ROMP-Facilitated Methodologies and Automated Library Development of Thiadiazepin-1,1-dioxide-4-ones

Toby R. Long

B.S., Missouri State University, 2002
M.S., Missouri State University, 2004

Submitted to the Department of Chemistry and the Faculty of the Graduate School of the University of Kansas in partial fulfillment of the requirements of the degree of Doctor of Philosophy

_____
Paul R. Hanson, chair

_____
Michael Rubin

_____
Minae Mure

_____
Helena Malinakova

_____
Jeffrey Aubé

Date Defended: _____

The Dissertation Committee for Toby R. Long certifies that this is the approved version of the following dissertation:

ROMP-Facilitated Methodologies and Automated Library Development of Thiadiazepin-1,1-dioxide-4-ones

_____

Paul R. Hanson, chair

_____

Michael Rubin

_____

Minae Mure

_____

Helena Malinakova

_____

Jeffrey Aubé

Date Approved: _____

Abstract

Toby R. Long, Ph.D.
Department of Chemistry, April 2010
University of Kansas

The use of ring-opening metathesis polymerization (ROMP) for polymer-assisted solution phase (PASP) synthesis is described herein. Multiple ROMP-based strategies will be discussed in the scope of this dissertation. These include the development and application of a multifaceted oligomeric phosphate as a facilitated leaving group in both S_N2 and S_N2' processes, as well as an in-situ generated sequestration reagent. We also investigate the use of ROMP in an atom-economical approach to generate a diverse collection of cyclic sulfonamides (sultams) whereby a vanishing support protocol imparts a traceless, chromatography-free synthesis of these motifs.

Also highlighted within is the ability to use ROMP technology to aid in the development of higher-loading magnetic nanoparticles for the purpose of supported catalysis. These cobalt-based ROMPgel nanoparticles were subsequently doped with Pd and demonstrated for use in several Suzuki-Miyaura coupling reactions. The nanoparticles were conveniently reclaimed via external magnetic field and recycled for later use.

Lastly, we present the design, validation, and completion of a 225-member library of thiadiazepin-1,1-dioxide-4-ones using both solution- and polymer-assisted solution phase protocols. The library was validated and conducted on an automated parallel synthesis platform in which a facile, two-step diversity-rendering sequence was performed.

In dedication to my Father,
my hero, Richard L. Long

To my wife Erica,
thank you for your unconditional love,
dedication and the many sacrifices you have made

To my brother Tyler,
you can accomplish anything

To my Mother, thank you for
your love and continual prayers

To my Step-Father, Richard Applegate
thank you for your love and
dedication to our family

To my second set of parents, Richard
and Cynthia Gummow,
thank you for your kind generosity
and support throughout
this process

Acknowledgments

I would first like to acknowledge my Lord and Savior, Jesus Christ. You never left my side. I would like to thank my family and friends for their prayers and amazing support. This was an incredible journey of learning, failures and successes, and a period of self-identity that contributed to the renewal of my long-time passion for the sciences.

I would like to thank my beautiful wife, Erica, for her unbridled support through my last three years. I can't wait to see what's next baby!

I would like to thank my father, Richard L. Long, who taught me the value of both working hard and playing hard. You had an incredible dedication to serve others; treating all people with respect despite who they were or how they treated you. You are my hero and a hero to the many people to who's lives fell into your hands over the short amount of time you had here on Earth. Thank you for encouraging me to seek my own answers and to pursue a college degree; I did it – three times over. You will be missed forever and one day we'll meet again to regale about the great times we had together. Love you Dad.

I would especially like to thank the key people throughout my life that fostered my love for science and the natural world. I would like to thank my father for taking me fossil hunting in the lime quarry. I would like to thank Gale Davis for my first and only telescope and for your musical talent that I still enjoy. To my first science teacher, Mrs. Denny, thank you for your stern, emotion-free face everyday and my

first experience with a chemistry lab. To Mrs. Latimer for teaching me the value of maintaining good ethics in science. To Mr. Reed, for keeping me awake during class. To all of my athletic coaches, thank you for always expecting more out of me. It has been one of my most valued lessons in life. To all of the professors in the chemistry department at Missouri State University, thank you for your amazing support and dedication to the student body. And, finally I would like to thank all of my professors, my colleagues, and the staff in the chemistry department at the University of Kansas, especially the Hanson Group for your dedication and support. I would like to thank my boss, Paul Hanson, for your support and patience. I will always remember your "soap box" speeches of encouragement and the countless emergency meetings throughout the five years of my Ph.D. I will always be indebted to you and Josh Waetzig for highlighting the importance of problem set and a good work ethic. To Josh, thank you for mentoring me and for your undying patience. To Professor Jeff Aubé, thank you for mentoring me and for your recommendation to intern at Abbott Laboratories in Chicago. It was an incredible learning experience. A special thanks to Conrad Santini, Ph.D., Frank Schoenen, Ph.D., and all of the participants in the KU-CMLD cores, especially Erik Fenster, Ph.D., David Hill, Kevin Frankowski, Ph.D., Ben Neuenswander, Gerald Lushington, Ph.D., Patrick Porubsky, Cagney Bennett, and all of the CMLD supporting staff. Thanks to all of the people I got to know behind the scenes – plumbers, electricians, janitorial staff, and anyone else that I forgot to mention.

ROMP-Facilitated Methodologies and Automated Library Development of Thiadiazepin-1,1-dioxide-4-ones

TABLE OF CONTENTS Page #

Abbreviations

AAS	atomic absorption spectroscopy
ADP	adenosine diphosphate
ATP	adenosine triphosphate
Ar	aryl
Bn	benzyl
BOC	*tert*-butoxycarbonyl
BPR	back-pressure regulator
cat	catalyst
CBZ	carbobenzyloxy
CDI	carbodiimide
CM	cross-metathesis
Cy	cyclohexyl
DBU	1,8-diazabicycloundec-7-ene
DCC	1,3-dicyclohexylcarbodiimide
DCE	dichloroethane
DEAD	diethyl azodicarboxylate
DMA	*N, N*-dimethylacetamide
DMAP	4-dimethylaminopyridine
DME	1,2-dimethoxyethane
DMF	*N*,*N*-dimethylformamide
DMSO	dimethylsulfoxide
DNA	deoxyribonucleic acid
EDC	1-ethyl-3-(3-dimethylaminopropyl) carbodiimide
EDX	energy-dispersive X-ray
ee	enantiomeric excess
equiv	equivalent
EVE	ethyl vinyl ether
GC	gas chromatography

HATU	2-(1H-7-Azabenzotriazol-1-yl)--1,1,3,3-tetramethyl uronium hexafluorophosphate Methanaminium
HOBt	*N*-hydroxybenzotriazole
HPLC	high-performance liquid chromatography
LP	low pressure
m-CPBA	metachloroperoxy benzoic acid
Mes	mesityl
MS	mass spectrometry
Nb	norbornene
NMI	*N*-methylimidazole
NMM	*N*-methylmorpholine
NMR	nuclear magnetic resonance
NP	nanoparticle
OACC	oligomeric alkyl cyclohexyl carbodiimide
OBP	oligomeric benzyl phosphate
OTPP	oligomeric triphenylphosphine
PASP	polymer-assisted solution phase
PEPPSI™	Pyridine-Enhanced Precatalyst Preparation Stabilization and Initiation.
PS	polystyrene
quant	quantitative
RCM	ring-closing metathesis
RNA	ribonucleic acid
ROM	ring-opening metathesis
ROMP	ring-opening metathesis polymerization
rt	room temperature
SEM	scanning electron microscopy
S_N2	bimolecular nucleophilic substitution
SPE	solid-phase extraction
SPOS	solid-phase organic synthesis
SPION	superparamagnetic iron oxide nanoparticles

TEM	transmission electron microscopy
TFA	trifluoroacetic acid
TFAA	trifluoroacetic anhydride
THF	tetrahydrofuran
TLC	thin layer chromatography
TMS	trimethylsilyl
VSM	vibrating sample magnetometer
VSP	vanishing support protocol

Chapter 1

Recent Advances in Polymer-Assisted Solution Phase Synthesis and Automated Protocols

1.1 Introduction

Over the last two decades, both organic synthesis and medicinal chemistry alike have been greatly impacted by the development of solid-phase synthesis and automated technologies.[1] Among these developments, polymer-assisted solution phase (PASP) synthesis[2] has brought about a new paradigm shift for drug discovery outside of the traditional "split and mix" combinatorial techniques of solid-phase chemistry. This has been gathered largely in part by a number of favorable attributes that allow for the simplification of synthetic processes including isolation and purification procedures. These attributes have been thoroughly reported throughout the literature[3] and include (i) having a larger commercially available set of immobilized reagents, catalysts, and scavengers at the chemist's disposal[4] (ii) the ability to facilitate cleaner and safer reaction profiles through immobilization of toxic/hazardous materials[5] (iii) reusability of the spent reagent (iv) ease of monitoring using conventional techniques (ie. TLC, LC-MS, GC, etc…) (v) and the ability to facilitate compound libraries that yield sufficient quantities (25–50 mg) of high-quality material.[6]

The roots of polymer-assisted synthesis dates back to the 1960's with seminal work performed by Bruce Merrifield in the development of facilitated peptide synthesis.[7] Since this time, these pivotal accomplishments have paved the way for the development of new facilitated approaches, not only in peptide chemistry[8], but have also aided in the assembly of complex natural products[9] and new synthetic materials.[10]

When one compares the attributes of PASP-synthesis to conventional solid-phase organic synthesis (SPOS), a clear separation is revealed (Figure 1.1). PASP-based methods eliminate the necessary synthetic steps to attach the substrate to the resin support and its subsequent release of the desired product. The reversed role played by PASP synthesis in which the substrates are solution-bound, facilitates overall cleaner reaction profiles having virtually eliminated side product formation due to incomplete "on-bead" conversions.

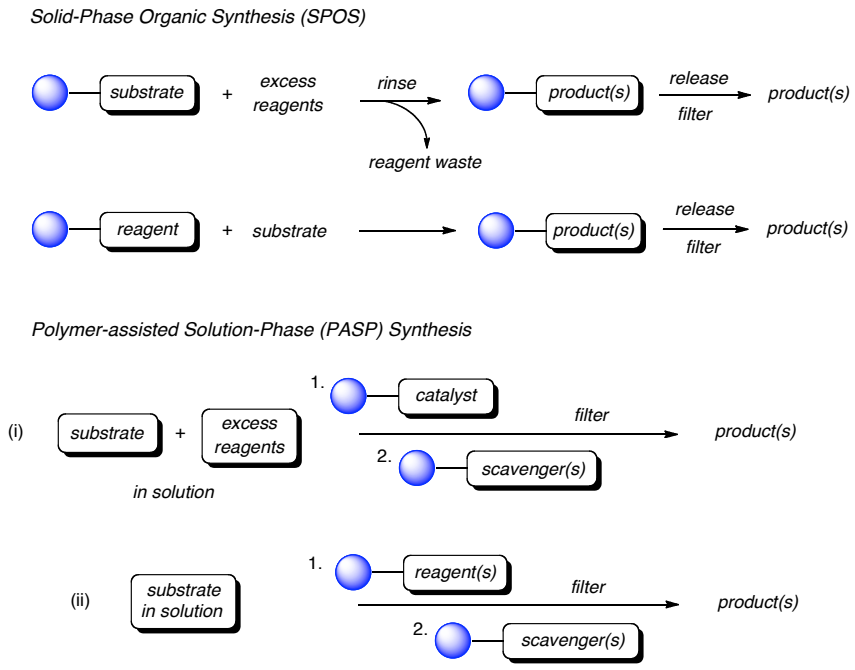

Figure 1.1 *Solid-phase organic synthesis vs. polymer-assisted solution phase synthesis*

PASP-based methods utilize excess reagents in solution (i), or polymer-bound (ii), to drive reactions to completion. These reagents, along with any byproducts that may

form, can conveniently be removed by either filtration, or via polymer-assisted chemoselective sequestration (ie. scavenging).[11]

Polymer-bound reagents can be categorized into a number of different areas related to their function and/or functionality present on the support (Figure 1.2). These include reagents used for oxidation[12] and reduction,[13] polymer-bound nucleophiles (electrophile scavengers),[14] polymer-bound electrophiles (nucleophile scavengers),[14a,15] amide coupling,[16] acidic,[17] basic,[18] and specialized reagents used for alkylation,[19] dehydration,[20] etc… Many of these chemical entities reside upon conventional polystyrene supports (PS) that are inexpensive and relatively easy to use. One caveat of PS-based supports is under certain conditions degradation can be observed thus leading to the development of a number of different alternative supports including metal-based nanoparticles,[21] silica,[22] cellulose,[23] zeolites,[24] and monoliths;[25] some of which will be discussed herein.

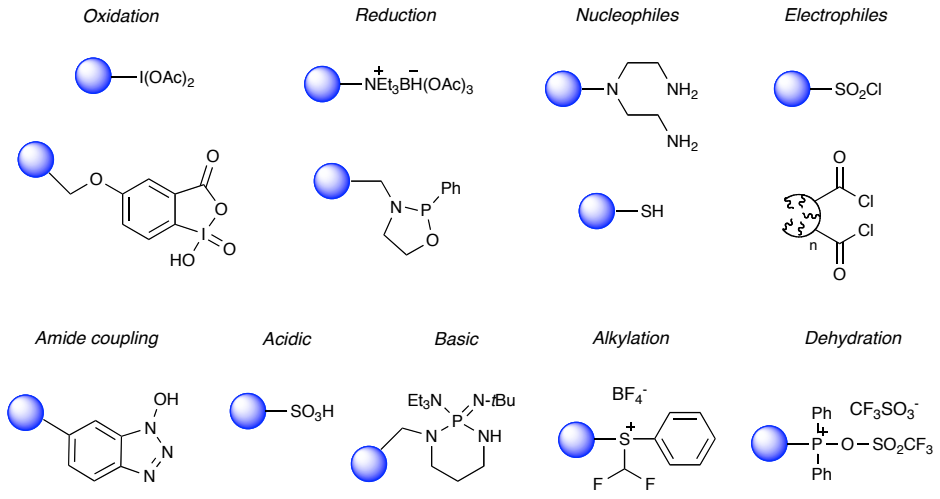

Figure 1.2 *Representative polymer-bound reagents used in PASP-synthesis*

To preface this discussion, this opening chapter will provide a brief review of some of the most recent and prominent advances in polymer-assisted solution phase (PASP) synthesis and automated technologies. This review will cover seminal reports and applications in the areas of (i) soluble and insoluble polymer-bound reagents, catalysts, and scavengers (ii) developments in flow-chemistry and new functionalized-materials (iii) as well as and other automated, PASP-friendly technologies and their use in small-molecule library development.

1.2 Recent Advances in Polymer-Bound Reagents, Catalysts and Scavengers

The use of polymer-supported chemical entities has steadily increased over the last several decades and continues to play a vital role in facilitating small-molecule synthesis.[26] This increase has come as a result of increased demands revolving around the drug-discovery process, and the need to produce diverse compound collections in a faster, more efficient manner. Over time, these demands have yielded a number of polymer-bound entities that have recently been used in PASP-facilitated library synthesis.[4b]

Parlow et. al. recently displayed use of a number of different polymer-bound reagents in the PASP-facilitated library synthesis of piperazinyl glutamate pyridines (Scheme 1.1).[27] Polymer-supported carbodiimide (CDI) (**1.1**) was used as an amide coupling reagent to piece together piperazine fragments (**1.2**) to a number of arylcarboxylic acids (**1.3**) in the presence of HOBt (coupling additive) and NMM. The authors used this fragment-based approach to optimize lead molecules (**1.4**) as $P2Y_{12}$ antagonists for inhibition of platelet aggregation.

Scheme 1.1 *Use of PASP synthesis in fragment-based lead optimization*

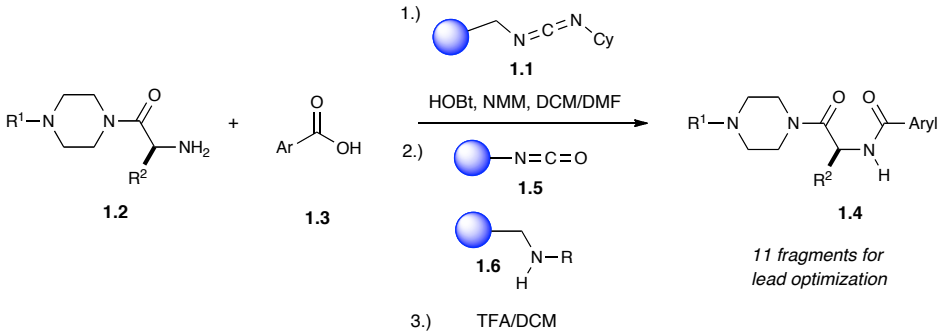

One of the more overlooked features of PASP-synthesis is the ability to incorporate and use otherwise incompatible functionalities together simultaneously in a single-pot reaction.[28] Highlighted above, the authors report the use of a polymer-bound isocyanate in the presence of a polymer-bound amine in a mixed-bed scavenging protocol. Isocyanate **1.5** was used to scavenge out excess HOBt and/or amine starting material, while amine **1.6** was used to remove any unreacted carboxylic acid (**1.3**). The decrease in reactivity of the two polymer-bound scavengers towards each other is mainly attributed to stabilization thorough overall spatial arrangement of the functional groups within the polymer matrix. The use of excess polymer-bound reagents is often a result of low resin-load capacities, but can also be related to this reduced reactivity. This, however, can also come at an advantage to the chemist as greater selectivity can sometimes be achieved as compared to the same non-supported reagent in solution.[29]

Parang and Ahmadibeni recently reported the development of solid-phase reagents for regioselective phosphoryation of carbohydrates and nucleosides.[30] Traditional phosphorylation and/or derivatization[31] of carbohydrates can utilize various

protection/deprotection schemes to achieve the desired mono-phosphorylated species, while unprotected systems often result in multi-phosphorylated compounds that must be separated; both scenarios are quite uneconomical for the purpose of library development. Reagent **1.7** was specifically designed to address these limitations through development of a more universal method for monophosphorylation of multi-hydroxylated compounds.

The activated phosphorus in this reagent is strategically placed for its preemptive release as a phosphate (**1.9**) via acid-mediated generation of a *p*-quinone methide. This resin-trapped methide is then quenched, releasing the newly phosphorylated products (**1.10**), and is then recycled for later use by various phosphitylating reagents.

Scheme 1.2 *Use of a solid-phase phosphoryating reagent*

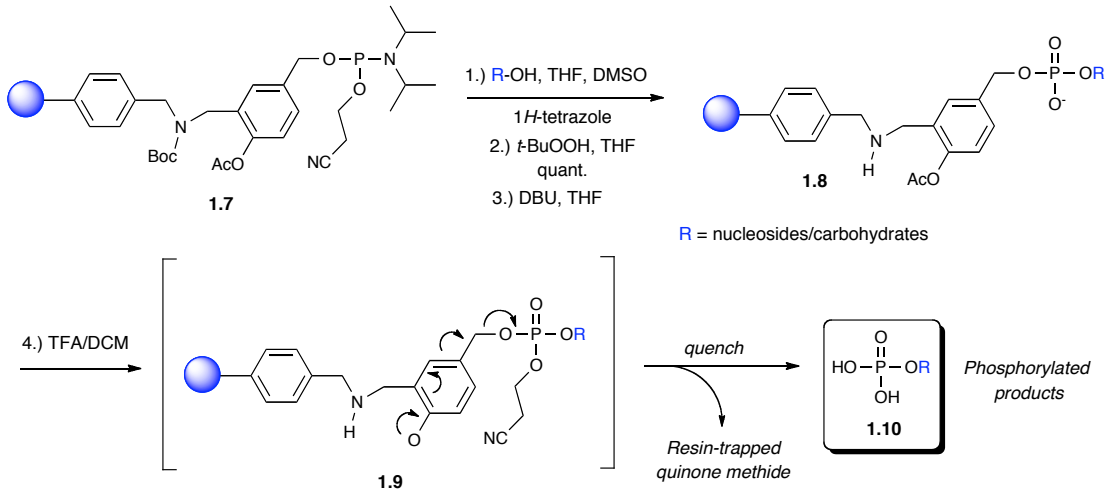

Recently, Chiara and Encinas reported on the usefulness of a supported dialkylformamide (**1.11**) as a catalyst for facilitated halogenation of protected sugar hemiacetals for the purpose of anomeric substitution (Scheme 1.3).[31] This was

conducted in the presence of oxalyl chloride, triphosgene, or oxalyl bromide thus demonstrating the fidelity of the support under harsh reagent conditions.

Scheme 1.3 *Use of a supported-dialkylformamide catalyst*

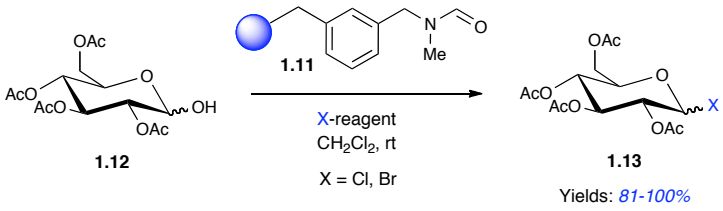

Recycling of this catalyst was also tested whereby 1 equiv. facilitated its use up to 6 times without any loss of activity (>99% yield for each). Reagent/catalyst recyclability is an important feature in polymer-assisted methods to prevent excess reagent waste and reduce the costs associated with their disposal.

The Huisgen [3+2] cycloaddition between an azide and an alkyne[32] (ie. "click" reaction)[33] represents itself well through its outstanding efficiency and reproducibility thereby making it prime for automated synthesis of 1,2,3-triazole-containing small-molecules. Triazoles and azoles in general, represent an interesting class of small-molecule heterocycles that are widely known for their use as powerful antifungal agents.[34] Recently, Girard and coworkers reported the development of a reusable polymer-supported copper catalyst for this reaction class.[35] This catalyst, based upon an Amberlyst A-21 dimethylamino resin, was tested in numerous alkyne/azide cycloadditions using a Chemspeed ASW-2000® parallel synthesizer[36]. Utilizing a loading capacity of 0.2 mol% CuI, the remaining (unactivated) dimethylamino

Scheme 1.4 *Use of a bifunctional solid-phase catalyst in Huisgen cycloadditions*

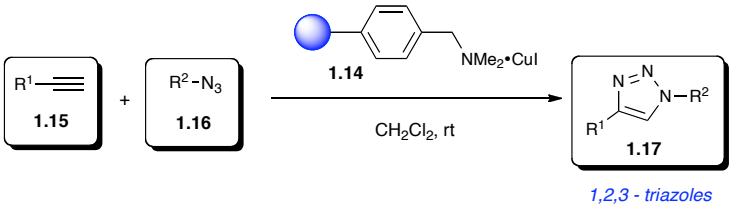

functionalities on the bead act as a resin-bound base, thus defining it as a bi-functional solid-phase catalyst. An average yield of 87% was obtained for the twenty-three triazoles (**1.17**) with the majority showing near quantitative conversions.

In a separate experiment, the catalyst was recycled up to 4 times having resulted in yields > 99% for each run. Use of this bi-functional catalyst in automated library synthesis will be further discussed in Chapter 5.

A modified version of this catalyst has also recently been reported in the production of various triazole-containing macrocycles (Scheme 1.5).[37] Although the authors report iodine incorporation with the use of the previously shown catalyst – no evidence supporting this claim was provided.

Scheme 1.5 *Intramolecular triazole formation via A-21•CuPF$_6$*

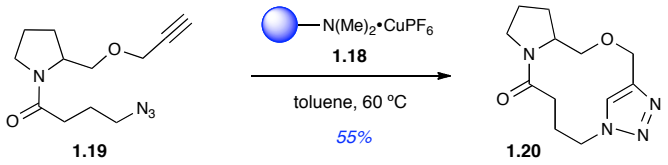

Despite considerable advances in the area of solid-phase reagent development, a number of technologies have emerged for use in more homogeneous environments. These soluble/partially-soluble reagents allow for greater substrate permeability and more favorable reaction kinetics when compared to standard immobilized reagents.

Janda and coworkers, over several years, have introduced the concept of employing more flexible cross-linkers into PS resins to increase the swelling properties of the polymeric support in various solvents.[38] The polymer, known commercially as JandaJel®, has been used in a number of different applications including catalysis,[39] multi-polymer transformations and peptide synthesis.[40] Recently, Janda and coworkers reported on the use of this polymeric support in a diversity-building cleavage reaction to facilitate the formation of various benzothiazoles (Scheme 1.6).

Scheme 1.6 *PASP-facilitated benzothiazole formation*

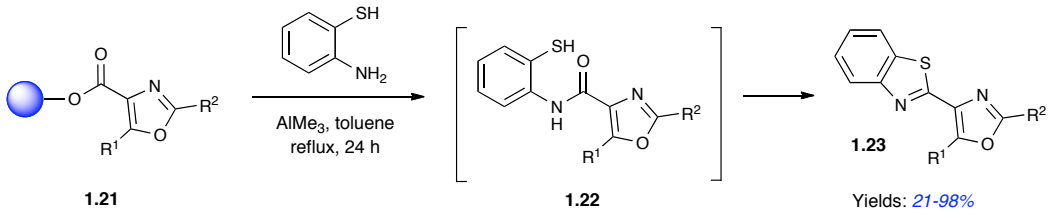

This unique strategy was discovered serendipitously by a Lewis-acid promoted cleavage of polymer-bound oxazole derivatives (**1.21**) in the presence of 2-amino thiophenol. Instead of isolating amide **1.22**, benzothiazole **1.23** was liberated, providing a facile polymer-assisted method towards this interesting class of heterocycles.

A number of homogeneous polymer-bound reagents have also been developed by both Barrett[41] and Hanson[42] using ring-opening metathesis polymerization (ROMP) of functionalized norbornenes. An oligomeric monoamine hydrochloride (OMAm•HCl) was reported in 2008 for use as a high-loading, electrophile scavenging reagent (Scheme 1.7).[42b] Previous attempts to generate this reagent as the free-amine were unsuccessful due to its nucleophilic nature and high reactivity towards catalysts in the

polymerization event. However, it was discovered that simple acidification of the monomeric free-amine **1.24** resulted in facile polymerization of monomer **1.25** to yield OMAm•HCl **1.26**.

Scheme 1.7 *Synthesis of oligomeric monoamine hydrochloride (OMAm•HCl)*

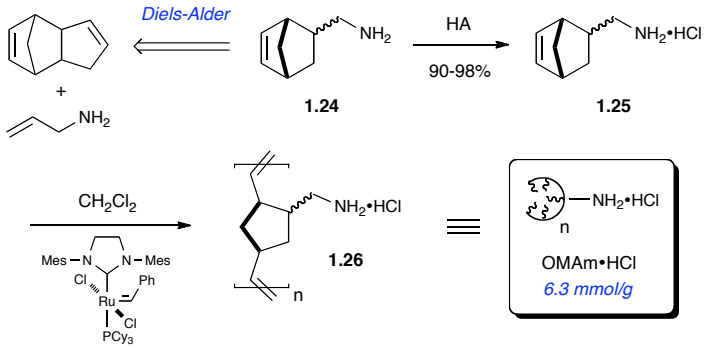

This reagent was used to facilitate the removal of a variety of chlorine-containing electrophiles (**1.27**) (benzoyl, benzyl, tosyl) as well as both isocyanates and aldehydes. These were used in excess for alkylation of various primary and secondary amines (**1.28**) (Scheme 1.8).

Scheme 1.8 *Use of OMAm•HCl in scavenging protocols*

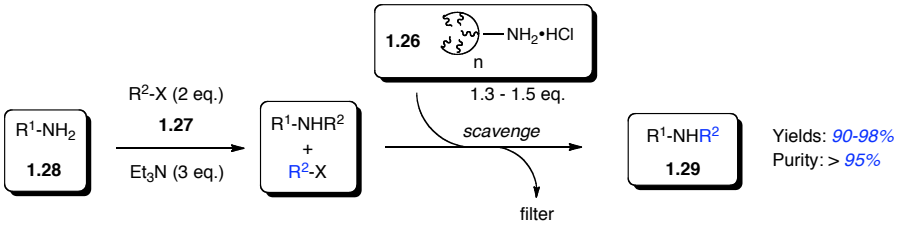

In the same year, Hanson and coworkers utilized ROMP-technology to aid in library synthesis of potential small-molecule inhibitors of methionine aminopeptidase; a metalloenzyme responsible for cell growth and proliferation.

Scheme 1.9 highlights the use of an oligomeric coupling reagent ($OACC_{100}$) for the synthesis of various substituted furans, thiophenes, and pyridines (not shown).

Scheme 1.9 *Facilitated amide formation via $OACC_{100}$ in a parallel format*

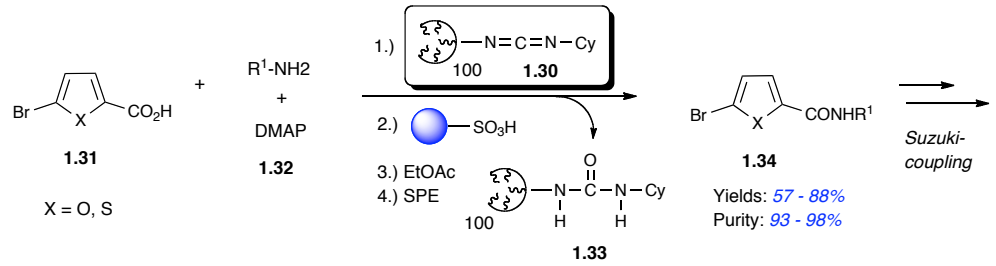

Commercially available 5-bromofuroic acid **1.31**, and analogs thereof were coupled to a number of different amines - including sulfonamides (**1.32**) in the presence of DMAP and reagent **1.30** to afford newly substituted furans **1.34** in good yields and excellent purities. The use of Amberlyst A-15 (sulfonic acid) was also employed to scavenge excess amine starting material **1.32** including DMAP. Both reagents were conveniently removed by SPE filtration.

1.3 Recent Developments in Flow-Chemistry and Functionalized Materials

With the advent of solid-phase-assisted synthesis, a number of automated technologies[1a] have further promoted development of these chemistries and enabled them quite user-friendly in terms of compound acquisition, organization and care, safety, and overall scalability. These have not only found themselves useful from an industrial pharmaceutical setting[43] but have also made their way into the academic laboratory for facilitating drug discovery efforts.[44] Ley and coworkers at Cambridge have demonstrated this transferal through a wide array of PASP-based techniques via continuous-flow synthetic methodologies (flow-chemistry).[45] This PASP-friendly

technology (Figure 1.3) uses polymer-bound cartridges that grant the user the ability to employ a variety of bound reagents, catalysts, or scavengers including the use of micro-scale reactors for performing homogeneous chemistry.[46]

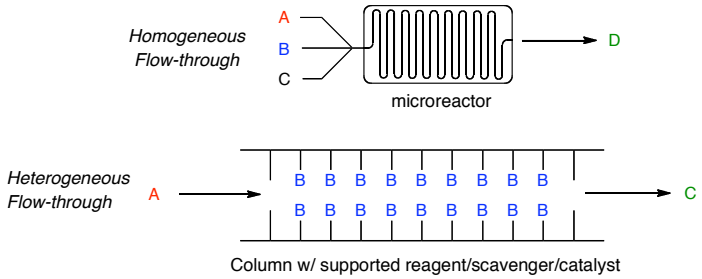

Figure 1.3 *General flow-chemistry scheme*

High reaction efficiency is often achieved in these systems using precisely controlled flow rates and efficient turbulent mixing patterns. This translates into greater control over stoichiometry and reaction kinetics (heat and mass transfer) often resulting in less byproduct formation as compared to the same reactions performed in a round-bottom flask. Another advantage to flow-chemistry is its ability to scale-out reactions via continuous-flow; providing that starting materials are continually being fed into the reaction stream. The ability to transition from milligram to kilogram quantities of material is merely a function of time.

One of most recent achievements by the Ley group demonstrates the power of PASP-synthesis in flow with the total synthesis of the (±)-oxomaritidine (Figure 1.4).[47] This synthesis was based upon their initial PASP-synthesis (not in flow) of the compound in 1999,[48] whereby polymer-supported reagents were used at every transformable step in the synthesis. These accomplishments represent a first in the

area of total synthesis having eliminated the need for chromatography or aqueous workup at any point in the synthesis. Other, more complex total-syntheses have also been reported by the Ley group in recent years using PASP-based methods.[49]

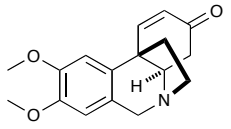

Figure 1.4 *Natural product (±)-oxomaritidine*

Scheme 1.10 highlights the synthesis of (±)-oxomaritidine in flow utilizing a variety of solid-phase reagents and catalysts. This synthesis was driven by the implementation of a number of different commercially available automated systems. The Syrris[50] AFRICA®, a highly-advanced modular flow-chemistry system, was used to deliver 4-(2-bromoethyl)phenol (**1.35**) through an azide exchange resin (column 1) to afford azido phenol **1.36**. This was carried into column 3 containing a polymer-bound phosphine to furnish the aza-Wittig intermediate trapped on the polymer support. Simultaneously, 3,4-dimethoxybenzyl alcohol (**1.37**) was flowed through column 2 containing resin-bound *N*-alkylammonium perruthenate (PSP) to facilitate oxidation to the corresponding aldehyde **1.38**. This is then flowed through column 3 to furnish imine **1.39** that is then subjected to flow-through hydrogenation utilizing a ThalesNano H-Cube® flow hydrogenator.[51] This unit utilizes a cartridge containing 10 % Pd on carbon catalyst and generates small amounts of hydrogen gas *in situ* via ionization of water; making the unit safe enough to use in a conventional laboratory setting.

Scheme 1.10 *Flow-through PASP-synthesis of (±)-oxomaritidine.*

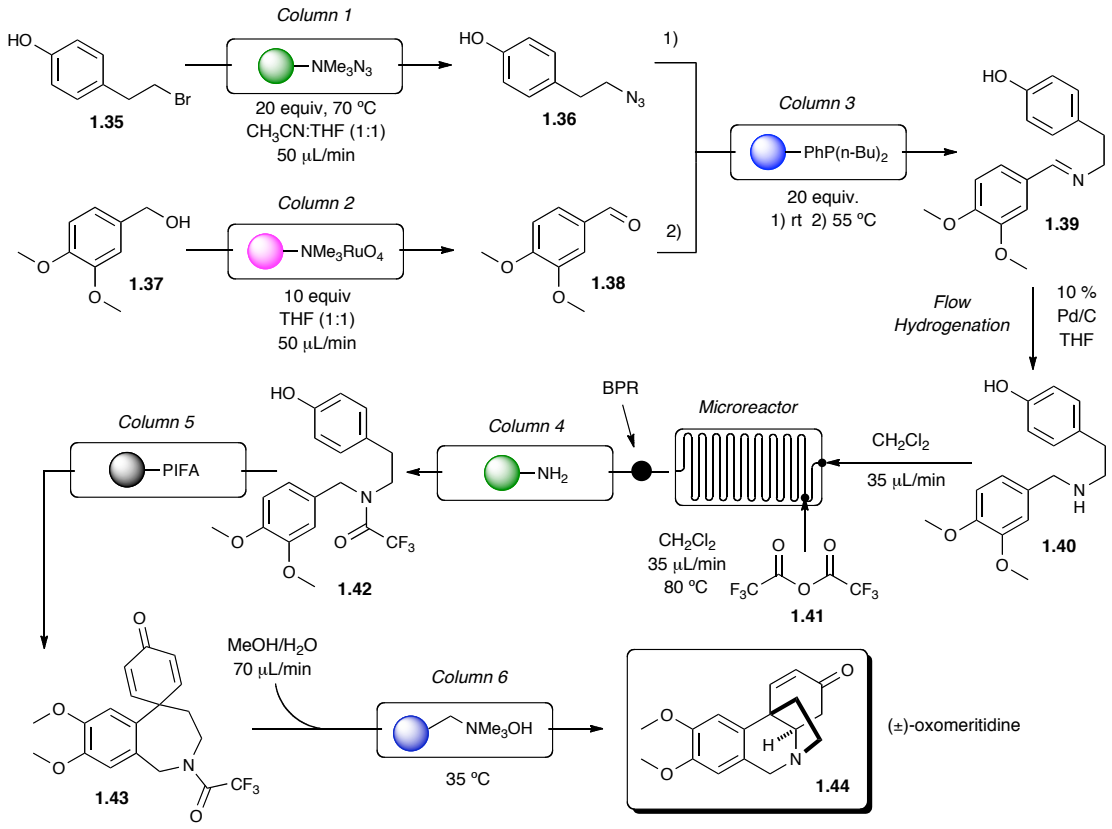

Secondary amine **1.40** in THF was then transferred via flow into a Biotage V-10® automated evaporation unit[14] and subjected to a solvent switch (CH_2Cl_2). This solution was then flowed through a glass microreactor on the Syrris system with TFAA (**1.41**) to afford trifluoroacylated amide **1.42**. At this stage in the synthesis, the use of a back-pressure regulator (BPR) allowed the reaction in CH_2Cl_2 to operate above reflux at 80 °C. With microchip ratings up to 300 bar, the ability to superheat reactions in this manner is easily achieved – often resulting in drastically increased reaction rates.

Also placed downstream from the reaction was column 4 containing a silica-supported primary amine[52] scavenger to rid the solution of excess TFAA. In the final steps of the synthesis, amide **1.42** was transformed to the spirotricyclic intermediate **1.43** with the use of polymer-supported (ditrifluoroacetoxyiodo)benzene (PS-PIFA) (column 5). This was then passed through column 6 containing a supported base to facilitate amide cleavage and subsequent 1,4 conjugate addition to afford the natural product (±)-oxomaritidine **1.44**.

Also impressive is Ley's use of flow-chemistry in the first total synthesis of neolignan natural product grossamide[53] (Scheme 1.11) performed in the same year. This synthesis was achieved via amide-bond coupling of ferulic acid (**1.45**) with tyramin (**1.47**) using polymer-supported HOBt (Reagent 1) whereby the activated ester initially formed on the surface of the reagent. Also reported was the use a sulfonic acid resin (Reagent 2) to scavenge out excess amine from the first reaction. More importantly, the Ley group has chosen to implement more exotic supported systems such as immobilized enzymes to facilitate key synthetic transformations.[54] "*Why use synthesis, when nature can do it for you.*" This statement has recently gained considerable attention with seminal advances in the area of microbial gene manipulation to produce natural products with desired chemical profiles.[55] Ley's use of a silica-immobilized horseradish peroxidase enzyme in buffered media conveniently afforded the natural product grossamide **1.49** without the need for purification via chromatography.

Scheme 1.11 *Ley group flow-through synthesis of grossamide.*

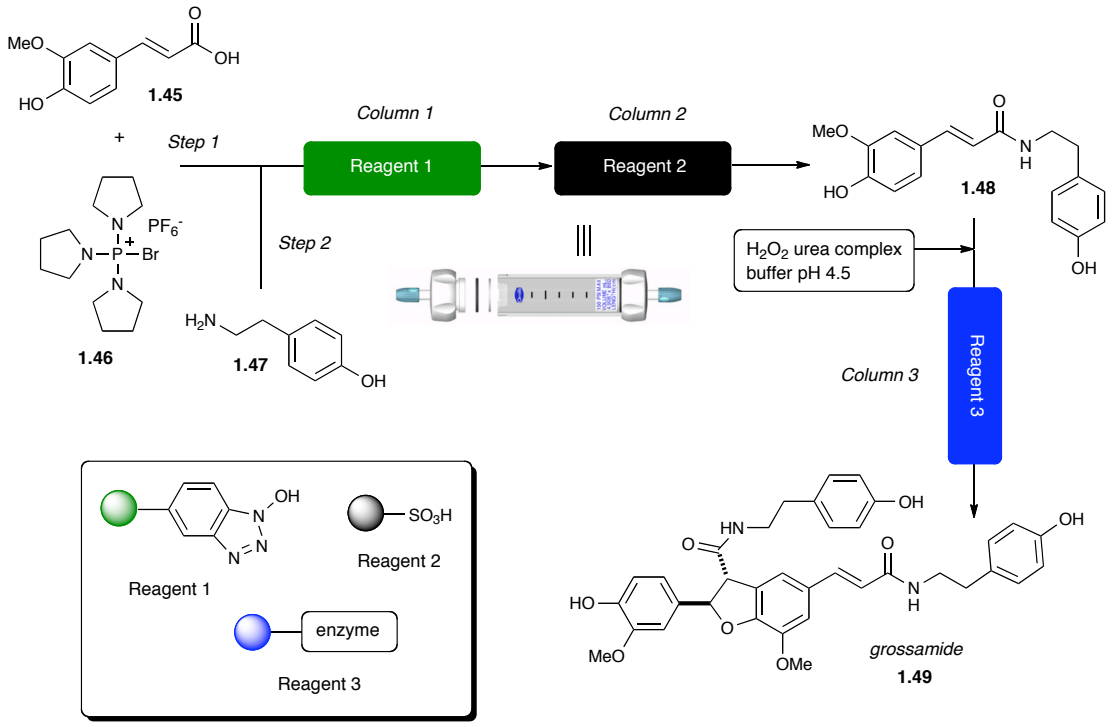

The modular approach of continuous-flow chemistry allows for an almost unlimited incorporation of hardened components including analytical equipment for *in situ* reaction monitoring and "on-the-fly" optimization and purification. With this notion, comes the flexibility to incorporate other types of reactors, equipment, and synthetic materials not previously mentioned.

Kirschning and coworkers, among others[56], have recently explored the use of functionalized magnetic nanoparticles inside microreactors (Figure 1.5) as solid supports for flow-chemical methodologies.[57] Using a magnetic field generator paired with an inductor, the investigators were able to achieve inductive heating of magnetic nanoparticles while in a continuous-flow environment. This system was also paired

with a preparative HPLC that could be used for in-stream reaction analysis as well as final purification of products being generated.

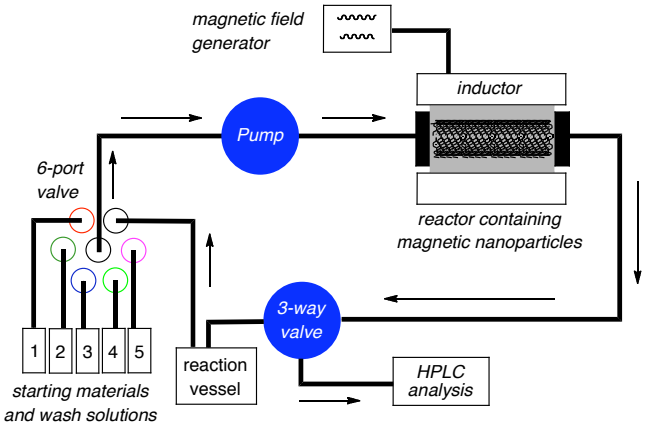

Figure 1.5 *Experimental setup for inductive magnetic manipulation of nanoparticles in a continuous-flow scenario.*

This method was subsequently applied to a variety of reactions highlighted in Scheme 1.12 including transesterification (i), condensation (not shown), Claisen rearrangement (ii), Hartwig-Buchwald amination (iii) and enyne metathesis (iv). Entry (iii) also highlights an observed increase in yield as compared to conventional heating. Included in this set of reactions were a number of Pd-catalyzed transformations that were achieved using Pd-functionalized magnetic nanoparticles. Previous examples shown merely used the catalyst in solution and the nanoparticles acted only as a source of heating. In this manner, Pd particles were obtained by reductive precipitation of ammonium-bound tetrachloropalladate salts to yield the catalyst bound nanoparticles **1.58**. The catalyst demonstrated good activity under flow-conditions for both the Suzuki-Miyaura (i) and Heck (ii) coupling reactions (Scheme 1.12).

Scheme 1.12 *Reactions performed using inductive heating of magnetic nanoparticles in flow.*

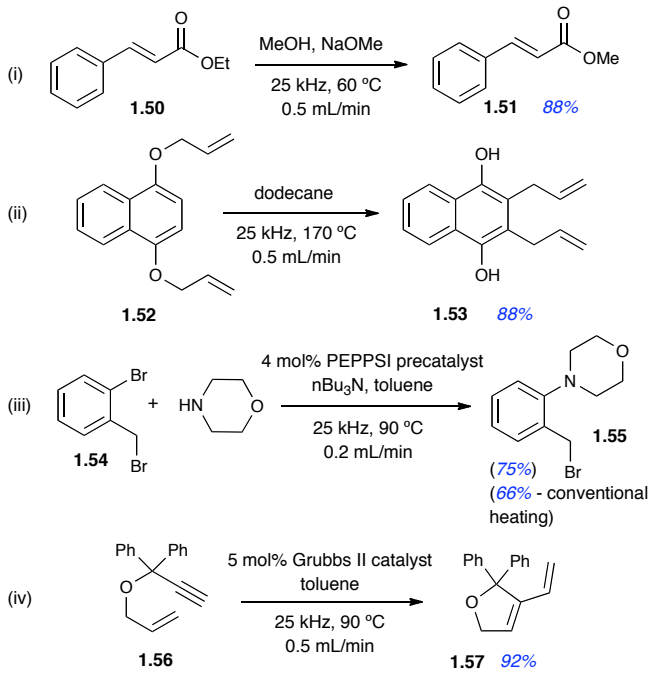

Scheme 1.13 *Use of Pd-functionalized nanoparticles in flow.*

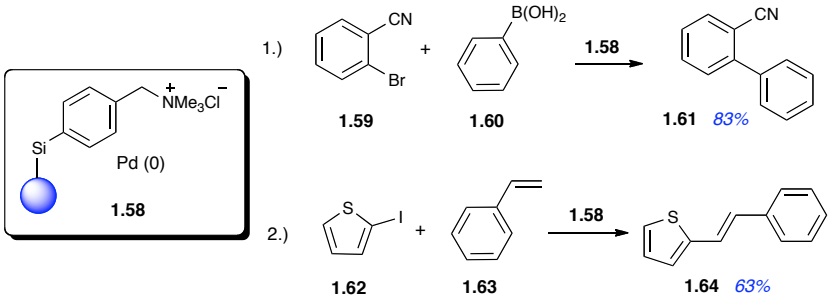

A number of different materials have been used in recent years for facilitating solution-phase chemistry,[58] especially in the area of flow-chemistry.[59] The development of these materials has addressed a number of limitations primarily associated with the nature of resin-packed columns. One such material is that of monolithic polymers. These materials were first developed as purification media in

LP/HP liquid chromatography[60] but have now found their place as alternative polymer-derived supports for PASP-based chemistries.[60b] Monolithic materials help circumvent problems associated with interstitial or void space between beads in fixed-bed cartridges that can often lead to undesired channeling. In this regard, monolithics inherently carry a much larger reactive surface area – owing to their extensive porosity making them very useful for heterogeneous continuous-flow chemistry. (Figure 1.6).

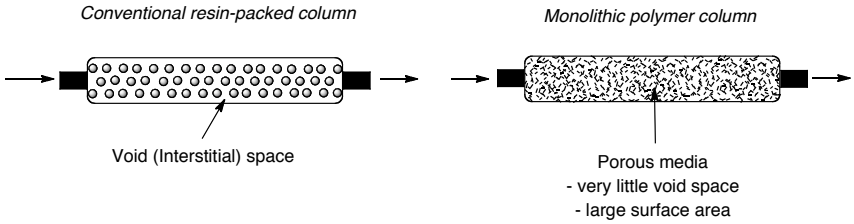

Figure 1.6 *Resin-packed columns vs. monolithic polymer columns*

Ley and coworkers recently demonstrated the use of monoliths in flow as alternative supports for azide-bearing reagents in the Curtius rearrangement. In this manner, the safety profile of the reagent was greatly increased by reducing the handling risks associated with azides including impact, shock, and exposure hazards.

Monolithic materials have also recently been generated by Buchmeiser et. al. with the use of previously mentioned ROMP-technology as a means to generate supports for organocatalysis[61]. These supports were prepared within a borosilicate column *vide supra* and subsequently used for numerous flow-thorough metathesis transformations.

These materials may prove valuable for the future of flow-chemistry in terms of developing more convenient PASP synthetic protocols providing that their cost effectiveness is on par with other polymer-bound entities and/or recyclability is a likely option.

1.4 Recent Advances in Automated Technologies for Small-Molecule Library Development

Despite considerable advances made in the field of PASP-facilitated continuous-flow synthesis, one of its current disadvantages is its inability to facilitate the production of medium to large compound collections for the purpose of drug discovery. Over the years, a number of automated technologies have been developed for this purpose alone,[62] but have likewise been used for the proliferation of other non-drug seeking chemistries.[63] One of the more minor, yet high-implicating contributors for small-molecule library development at the present time is the use of microwave synthesizers.

Microwave chemistry over the last decade has seen an explosion of applications and devices for facilitating numerous reactions that are often burdensome under traditional heating methods.[64] Only until recently, however, have commercial microwave (multi-mode) synthesizers been developed for the purpose of parallel reaction synthesis.[65] Mono-mode microwaves (ie. one vial, one condition set) have already seen substantial use in the pharmaceutical industry in conjunction with various autosamplers and robotics to facilitate sequential compound synthesis.

Sauer and coworkers at Abbott Laboratories have recently utilized this technology in conjunction with polymer-bound reagents to aid in the formation of numerous medicinally relevant heterocycles.[66] They also demonstrated the use and thermal stability of a new class of polymer-bound catalysts (Pd-bound FibreCat®) for microwave assisted Suzuki-Miyaura coupling reactions (Scheme 1.14).[67] A number of different catalysts were explored including a PS-based Pd source. These were compared to several Pd-bound FibreCat® catalysts (FC-X) where higher conversions were observed with the use of EtOH as the primary solvent. Silica-bound carbonate (Si-Carbonate) was also utilized for the purpose of removing excess boronic acid (**1.66**) from the reaction and complete sequestration was noted when a 10-fold excess of this supported base was used during crude reaction filtration.

Scheme 1.14 *PASP-microwave assisted Suzuki-Miyaura coupling*

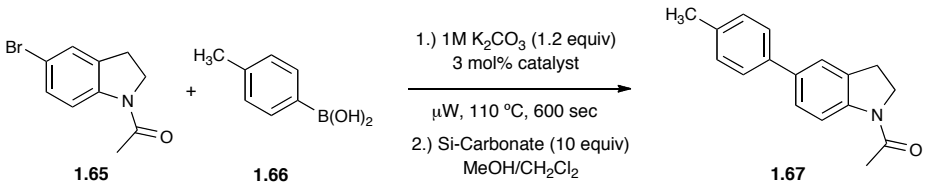

catalyst	solvent	conversion[a]
$Pd(PPh_3)_2Cl_2$	DME/EtOH (1:1)	*88%*
$PS\text{-}PPh_3\text{-}Pd$	DME/EtOH (1:1)	*81%*
FC-1001	EtOH	*100%*
FC-1007	EtOH	*100%*
FC-1032	EtOH	*100%*

[a] Determined by ^{1}H-NMR and LC/MS.

In 2008, Clapham and Sauer et. al. also demonstrated the use of the previously mentioned ThalesNano H-Cube® flow-hydrogenator as a means for facilitating high-throughput parallel deprotection. The automated system, shown in Figure 1.7, was

constructed on a Bohdan® robot[68] platform and machined to accept eight custom vial racks that accept 12–20 mL scintillation vials for both starting materials and product collection on a large scale.

Figure 1.7 *Custom parallel flow-hydrogenation robot*[69]

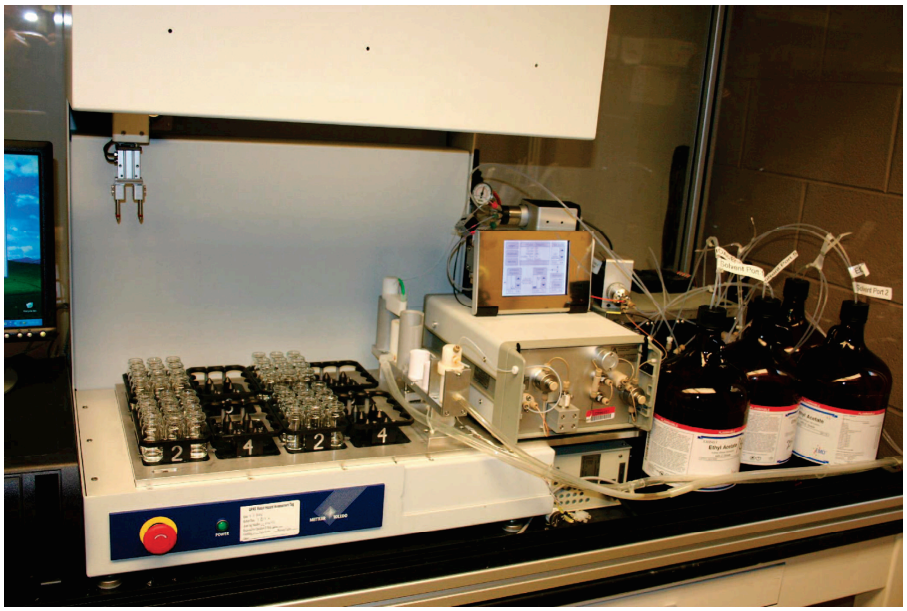

The automated system was tested for use on two separate pilot-scale libraries: (i) – CBZ protected and (ii) – benzyl ether protected (Scheme 1.15). Good to excellent yields were obtained for both libraries, having demonstrated the utility of pairing robotic automation with mono-mode systems to successfully achieve parallel synthesis.

Scheme 1.15 *High-throughput deprotection using hydrogenation*

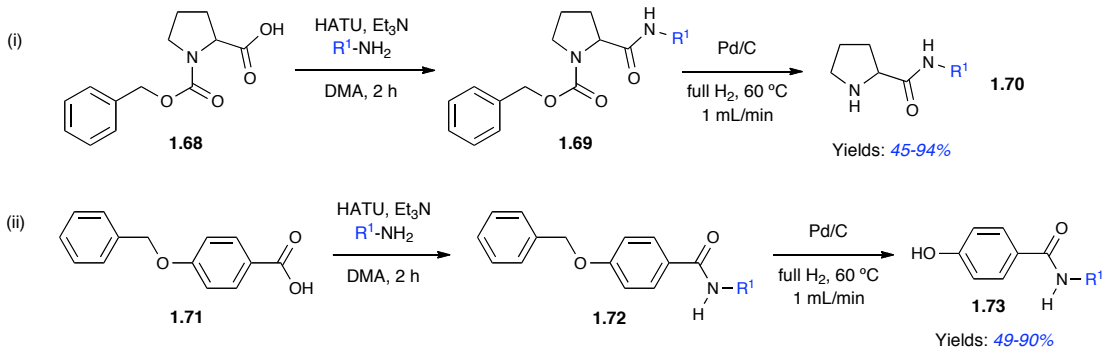

Fully automated systems, like the one mentioned above, have several advantages and disadvantages associated with their use in library production. Typically, the user must either have full working knowledge of the automated system, or a full-time dedicated technician must oversee all projects taking place on the parallel platform. Despite the more hands-off approach, the technician must be able to troubleshoot and correct any foreseeable problem at a moments notice to prevent material loss. Other, more semi-automated systems, however, can be prepared by multiple people and often have a lesser amount of problems due to their more simplistic design.

Recently, Aubé and Hanson et. al. utilized two parallel synthetic platforms, both semi- (i) and fully automated (ii), in a library comparison study to synthesize various 1,4-diazepin-5-ones as γ-turn peptidomimetics (Scheme 1.16).[44a] Both the Bohdan MiniBlock XT® (i)[68] and the Chemspeed SLT-100® (ii)[36] platforms were tested – each having resulted in comparable yields and purities for the three-component reaction sequence.

Scheme 1.16 *Automated parallel synthesis of 1,4-diazepine-5-ones*

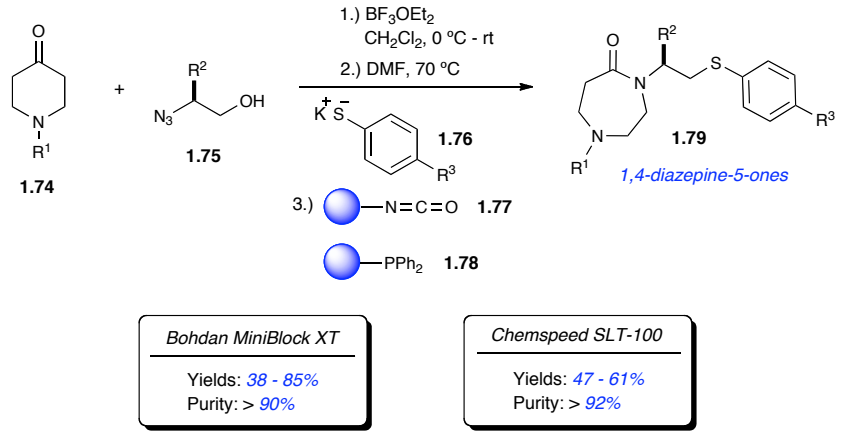

During validation, a number of polymer-supported scavengers were used to aid in subsequent purification of crude products. Polymer-bound isocyanate **1.77** was used to remove excess thiophenoxides (**1.76**) while excess hydroxyazides (**1.75**) were sequestered by polymer-bound triphenylphosphine **1.78**. Using the liquid handling capabilities of the Chemspeed robotic platform, the three-component sequence was conveniently simplified by introducing a basic wash (NaOH) step – replacing both polymer-bound scavengers for the removal of excess starting materials. The hydroxyazides were also easily removed from the crude reaction mixtures via silica SPE filtration. This more cost-efficient method was ultimately chosen for final library production – highlighting the flexibility of using various automated platforms – even without the use of immobilized scavengers/reagents.

1.5 Conclusions

The development of new materials and automated technologies has produced a number of prime examples in recent years where polymer-assisted solution phase protocols have played a key role in facilitating the reaction process. Undoubtedly, the bodies of work discussed herein represent the front lines for future advancement in the areas of both natural product synthesis and small-molecule library development. These contributions will not only enable further advancement in these areas in the near future, but will likely have far-reaching implications into other closely related scientific disciplines.

References

(1) (a) Koppitz, M.; Eis, K., Automated medicinal chemistry. *Drug Discov. Today* **2006**, *11*, 561–568. (b) Koppitz, M., Maximizing Efficiency in the Production of Compound Libraries *J. Comb. Chem.* **2008**, *10,* 573–579 (c) Hird, N. W. Automated synthesis: new tools for the organic chemist. *Drug Discov. Today* **1999**, *4*, 265–274.

(2) (a) Flynn, D. L.; Devraj, R. V.; Naing, W.; Parlow, J. J.; Weidner, J. J.; Yang, S., Polymer-assisted solution phase (PASP) chemical library synthesis. *Med. Chem. Res.* **1998**, *8*, 219–243. (b) Parlow, J. J., Polymer-assisted solution-phase chemical library synthesis. *Curr. Opin. Drug Disc.* **2005**, *8*, 757–775.

(3) (a) Salimi, H.; Rahimi, A.; Pourjavadi A., Applications of Polymeric Reagents in Organic Synthesis. *Monatshefte fur Chemie* **2007**, *138*, 363–379. (b) Boldt, G. E.; Dickerson, T. J.; Janda, K. D., Emerging chemical and biological approaches for the preparation of discovery libraries. *Drug Discov. Today* **2006**, 11, 143–148. (c) Colombo M.; Peretto, I., Chemistry strategies in early drug discovery: an overview of recent trends. *Drug Discov. Today* **2008**, *13*, 677–684. (d) Kennedy, J. P.; Williams, L.; Bridges, T. M.; Daniels, R. N.; Weaver, D.; Lindsley, C. W., Application of Combinatorial Chemistry Science on Modern Drug Discovery. *J. Comb. Chem.* **2008**, *10*, 345–354.

(4) (a) Bhattacharyya, S., New developments in polymer-supported reagents, scavengers and catalysts for organic synthesis. *Curr. Opin. Drug Disc.* **2004**, *7*, 752–764. (b) Dolle, R. E.; Le Bourdonnec, B.; Goodman, A. J.; Morales, G. A.; Thomas, C. J.; Zhang, W., Comprehensive Survey of Chemical Libraries for Drug Discovery and Chemical Biology: 2008. *J. Comb. Chem.* **2009**, *11*, 739–790. (c) Rademann, J., Advanced polymer reagents based on activated reactants and reactive intermediates: powerful novel tools in diversity-oriented synthesis. *Method. Enzymol.* **2003**, *369* (Combinatorial Chemistry, Part B), 366–390. (d) Ley, S. V.; Baxendale, I. R.; Bream, R. N.; Jackson, P. S.; Leach, A. G.; Longbottom, D. A.; Nesi, M.; Scott, J. S.; Storer, R. I.; Taylor, S. J., Multi-step organic synthesis using solid-supported reagents and scavengers: a new paradigm in chemical library generation. *J. Chem. Soc. Perk. T. 1.* **2000**, *23*, 3815–4195.

(5) (a) Sinfelt, J. H.; Yates, D. J. C., Studies of ethane hydrogenolysis over Group VIII metals: supported osmium and iron. *J. Catal.* **1968**, *10*, 362–367. (b) Lee, B. S.; Mahajan, S.; Janda, K. D., Asymmetric dihydroxylation catalyzed by ionic polymer-supported osmium tetroxide. *Tetrahedron Lett.* **2005**, *46*, 4491–4493.

(6) Li, K.; Tunge, J. A., Chemical Libraries via Sequential C-H Functionalization of Phenols. *J. Comb. Chem.* **2008**, *10*, 170–174.

(7) (a) Merrifield, R. B., Solid phase peptide synthesis. I. The synthesis of a tetrapeptide. *J. Am. Chem. Soc.* **1963**, *85*, 2149–2154. (b) Merrifield, R. B., Solid phase peptide synthesis. II. Synthesis of bradykinin. *J. Am. Chem. Soc.* **1964**, *86*, 304–305.

(8) (a) Mutulis, F.; Tysk, M.; Mutule, I.; Wikberg, J. E. S., A Simple and Effective Method for Producing Nonrandom Peptide Libraries Using Cotton as a Carrier in Continuous Flow Peptide Synthesizers. *J. Comb. Chem.* **2003**, *5*, 1–7. (b) Baxendale, I. R.; Ley, S. V.; Smith, C. D.; Tranmer, G. K., A flow reactor process for the synthesis of peptides utilizing immobilized reagents, scavengers and catch and release protocols. *Chem. Commun.* **2006**, *46*, 4835–4837. (c) France, S.; Bernstein, D.; Weatherwax, A.; Lectka, T., Performing the Synthesis of a Complex Molecule on Sequentially Linked Columns: Toward the Development of a "Synthesis Machine". *Org. Lett.* **2005**, *7*, 3009–3012.

(9) Winssinger, N.; Barluenga, S.; Dakas, P.-Y., High-throughput synthesis of natural products. In *Power of Functional Resins in Organic Synthesis*. Wiley-VCH Verlag GmbH&Co. KGaA, Weinheim, Germany, 2008; pp 613–640. Mentel, M.; Breinbauer, R., Combinatorial solid-phase natural product chemistry. *Top. Curr. Chem.* **2007**, *278* (Combinatorial Chemistry on Solid Supports), 209–241. Ganesan, A., Solid-phase synthesis in the twenty-first century. Mini-Reviews in Medicinal Chemistry **2006**, *6*, 3–10. Baxendale, I. R.; Ley, S. V. Synthesis of alkaloid natural products using solid -supported reagents and scavengers. *Curr. Org. Chem.* **2005**, *9*, 1521–1534. Nandy, J. P.; Prakesch, M.; Khadem, S.; Reddy, P. Thirupathi; S., U.; Arya, P. Advances in Solution- and Solid - Phase Synthesis toward the Generation of Natural Product-like Libraries. *Chem. Rev.* **2009**, *109*, 1999–2060.

(10) (a) Schultz, P. G.; Xiang, X.-D., Combinatorial approaches to materials science. *Curr. Opin. Solid St. M.* **1998**, *3*, 153–158. (b) Meier, M. A. R.; Schubert, U. S., Combinatorial polymer research and high-throughput experimentation: powerful tools for the discovery and evaluation of new materials. *J. Mater. Chem.* **2004**, *14*, 3289–3299. (c) Petro, M.; Nguyen, S. H.; Liu, M.; Kolosov, O., Combinatorial exploration of polymeric transport agents for targeted delivery of bioactives to human tissues. *Macromol. Rapid Comm.* **2004**, *25*, 178–188.

(11) (a) Keating, T. A.; Armstrong, R. W., Postcondensation Modifications of Ugi Four-Component Condensation Products: 1-Isocyanocyclohexene as a Convertible Isocyanide. Mechanism of Conversion, Synthesis of Diverse Structures, and Demonstration of Resin Capture. *J. Am. Chem. Soc.* **1996**, *118*, 2574–2583.

(12) (a) Boehlow, T. R.; Harburn, J. J.; Spilling, C. D., Approaches to the Synthesis of Some Tyrosine-Derived Marine Sponge Metabolites: Synthesis of Verongamine and Purealidin N. *J. Org. Chem.* **2001**, *66*, 3111–3118. (b) Lei, Z. Q.; Ma, H. C.; Zhang, Z.; Yang, Y. X., Synthesis and oxidation reactions of a polymer-supported IBX reagent. *React. Funct. Polym.* **2006**, *66*, 840–844.

(13) (a) Bhattacharyya, S.; Rana, S.; Gooding, O. W.; Labadie, J., Polymer-supported triacetoxyborohydride: a novel reagent of choice for reductive amination. *Tetrahedron Lett.* **2003**, *44*, 4957–4960. (b) Ley, S. V.; Taylor, S. J., A polymer-supported [1,3,2]oxazaphospholidine for the conversion of iso-thiocyanates to isocyanides and their subsequent use in an Ugi reaction. *Bioorg. Med. Chem. Lett.* **2002**, *12*, 1813–1816.

(14) (a) Biotage Home Page. http://www.biotage.com (accessed April 14, 2010). (b) Booth, R. J.; Hodge, J. C., Polymer-Supported Quenching Reagents for Parallel Purification. *J. Am. Chem. Soc.* **1997**, *119*, 4882–4886.

(15) (a) Moore, J. D.; Byrne, R. J.; Vedantham, P.; Flynn, D. L.; Hanson, P. R., High-Load, ROMP-Generated Oligomeric Bis-acid Chlorides: Design of Soluble and Insoluble Nucleophile Scavengers. *Org. Lett.* **2003**, *5*, 4241–4244.

(16) Pop, Iuliana E.; Deprez, Benoit P.; Tartar, Andre L., Versatile Acylation of N-Nucleophiles Using a New Polymer-Supported 1-Hydroxybenzotriazole Derivative. *J. Org. Chem.* **1997**, *62*, 2594–2603.

(17) (a) Flynn, D. L.; Crich, J. Z.; Devraj, R. V.; Hockerman, S. L.; Parlow, J. J.; South, M. S.; Woodard, S. S., Chemical Library Purification Strategies Based on Principles of Complementary Molecular Reactivity and Molecular Recognition. *J. Am. Chem. Soc.* **1997**, *119*, 4874–4881. (b) Gayo, L. M.; Suto, M., Ion-exchange resins for solution phase parallel synthesis of chemical libraries. *Tetrahedron Lett.* **1997**, *38*, 513–516.

(18) (a) Paquette, L. A., *Encyclopedia of Reagents for Organic Synthesis;* John Wiley and Sons, 1995, Vol. 6, p 4110. (b) Schwesinger, R.; Willaredt, J.; Schlemper, H.; Keller, M.; Scmitt, D.; Fritz, H., Novel, very strong, uncharged auxiliary bases; design and synthesis of monomeric and polymer-bound triaminoiminophosphorane bases of broadly varied steric demand. *Chem. Ber.* **1994**, *127*, 2435–2454.

(19) Prakash, G. K. S.; Weber, C.; Chacko, S.; Olah, G. A., New Solid-Phase Bound Electrophilic Difluoromethylating Reagent. *J. Comb. Chem.* **2007**, *9*, 920–923.

(20) Fairfull-Smith (née Elson), K. E.; Jenkins, I. D.; Loughlin, W. A., Novel polymer-supported coupling/dehydrating reagents for use in organic synthesis. *Org. Biomol. Chem.,* **2004**, *2*, 1979–1986.

(21) See Chapter 4 for references on metal-based nanoparticles.

(22) (a) Akelah, A., Use of functionalized silica in catalysis and organic synthesis. British Polymer Journal **1981**, *13*, 107–110. (b) Mayr, M.; Buchmeiser, M. R.; Wurst, K., Synthesis of a silica-based heterogeneous second generation Grubbs catalyst. *Adv. Synth. Catal.* **2002**, *344*, 712–719.

(23) De Luca, L.; Giacomelli, G.; Porcheddu, A.; Salaris, M.; Taddei, M., Cellulose Beads: a New Versatile Solid Support for Microwave-Assisted Synthesis. Preparation of Pyrazole and Isoxazole Libraries. *J. Comb. Chem.* **2003**, *5*, 465–471.

(24) Heravi, M. M.; Hydarzadeh, F.; Farhangi, Y.; Ghassemzadeh, M., Zeolite - supported chromium(VI) oxide. A mild, efficient, and inexpensive reagent for oxidative deprotection of trimethylsilyl ethers under microwave irradiation. *Phosphorus Sulfur* **2004**, *179*, 1473–1475.

(25) Garg, Dipti; Ahn, J.-H.; Chauhan, Ghanshyam S., Proline-based polymeric monoliths : Synthesis , characterization, and applications as organocatalysts in aldol reaction. *J. Polym. Sci. A1* **2010**, *48*, 1007–1015.

(26) Storer, R. I.; Takemoto, T.; Jackson, P. S.; Brown, D. S.; Baxendale, I. R.; Ley, S. V., Multi-step application of immobilized reagents and scavengers: A total synthesis of epothilone C. *Chem-Eur. J.* **2004**, *10*, 2529–2547.

(27) Parlow, J. J.; Burney, M. W.; Case, B. L.; Girard, T. J.; Hall, K. A.; Harris, P. K.; Hiebsch, R. R.; Huff, R. M.; Lachance, R. M.; Mischke, D. A.; Rapp, S. R.; Woerndle, R. S.; Ennis, M. D. Piperazinyl glutamate pyridines as potent orally bioavailable P2Y12 antagonists for inhibition of platelet aggregation. *J. Med. Chem.* **2010**, *53*, 2010–2037.

(28) Parlow, J. J., Simultaneous multistep synthesis using polymeric reagents. *Tetrahedron Lett.,* **1995**, *36*, 1395–1396.

(29) Novabiochem Catalogue, **2002**, p 359.

(30) Ahmadibeni, Y.; Parang, K., Solid-Phase Reagents for Selective Mono-Phosphorylation of Carbohydrates and Nucleosides. *J. Org. Chem.* **2005**, *70*, 1100–1103.

(31) Encinas, L.; Chiara, J. L., Polymer-Assisted Solution-Phase Synthesis of Glycosyl Chlorides and Bromides Using a Supported Dialkylformamide as Catalyst. *J. Comb. Chem.* **2008**, *10*, 361–363.

(32) (a) Huisgen, R.; Knorr, R.; Moebius, L.; Szeimies, G., 1,3-Dipolar cycloadditions. XXIII. Addition of organic azides to C--C triple bonds. *Chem. Ber.* **1965**, *98*, 4014–4021. (b) Huisgen, R.; Szeimies, G.; Moebius, L., 1,3-Dipolar cycloadditions. XXXII. *Chem. Ber.* **1967**, *100*, 2494–2507.

(33) Kolb, H. C.; Finn, M. G.; Sharpless, K. B., Click chemistry: diverse chemical function from a few good reactions. *Angew. Chem. Int. Ed.* **2001**, *40*, 2004–2021.

(34) (a) Buchel, K. H.; Draber, W.; Regel, E.; Plempel, M., Synthesis and properties of clotrimazole and other antimycotic 1-triphenylmethylimidazoles. *Arzneim-Forsch.* **1972**, *22*, 1260–1272. (b) Heeres, J.; Backx, L. J. J.; Mostmans, J. H.; Van Cutsem, J., Antimycotic imidazoles. Part 4. Synthesis and antifungal activity of ketoconazole, a new potent orally active broad-spectrum antifungal agent. *J. Med. Chem.* **1979**, *22*, 1003–1005. (c) Koltin, Y., Targets for antifungal drug discovery. *Annu. Rep. Med. Chem.* **1990**, *25* 141–148. (d) Park, J. S.; Yu, K. A.; Kang, T. H.; Kim, S.; Suh, Y.-G., Discovery of novel indazole-linked triazoles as antifungal agents. *Bioorg. Med. Chem. Lett.* **2007**, *17*, 3486–3490.

(35) Girard, C.; Oenen, E.; Aufort, M.; Beauviere, S.; Samson, E.; Herscovici, J., Reusable Polymer-Supported Catalyst for the [3+2] Huisgen Cycloaddition in Automation Protocols. *Org. Lett.* **2006**, *8*, 1689–1692.

(36) Chemspeed Technologies Home Page. http://www.chemspeed.com/ (accessed April, 10, 2010).

(37) Kelly, A. R.; Wei, J.; Kesavan, S.; Marie, J.-C.; Windmon, N.; Young, D. W.; Marcaurelle, L. A. Accessing Skeletal Diversity Using Catalyst Control: Formation of n and n + 1 Macrocyclic Triazole Rings. *Org. Lett.* **2009**, *11*, 2257–2260.

(38) Toy, P. H.; Reger, T. S.; Janda, K. D., Tailoring polystyrene solid-phase synthesis resins: incorporation of flexible cross-linkers. *Aldrichim. Acta* **2000**, *33*, 87–93.

(39) Dickerson, T. J.; Reed, N. N.; Janda, K. D., Soluble polymers as catalyst and reagent platforms: liquid-phase methodologies. In *Polymeric Materials in Organic Synthesis and Catalysis,* Wiley-VCH Verlag GmbH&Co. KGaA, Weinheim, Germany 2003, pp 241–276.

(40) (a) Ahn, J.-M.; Wentworth, P., Jr.; Janda, K. D., Soluble polymer-supported convergent parallel library synthesis. *Chem. Commun.* **2003**, *4*, 480–481. (b) Moss, J. A.; Dickerson, T. J.; Janda, K. D., Solid phase peptide synthesis on JandaJel™ resin. *Tetrahedron Lett.* **2001**, Vol. Date **2002**, *43*, 37–40.

(41) (a) Barrett, A. G. M.; Cramp, S. M.; Roberts, R. S., ROMP-Spheres: A Novel High-Loading Polymer Support Using Cross Metathesis between Vinyl Polystyrene and Norbornene Derivatives. *Org. Lett.* **1999**, *1*, 1083–1086. (b) Barrett, A. G. M.; Hopkins, B. T.; Koebberling, J., ROMPgel Reagents in Parallel Synthesis. *Chem. Rev.* **2002**, *102*, 3301–3323.

(42) (a) Rolfe, A.; Probst, D.; Volp, K.; Omar, I.; Flynn, D.; Hanson, P. R., High-load, Oligomeric dichlorotriazine (ODCT): A Versatile ROMP-derived Reagent and Scavenger. *J. Org. Chem.* **2008**, *73*, 8785–8790. (b) Stoianova, D. S.; Yao, L.; Rolfe, A.; Samarakoon, T.; Hanson, P. R. High-load, Oligomeric Monoamine Hydrochloride: Facile Generation via ROM Polymerization and Application as an Electrophile Scavenger. *Tetrahedron Lett.* **2008**, *49*, 4553–4555.

(43) Clapham, B.; Wilson, N. S.; Michmerhuizen, M. J.; Blanchard, D. P.; Dingle, D. M.; Nemcek, T. A.; Pan, J. Y.; Sauer, D. R., Construction and Validation of an Automated Flow Hydrogenation Instrument for Application in High-Throughput Organic Chemistry. *J. Comb. Chem.* **2008**, *10*, 88–93.

(44) (a) Fenster, E.; Rayabarapu, D. K.; Zhang, M.; Mukherjee, S.; Hill, D.; Neuenswander, B.; Schoenen, F.; Hanson, P. R.; Aube, J., Three-component synthesis of 1,4-diazepin-5-ones and the construction of γ -turn-like peptidomimetic libraries. *J. Comb. Chem.* **2008**, *10*, 230–234. (b) Griffiths-Jones, C. M.; Hopkin, M. D.; Joensson, D.; Ley, S. V.; Tapolczay, D. J.; Vickerstaffe, E.; Ladlow, M., Fully Automated Flow-Through Synthesis of Secondary Sulfonamides in a Binary Reactor System. *J. Comb. Chem.* **2007**, *9*, 422–430.

(45) (a) Hopkin, M. D.; Baxendale, I. R.; Ley, S. V., A flow-based synthesis of Imatinib: the API of Gleevec. *Chem. Commun.* **2010**, *46*, 2450–2452. (b) Baxendale, I. R.; Ley, S. V.; Smith, C. D.; Tamborini, L.; Voica, A.-F., A Bifurcated Pathway to Thiazoles and Imidazoles Using a Modular Flow Microreactor. *J. Comb. Chem.* **2008**, *10*, 851–857.

(46) Fletcher, P. D. I.; Haswell, S. J.; Pombo-Villar, E.; Warrington, B. H.; Watts, P.; Wong, S. Y. F.; Zhang, X., Micro reactors: principles and applications in organic synthesis. *Tetrahedron* **2002**, *58*, 4735–4757.

(47) Baxendale, I. R.; Deeley, J.; Griffiths-Jones, C. M.; Ley, S. V.; Saaby, S.; Tranmer, G. K., A flow process for the multi-step synthesis of the alkaloid natural product oxomaritidine: a new paradigm for molecular assembly. *Chem. Commun.* **2006**, 2566–2568.

(48) Ley, S. V.; Schucht, O.; Thomas, A. W.; Murray, P. J., Synthesis of the alkaloids (±)-oxomaritidine and (±)-epimaritidine using an orchestrated multi-step sequence of polymer supported reagents. *J. Chem. Soc. Perk. T. 1.* **1999**, 1251–1252.

(49) Storer, R. I.; Takemoto, T.; Jackson, P. S.; Brown, D. S.; Baxendale, I. R.; Ley, S. V., Multi-step application of immobilized reagents and scavengers: A total synthesis of epothilone C. *Chem-Eur. J.* **2004**, *10*, 2529–2547.

(50) Syrris Home Page. http://www.syrris.com/ (accessed April 10, 2010).

(51) ThalesNano Home Page. http://www.thalesnano.com/ (accessed April 10, 2010).

(52) Soluble, high-loading ROMP-derived primary amine scavengers have also been reported recently: Stoianova, D. S.; Yao, L.; Rolfe, A.; Samarakoon, T.; Hanson, P. R., High-load, oligomeric monoamine hydrochloride: facile generation via ROM polymerization and application as an electrophile scavenger. *Tetrahedron Lett*. **2008**, *49*, 4553–4555.

(53) Baxendale, I. R.; Griffiths-Jones, C. M.; Ley, S. V.; Tranmer, G. K., Preparation of the neolignan natural product grossamide by a continuous-flow process. *Synlett* **2006**, 427–430.

(54) Baxendale, I. R.; Ley, S. V.; Ernst, M.; Krahnert, W.-R., Application of polymer-supported enzymes and reagents in the synthesis of gamma-aminobutyric acid (GABA) analogues. *Synlett* **2002**, 1641–1644.

(55) Eustáquio, A. S.; O'Hagan, D.; Moore, B. S., Engineering Fluormetabolite Production: Fluorinase Expression in *Salinispora tropica* Yields Fluorosalinosporamide. *J. Nat. Prod*. **2010**, *73*, 378–382.

(56) (a) Wittmann, S.; Schaetz, A.; Grass, R. N.; Stark, W. J.; Reiser, O., A Recyclable Nanoparticle-Supported Palladium Catalyst for the Hydroxycarbonylation of Aryl Halides in Water. *Angew. Chem. Int. Ed*. **2010**, *49*, 1867–1870. (b) Schaetz, A.; Grass, R. N.; Kainz, Q.; Stark, W. J.; Reiser, O., Cu(II)-Azabis(oxazoline) Complexes Immobilized on Magnetic Co/C Nanoparticles: Kinetic Resolution of 1,2-Diphenylethane-1,2-diol under Batch and Continuous-Flow Conditions. *Chem. Mater*. **2010**, *22*, 305–310.

(57) Ceylan, S.; Friese, C.; Lammel, C.; Mazac, K.; Kirschning, A., Inductive heating for organic synthesis by using functionalized magnetic nanoparticles inside microreactors. *Angew. Chem. Int. Ed*. **2008**, *47*, 8950–8953.

(58) (a) Frechet, J. M. J.; Svec, F., New designs of macroporous polymers as supports for separation media, solid-phase reactions, and catalysis. *Polymeric Materials Science and Engineering* **1995**, *73*, 451.

(59) (a) Nguyen, A. M.; Dinh, N. P.; Cam, Q. M.; Sparrman, T.; Irgum, K. Preparation and characterization of sizable macroporous epoxy resin-based monolithic supports for flow-through systems. *J. Sep. Sci.* **2009**, *32*, 2608–2618. (b) Jones, R. C.; Canty, A. J.; Deverell, J. A.; Gardiner, M. G.; Guijt, R. M.; Rodemann, T.; Smith, J. A.; Tolhurst, V.-A., Supported palladium catalysis using a heteroleptic 2-methylthiomethylpyridine-N,S-donor motif for Mizoroki-Heck and Suzuki-Miyaura coupling, including continuous organic monolith in capillary microscale flow-through mode. *Tetrahedron* **2009**, *65*, 7474–7481.

(60) (a) Hansen, L. C.; Sievers, R. E., Highly permeable open pore polyurethane columns for liquid chromatography. *J. Chromatogr.* **1974**, *99*, 123–33. (b) Hjerten, S.; Liao, J. L.; Zhang, R., High-performance liquid chromatography on continuous polymer beds. *J. Chromatogr.* **1989**, *473*, 273–275.

(61) Lu, J.; Toy, P. H., Organic Polymer Supports for Synthesis and for Reagent and Catalyst Immobilization. *Chem. Rev.* **2009**, *109*, 815–838.

(62) Koppitz, M.; Eis, K., Automated medicinal chemistry. *Drug Discov. Today* **2006**, *11*, 561–568.

(63) Meier, M. A. R.; Hoogenboom, R.; Schubert, U. S., Combinatorial methods, automated synthesis and high-throughput screening in polymer research: The evolution continues. *Macromol. Rapid Comm.* **2004**, *25*, 21–33.

(64) For reviews in microwave synthesis see: (a) Kappe, C. O.; Dallinger, D., Controlled microwave heating in modern organic synthesis : highlights from the 2004–2008 literature. *Mol. Divers.* **2009**, *13*, 71–193. (b) Matloobi, M.; Kappe, C. O., Microwave synthesis in high-throughput environments. *Chim. Oggi* **2007**, *25*, 26–27, 30–31. (c) Kappe C. O.; Dallinger D., The impact of microwave synthesis on drug discovery. *Nature Rev. Drug Discov.* **2006**, *5*, 51–63. (d) Hayes, B. L., Recent advances in microwave-assisted synthesis. *Aldrichim. Acta* **2004**, *37*, 66–77. (e) Collins, M. J., Jr. Future trends in microwave synthesis. *Future Medicinal Chemistry* **2010**, *2*, 151–155.

(65) Anton-Paar Home Page. http://www.anton-paar.com/US/en/1 (accessed April 7, 2010)

(66) (a) Wang, Y.; Miller, R. L; Sauer, D. R; Djuric, S. W., Rapid and efficient synthesis of 1,2,4-oxadiazoles utilizing polymer-supported reagents under microwave heating. *Org. Lett.* **2005**, *7*, 925–928. (b) Wang, Y.; Sauer, D. R.; Djuric, S. W. A simple and efficient one step synthesis of 1,3,4-oxadiazoles utilizing polymer-supported reagents and microwave heating. *Tetrahedron Lett.* **2005**, Vol. Date **2006**, *47*, 105–108.

(67) Wang, Y.; Sauer D. R., Use of polymer-supported Pd reagents for rapid and efficient Suzuki reactions using microwave heating. *Org. Lett.* **2004**, *6*, 2793–2796.

(68) Mettler Toledo Home Page: http://us.mt.com/us/en/home.html (accessed April 11, 2010).

(69) Permission to use this photo was granted by Daryl R. Sauer at Abbott Laboratories, Abbott Park, IL. April 4, 2010.

Chapter 2

A Multifaceted ROMP-derived Oligomeric Phosphate
and Its Use in PASP-Facilitated Protocols

2.1 Introduction

Throughout nature, phosphates have been uniquely designed to play vital roles in the existence of all living things. The essence of these unique and irreplaceable structures comprise the biomolecular constructs of ADP, ATP, creatine phosphate, phospholipid bilayers, and more importantly proteins and genetic material (RNA/DNA). The intracellular addition of phosphates (ie. phosphorylation) is regulated by numerous protein kinase enzymes which are triggered by extracellular stimuli. The process of phosphorylation is necessary for a wide array of cellular functions including signal transduction, cell division, membrane transport, and apoptosis (cell death) just to name a few. In contrast, dephosphorylation, is the action of phosphate removal via hydrolysis and is controlled by various protein phosphatase enzymes. Without ultimate control of these two independant processes, life as we know it would cease to exist.

Within the last two decades, organophosphates have emerged as important reagents that have found regular employment in synthetic protocols. Many of these protocols reside within the area of natural product synthesis,[1] but also play important roles in the pharmaceutical[2] and agrochemical industries.[3] This newly selected use of phosphates in synthesis is primarily due to their hydrolytic stability, facile assembly, and ideal monoanionic pKa profiles thereby placing them within the circle of other commonly employed leaving groups.

A seminal paper in 1987 by F.H. Westheimer entitled, "*Why Nature Chose Phosphates",* concludes that organic chemists cannot afford to use compounds as

stable as phosphate anions due their lack of reactivity. Furthermore, Westheimer also notes that likewise nature cannot afford to utilize alkyl halides, as their reactivity is directly related to their toxicity.[4] Synthetic organic chemists, however, have presented their case that phosphates can provide more stable, leaving group-armed intermediates that are more easily separable from valued material.[5] This chapter will focus on the development and utilization of a multi-faceted, ROMP-derived oligomeric phosphate and its utility as a chemical tag, a sequestration reagent, and a supported leaving group in both S_N2 and S_N2' processes.

2.1.1 Background and Significance

Synthetic oligomeric phosphates and other phosphorous-laden materials have primarily found applications in the production of flame-retardant materials,[6] but have also found themselves useful as immobilized reagents within the realms of both pharmaceutical[7] and medicinal chemistry.[8] Hawthorne and coworkers[9] highlight one such application in the assembly of boron-rich oligophosphates (Figure 2.1) for use in boron-neutron capture therapy (BNCT).

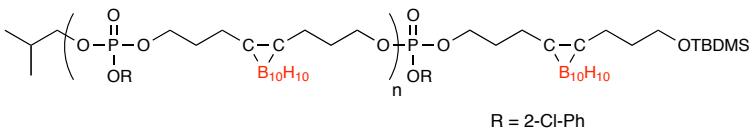

Figure 2.1 *Boron-rich oligophosphate*

This chemotherapeutic treatment relies on the ability to deliver large quantities of ^{10}B atoms directly to the site of the tumor where emission of α-particles takes place. The solubility and biocompatability of these delivery units is of high-importance and thus

substantiates the incorporation of the oligophosphate backbone. Once the process is complete, the oligomers are easily metabolized and excreted from the body. Others have also utilized phosphorous-based oligomers in hybrid, solid-phase supports for the synthesis of multiple labelled-carbohydrate oligonucleotides (Figure 2.2).[10] These nucleotide-bearing complexes are currently being studied for their potential use in various biomedical, therapeutic, and diagnostic applications.

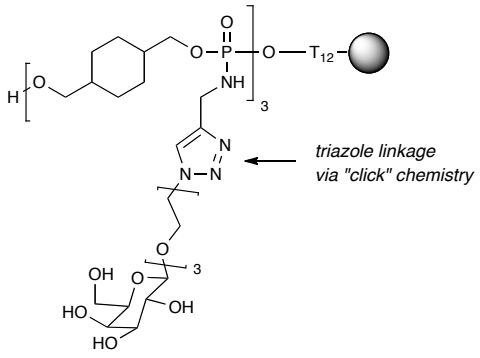

Figure 2.2 *Carbohydrate oligonucleotides on hybrid solid-phase support*

As previously discussed, solid-phase synthesis and immobilized reagents have played an integral role in combinatorial chemistry and the search for biologically relevant molecules. However, despite huge advances in this area, limitations are widely noted throughout the literature.[11] Many resin-bound reagents/scavengers inheriently carry low load capacities (typically <1 mmol/g) due to the overall molecular weight of the primary support, thus requiring the use of a gross excess of bound reagent/scavenger. Solid supports and linkers used in SPOS can be expensive to purchase on large-scale and can limit the possible chemistry that can be achieved. This is especially true when larger quantities of final product is desired. Non-ideal,

heterogeneous reaction kinetics also hinder many of these reactions and result in elongated validation times during the transfer of chemistry from solution.

Over the years, a number of alternative technologies have been developed as a result of the aforementioned limitations of solid-phase systems. Curran and coworkers have developed a unique strategy known as "fluorous synthesis" that is based upon the chemical tagging of small-molecules with fluorine atoms in a homogeneous environment.[12] This concept, first introduced by Horváth and Rabái in 1994,[13] uses F-tagged molecules (substrates/reagents/catalysts) that can be differentiated through the use of fluorophilic and fluorophobic solvents or materials allowing for their facile separation/purification. Curran and coworkers recently demonstrated the power of this technology for library development of a diverse collection of piperazinediones (Figure 2.3). Using this approach, over 600 diverse analogs were efficiently prepared from a single fluorous-tagged scaffold.

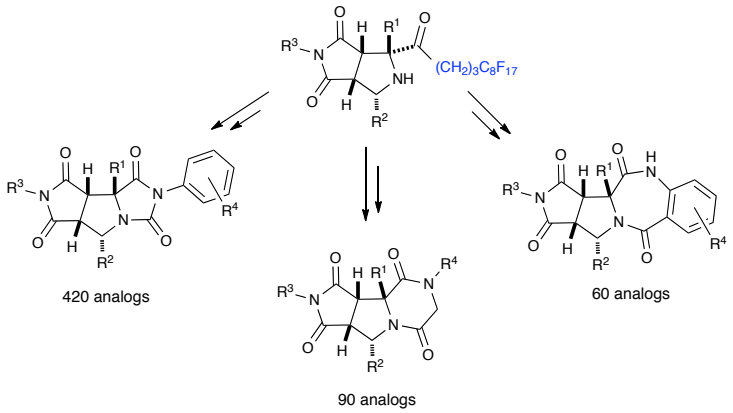

Figure 2.3 *Collection of piperazindiones via fluorous-tagging*

Another powerful technology that has surfaced as an alternative to solid-phase chemistries is ring-opening metathesis polymerization (ROMP) of functionalized

norbornenes.[14] The advantages of this polymer-assisted technology can clearly be seen in a number of different attributes: (i) starting materials containing a norbornene functionality can easily be prepared and scaled-up via Diels-Alder reaction with either cyclopentadiene or furan and a suitable dienophile. (ii) all reaction components are contained within a homogenous reaction environment thereby incorporating the advantages of solution-phase reaction kinetics (iii) ROMP is a user-friendly technique that does not require the use of special equipment or materials. These attributes directly translate into chemistry derived from proven solution phase conditions which can be easily translated into the world of facilitated synthesis.

ROM-polymerization is now a well-defined and well-understood system (Scheme 2.1) whereby reactions take place under mild conditions without the need for cocatalysts, additives, or high-temperatures. This achievement was made possible through early work by Yves Chauvin[15] in the fields of organometallics and catalysis and later by both Richard R. Schrock[16] and Robert S. Grubbs.[17] These Nobel-prize worthy efforts have resulted in the advancement and preparation of numerous, well-defined metal carbene catalysts (Figure 2.4). It is with the development and use of these unique complexes that now defines olefin metathesis in synthetic chemistry today. For the remainder of this dissertation, Grubbs' catalysts **2.3**, **2.4,** and **2.6** will be refered to as **1G**, **2G** and **3G**.

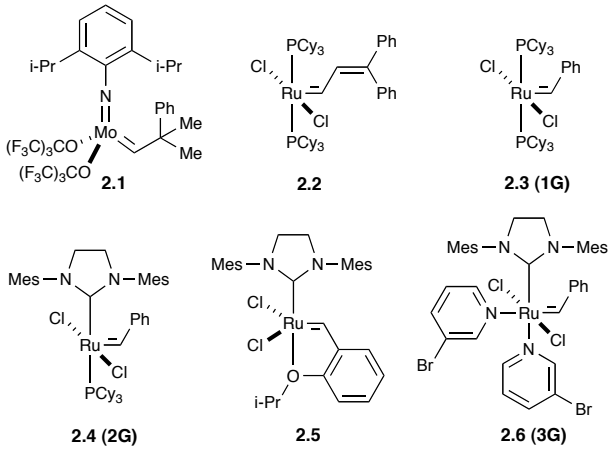

Figure 2.4 *Mo and Ru-based metathesis catalysts*

The inherent ring strain of various systems[18] including norbornene, is the key component for achieving ROM-polymerization. The first step in this process involves the dissociation of a phosphine ligand from the precatalyst **2.7**. The resulting 14-electron complex **2.8** subsequently adds across the strained olefin of the norbornene to form metallocyclobutane intermediate **2.9**. This intermediate was first postulated by Chauvin in 1971[19] and later proven by isolation of a similar titanium-based Tebbe intermediate by Grubbs and coworkers in 1980.[20] This newly formed strained intermediate is relieved via the ring-opening event to form the terminal "activated" carbene species **2.11**. This intermediate then undergoes propagation with additional monomeric units until **2.9** is completely consumed. This continual process then affords living oligomer **2.12** that is still activated with the metal carbene. This carbene containing oligomer is then terminated with the addition of ethyl vinyl ether to yield the final oligomeric product **2.14** and allowing Fisher carbene-type complex **2.13** to easily be discarded. This well-defined system results in similar initiation (k_i) and propagation rates (k_p) allowing for greater control over molecular weight

distribution as compared to previous processes of this type.[21] This is readily achieved by changing the amount of precatalyst **2.7** being used in the reaction whereby oligomeric length n = 100/mol % catalyst.

Scheme 2.1 *Mechanism of ROM-polymerization of norbornene-based systems*

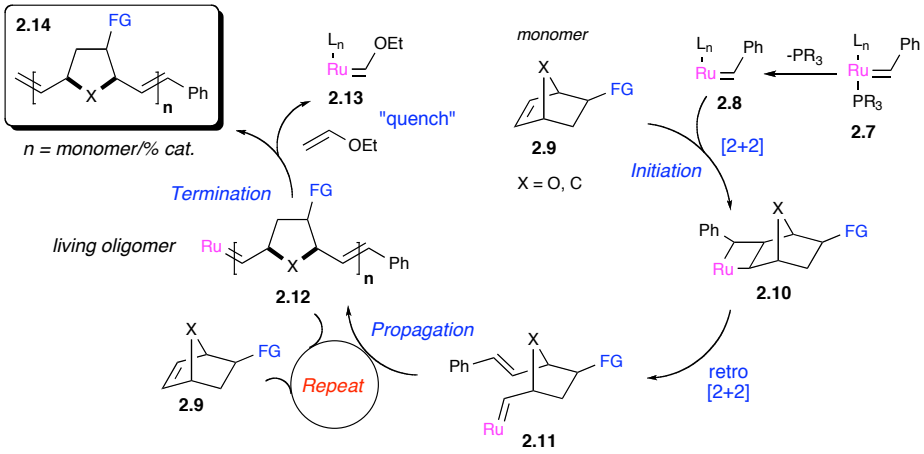

2.1.2 Capture/ROMP/Release Strategies

A large portion of our work in the area of ROMP has focused on the development of high-loading oligomeric reagents and scavengers.[22,23] Alongside these methods, however, comes the ability to attach small-molecules to a norbornene tag for the purpose of solution-phase trafficking.[24] During this event (Figure 2.5), the molecule of interest **2.15** (ie. precious scaffold) is tagged or "captured" via norbornene linker (NB-tagged **2.16**) and then subjected to ROM-polymerization enabling the soluble, bound scaffold **2.17** to be operated on synthetically via facilitated methods. These methods allow for the "captured" scaffold to be subjected to facile diversification reactions to afford tagged **2.18** under homogeneous conditions and then subsequently released yielding the newly diversified scaffold **2.19** and the spent oligomer.

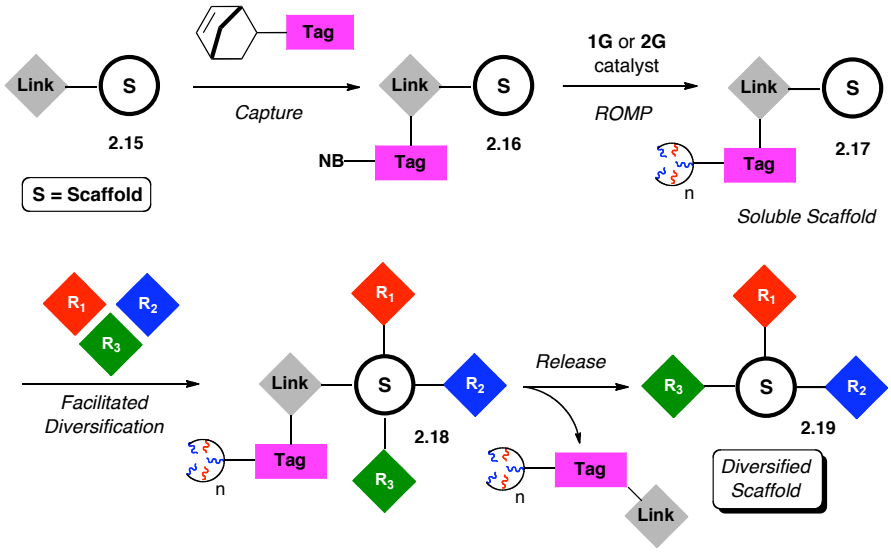

Figure 2.5 *Phase trafficking via ROMP*

These bimolecular systems are conveniently soluble in organic solvents such as CH_2Cl_2, $CHCl_3$, DMF, THF, and correspondingly insoluble in polar solvents such as MeOH, EtOH, EtOAc, and Et_2O. This differential solubility profile allows for a facile precipitation/filtration event allowing all other reagents to be washed away from the final product typically without the need for additional purification. One such example published within our group (Scheme 2.2) demonstrated the ability to utilize a Mitsunobu capturing event of various 1° and 2° alcohols onto a *N*-hydroxy-succinamide-derived norbornene tag **2.20**. ROM-polymerization affords **2.21** and subsequent release via hydrazine removes the Mitsunobu byproducts rendering the newly formed amines **2.22** in moderate to excellent yields without the need for chromatography.

Scheme 2.2 *Capture-ROMP-release: application to the synthesis of amines*

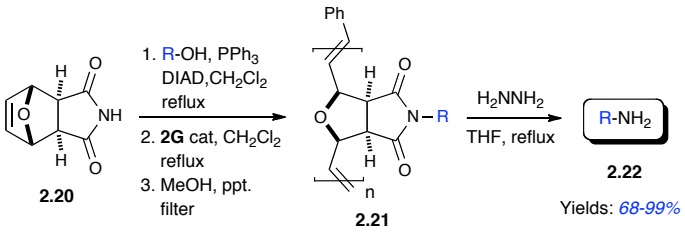

2.2 Results and Discussion (I)

Subsequent work in metathesis-based transformations on bicyclic phosphate tri-esters led to the development of a phosphate-based tag (Scheme 2.3) for its utility in ROMP-derived phase-trafficking. During the initial stages of development, it was determined that the *endo* isomer of the phosphate-based system was not readily polymerized by either catalyst **1G** or **2G** and focus turned to the synthesis of the corresponding *exo* isomer. It was hypothesized that both steric and electronic interactions of the P=O bond (Figure 2.6) of the resulting *endo* isomer could interfere with catalyst/olefin activation or subsequent propagation step.

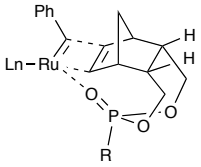

Figure 2.6 *Proposed endo P=O bond interactions w/ catalysts **1G** and **2G***

Synthesis of the *exo* isomer was readily achieved, however, on a large scale via thermal isomerization of *endo* carbic anhydride **2.23** using classical methods[25] to yield the exo product **2.24** with diastereomeric ratios ranging from 20:1 up to 84:1. Reduction of **2.24** with $LiAlH_4$ yielded diol **2.25** as a clear, viscous oil.

Phosphorylation of *exo* diol **2.25** was performed using freshly distilled $POCl_3$ and Et_3N in the presence of catalytic DMAP and/or *N*-methylimidazole (NMI) to yield phosphorochloridate **2.26** as a white solid in moderate yields.

Scheme 2.3 *Synthesis of the norbornenyl phosphorochloridate tag*

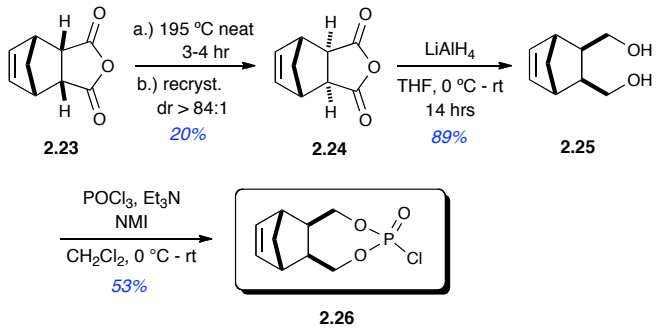

2.23 **2.24** **2.25** **2.26**

Initial interest in the utilization of **2.26** was derived from the idea of coupling this tag with allyl alcohol, thus setting the stage for a possible capturing event via selective cross-metathesis reaction in the presence of the internal norbornene. A number of experiments were performed using catalysts **1G**, **2G**, **3G** and Hoveyda-Grubbs 2nd generation catalyst **2.5** but all resulted in the subsequent polymerization of the norbornene affording only insoluble oligomeric gels. As a result, focus turned towards the installation of allyl alcohol into oligomeric phenyl phosphate ester **2.27**. This addition was not very reproducible due to various insolubilities at low temperatures and difficulty in the purification of oligomeric allylic phosphate ester **2.28**. From these results, the addition of 3-methyl 2-butene 1-ol into **2.26** was attempted, but it easily became apparent that compound **2.29** was unstable and could not be isolated.

Scheme 2.4 *Synthesis of the oligomeric allylic phosphate ester*

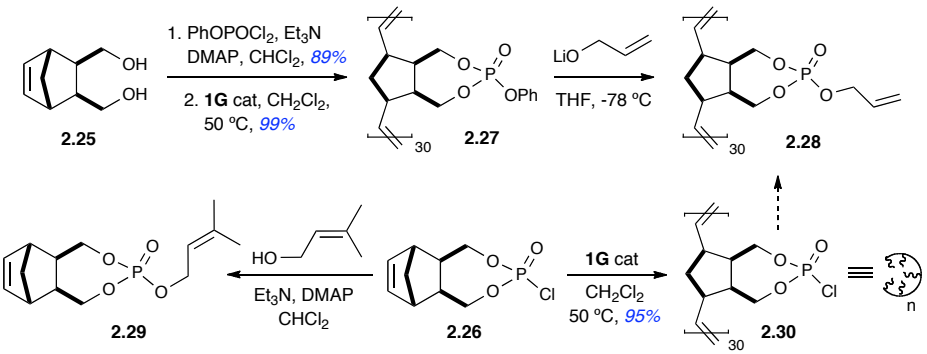

The possibility of polymerizing **2.26** was also explored as previous examples have highlighted the fidelity of the Grubbs catalysts in the presence of highly reactive functional groups including phosphonyl dichlorides.[26] Polymerization in the presence of catalyst **1G** afforded oligomeric product **2.30** in excellent yield, however solubility and purification issues continued to plague the synthesis of **2.28** resulting its overall abandonment.

Interest in the development of supported allylic phosphate esters resided with known literature precedence *vide supra* of the extensive use of this functionality in highly selective copper-mediated S_N2' displacements. In this manner, we planned a preemptive "release" mechanism by which an element of diversity (ie. carbon nucleophile) could be incorporated into the scaffold within the same step. In separate reports by Tanaka[27] and Yamamoto[28], each touted the superiority of allylic phosphates as leaving groups in comparison to their chloride and sulfonate counterparts in terms of regioselectivity, preferential *anti*-addition relative to the phosphate, geometry of the olefin formed, and high levels of chirality transfer. These highly selective S_N2', γ-

regioselective displacement reactions occur through use of both mixed zinc-copper and magnesium-copper-based reagents.[29] The use of CuCN is typical for S_N2' displacements demonstrating high preference for addition at the γ-position of the electrophilic species. This reagent is used in the presence of dialkyl zincates to form the active nucleophilic cuprate. Due to the high specificity and nature of the Cu/Zn complex, this reagent was herein chosen for this investigation.

Figure 2.7 highlights a general mechanism postulated by Corey for the reaction of Cu(I) reagents with allylic phosphate esters. He attributes this highly selective transformation to the occupied d-orbitals of copper having overlapped with both the π^* and σ^* orbitals of the allylic ester shown as **2.31**.[30] Experimental evidence for a Cu(III) intermediate has also been reported in which addition of the copper reagent first occurs at the γ-position (**2.33a**).[31] Cu(III) complex **2.33a** can subsequently undergo either reductive elimination to form the γ-coupled **2.34**, or can shift to π-allyl intermediate **2.33b**. This species is in equilibrium with the α-complex (**2.33c**), which can undergo reductive elimination to afford the α-coupled product **2.35**.

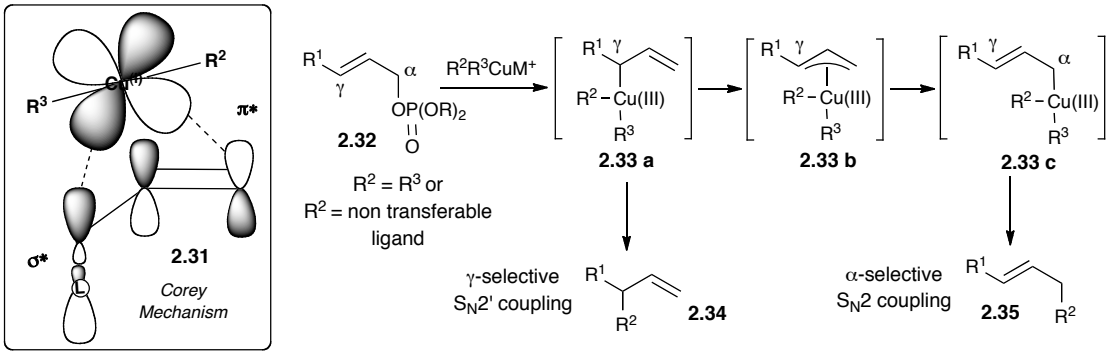

Figure 2.7 *Mechanisms for copper-mediated displacement of allylic phosphate esters*

After several failed attempts to generate a supported allylic phosphate ester, we began to explore a number of scaffolds which contained an internal allylic alcohol functionality that could be subsequently coupled to the norbornenyl monochloro-phosphate tag **2.26**. A model system was first developed to test the fidelity of the oligomeric phosphate tag under the harsh conditions of the S_N2' cuprate addition. A *cis/trans* mixture of cinnamyl alcohol was combined with **2.26** yielding a diastereomeric cinnamyl phosphate **2.36** which was polymerized affording oligomer **2.37**. This was then subjected to Et_2CuZn (generated *in situ*) rendering the release of racemic **2.38**. Isolation of the product proved difficult due to its low molecular weight, but was later confirmed by GC/MS traces. Noticeable precipitation of the monoanionic phosphate **2.39** also occurred upon the addition of the cuprate at -30 ºC and remained insoluble in THF upon warming to rt.

Scheme 2.5 *Model system for S_N2' cuprate release*

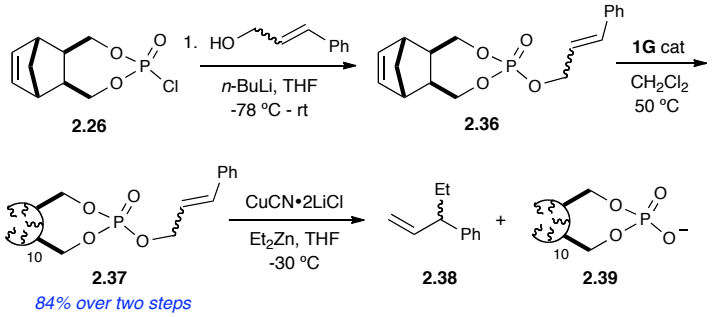

With this successful demonstration, a catch and release sequence was then tested on a six-membered phosphonosugar (*P*-sugar) template, previously developed in our laboratory,[32] that contains the requisite internal allylic alcohol functionality. Scheme 2.5 highlights the resynthesis efforts of this scaffold.

The synthesis begins with the highly reactive allyl phosphonyl dichloride **2.40** whereby addition of excess phenol affords diphenyl phosphonate **2.41**. Allylic alcohol **2.43** is generated via treatment of trimethylsulfonium iodide in *n*-BuLi with the corresponding (*S*)(−) glycidyl epoxide **2.42**. This newly generated allylic fragment is coupled to allyl phosphonate **2.41** affording the diallyl fragment **2.44** as a mixture of *P*-epimers. This is subjected to ring-closing metathesis conditions via catalyst **1G** affording six-membered allyl phosphonate **2.45** where the major *anti*(−) product in respect to the phenoxy group is separated by silica column chromatography. Transformation to the corresponding *syn*-diol **2.46** is achieved via Sharpless diastereoselective dihydroxylation.[33] Lastly, the diol is protected as the carbonate using triphosgene and subsequently eliminated via excess base (Et_3N) in a one-pot process affording the cyclic phosphonate **2.47** containing the requisite internal allylic alcohol.

Scheme 2.5 *Resynthesis efforts of the P-sugar template*

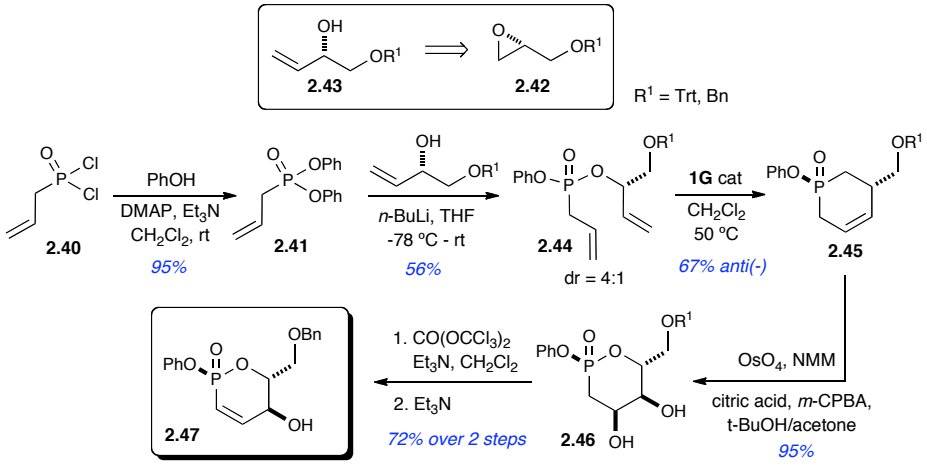

Scaffold **2.47** was next subjected to the capturing event via tag **2.26** rendering tagged scaffold **2.48** as a mixture of *P*-diastereomers (Scheme 2.6). This was then polymerized via catalyst **1G** yielding the soluble oligomeric phostone **2.49**. The nucleophilic cuprate was generated in situ from the corresponding zincate/CuCN mixture in THF. This was then added via cannulation to a solution of **2.49** thereby faciliting the diversify/release step affording products **2.50**–**2.52** in moderate yields, good purity and high diastereoselectivity (ds >20:1). This same catch and release process was repeated on other relevant scaffolding demonstrating its general compatibility with other heterocyclic systems.[34] After addition of the cuprate, an interesting observation was made whereby the blue coloration of the resulting copper salts began to quickly disappear, but upon quenching the reaction with 10% $HCl_{(aq)}$ the salts reappeared once more.

Scheme 2.6 *Capture/ROMP/cuprate release of phosphonate* ***2.47***

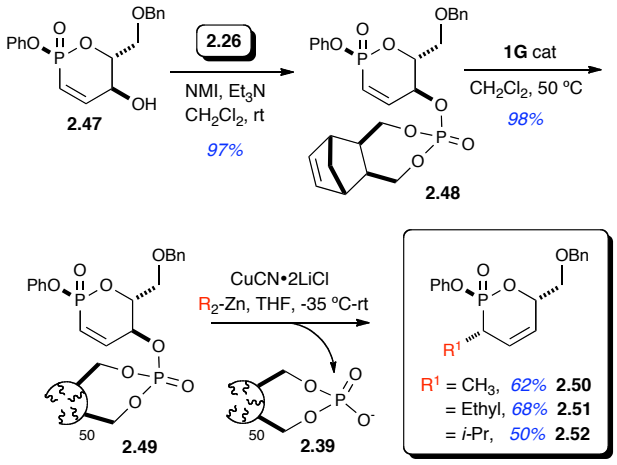

It was discovered that the resulting monoanionic phosphate oligomer **2.39** must be sequestering the copper salts during the progression of the cuprate addition. Upon

quenching the reaction, the phosphate acid once formed relinquishes the copper back into solution. It was noted that without the quench crude filtration of the reaction through a silica SPE successfully eliminated the need for the typical acidic workup. To test the sequestering ability of the oligomeric phosphate acid by itself, the reagent was added to an aqueous solution of known concentration containing $CuCl_2$ salts. The reaction mixture was stirred and monitored over several hours using UV/Vis detection, however no change in absorption was noted during this time period. It was concluded that the *in situ* generated monoanionic phosphate **2.39** is likely responsible for chelation in this sequestration process.

2.3 Development and Application of a ROMP-Derived Benzylating Reagent

Due to its ease of incorporation and removal, benzylation continues to serve as one of the most exploited protecting groups in organic synthesis.[4b,35,36] In addition, the hydrophobic, aromatic properties inherent to the benzyl group make it an ideal diversity element in combinatorial chemistry.[37] This can be often attributed to various structure-activity-relationships (SAR) associated with its size and shape and its ability to undergo π-stacking interactions. The intent to incorporate this element into our own facilitated efforts towards pilot-scale library production is demonstrated herein.

Several reports within our group alone have explored a number of different leaving group-armed, ROMP-based supports for achieving facilitated benzylation. Each of these reagents are stable, free-flowing powders that can be conveniently stored over extended periods of time. Efforts in our group, lead by Zhang and Moore, utilized benzyl sulfonate esters **2.54** (Figure 2.8) as reagents for benzylation derived

from oligomeric sulfonyl chloride (OSC) **2.53**; a reagent that had previously been reported for use as an effective nucleophile scavenger.[38] Treatment of this reagent with various benzyl alcohols provided a number of different analogs for use in benzylation. Treatment with a variety of amines produced the desired benzylated products in excellent yields after crude filtration.

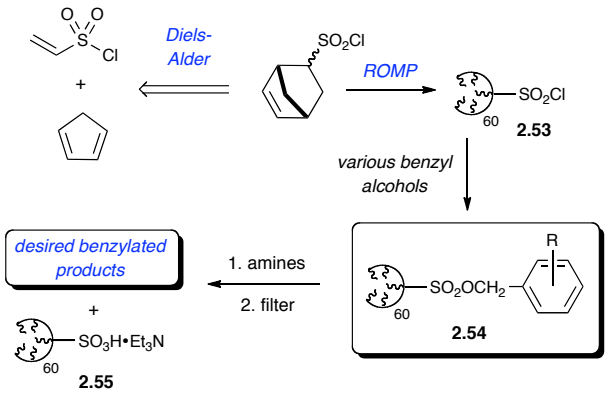

Figure 2.8 *Facilitated benzylation via oligomeric sulfonate esters*

Another method highlighted below utilized oligomeric sulfonium salts **2.57** to achieve facile benzylation.[39] Despite the insolubility of this reagent in common organic solvents, the notion for its use in flow-through, automated synthetic protocols may prove viable in the near future.

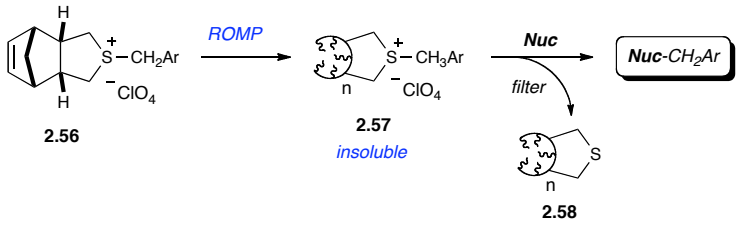

Figure 2.9 *Facilitated benzylation via oligomeric sulfonium salts*

Phosphates, as previously discussed, have been used extensively throughout the literature for S_N2' related pathways but are quite deficient in their use for S_N1 or direct S_N2 displacement reactions.[40] Only until recently have phosphates been demonstrated as effective leaving groups in Pd-catalyzed C-arylation/benzylation reactions; even having demonstrated drastic improvements in yield as compared to benzyl bromide.[41] In light of this gap, an oligomeric phosphate was pursued as a logical starting point for the development of a new reagent for facilitated benzylation. In this regard, the development and application of a new ROMP-based oligomeric benzyl phosphate (OBP) and its derivatives thereof were pursued as a *green* alternatives to the standard set of commercially available, halogen-based, benzylating reagents. Others have followed this pathway in the search for greener alkylating reagents[42] but few have exploited their use on polymer-based supports.[43] To our knowledge there are no reports of phosphate-based benzylating or alkylating reagents in the literature.

2.4 Results and Discussion (II)

Initial interest in the development of substituted oligomeric phosphates led to the idea of utilizing the oligomeric phosphorochloridate **2.30** as a means for producing tertiary amines in a one-pot, two-step protocol from substituted propargylic alcohols (Scheme 2.7). It was with this observation that we began to look more closely at the phosphate as an oligomeric leaving group that could be exploited in similar S_N2 displacement reactions; primarily that of benzylation.

Scheme 2.7 *One-pot synthesis of a propargylic tertiary amine*

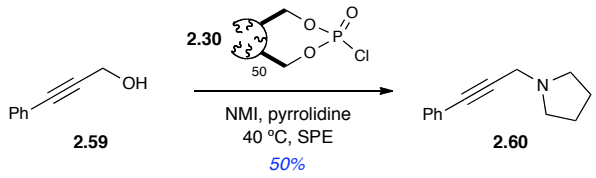

With this idea in hand, we envisaged an oligomeric benzylic phosphate and its synthesis starting from benzyl alcohol (Scheme 2.8). Experimentation began with the addition of the phosphorochloridate tag **2.26** into a solution containing benzyl alcohol, NMI, and CH_2Cl_2 at room temperature cleanly affording the benzyl phosphate **2.61** in good yields and purity. Polymerization of **2.61** and other phosphate analogs of this type in the presence of catalyst **2G** occurred rapidly at room temperature resulting in formation of insoluble and unusable gels. Subsequent ROM polymerization with catalyst **1G**, however, cleanly afforded the oligomeric benzyl phosphate (OBP_n) **2.62** with desirable characteristics.[44] Following polymerization, the reaction was quenched with ethyl vinyl ether (EVE) and stirred for 30 minutes. A basic workup involving the Pederson protocol[45] was also investigated and surprisingly no degradation of the phosphate was observed. This was then applied to the system on a large-scale and reflux was continued until the purple solution turned clear yielding a yellow precipitate. The resulting solution was washed several times with water and the organic polymer-containing layer was dried ($MgSO_4$), concentrated to critical viscocity[46] and precipitated dropwise into anhydrous Et_2O. The free-flowing, white reagent (OBP_n) **2.62** was then filtered off, rinsed thoroughly w/ anhydrous Et_2O, and placed under vacuum to dry.

Scheme 2.8 *Synthesis of the oligomeric benzyl phosphate (OBP_n)*

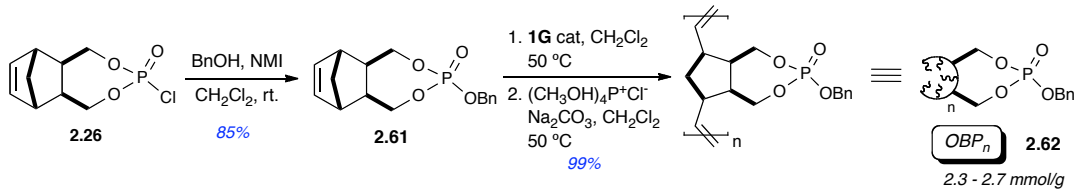

The oligomeric benzyl phosphate (OBP_{20}) was tested in benzylation reactions using a number of cyclic and acyclic amines as well as O, and S nucleophiles (Table 2.1). The reagent was delivered in excess (1.5–3.0 equiv) as either a free-flowing powder[47] or as a stock solution in anhydrous $CHCl_3$, with a catalytic amount of tetra-butylammonium iodide (Bu_4NI).[48] New formulations of this reagent and others are also currently being explored (Figure 2.10) including a tablet formulation (ROMP-tabs) that enables the user to take advantage of pre-measured loadings without the potential for large-scale inhalation hazards.

Figure 2.10 *OBP_{20} ROMP-tabs in comparison to free-flowing OBP_{20}*

Table 2.1 *Facilitated benzylation using oligomeric benzyl phosphate (OBP_n)*

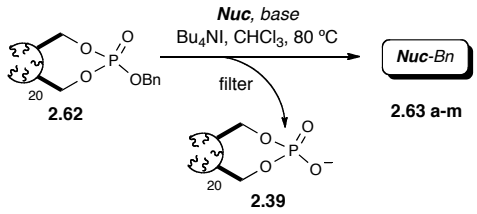

nucleophile	products **2.63**	yield (%)	purity (%)[a]
	**a**	99	98
	**b**	93	98
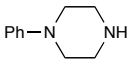	**c**	98	99
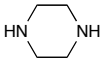	**d**	95	97
	**e**	80	99
	**f**	73	99
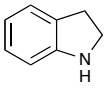	**g**	98	85
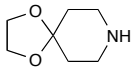	**h**	69	97
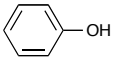	**i**	80	95
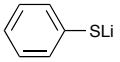	**j**	98	96
$Bn\text{-}NH_2$	**k/l**	99[b]	4:1[c]
Ph-NHEt	**m**	81	89
$Cy\text{-}NHCH_3$	n/a	nr	n/a

[a]Purities calculated using GC and further confirmed by ^{1}H NMR. [b],[c]Percent conversion and ratio of mono to dibenzylated amine calculated by GC/MS.

During benzylation, precipitation of the oligomeric phosphate monoanion **2.39** typically occured within a 0.5–2 hour period after addition of the nucleophile.

Reactions were allowed to cool to rt and the soluble contents were removed via syringe and either transferred and concentrated over silica or precipitated into Et_2O. This mixture was then passed through a silica SPE cartridge and concentrated under vacuum to afford the corresponding benzylated products **2.63a–m**. Monoanion **2.39** was found to be water soluble at elevated temperatures and remained indefinitely soluble on cooling to room temperature. This cleanup procedure is of particular importance for large-scale benzylation thus having eliminated the potential need for solvent change during the precipitation event.

A number of monomeric analogs (**2.61a–l**) of OBP were also prepared using several substituted benzyl alcohols (Table 2.2) and the corresponding oligomers **2.62 a–l** were tested accordingly (Table 2.3). Interestingly, efforts towards production of monomeric phosphates **2.61a–d** did not afford the desired products. This is likely due to an eliminative degradation pathway although no conclusive evidence for this has been obtained. With this notion, the corresponding oligomers **2.62e–l** were subjected to established benzylation conditions to afford the desired benzylated products in moderate to good yields (Table 2.3).

Table 2.2 *Synthesis of various OBP analogs*

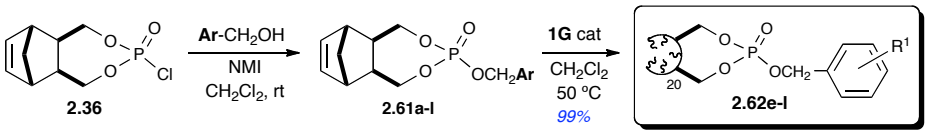

2.61	Ar	yield (%)
a	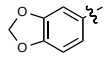	*23%*
b	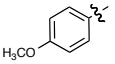	*21%*
c		*< 10%*
d		*< 10%*

2.61	R^1	yield (%)
e	*o*-CH_3	*75%*
f	3,5-$(OCH_3)_2$	*70%*
g	*p*-Br	*79%*
h	*p*-Cl	*76%*
i	*p*-F	*80%*
j	*p*-NO_2	*70%*
k	*m*-$N(CH_3)_2$	*73%*
l	*p*-CF_3	*77%*

Table 2.3 *Benzylation of amines using various OBP analogs*

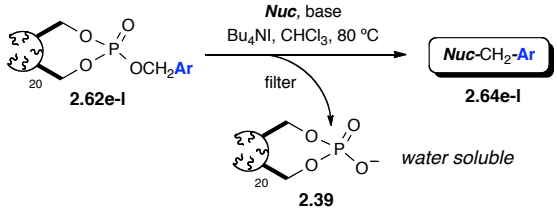

entry	sm **2.62**	products **2.64**		yield (%)	purity (%)[a]
1	**e**	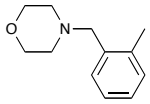	**e**	64	94
2	**f**	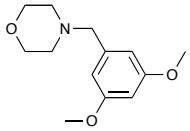	**f**	54	89
3	**g**	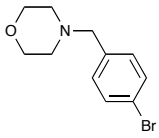	**g**	82	93

4	**h**	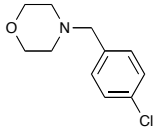	**h**	67	97
5	**i**	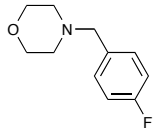	**i**	70	96
6	**j**	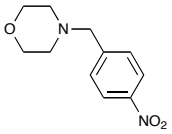	**j**	74	93
7	**k**	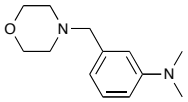	**k**[b]	78	98
8	**k**	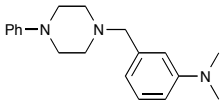	**k′**[c]	93	98
9	**l**	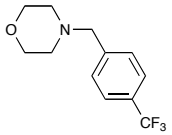	**l**	68	95

[a]Purities calculated using GC and further confirmed by ^{1}H NMR.
[b],[c] Despite their simplicity each compound is classified as a NCE.

The integration of ROMP-derived oligomeric reagents for application in small-molecule library development is of utmost importance to our research. With this in mind, OBP_{20} was tested on a select benzofused sultam scaffold for benzylation (Table 2.4). The reagent was added to a THF solution containing benzothiaoxazepine-1,1-dioxide (**2.65a**) in the presence of K_2CO_3 and Bu_4NI and stirred at 80 ºC overnight. The resulting mother liquor was precipitated from a Et_2O/EtOAc mixture. Subsequent filtration employing a silica SPE cartridge, and evaporation of solvent

afforded the desired benzylated product **2.66a** in excellent yield and high purity. With this result in place, sultams **2.65a/b** were subjected to benzylation employing OBP derivatives **2.62f,i** utilizing the condtions established above to afford the desired products (**2.66b–d**) in good to excellent yields and purities.

Table 2.4 *Pilot-scale benzylation of benzo-fused sultams*

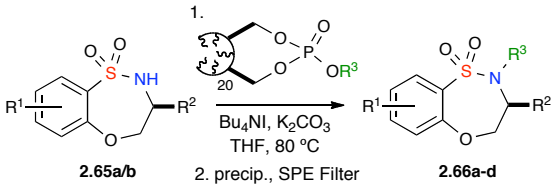

entry	sm **2.65**	R^1	R^2	R^3	product **2.66**	yield (%)[a]
1	**a**	4-Br	Ph	Bn	**a**	99
2	**a**	4-Br	Ph	3,5-diMeO-Bn	**b**	72
3	**a**	4-Br	Ph	4-F Bn	**c**	85
4	**b**	4-Br	^{i}Bu	4-F Bn	**d**	97

[a]Yields after filtration via silica SPE.

2.5 Conclusion and Future Outlook

In conclusion we have developed a multifaceted oligomeric phosphate that can serve as both a support and a leaving group in S_N2' processes for facilitated "catch and release" synthesis, as well as an *in situ* generated copper sequestration reagent. It has also been demonstrated as an efficient benzylating reagent for a variety of nucleophiles and was applied in the pilot-scale diversification of benzo-fused sultams. We are currently exploring new ways to widen the scope and utility of this system including the development of an oligomeric propargylic phosphate variant and its use in facilitated triazole formation and azide scavenging. Current efforts are also aimed at using this reagent in pilot-scale library production.

References

(1) (a) Yanagisawa, A.; Nomura, N.; Noritake, Y.; Yamamoto, H., Highly S_N2'-, (E)-, and antiselective alkylation of allylic phosphates. Facile synthesis of coenzyme Q10. *Synthesis* **1991**, *12,* 1130–1136. (b) Torneiro, M.; Fall, Y.; Castedo, L.: Mourino, A., Short, Efficient Copper-Mediated Synthesis of 1α, 25-Dihydroxyvitamin D2 (1α,25-Dihydroxyergocalciferol) and C-24 Analogs. *J. Org. Chem.* **1997**, *62*, 6344–6352. (c) Murphy, K. E.; Hoveyda, A. H., Enantioselective Synthesis of α-Alkyl-β,γ-unsaturated Esters through Efficient Cu-Catalyzed Allylic Alkylations., *J. Am. Chem. Soc.* **2003**, *125*, 4690–4691. (d) Williams, D. R.; Heidebrecht, R. W. Jr., Total Synthesis of (+)-4,5-Deoxyneodolabelline. *J. Am. Chem. Soc.* **2003**, *125*, 1843–1850. (e) Fuwa, H.; Sasaki, M., Total synthesis of isoindolobenzazepine alkaloids, lennoxamine and chilenine, based on palladium-catalyzed reduction of alkenyl phosphates. *Heterocycles* **2008**, *76*, 521–539. (f) Thomas, C. D.; McParland, J. P.; Hanson, P. R., Divalent and Multivalent Activation in Phosphate Triesters: A Versatile Method for the Synthesis of Advanced Polyol Synthons. *Eur. J. Org. Chem.* **2009**, 5487–5500.

(2) Bookser, B. C.; Raffaele, N. B. High-throughput Synthesis of HepDirect Prodrugs of Nucleoside Monophosphates. *J. Comb. Chem.* **2008**, *10*, 567–572.

(3) (a) Franchetti, P.; Cappellacci, L.; Grifantini, M.; Messini, L.; Sheikha, G. A.; Loi, A. G.; Tramontano, E.; Montis, A. D.; Spiga, M. G.; Colla, P. L., Synthesis and Evaluation of the Anti-HIV Activity of Aza and Deaza Analogues of IsoddA and Their Phosphates as Prodrugs. *J. Med. Chem.* **1994,** *37*, 3534–3541. (b) Eto, M., Functions of Phosphorous Moiety in Agrochemical Molecules. *Biosci., Biotechnol., Biochem.* **1997,** *61*, 1–11.

(4) (a) Westheimer, F. H., Why Nature Chose Phosphates. *Science* **1987**, *235,* 1173–1178. (b.) Paquette, L. A., *Encyclopedia of Reagents for Organic Synthesis*; 1st Edition, John Wiley and Sons, 1995, pp 316–318. The most common reagents to achieve this process are the benzylic bromides, which present both safety and toxicity issues, most notably they are severe lachrymators.

(5) Nicolaou, K. C.; Shi, G. Q.; Gunzner, J. L.; Gaertner, P.; Yang, Z., Palladium-Catalyzed Functionalization of Lactones via Their Cyclic Ketene Acetal Phosphates. Efficient New Synthetic Technology for the Construction of Medium and Large Cyclic Ethers. *J. Am. Chem. Soc.* **1997**, *119,* 5467–5468.

(6) Morgan, A. B.; Tour, J. M., Synthesis and testing of nonhalogenated alkyne/phosphorus-containing polymer additives: potent condensed-phase flame retardants. *J. Appl. Polym. Sci.* **1999**, *73,* 707–718.

(7) (a) Ahmadibeni, Y.; Parang, K., Solid-Phase Reagents for Selective Mono-Phosphorylation of Carbohydrates and Nucleosides. *J. Org. Chem.* **2005**, *70*, 1100–1103. (b) Ahmadibeni, Y.; Parang, K. Polymer-bound oxathia-phospholane: a solid-phase reagent for regioselective monothiophosphorylation and monophosphorylation of unprotected nucleosides and carbohydrates. *Org. Lett.* **2005**, *7*, 1955–1958.

(8) Wang, J.; Mao, H.-Q.; Leong, K. W., A Novel Biodegradable Gene Carrier Based on Polyphosphoester. *J. Am. Chem. Soc.* **2001**, *123*, 9480–9481.

(9) Kane, R. R.; Lee, C. S.; Drechsel, K.; Hawthorne, M. F., Solution-phase synthesis of boron-rich phosphates. *J. Org. Chem.* **1993**, *58*, 3227–3228.

(10) Bouillon, C.; Meyer, A.; Vidal, S.; Jochum, A.; Chevolot, Y.; Cloarec, J.-P.; Praly, J.-P.; Vasseur, J.-J.; Morvan, F., Microwave Assisted "Click" Chemistry for the Synthesis of Multiple Labeled-Carbohydrate Oligonucleotides on Solid Support. *J. Org. Chem.* **2006**, *71*, 4700–4702.

(11) (a) Flynn, D. L.; Devraj, R. V.; Naing, W.; Parlow, J. J.; Weidner, J. J.; Yang, S., Polymer-assisted solution phase (PASP) chemical library synthesis. *Med. Chem. Res.* **1998**, *8*, 219–243. (b) Yoshida J.-I.; Itami K., Tag strategy for separation and recovery. *Chem. Rev.* **2002**, *102*, 3693–716. (c) Boldt, G. E.; Dickerson, T. J.; Janda, K. D., Emerging chemical and biological approaches for the preparation of discovery libraries. *Drug Discov. Today* **2006**, *11*, 143–148.

(12) (a) Curran, D. P.; Hoshino, M., Stille Couplings with Fluorous Tin Reactants: Attractive Features for Preparative Organic Synthesis and Liquid-Phase Combinatorial Synthesis. *J. Org. Chem.* **1996**, *61*, 6480–6481. (b) Curran, D. P.; Hadida, S., Tris(2-(perfluorohexyl)ethyl)tin Hydride: A New Fluorous Reagent for Use in Traditional Organic Synthesis and Liquid Phase Combinatorial Synthesis. *J. Am. Chem. Soc.* **1996**, *118*, 2531–2532.

(13) Horváth, I. T.; Rabái, J., Facile catalyst separation without water: fluorous biphase hydroformylation of olefins. *Science* **1994**, *266*, 72–75.

(14) (a) Barrett, A. G. M.; Hopkins, B. T.; Kobberling, J., ROMPgel Reagents in Parallel Synthesis. *Chem. Rev.* **2002**, *102,* 3301–3324. (b) Harned, A. M.; Probst, D. A.; Hanson, P. R., *Handbook of Metathesis, Vol. 2,* Grubbs, R. H., Ed.: Wiley-VCH: Weinheim, 2003. pp 361–402. (c) Flynn, D. L.; Hanson, P. R.; Berk, S. C.; Makara, G. M., New developments in chemical library synthesis. Norbornenyl tags for use in phase-switching, sequestration, capture-release and soluble support applications. *Curr. Opin. Drug Discov. Devel.* **2002**, 5, 571–579.

(15) (a) Phung-Nhu-Hung; Chauvin, Y.; Lefebvre, G., Application of mobile isomerization equilibrium to the polymerization of olefin mixtures. II. Prototropic displacement by the salts and complexes of noble metals. *B. Soc. Chim. Fr.* **1967**, *10*, 3618–3626. (b) Herisson, J. L.; Chauvin, Y.; Phung-Nhu-Hung; Lefebvre, G., Transformation of acyclic olefins by homogeneous and heterogeneous tungsten-based catalysts. *Cr. Acad. Sci. C. Chim.* **1969**, *269*, 661–664. (c) Soufflet, J. P.; Commereuc, D.; Chauvin, Y., Transformation of olefins catalyzed by tungsten complexes. Possible forms of the intermediates. *Cr. Acad. Sci. C. Chim.* **1973**, *276*, 169–171. (d) Bre, A.; Chauvin, Y.; Commereuc, D., Mode of decomposition of titanacyclopentanes, model of the intermediate species in the dimerization of olefins catalyzed by titanium complexes. *Nouv. J. Chim.* **1986**, *10*, 535–537.

(16) Schrock, R. R., The Discovery and Development of High Oxidation State Mo and W Imido Alkylidene Complexes for Alkene Metathesis. In *Handbook of Metathesis, Volume 1*; Grubbs, R. H., Ed.; Wiley-VCH: New York, 2003; pp 8–32.

(17) Nguyen, S. T.; Trnka, T. M., The Discovery and Development of Well-Defined, Ruthenium-based Olefin Metathesis Catalysts. In *Handbook of Metathesis, Volume 1*; Grubbs, R. H., Ed.; Wiley-VCH: New York, 2003; pp 61–85.

(18) (a) Chauvin, Y.; Commereuc, D.; Cruypelinck, D., Catalysis of olefin transformation by tungsten complexes, 5. Tungsten carbonyl carbenes activated by titanium tetrahalides as catalysts for the ring-opening polymerization of cyclopentene. *Makromolekul. Chem.* **1976**, *177*, 2637–2646.

(19) Hérisson, P. J-L.; Chauvin, Y., Catalyse de transformation des oléfines par les complexes du tungstène. II. Télomérisation des oléfines cycliques en présence d'oléfines acycliques. *Makromolekul. Chem.* **1971**, *141*, 161–176.

(20) Howard, T. R., Lee J. B., Grubbs, R. H., Titanium metallacarbene-metallacyclobutane reactions: stepwise metathesis. *J. Am. Chem. Soc.* **1980**, *102*, 6876–6878.

(21) Nguyen, S. T.; Grubbs, R. H.; Ziller, J. W., Syntheses and activities of new single-component, ruthenium-based olefin metathesis catalysts**.** *J. Am. Chem. Soc.* **1993**, *115*, 9858–9859.

(22) (a) Harned, A. M.; Zhang, M.; Vedantham, P.; Mukherjee, S.; Herpel, R. H.; Flynn, D. L.; Hanson, P. R., ROM Polymerization in Facilitated Synthesis. *Aldrichimica Acta*, **2005**, *38,* 3–16. (b) Zhang, M., Vedantham, P.; Flynn, D. L.; Hanson, P. R., High-Load, Soluble Oligomeric Carbodiimide: Synthesis and Application in Coupling Reactions. *J. Org. Chem.* **2004**, *69*, 8340–8344. (c) Harned, A. M.; Sherrill, W. M.; Flynn, D. L.; Hanson, P. R., High-Load, Soluble Oligomeric Benzenesulfonyl Azide: Applications to Facile Diazo-Transfer Reactions. *Tetrahedron* **2005**, *61*, 12093–12099. (d) Rolfe, A.; Probst, D.; Volp, K.; Omar, I.; Flynn, D.; Hanson, P. R., High-load, Oligomeric dichlorotriazine (ODCT): A Versatile ROMP-derived Reagent and Scavenger. *J. Org. Chem.* **2008**, *73*, 8785–8790.

(23) For use of ROMP reagents in library synthesis, see: Vedantham, P.; Zhang, M.; Gor, P. J.; Huang, M.; Georg, G. I.; Lushington, G. H.; Mitscher, L. A.; Ye, Q.-Z.; Hanson, P. R., Studies Towards the Synthesis of Methionine Aminopeptidase Inhibitors: Diversification Utilizing a ROMP-Derived Coupling Reagent. *J. Comb. Chem.* **2008**, *10*, 195–203.

(24) Harned, A. M.; Mukherjee, S.; Flynn, D. L; Hanson, P. R., Ring-Opening Metathesis Phase-Trafficking (ROMpt) Synthesis: Multistep Synthesis on Soluble ROM Supports. *Org. Lett.* **2003**, *5*, 15–18.

(25) Craig, D. The Rearrangement of *endo*-3,6-Methylen-1,2,3,6-tetrahydro-*cis*-phthalic Anhydride. *J. Am. Chem. Soc.* **1951**, *73*, 4889–4892.

(20) (a) Moore, J. D.; Byrne, R. J.; Vedantham, P.; Flynn, D. L.; Hanson, P. R., High-Load, ROMP-Generated Oligomeric Bis-acid Chlorides: Design of Soluble and Insoluble Nucleophile Scavengers. *Org. Lett.* **2003**, *5*, 4241–4244. (b) Rolfe, A.; Probst, D.; Volp, K.; Omar, I.; Flynn, D.; Hanson, P. R., High-load, Oligomeric dichlorotriazine (ODCT): A Versatile ROMP-derived Reagent and Scavenger. *J. Org. Chem.* **2008**, *73*, 8785–8790. (c) Herpel, R. H.; Vedantham, P.; Flynn, D. L.; Hanson, P. R., High-load, Oligomeric Phosphonyl

Dichloride: Facile Generation via ROM Polymerization and Applications to Scavenging Amines. *Tetrahedron Lett*. **2006**, *47*, 6429–6432.

(27) Tanaka, T.; Bannai, K.; Hazato, A.; Koga, M.; Kurozumi, S.; Kato, Y., Prostaglandin chemistry. Part XXXV. Short synthesis of isocarbacyclin by regioselective SN2' alkylation of bicyclic allylic esters with zinc-copper reagents. *Tetrahedron* **1991**, *47*, 1861–1876.

(28) Yanagisawa, A.; Noritake, Y.; Nomura, N.; Yamamoto, H., Superiority of phosphate ester as leaving group for organocopper reactions. Highly SN2'-, (E)-, and antiselective alkylation of allylic alcohol derivatives. *Synlett* **1991**, *4*, 251–253.

(29) Thaler, T.; Knochel, P., Copper-catalyzed asymmetric Michael addition of magnesium, zinc, and aluminum organometallic reagents: efficient synthesis of chiral molecules. *Angew. Chem. Int. Ed*. **2009**, *48*, 645–648.

(30) Corey, E. J.; Boaz, N. W. d-Orbital Stereoelectronic Control of the Stereochemistry of S_N2' Displacements by Organocuprate Reagents. *Tetrahedron Lett*. **1984**, *25*, 3063–3066.

(31) For experimental and theoretical studies, see: (a) Karlstrom, A. S. E.; Backvall, J.-E., Experimental evidence supporting a CuIII intermediate in cross-coupling reactions of allylic esters with diallylcuprate species. *Chem.-Eur. J*. **2001**, *7*, 1981–1989. (b) Backvall, J.-E.; Sellen, M.; Grant, B. Regiocontrol in copper-catalyzed Grignard reactions with allylic substrates. *J. Am. Chem. Soc*. **1990**, *112*, 6615–6621 and references therein. (c) Dorigo, A. E.; Wanner, J.; von Rague Schleyer, P. Computational evidence for the existence of CuIII intermediates in addition and substitution reactions with dialkylcuprates. *Angew. Chem., Int. Ed. Engl*. **1995**, *34*, 476–478. (d) Mori, S.; Hirai, A.; Nakamura, M.; Nakamura, E. Correlation of reactivities of organocuprate(I) and zincate(II) with d-orbital energies of ate complexes. *Tetrahedron* **2000**, *56*, 2805–2809. (e) Goering, H. L.; Kantner, Steven, S. Alkylation of allylic derivatives. Loss of double-bond configuration associated with α-alkylation of allylic carboxylates with dialkylcuprates. *J. Org. Chem*. **1983**, *48*, 721–724.

(32) Stoianova, D.S.; Whitehead, A.; Hanson, P. R. *P*-Heterocyclic Building Blocks: Application to the Stereoselective Synthesis of *P*-Sugars. *J. Org. Chem*. **2005**, *70*, 5880–5889.

(33) Sharpless, K. B.; Amberg, W.; Bennani, Y. L.; Crispino, G. A.; Hartung, J.; Jeong, K. S.; Kwong, H. L.; Morikawa, K.; Wang, Z. M.; Xu, D.; Zhang, X-L., The osmium-catalyzed asymmetric dihydroxylation : a new ligand class and a process improvement. *J. Org. Chem.* **1992**, *57*, 2768–2771.

(34) Jimenez, M. D. S., Synthesis of sultams and related sulfur heterocycles using the ring-closing metathesis reaction. Ph.D. Dissertation, University of Kansas, Lawrence, KS, 2008.

(35) March, J. *Advanced Organic Chemistry*, 4th ed.; John Wiley and Sons: New York, 1991.

(36) Greene, T. W.; Wuts, P. G. M. In *Protective Groups in Organic Synthesis*, 4th ed.; John Wiley and Sons: New York, 2007; pp 102–148.

(37) Dolle, R. E.; Le Bourdonnec, B.; Goodman, A. J.; Morales, G. A.; Thomas, C. J.; Zhang, W., Comprehensive Survey of Chemical Libraries for Drug Discovery and Chemical Biology: 2008. *J. Comb. Chem.* **2009**, *11*, 739–790.

(38) Zhang, M.; Moore, J. D.; Flynn, D. L.; Hanson, P. R., Development of High-Load, Soluble Oligomeric Sulfonate Esters via ROM Polymerization: Application to the Benzylation of Amines. *Org. Lett.* **2004**, *6*, 2657–2660.

(39) Zhang, M.; Flynn, D. L.; Hanson, P. R., Oligomeric Benzylsulfonium Salts: Facile Benzylation via High-Load ROMP Reagents. *J. Org. Chem.* **2007**, *72*, 3194–3198.

(40) (a) Zeller, E.; Sajus, H.; Grierson, D. S., Carbon-carbon bond forming reactions of α -aminonitriles under dissolving metal conditions: synthesis of gephyrotoxin-167B. *Synlett* **1991**, *12,* 44–46. (b) Zeller, E.; Grierson, D. S. Reactions of α -amino nitriles under dissolving metal conditions: a concise synthesis of (±)-monomorine-I. *Synlett* **1991**, *12*, 878–880. (c) Rychnovsky, S. D.; Takaoka, L. R., Spiroannulation by alkylation and reductive cyclization of nitriles. *Angew. Chem., Int. Ed.* **2003**, *42*, 818–820. (d) Morin, M. D.; Rychnovsky, S. D., Reductive Spiroannulation of Nitriles with Secondary Electrophiles. *Org. Lett.* **2005,** *7*, 2051–2053. (e) Wolckenhauer, S. A.; Rychnovsky, S. D. Generation and Utility of Tertiary α-Aminoorganolithium Reagents. *Org. Lett.* **2004**, *6*, 2745–2748. (f) Wolckenhauer, S. A.; Rychnovsky, S. D., Stereochemical course of the reductive spiroannulations of *N*-Boc and *N*-benzyl 2-cyanopiperidines. *Tetrahedron* **2005**, *61*, 3371–3381. (g) La Cruz, T. E.; Rychnovsky, S. D., A Reductive Cyclization Approach to

Attenol A. *J. Org. Chem.* **2007**, *72*, 2602–2611.

(41) (a) Ackermann, L.; Barfuesser, S.; Pospech, J., Palladium-Catalyzed Direct Arylations, Alkenylations, and Benzylations through C-H Bond Cleavages with Sulfamates or Phosphates as Electrophiles. *Org. Lett.* **2010,** *12*, 724–726. (b) Lapointe, D.; Fagnou, K., Palladium-catalyzed benzylation of heterocyclic aromatic compounds. *Org. Lett.* **2009**, *11*, 4160–4163.

(42) (a) Shieh, W.-C.; Dell, S.; Repic, O., 1,8-Diazabicyclo[5.4.0]undec-7-ene (DBU) and Microwave-Accelerated Green Chemistry in Methylation of Phenols, Indoles, and Benzimidazoles with Dimethyl Carbonate. *Org. Lett.* **2001**, 3, 4279–4281. (b) Shieh, W.-C.; Lozanov, M.; Loo, M.; Repic, O.; Blacklock, T. J., DABCO- and DBU-accelerated green chemistry for N-, O-, and S-benzylation with dibenzyl carbonate. *Tetrahedron Lett.* **2003**, *44*, 4563–4565. (c) Loris, A.; Perosa, A.; Selva, M.; Tundo, P. J., Selective *N*,*N*-Di-benzylation of Primary Aliphatic Amines with Dibenzyl Carbonate in the Presence of Phosphonium Salts. *Org. Chem.* **2004**, *69*, 3953–3956. (d) Poon, K. W. C.; House, S. E.; Dudley, G. B., A bench-stable organic salt for the benzylation of alcohols. *Synlett* **2005**, *20*, 3142–3144.

(43) (a) Hanessian, S.; Huynh, H. K., Solution and solid-phase p-alkoxybenzylation of alcohols under neutral conditions. *Tetrahedron Lett.* **1999**, *40*, 671–674. (b) Baxter, E. W.; Rueter, J. K.; Nortey, S. O.; Reitz, A. B., Arylsulfonate esters in solid phase organic synthesis. II. Compatibility with commonly-used reaction conditions. *Tetrahedron Lett.* **1998**, *39*, 979–982. (c) Rueter, J. K.; Nortey, S. O.; Baxter, E. W.; Leo, G. C.; Reitz, A. B., Arylsulfonate esters in solid phase organic synthesis. I. Cleavage with amines, thiolate, and imidazole. *Tetrahedron Lett.* **1998**, *39*, 975–978. (d) Prakash, G. K. S.; Weber, C.; Chacko, S.; Olah, G. A., New Solid-Phase Bound Electrophilic Difluoromethylating Reagent. *J. Comb. Chem.* **2007**, *9*, 920–923.

(44) Desirable characteristics included overall solubility of the oligomeric reagent, and its ability to be purified in a one-pot process as noted in the text.

(45) Pederson, R. L.; Fellows, I. M.; Ung, T. A.; Ishihara, H.; Hajela, S. P., Applications of olefin cross metathesis to commercial products. *Adv. Synth. Catal.* **2002**, *344*, 728–735.

(46) Critical viscosity is described as the optimal viscosity needed to achieve a free-flowing powder during the precipitation event.

(47) Hazards/toxicity relating to the inhalation of these powders have not been studied or tested and precautions should be taken when in use.

(48) (a) Conditions used for benzylation were modified from previously reported conditions used in our group. See ref. 36. (b) Observation of a catalytic amount of benzyl iodide during the reaction period was confirmed by GC/MS in two specific cases.

Chapter 3

A ROMP-Based Strategy Towards Skeletally Diverse Sultams

3.1 Introduction

The emergence of designer polymers and associated technologies continues to bring new opportunities for facilitating the drug discovery process.[1] Conventionally, this goal been achieved by operating on resin-bound substrates (i) with excess reagents or treating solution phase substrates with excess immobilized reagents (ii) (Figure 3.1). Both scenarios, although deemed uneconomical,[2] have been extensively represented in the literature as highlighted in previous chapters. Alternatively, a third scenario is presented (iii) that employs the use of excess substrate (normally considered the precious component) and is rarely used due to obvious reasons. However, if excess substrate is warranted in a reaction and can be further processed in a parallel, chromatography-free manner, ie, "reclaimed", this unfavorable scenario is then deemed quite favorable. This recycling process would allow for the possibility of generating a new set of products derived from the parent substrate.

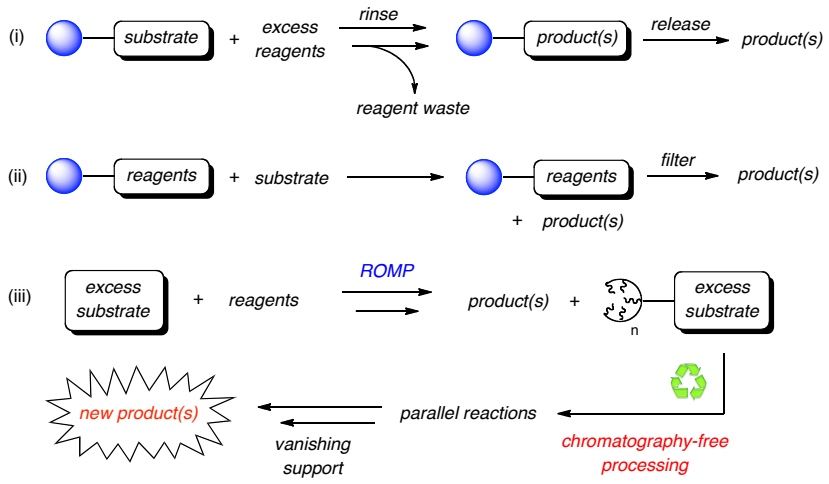

Figure 3.1 *General scheme for facilitated reactions (i-iii).*

Sulfonamides have long been recognized as an important class of compounds in drug discovery for their rich biological and chemical profiles. This has been augmented by a number of favorable chemical properties (ie. pKa's) inherent to these structures enabling them to undergo facile coupling/alkylation pathways, stability to hydrolysis, overall polarity, and their crystalline nature. Like their acyclic counterparts, sultams (cyclic sulfonamides), despite their absence in nature, exhibit a wide-array of potent biological activities (Figure 3.2) including COX-2 inhibition[3] (**3.1**, **3.2**) antiviral and anticancer[4] (**3.3**), treatments for glaucoma[5] (**3.4**) and epilepsy[6] (**3.5**), as well as calpain I inhibition[7] (**3.6**). This information has opened the door for aggressively mining underrepresented chemical space of this particular chemotype.

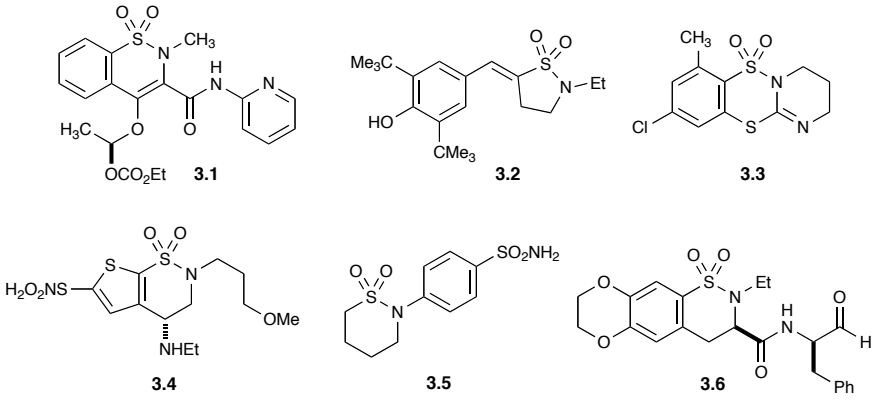

Figure 3.2 *Examples of known bioactive sultams*

Within the context of this chapter, a unique, ROMP-based synthetic protocol will be presented for use in the atom-economical synthesis of various skeletally diverse sultams starting from a single norbornene-based scaffold. The use of a vanishing support protocol is also demonstrated as a traceless means for polymer-assisted synthesis.

Our continued interest in norbornene-based structures has led to the development of new methods employing metathesis as a key reaction in accessing skeletally diverse sultams (Scheme 3.1).[8] The idea of utilizing ring-strain as a facilitated protocol for creating diversity however, is by no means a new concept. Outside of traditionally accomplished Diels-Alder chemistry, many others have also capitalized on the use of norbornene-systems as reliable diversity-creating substructures.[9a,b]

Scheme 3.1 *Cascade metathesis reactions towards diverse sultams*

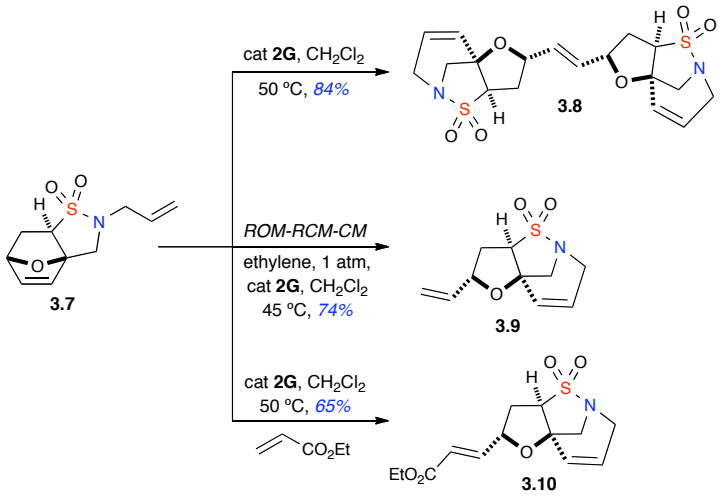

Recently, Spring and coworkers demonstrated the power of this concept in the search for new antibiotic small-molecule probes.[10] This strategy utilized a solid-supported phosphonate (**3.11**) for the stereoselective formation of α, β-unsaturated acyl imidazolidinones **3.12** (Scheme 3.2). These twelve compounds were subsequently used to produce a 242-member library of a wide array of diverse scaffolding. In this search, three compounds, including **3.14**, were identified having

displayed antibiotic activity. Compound **3.14** named (–)-gemmacin, also showed inhibitory activity towards a methicillin-resistant strain of *Staphylococcus aureus* (MRSA).

Scheme 3.2 *Norbornene-based DOS strategy for drug discovery*

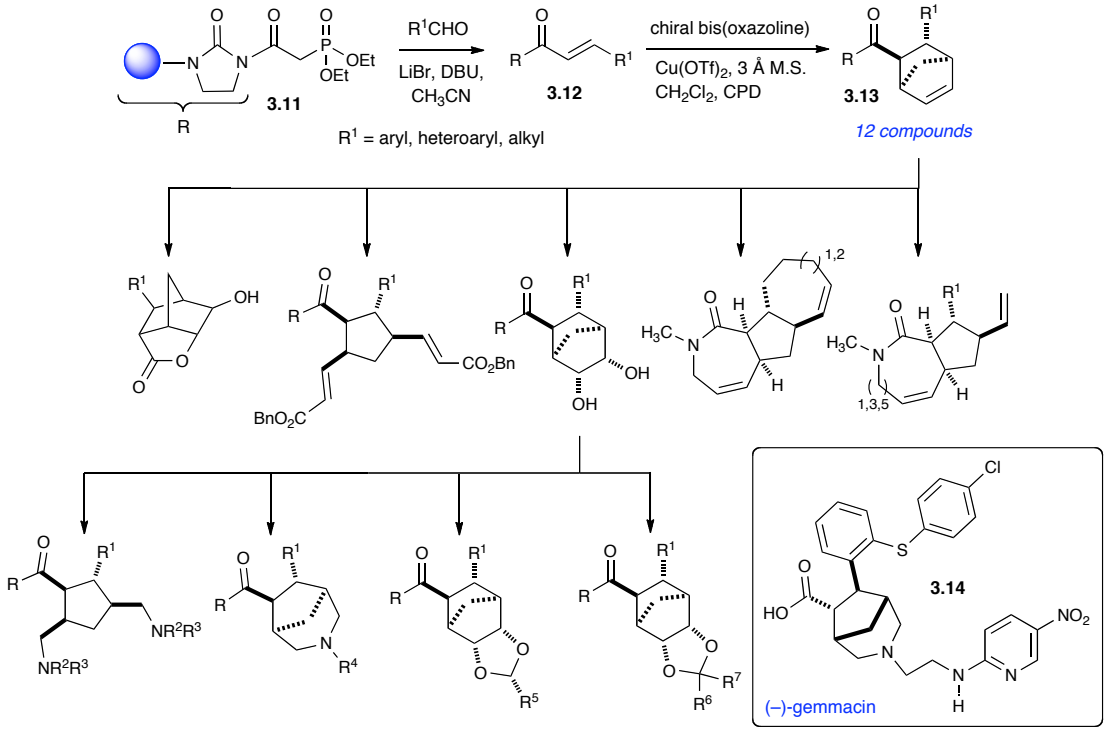

Our general method, highlighted in Figure 3.3, incorporates the following diversity-generating sequence: (i) performing reactions on the internal olefin of an oxa-norbornene-based scaffold used in excess, (ii) reclamation of this excess scaffold via ROMP followed by subsequent diversification via parallel reactions, and (iii) the use of a vanishing support protocol (VSP)[11] to relinquish the newly diversified collection of products in high purity. The representative oxa-norbornene-based scaffold herein is not only inherently armed for diversity but also for ROM-polymerization. After

completion of the parent reaction, which transforms the olefin moiety into a new functional group, excess monomeric scaffold (S-1) is sequestered via *in situ* ROM polymerization.[11a,12] Filtration of the parent reaction yields pure products (P-1) as well as reclaimed oligomeric sultam (O-1) (ie. the precious component.) In contrast to the aforementioned scenarios, the oligomeric sultam does not constitute as waste since added diversification can take place and ultimately, additional products (P-2 to P-4) can be relinquished via polymer annihilation using a vanishing support protocol (VSP). Overall, this chromatography-free process provides access to diverse sultam scaffolds in a parallel manner by integrating the virtues of solid phase and solution-phase chemistries through an atom-economical approach.

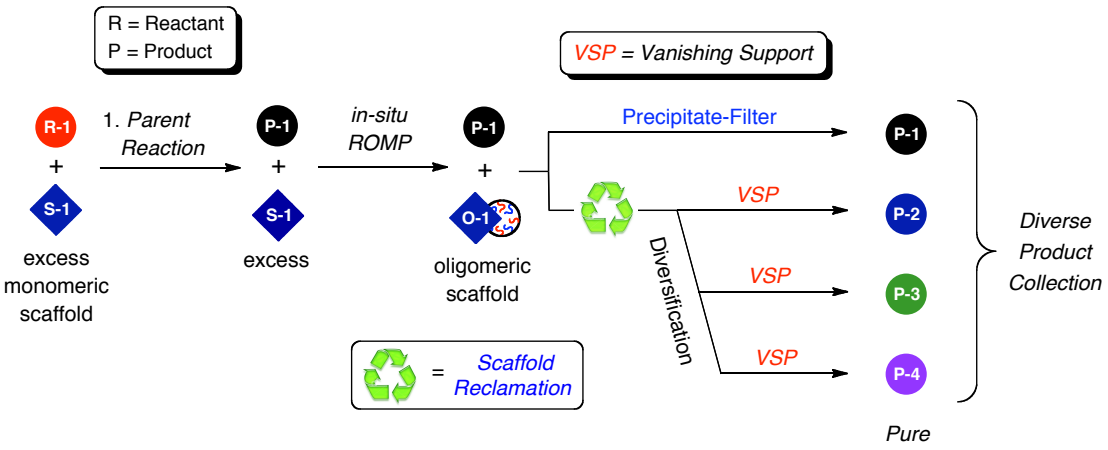

Figure 3.3 *Parallel processing via scaffold reclamation*

3.2 Results and Discussion

The initial route began with the synthesis of tricyclic sultam **3.15** using precedent set by Metz and coworkers (Scheme 3.3).[13] Treatment of furfuryl amine with 2-chloroethanesulfonyl chloride and subsequent Boc-protection afforded a vinyl

sulfonamide, which upon heating gave the desired intramolecular Diels-Alder adduct **3.15** with excellent yield and exo-adduct selectivity (dr > 19:1). This scaffold was subjected to reductive Heck conditions[14] using $Pd(OAc)_2$, Zn and excess aromatic iodides (1.5 equiv.) to afford sultam **3.16** in < 60% yield with excellent regio- and diastereoselectivity (dr > 19:1). During an initial study, however, it was discovered that using excess scaffold (1.5 equiv.) increased the yield of this reaction up to 89%. However, chromatographic purification became tedious due to the similarity in R_f between sultams **3.15** and **3.16**. At this juncture, the notion of sequestering excess scaffold became apparent when it was discovered that **3.15** underwent facile ROM-polymerization. The method was implemented in a sequence by performing the Heck reaction of an aromatic iodide with excess sultam **3.15** in the presence of $Pd(OAc)_2$ and Zn in DMF at 60 ºC.

Scheme 3.3 *ROMP-facilitated DOS-strategy*

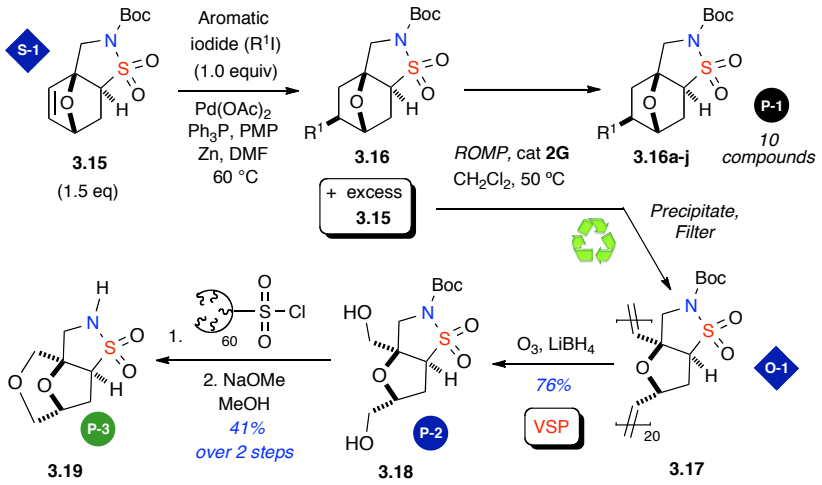

After completion of the reaction, the mixture was filtered through Celite (to remove Zn), concentrated and subjected to *in situ* ROM-polymerization using catalyst **2G** where simple precipitation and filtration afforded the desired Heck products **3.16a–j** in good yields and excellent purity (Table 3.1). The reclaimed oligomeric scaffold **3.17** was then subjected to additional processing via reductive ozonolysis[15] to generate sultam **3.18**. Moreover, capture of **3.18** with oligomeric benzene sulfonyl chloride ($OBSC_{60}$) followed by release with NaOMe afforded cyclized product **3.19** in 41% yield over the two-step sequence.

Table 3.1 *Reductive Heck products **3.16a–j***

entry	substrate	R^1	yield %[a]
1	**a**	*p*-Ac-Ph	82
2	**b**	*p*-F-Ph	77
3	**c**	*p*-CO_2CH_3-Ph	86
4	**d**	*p*-OH-Ph	89
5	**e**	*m*-F-Ph	82
6	**f**	3,5 di-CH_3-Ph	76
7	**g**	*p*-CH_3-Ph	75
8	**h**	2-thiophene-Ph	81[b]
9	**i**	*p*-CF_3O-Ph	73[c]
10	**j**	*p*-CN-Ph	65[c]

[a]Purities > 95%. [b] dr = 3:1, [c] dr = 4:1

Alternatively, oligomer **3.17** underwent facile deprotection, alkylation and reductive ozonolysis (ie. VSP) to afford the alkylated sultam **3.21** in excellent yield (Scheme 3.4). The purity in both sequences was excellent and X-ray quality crystals (Figure 3.4) were obtained via simple filtration thru a SiO_2 SPE followed by concentration.

The diversification reaction in this protocol was further extended to incorporate the Suzuki-Miyaura coupling reaction. Thus, deprotected oligomer **3.20** was also alkylated with *p*-iodobenzyl bromide to yield oligomer **3.22** that was subjected to the coupling reaction,[16] followed by reductive ozonolysis to afford sultams **3.23a–b** in excellent yields and purities.

Scheme 3.4 *Incorporation of the Suzuki-Miyaura coupling reaction*

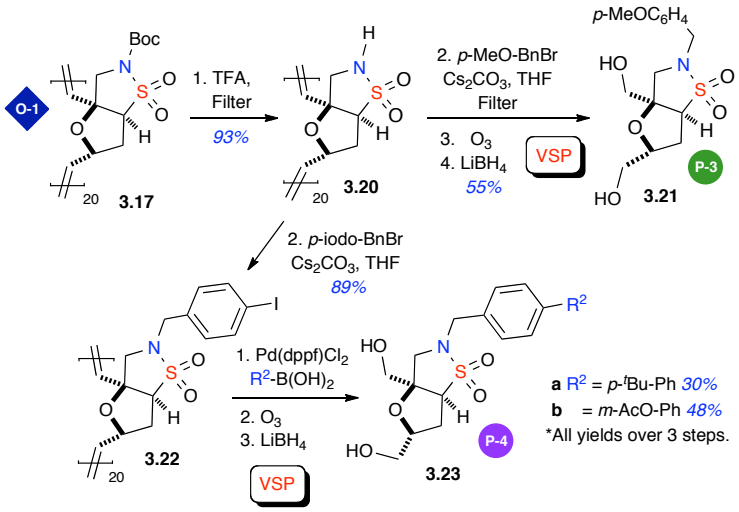

Overall, this method offers several advantages, including (i) atom economy; where all of the oligomer (ie. reclaimed scaffold) is converted to product(s) after annihilation, (ii) no additional linker is required (in contrast to traditional SPOS), (iii) a single starting scaffold affords four different scaffolds via parallel processing with minimal waste stream.

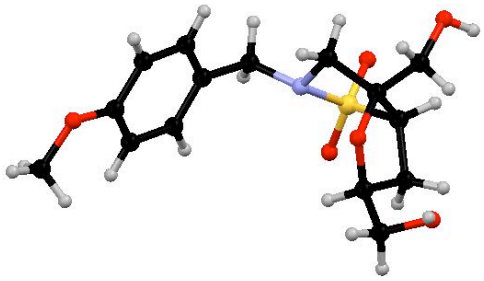

Figure 3.4 *X-ray crystal structure (**3.21**) depicted as a single enantiomer*

In a proof-of-concept experiment, sultam **3.24**, a derivative of **3.15**, was subjected to Sharpless dihydroxylation conditions with *N*-methyl morpholine *N*-oxide (oxidant) as the limiting reagent (Scheme 3.5).[17] After depletion of the oxidant, diol **3.25** was immediately liberated via crystallization during the polymerization event of **3.24** affording x-ray quality crystals (Figure 3.5) after simple filtration and concentration. The reclaimed scaffold **3.26** was then further processed via Suzuki-Miyaura coupling as previously described, followed again by reductive ozonolysis to afford products **3.28a–b** in good yields and excellent purity over the three-step sequence. This proof-of-concept experiment demonstrated the overall compatibility and functional group tolerance of ROM-polymerization processes while having highlighted the purity of the initial parent product as a result of the polymerization event.

Scheme 3.5 *Proof-of-concept purification experiment*

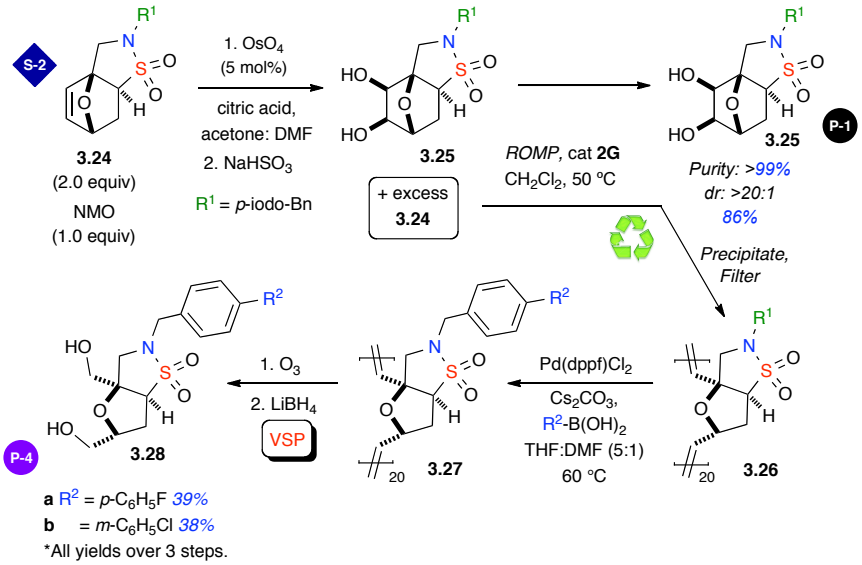

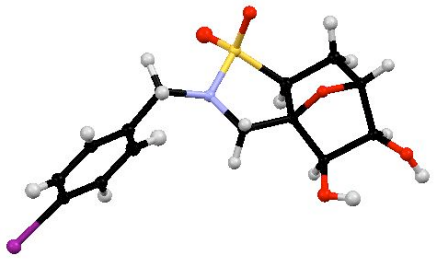

Figure 3.5 *X-ray crystal structure (**3.25**) depicted as a single enantiomer*

3.3 Conclusions and Future Outlook

In conclusion, a new atom-economical method utilizing ROM-polymerization and a vanishing support protocol has been described. This strategy allows for parallel processing of a reductive Heck product as well as reclamation of excess sultam oligomer that is further diversified and annhilated to yield an array of skeletally diverse sultam scaffolds. This method was extended to a diastereoselective dihydroxylation reaction demonstrating the compatibility and functional group tolerance of ROM-polymerization processes. Future work focusing on additional scaffolds and diversity-generating reaction pathways for library development will be reported in due course including new ROMP-derived strategies for facile purification and PASP reaction processing.

References

(1) (a.) Ley, S. V.; Ladlow, M.; Vickerstaffe, E., *Exploiting Chemical Diversity for Drug Discovery;* Bartlett, P. A.; Entzeroth, M., Eds.; Royal Society of Chemistry, Cambridge, UK, 2006, pp 3–32. (b.) Hart, T., Future combinatorial strategies for chemistry and biology. *Drug Discov. Today,* **2001**, *6*, 937–939.

(2) Although reagents used in excess represent waste, their use streamlines the purification process.

(3) Rabasseda, X.; Hopkins, S. J., Ampiroxicam: A prodrug of piroxicam devoid of gastrointestinal toxicity. *Drugs of Today* **1994**, *30*, 557–563.

(4) Brzozowski, Z.; Saczewski, F.; Neamati, N., Synthesis and anti-HIV-1 activity of a novel series of 1,4,2-benzodithiazine-dioxides. *Bioor. Med. Chem. Lett.* **2006**, *16*, 5298–5302.

(5) Wroblewski, T.; Graul, A.; Castaner, J., Brinzolamide. *Drugs Future* **1998**, *23*, 365–369.

(6) Tanimukai, H.; Inui, M.; Harigushi, S.; Kaneko, J., Antiepileptic property of inhibitors of carbonic anhydrase. *Biochem. Pharmacol.* **1965**, *14*, 961–970.

(7) Wells, G. J.; Tao, M.; Josef, K. A.; Bihovsky, R., 1,2-Benzothiazine 1,1-dioxide P(2)-P(3) peptide mimetic aldehyde calpain I inhibitors. *J. Med. Chem.* **2001**, *44*, 3488–3503.

(8) (a) Jiménez-Hopkins, M.; Hanson, P. R., An RCM Strategy to Stereodiverse δ-Sultam Scaffolds. *Org. Lett.* 2000, **2**, 709–712. (b) Jeon, K. O.; Rayabarapu, D.; Rolfe, A.; Volp, K.; Omar, I.; Hanson, P. R. Metathesis Cascade Strategies (ROM-RCM-CM): A DOS Approach to Skeletally Diverse Sultams. *Tetrahedron* **2009**, *65*, 4992–5000.

(9) (a) Schindler, C. S.; Carreira, E. M., Rapid formation of complexity in the total synthesis of natural products enabled by oxabicyclo[2.2.1]heptene building blocks., *Chem. Soc. Rev.* **2009**, *38*, 3222–3241. (b) Singh, V.; Sahu, P. K.; Sahu, B. C.; Mobin, S. M., Diels-Alder Cycloaddition and Ring-Closing Metathesis: A Versatile, Stereoselective, and General Route to Embellished Bridged Bicyclic Systems, Carbocyclic Framework of Secoatisanes, and Homologues *J. Org. Chem.*, **2009**, *74*, 6092–6104. (c) Lee, D.; Sello, J. K.; Schreiber, S. L.,

Pairwise Use of Complexity-Generating Reactions in Diversity-Oriented Organic Synthesis. *Org. Lett.* **2000**, *2*, 709–712. (d) Di Micco, S.; Vitale, R.; Pellecchia, M.; Rega, M. F.; Riva, R.; Basso, A.; Bifulco, G. Identification of Lead Compounds as Antagonists of Protein Bcl-xL with a Diversity-Oriented Multidisciplinary Approach. *J. Med. Chem.* **2009**, *52*, 7856–7867.

(10) Thomas, G. L.; Spandl, R. J.; Glansdorp, F. G.; Welch, M.; Bender, A.; Cockfield, J.; Lindsay, J. A.; Bryant, C.; Brown, D. F. J.; Loiseleur, O.; Rudyk, H.; Ladlow, M.; Spring, D. R., Anti-MRSA agent discovery using diversity-oriented synthesis. *Angew. Chem. Int. Ed.* **2008**, *47*, 2808–2812.

(11) Of notable importance is the seminal advances made by Barrett and coworkers demonstrating the concepts of reagent annihilation (norbornenyl-tagged DEAD) and polymer backbone degradation. (a) Barrett, A. G. M.; Roberts, R. S.; Schröder, J., Impurity Annihilation: Chromatography-Free Parallel Mitsunobu Reactions. *Org. Lett.*, **2000**, *2*, 2999–3002. (b) Ball, C. P.; Barrett, A. G. M.; Poitout, L. F.; Smith, M. L.; Thorn, Z. E., Polymer backbone disassembly: polymerizable templates and vanishing supports in high loading parallel synthesis. *Chem. Commun.* **1998**, 2453–2454.

(12) Moore, J. D.; Harned, A. M.; Henle, J.; Flynn, D. L.; Hanson, P. R., Scavenge-ROMP-Filter: A Facile Strategy for Soluble Scavenging via Norbornenyl Tagging of Electrophilic Reagents. *Org. Lett.* **2002**, *4*, 1847–1849.

(13) Metz, P.; Seng, D.; Frohlich, R.; Wibbeling, B., Intramolecular Diels-Alder reactions of vinylsulfonamides. *Synlett* **1996**, 741–742.

(14) (a) Chen, C. L.; Martin, S. F., Facile Synthesis of 2-Substituted 1,2-Dihydro-1-naphthols and 2-Substituted 1-Naphthols. *Org. Lett.* **2004**, *6*, 3581–3584. (b) Duan, J. P.; Cheng, C. H., Palladium-catalyzed stereoselective reductive coupling reactions of organic halides with 7-heteroatom norbornadienes. *Tetrahedron Lett.* **1993**, *34*, 4019–4022.

(15) Cheng, C.; Qi, K.; Khoshdel, E.; Wooley, K. L., Tandem Synthesis of Core-Shell Brush Copolymers and Their Transformation to Peripherally Cross-Linked and Hollowed Nanostructures. *J. Am. Chem. Soc.* **2006**, *128*, 6808–6809.

(16) Notably, the Suzuki reaction of monomeric **8** afforded an inseparable mixture of products (Suzuki product as well as product resulting from the double Heck-addition across the double bond), thus further substantiating the use of the entitled process.

(17) Sharpless, K. B.; Amberg, W.; Youssef, B. L.; Crispino, G. A.; Hartung, J.; Jeong, K.; Kwong, H.; Morikawa, K.; Wang, Z.; Daqiang, X.; Zhang, X., The osmium-catalyzed asymmetric dihydroxylation: a new ligand class and a process improvement. *J. Org. Chem.,* **1992**, *57*, 2768–2771.

Chapter 4

The Development and Application of Cobalt-based ROMPgel Magnetic Nanoparticles

4.1 Introduction

Developmental research of magnetic nanomaterials for applications in the medical[1] and chemical[2] fields has steadily increased in the last several decades. As a result, several strategies have surfaced for the facile assembly of diverse inorganic and organic frameworks with inherent magnetic properties. These studies include pioneering efforts made in the area of supported-catalysis where materials such as silica, carbon or polymers have been doped with magnetic nanoparticles.[3]

In recent years, a substantial number of reports have also focused on defined core/shell assemblies based on superparamagnetic iron oxide nanoparticles (SPION), such as magnetite.[3,4] A lack of magnetic remanence in this material in the absence of an external magnetic field is especially beneficial for the dispersability of these nanoparticles in a heterogeneous reaction environment. However, this advantage is accompanied by a relatively low saturation moment of these ferrites ($M_{S,bulk} \leq 92$ emu/g). When compared to bulk, this moment is usually far lower in the nano-sized mater due to partial oxidation on the surface, and sometimes diminished further through its requisite outer protective shell.[5] As a consequence, hybrid materials that rely on iron oxide nanoparticles require a high metal content for effective magnetic susceptibility, thus limiting functional group load capacity and their use as supported reagents. Nanoparticles derived from pure metals, however, exhibit superior magnetic properties as compared to oxides, but their synthesis had been limited to small-scale operations.[6,7]

Recently, Grass and coworkers[8] reported on a continuous process, in which large amounts of carbon coated ferromagnetic nanoparticles (> 30 g/h) are accessible via reducing flame-spray pyrolysis.[9] Despite the comparatively thin graphene layer (1 nm), the built-in pyrophoric cobalt cores reveal remarkable thermal and chemical stability[10] and more importantly, the protective carbon layer surrounding the cobalt core had no detrimental effect on the overall magnetization (158 emu/g). From a synthetic perspective, Co/C-nanomagnets allow for simple and rapid separation via magnetic decantation but are limited by their loading (0.1 mmol/g)[8] due to the sheer mass of the carbon/cobalt framework. As a result, their usefulness as magnetically recoverable supports in facilitated synthesis was deemed quite limited.

Reported herein is a brief investigation that was conducted to combine the favorable attributes of ROMP technology to facilitate increased load capacities of cobalt/carbon-nanoparticles (Co/C-NP) for the purpose of supported-catalysis. This was readily achieved through the development of new ROMP-hybrid, magnetic materials that were used as magnetically recoverable and recyclable Pd catalysts in Suzuki-Miyaura coupling reactions.

4.2 Results and Discussion

In order to combine these two different technologies, we envisaged the covalent attachment of a norbornene-tag (Nb-tag) onto the surface of the Co/C-NP (Scheme 4.1), followed by ROM-polymerization in the presence of a Nb-tagged ligand to ultimately immobilize the ligand onto the surface of the Co/C-NPs. Buchmeiser[11] Grubbs[12] and Whitesides,[13] all have demonstrated ROM-polymerization on silica

surfaces, while Buchmeiser and Barrett have also reported ROM-polymerization on polystyrene resins.[14] In 2003, Barrett et. al. used a ROMPgel supported triphenyl-phosphine as a supported ligand for the attachment of Wilkinson's catalyst.[15] Numerous imidazolium norbornene units (**4.2**) were also incorporated into the polymer backbone to create a bi-functional ROMPgel **4.3** that retained the attributes of an ionic liquid (Figure 4.1). Catalyst **4.4** was successfully used to facilitate hydrogenation of a collection of olefin-containing compounds.

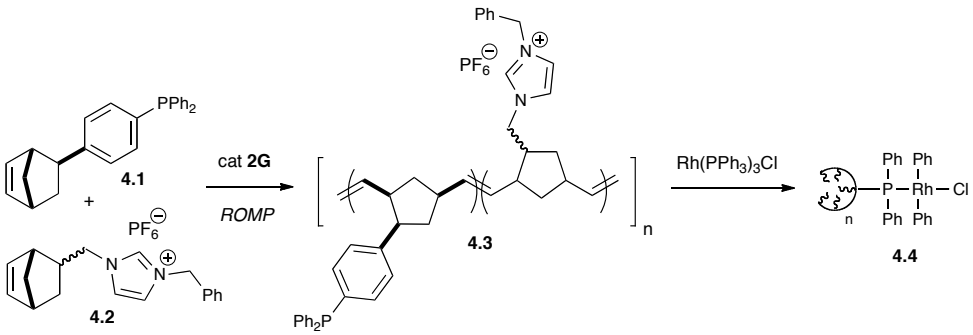

Figure 4.1 *Ionic ROMPgel-supported Wilkinson's catalyst for hydrogenation*

ROMP-derived oligomers themselves have also been used as surfactants to stabilize maghemite nanoparticles, although the magnetization of the resulting composite was not reported.[16] The covalent attachment of a ROMP-derived oligomer onto magnetic nanoparticles, however, is unprecedented.

Synthesis of the azide-tagged nanoparticles (Scheme 4.1) was achieved in a concise two-step reaction based on the covalent attachment of diazonium compounds on graphene layers as described previously.[8a,17] An azide-loading of 0.1 mmol/g was obtained for **4.6** as determined by elemental microanalysis. This was subjected to the

Huisgen [3+2] cycloaddition ("click") reaction[18] to graft propargylated norbornene

Scheme 4.1 *Functionalization of azide-tagged Co/C-nanoparticles with $OTPP_{50}$*

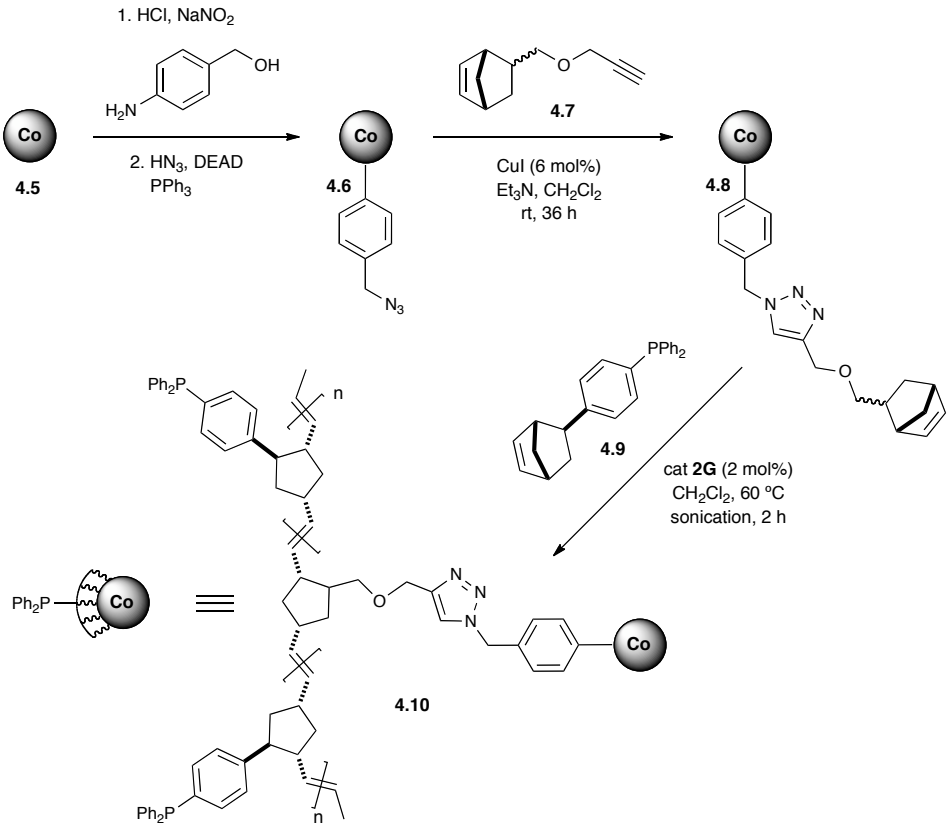

derivative **4.7** onto azide functionalized Co/C-NPs **4.6**. In this combined strategy, Nb-tagged **4.8** now presented the necessary linkage for which ROM-copolymerization could be effectively achieved. This reaction was monitored by solid-phase IR spectroscopy with the disappearance of the azide peak at ~2100 cm^{-1}.

Nb-tagged Co/C-NPs **4.8** were then placed in sealed pressure tube in a tempered (60 °C) ultrasonic bath and the nanopowder was dispersed in degassed CH_2Cl_2 via sonication under an inert atmosphere (argon). After which time a solution of catalyst **2G** (2 mol% in respect to **4.9**) was added to the mixture. ROM-copolymerization was

carried out using PPh_3-functionalized norbornene **4.9**[19] (50.0 equiv. in respect to **4.8** @ 0.1 mmol/g) under conditions suitable for theoretical formation of a grafted 50mer. During the course of the reaction, the voluminous, black Co/C-ROMPgel **4.10** was formed, leaving behind little residual solvent. Assuming that all Co/C-nanoparticles were coated with the available amount of oligomer, one would expect a Co-content of approximately 33% in the resulting hybrid material, a value that was confirmed by elemental microanalysis. TEM images confirmed the embedment of Co/C-particles in a polymer matrix, reducing the otherwise densely packed clusters to a more spatial arrangement (Figure 4.2). No evidence of cross linking was observed in agreement with earlier studies in which metathesis between an immobilized norbornene derivative and dissolved olefins was carried out.[20]

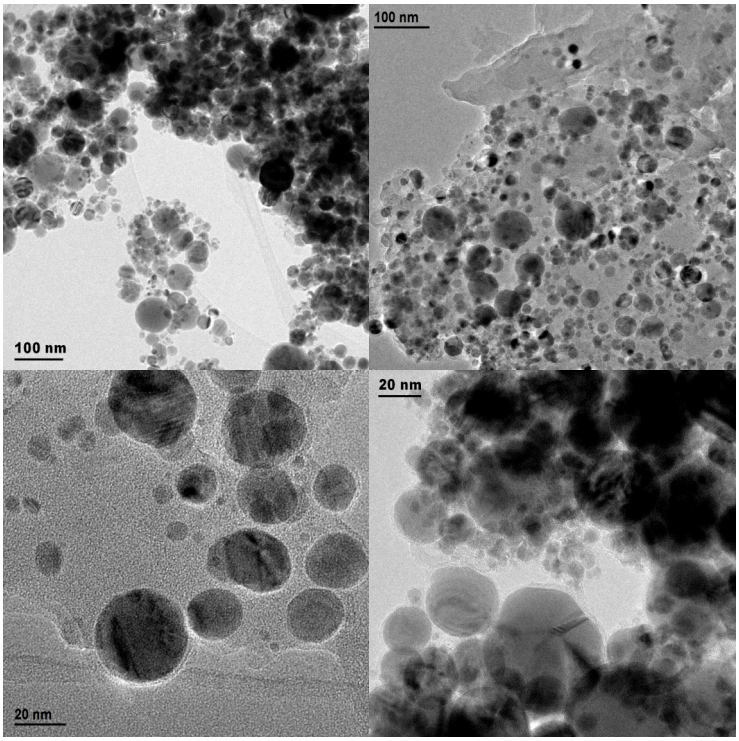

Figure 4.2 *TEM Images of Co/C-nanoparticles **4.5**(left) and Co/C-ROMPgel **4.10** (right)*

A control experiment utilizing azide-functionalized Co/C-NPs **4.6** instead of Nb-tagged nanoparticles **4.8** was conducted to ensure that the polymer did not only encapsulate the nanomagnets but was instead covalently attached to the carbon shell. In contrast to the previous observation, no gel was formed during this control and the nanoparticles remained in solution as heterogeneous particulates. The oligomer remained soluble in solution until precipitated from MeOH. The swelling behavior of Co/C-ROMPgel **4.10** was found to be in line with the general properties of ROMPgels, showing a pronounced volume increase in THF and CH_2Cl_2 whereas solvents such as MeOH or Et_2O did not provoke a significant effect.[21]

The morphology of this new hybrid material was clearly distinct from both parent materials as observed in scanning electron micrographs (SEM) (Figure 4.3). The aforementioned oligomeric triphenylphosphine ($OTPP_{50}$)[19b] obtained from the control experiment (Figure 4.2a) was analyzed next to unmodified Co/C-nanoparticles **4.5** (Figure 4.2b). In addition, the specimen stub was coated with atomized silver prior to deposition of Co/C-ROMPgel **4.10** to prevent the accumulation of static electric charge on the sample and to display its inherent magnetic field (Figure 4.3c). Energy dispersive X-ray (EDX) (Figure 4.2d) and ^{31}P NMR[22] confirmed the presence of phosphorus in the hybrid material. The fraction of phosphorus was assessed via elemental microanalysis (3.45%), corresponding to 1.1 mmol/g *P*-loading. Hence, approximately 30% of the hybrid material consists of triphenylphosphine (TPP). The immobilized TPP was expected to render the nanocomposite with the ability to serve

as a separable reagent/ scavenging agent[23] or a ligand, i.e. for the formation of a recyclable palladium complex.

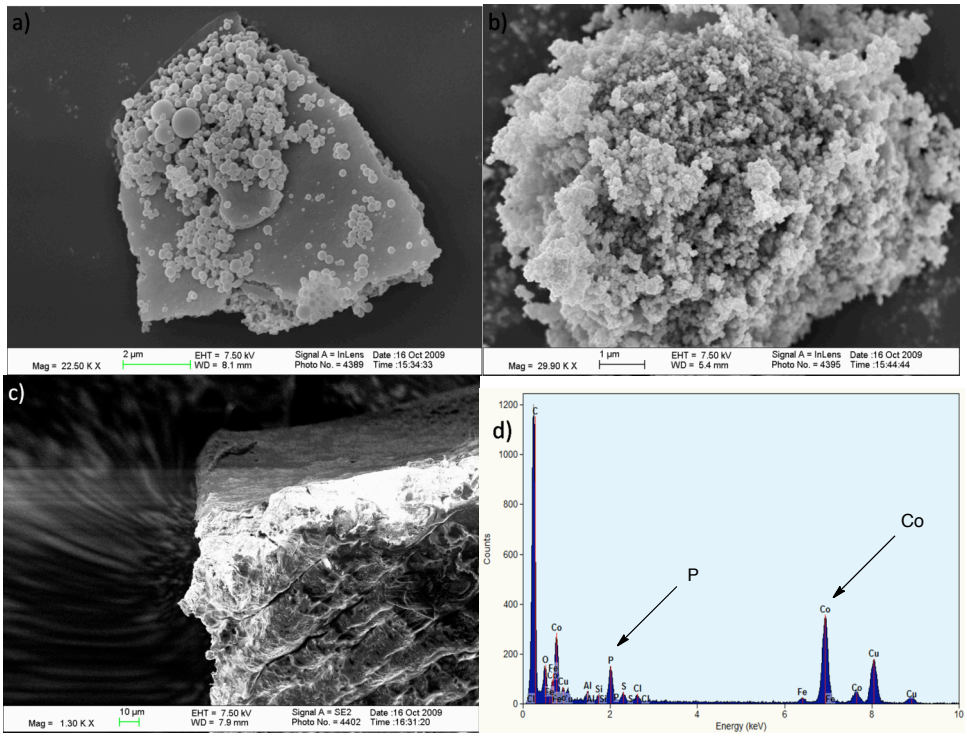

Figure 4.3 *SEM images of $OTPP_{50}$ (a), Co/C-nanoparticles **4.5** (b), and Co/C-ROMPgel **4.10** (c), EDX-Spectrum of **4.10** (d)*[24]

4.2.1 Catalysis with a Co/C-ROMPgel immobilized Pd-complex

A number of examples of palladium complexes anchored on different magnetic iron oxide nanoparticles have been reported in the past years.[4,25] However, highly functionalized architectures that relied on stabilized ferrite cores were naturally less susceptible to magnetic separation as previously discussed. The doping of such complexes with palladium is typically achieved by mixing the metal source together with the ligand-functionalized scaffold (Scheme 4.2). This is often prone to further diminish the mass magnetization making for a difficult recovery process. However,

the magnetization of composite **4.11**, which was measured via vibrating sample magnetometer (VSM), was found to be 34 emu/g, a value consistent with the mass percentage of the ferromagnetic cobalt core in the sample. This level is comparable to surfactant stabilized SPIONs, however, polymer or silica coated iron oxide NPs which resembles **4.11** in terms of durability, exhibit significantly lower magnetization.[5]

Scheme 4.2 *Heterogeneous Palladium-metathesis onto PPh_3-functionalized Co/C-ROMPgel **4.10**. The Pd-content of **4.11** was assessed by AAS (0.48 mmol/g)*

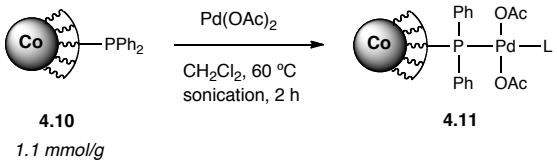

4.10
1.1 mmol/g

4.11

To determine the catalytic efficacy of Pd-catalyst **4.11**, we subjected it to several consecutive Suzuki-Miyaura cross-coupling reactions[26] of aryl halides with phenylboronic acids (Table 4.1). As it is common in such reactions, iodides are consistently more reactive than bromides or chlorides, therefore when iodobenzene was chosen as substrate (entries 1, 3, 4 and 6), good to excellent yields were achieved. Importantly, catalyst **4.11** was quantitatively recovered after each reaction and reused in the next run, proving the suitability of the new Co/C-ROMPgel as a high-capacity support that can be readily recovered and recycled by magnetic separation.

Table 4.1 *Suzuki-Miyaura cross-coupling reactions catalyzed by recyclable Co/C-ROMPgel immobilized Pd-complex* ***4.11***

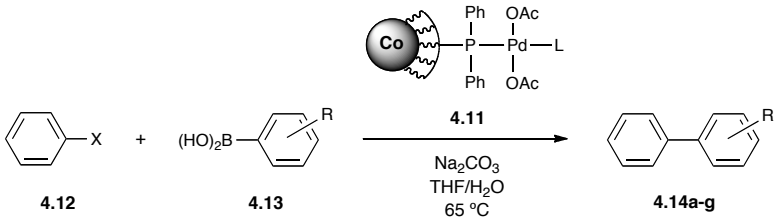

entry	run	X	R	time (h)	yield (%)
1	1	I	H	2	96
2	2	Cl	H	6	38
3	3	I	2-Br	2	95
4	4	I	2-Me	2	90
5	5	Br	H	12	92
6	6	I	4-*t*-Bu	4	86
7	7	I	H	4	90

[a] Reagents and conditions: Phenylhalide (0.5 mmol), phenylboronic acid (0.55), Na_2CO_3 (1.5 mmol), 1.1 mol% cat **4.11**, 65 °C, solvent 3 mL THF/H_2O (1:2 v/v)

4.3 Conclusions and Future Outlook

In conclusion we have demonstrated the ability to incorporate the favorable, high-loading attributes of ROMP technology with cobalt-based, magnetic nanoparticles to create a new hybrid material (Co/C-ROMPgel). We have also highlighted the use of this material as a support for Pd-catalysis – having demonstrated its use in Suzuki-Miyaura coupling reactions and revealed its ability to be recycled via magnetic recovery.

This composite might also be suitable for alternative assemblies that rely on iron oxides as magnetic core material. More importantly, from a synthetic application standpoint, these will likely prove useful in automated synthesis where manipulation via magnetic field could readily be achieved.

Currently, this hybrid material is proving useful in a number of other applications including the Mitsunobu reaction. This material allows for the convenient sequestration and removal of monomeric norbornene-based reagents (Ph_3P and DEAD) via *in situ* ROM-polymerization and magnetic decantation. This may also prove effective as a magnetically recoverable and reusable source of triphenylphosphine. Results of these endeavors will be reported in due course.

References

(1) (a) Lee, H.; Lee, E.; Kim, D. K.; Jang, N. K.; Jeong, Y. Y.; Jon, S., Antibiofouling Polymer-Coated Superparamagnetic Iron Oxide Nanoparticles as Potential Magnetic Resonance Contrast Agents for in Vivo Cancer Imaging. *J. Am. Chem. Soc.* **2006**, *128*, 7383–7389. (b) Xu, Z. P.; Zeng, Q. H.; Lu, G. Q.; Yu, A. B., Inorganic nanoparticles as carriers for efficient cellular delivery. *Chem. Eng. Sci.* **2005**, Vol. Date **2006**, *61*, 1027–1040; (c) Kim, J.; Kim, H. S.; Lee, N.; Kim, T.; Kim, H.; Yu, T.; Song, I. C.; Moon, W. K.; Hyeon, T., Multifunctional uniform nanoparticles composed of a magnetite nanocrystal core and a mesoporous silica shell for magnetic resonance and fluorescence imaging and for drug delivery. *Angew. Chem. Int. Ed.* **2008**, *47*, 8438–8441. (d) Park, K.; Lee, S.; Kang, E.; Kim, K.; Choi, K.; Kwon, I. C., New generation of multifunctional nanoparticles for cancer imaging and therapy. *Adv. Funct. Mater.* **2009**, *19*, 1553–1566; (e) Gleeson, O.; Tekoriute, R.; Gun'ko, Y. K.; Connon, S. J., The First Magnetic Nanoparticle-Supported Chiral DMAP Analogue: Highly Enantioselective Acylation and Excellent Recyclability. *Chem. Eur. J.* **2009**, *15*, 5669–5673.

(2) (a) Shokouhimehr, M.; Piao, Y.;Kim, J.; Jang, Y.; Hyeon, T., A magnetically recyclable nanocomposite catalyst for olefin epoxidation. *Angew. Chem. Int. Ed.* **2007**, *46*, 7039–7043; (b) Sobal, N. S.; Hilgendorff, M.; Möhwald, H.; Giersig, M., Synthesis and Structure of Colloidal Bimetallic Nanocrystals: The Non-Alloying System Ag/Co. *Nano Lett.* **2002**, *2*, 621–624. (c) Ceylan, S.; Friese, C.; Lammel, C.; Mazac, K.; Kirschning, A., Inductive heating for organic synthesis by using functionalized magnetic nanoparticles inside microreactors. *Angew. Chem. Int. Ed.* **2008**, *47*, 8950–8953.

(3) (a) Lu, A.-H.; Li, W. C.; Kiefer, A.; Schmidt, W.; Bill, E.; Fink, G.; Schüth, F., Fabrication of Magnetically Separable Mesostructured Silica with an Open Pore System. *J. Am. Chem. Soc.* **2004**, *126*, 8616–8617. (b) Lu, A.-H.; Schmidt, W.; Matoussevitch, N.; Bönnemann, H.; Spliethoff, B.; Tesche, B.; Bill, E.; Kiefer, W.; Schüth, F., Magnetic carbon: Nanoengineering of a magnetically separable hydrogenation catalyst. *Angew. Chem. Int. Ed.* **2004**, *43*, 4303–4306; (c) Lu, A-H.; Li, W.; Matoussevitch, N.; Spliethoff, B.; Pennemann, H. B.; Schüth, F., Highly stable carbon-protected cobalt nanoparticles and graphite shells. *Chem. Commun.* **2005**, 98–100.

(4) (a) Stevens, P. D.; Fan, J.; Gardimalla, H. M. R.; Yen, M.; Gao, Y., Superparamagnetic Nanoparticle-Supported Catalysis of Suzuki Cross-Coupling Reactions. *Org. Lett.* **2005**, *7*, 2085–2088. (b) Duanmu, C.; Saha, I.; Zheng, Y.;

Goodson, B. M.; Gao, Y., Dendron-Functionalized Superparamagnetic Nanoparticles with Switchable Solubility in Organic and Aqueous Media: Matrices for Homogeneous Catalysis and Potential MRI Contrast Agents. *Chem. Mater.* **2006**, *18*, 5973–5981. (c) Abu-Reziq, R.; Alper, H.; Wang, D.; Post, M. L., Metal supported on dendronized magnetic nanoparticles: highly selective hydroformylation catalysts. *J. Am. Chem. Soc.* **2006**, *128*, 5279–5282. (d) Arai, T.; Sato, T.; Kanoh, H.; Kaneko, K.; Oguma, K.; Yanagisawa, A., Organic-inorganic hybrid polymer-encapsulated magnetic nanobead catalysts. *Chem. Eur. J.* **2008**, *14*, 882–885.

(5) (a) Butterworth, M. D.; Illum, L.; Davis, S. S., Preparation of ultrafine silica- and PEG-coated magnetite particles. *Colloids and Surfaces A: Physicochem. Eng. Aspects* **2001**, *179*, 93–102. (b) Sun, H. Y.; Feng, S. Z.; Nie, X. F.; Sun, Y. P., Effect of Co layer thickness on structural and magnetic properties of C/Co/C films. *J. Magn. Magn. Mater.* **2005**, Vol. Date **2006**, *299*, 70–74. (c) Deng, Y.-H.; Wang, C.-C.; Hu, J.-H.; Yang, W.-L.; Fu, S.-K., Investigation of formation of silica-coated magnetite nanoparticles via sol-gel approach. *Colloids and Surfaces A: Physicochem. Eng. Aspects* **2005**, *262*, 87–93.

(6) (a) Saito, Y., Nanoparticles and filled nanocapsules. *Carbon* **1995**, *33*, 979–988. (b) Scott, J. H. J.; Majetich, S. A., Morphology, structure, and growth of nanoparticles produced in a carbon arc. *Phys. Rev. B* **1995**, 52, 12564–12571. (c) Jiao, J.; Seraphin, S.; Wang, X.; Withers, J. C., Preparation and properties of ferromagnetic carbon-coated Fe, Co, and Ni nanoparticles. *J. Appl. Phys.* **1996**, *80*, 103–108.

(7) (a) Wang, Z. H.; Choi, C. J.; Kim, B. K.; Kim, J. C.; Zhang, Z. D., Characterization and magnetic properties of carbon-coated cobalt nanocapsules synthesized by the chemical vapor-condensation process. *Carbon* **2003**, *41*, 1751–1758. (b) Flahaut, E.; Agnoli, F.; Sloan, J.; O'Connor, C.; Green, M. L. H., CCVD Synthesis and Characterization of Cobalt-Encapsulated Nanoparticles. *Chem. Mater.* **2002**, *14*, 2553–2558.

(8) (a) Grass, R. N.; Athanassiou, E. K.; Stark, W. J., Covalently functionalized cobalt nanoparticles as a platform for magnetic separations in organic synthesis. *Angew. Chem. Int. Ed.* **2007**, *46*, 4909–4912. (b) Herrmann, I. K.; Grass, R. N.; Mazunin, D.; Stark, W. J., Synthesis and Covalent Surface Functionalization of Nonoxidic Iron Core-Shell Nanomagnets. *Chem. Mater.* **2009**, *21*, 3275–3281. (c) Grass, R. N.; Stark, W. J., Gas phase synthesis of fcc-cobalt nanoparticles. *J. Mater. Chem.* **2006**, *16*, 1825–1830; (d) Wittmann, S.; Schätz, A.; Grass, R. N.; Stark, W. J.; Reiser, O., A Recyclable Nanoparticle-Supported Palladium

Catalyst for the Hydroxycarbonylation of Aryl Halides in Water. *Angew. Chem.* **2010**, *49*, 1867–1870.

(9) Stark, W. J.; Madler, L.; Maciejewski, M.; Pratsinis, S. E.; Baiker, A., Flame synthesis of nanocrystalline ceria-zirconia: effect of carrier liquid. *Chem. Commun.* **2003**, 588–589.

(10) (a) Koehler, F. M.; Rossier, M.; Waelle, M.; Athanassiou, E. K.; Limbach, L. K.; Grass, R. N.; Günther, D.; Stark, W. J., Magnetic EDTA: Coupling heavy metal chelators to metal nanomagnets for rapid removal of cadmium, lead and copper from contaminated water. *Chem. Commun.* **2009**, *32*, 4862–4864. (b) Rossier, M.; Koehler, F. M.; Athanassiou, E. K.; Grass, R. N.; Aeschlimann, B.; Günther, D.; Stark, W. J., Gold adsorption on the carbon surface of C/Co nanoparticles allows magnetic extraction from extremely diluted aqueous solutions. *J. Mater. Chem.* **2009**, *19*, 8239–8243.

(11) (a) Buchmeiser, M. R.; Seeber, G.; Mupa, M.; Bonn, G. K., ROMP-based, highly hydrophilic poly(7-oxanorborn-2-ene-5,6-dicarboxylic acid)-coated silica for analytical and preparative scale high-performance ion chromatography. *Chem. Mater.* **1999**, *11*, 1533–1540. (b) Buchmeiser, M. R.; Sinner, F. M.; Mupa, M.; Wurst, K., Ring-opening metathesis polymerization for the preparation of surface-grafted polymer supports. *Macromolecules* **2000**, *33*, 32–39. (c) Gatschelhofer, C. C. Magnes, Pieber, T. R.; Buchmeiser, M. R., Sinner, F. M., Evaluation of ring-opening metathesis polymerization (ROMP)-derived monolithic capillary high performance liquid chromatography columns. *J. of Chrom. A.* **2005**, *1090*, 81–89.

(12) Rutenberg, I. M.; Scherman, O. A.; Grubbs, R. H.; Jiang, W.; Garfunkel, E.; Zhenan, B., Synthesis of Polymer Dielectric Layers for Organic Thin Film Transistors via Surface-Initiated Ring-Opening Metathesis Polymerization. *J. Am. Chem. Soc.* **2004**, *126*, 4062–4063.

(13) Kim, N. Y.; Jeon, N. L.; Hoi, I. S.; Takami, S.; Harada, Y.; Finnie, K. R.; Girolami, G. S.; Nuzzo, R. G.; Whitesides, G. M.; Laibinis, P. E.; *Macromolecules* **2000**, *33*, 2793–2795.

(14) Barrett, A. G. M.; Cramp, S. M.; Roberts, R. S.; ROMP-Spheres: A Novel High-Loading Polymer Support Using Cross Metathesis between Vinyl Polystyrene and Norbornene Derivatives. *Org. Lett.* **1999**, 7, 1083–1086.

(15) Årstad, E.; Barrett, A. G. M.; Tedeschi, L., ROMPgel-supported tris(triphenylphosphine)rhodium(I) chloride: a selective hydrogenation catalyst for parallel synthesis., *Tetrahedron Lett*. **2003**, *44*, 2703–2707.

(16) Belfield, K. D.; Zhang, L., Norbornene-Functionalized Diblock Copolymers via Ring-Opening Metathesis Polymerization for Magnetic Nanoparticle Stabilization. *Chem. Mater*. **2006**, *18*, 5929–5936.

(17) (a) Schätz, A.; Grass, R. N.; Stark, W. J.; Reiser, O., Dependence of enantioselectivity on the ligand/metal ratio in the asymmetric Michael addition of indole to benzylidene malonates: electronic influence of substrates. *Chem. Eur. J*. **2008**, 14, 8262–8266. (b) Schätz, A.; Grass, R. N.; Kainz, Q.; Stark, W. J.; Reiser, O., Cu(II)-Azabis(oxazoline) Complexes Immobilized on Magnetic Co/C Nanoparticles: Kinetic Resolution of 1,2-Diphenylethane-1,2-diol under Batch and Continuous-Flow Conditions, *Chem. Mater*. **2010**, *22*, 305–310.

(18) (a) Tornøe, C. W.; Meldal, M., Peptidotriazoles: copper(I)-catalyzed 1,3-dipolar cycloadditions on solid-phase. In *American Peptide Symposium;* M. Lebl, R. A. Houghten, Eds., American Peptide Society and Kluwer Academic Publishers: San Diego, CA, 2001, pp 263–264. (b) Rostovtsev, V. V.; Green, L. G.; Fokin, V. V.; Sharpless, K. B., A stepwise Huisgen cycloaddition process: copper(I)-catalyzed regioselective "ligation" of azides and terminal alkynes. *Angew. Chem. Int. Ed*. **2002**, *41*, 2596–2599. (c) Tornøe, C. W.; Christensen, C.; Meldal, M., Peptidotriazoles on solid phase: [1,2,3]-triazoles by regiospecific copper(i)-catalyzed 1,3-dipolar cycloadditions of terminal alkynes to azides. *J. Org.Chem*. **2002**, *67*, 3057–3064.

(19) (a) ROMPgel-supported PPh_3: Årstad, E.; Barrett, A. G. M.; Hopkins, B. T.; Köbberling, J., ROMPgel-Supported Triphenylphosphine with Potential Application in Parallel Synthesis. *Org. Lett*. **2002**, *4*, 1975–1977. (b) Harned, A. M.; Song He, H.; Toy P. H., Flynn, D. L.; Hanson, P. R., Multipolymer Solution-Phase Reactions: Application to the Mitsunobu Reaction. *J. Am. Chem. Soc*. **2005**, *127*, 52–53. (c) Yang, Y.-C.; Luh, T.-Y. Polymeric Phosphine Ligand from Ring-Opening Metathesis Polymerization of a Norbornene Derivative. Applications in the Heck, Sonogashira, and Negishi Reactions. *J. Org. Chem*. **2003**, *68*, 9870-9873.

(20) (a) Cuny, G. D.; Cao, J.; Hauske, J. R., Ring opening cross-metathesis on solid support. *Tetrahedron Lett*. **1997**, *38*, 5237–5240. (b) Cao, J.; Cuny, G. D.; Hauske, J. R., Ring opening cross-metathesis on solid support: a combinatorial library synthesis of highly functionalized cyclopentanes. *Mol. Diversity* **1998**,

3, 173–179. (c) Week, M.; Jackiw, J. J.; Rossi, R. R.; Weiss, P. S.; Grubbs, R. H., Ring-opening metathesis polymerization from surfaces. *J. Am. Chem. Soc.* **1999**, *121*, 4088–4089. (d) Barrett, A. G. M.; Cramp, S. M.; Roberts, R. S., ROMP-Spheres: A Novel High-Loading Polymer Support Using Cross Metathesis between Vinyl Polystyrene and Norbornene Derivatives. *Org. Lett.* **1999**, *1*, 1083–1086 (e) Årstad, E.; Barrett, A. G. M.; Hopkins, B. T.; Koebberling, J., ROMPgel-Supported Triphenylphosphine with Potential Application in Parallel Synthesis. *Org. Lett.* **2002**, *4*, 1975–1977. (f) Roberts, R. S., ROMPgel beads in IRORI format: acylations revisited. *J. Comb. Chem.* **2005**, *7*, 21–32.

(21) Santini, R.; Griffith, M. C.; Qi, M., ROMPgel beads in IRORI format: acylations revisited. *Tetrahedron Lett.* **1998**, *39*, 8951–8954.

(22) See Appendix A for spectrum.

(23) (a) McKinley, S. V.; Rakshys, J. W., Wittig resins. Preparation and application of insoluble polymeric phosphoranes. *J. Chem. Soc., Chem. Commun.* **1972**, 134–135. (b) Bernard, M.; Ford, W. T., Wittig reagents bound to crosslinked polystyrenes. *J. Org. Chem.* **1983**, *48*, 326–332. (c) Tunoori, A. R., Dutta, D.; Georg, G. I., Polymer-bound triphenylphosphine as traceless reagent for Mitsunobu reactions in combinatorial chemistry: synthesis of aryl ethers from phenols and alcohols. *Tetrahedron Lett.* **1998**, *39*, 8751–8754. (d) Regen, S. L.; Lee, D. P., Solid phase phosphorus reagents. Conversion of alcohols to alkyl chlorides. *J. Org. Chem.* **1975**, *40*, 1669–1670.

(24) The Cu-signal in the EDX-spectrum originated from the copper grid, on which the sample was supported during measurement, not residual copper from the "click"- reaction. No traces of the ruthenium-based catalyst **2G** appeared in any spectrum.

(25) (a) Stevens, P. D.; Li, G.; Fan, J.; Yenb, M.; Gao, Y., Recycling of homogeneous Pd catalysts using superparamagnetic nanoparticles as novel soluble supports for Suzuki, Heck, and Sonogashira cross-coupling reactions. *Chem. Commun.* **2005**, 4435–4437. (b) Zheng, Y.; Stevens, P. D.; Gao, Y., Magnetic Nanoparticles as an Orthogonal Support of Polymer Resins: Applications to Solid-Phase Suzuki Cross-Coupling Reactions. *J. Org. Chem.* **2006**, *71*, 537–542. (c) Baruwati, B.; Reddy, K. M.; Manorama, S. V., Singh, R. K.; Parkash, O., Tailored conductivity behavior in nanocrystalline nickel ferrite. *Appl. Phys. Lett.* **2004**, *85*, 2833–2835. (d) Guin, D.; Baruwati, B.; Manorama, S. V., A simple chemical synthesis of nanocrystalline AFe2O4

(A=Fe, Ni, Zn): An efficient catalyst for selective oxidation of styrene. *J. Mol. Catal. A. Chem.* **2005**, *242*, 26–31.

(26) (a) Miyaura, N.; Yamada, K.; Suzuki, A., A new stereospecific cross-coupling by the palladium-catalyzed reaction of 1-alkenylboranes with 1-alkenyl or 1-alkynyl halides. *Tetrahedron Lett.* **1979**, *20*, 3437–3440. (b) Miyaura, N.; Suzuki, A., Palladium-Catalyzed Cross-Coupling Reactions of Organoboron Compounds. *Chem. Rev.* **1995**, *95*, 2457–2483. (c) Barder, T. E.; Walker, S. D.; Martinelli, J. R.; Buchwald, S. L., Catalysts for Suzuki-Miyaura Coupling Processes: Scope and Studies of the Effect of Ligand Structure. *J. Am. Chem. Soc.* **2005**, *127*, 4685–4696.

Chapter 5

Automated Library Synthesis of Thiadiazepin-1,1-dioxide-4-ones

5.1 Introduction

The continued search for biologically relevant small-molecules is of utmost importance for the advancement of human health.[1] With this notion, the area of diversity-oriented synthesis has emerged in recent years as a powerful strategy to embark upon this ever-demanding challenge.[2] This objective is currently being fueled by various functional group pairing (FG-pairing) strategies that render the ability to generate diverse collections of molecules in the fewest number of steps possible.[3] These key concepts are at the heart of the "Build/Couple/Pair (BCP)" strategy set forth by Schreiber and coworkers in 2008[4] and continues to be the impetus for DOS-based library efforts in medicinal chemistry.[5] Once such strategy by Porco and coworkers[3a] recently demonstrated a FG-pairing concept for the generation of skeletally diverse systems.

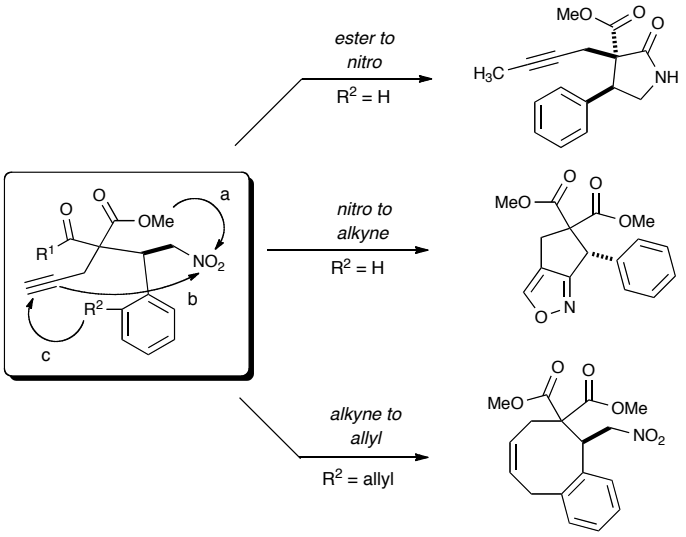

Figure 5.1 *Porco FG-pairing strategy*

To successfully facilitate a process in this manner, each FG-pairing pathway must be compatible with the functionality residing in other regions on the molecule, taking in consideration these may provide additional handles for future appendage attachment.

Our strategy entitled "*Click, Click, Cyclize*", highlighted below, utilizes a multi-functional linchpin approach[3b,6] wherein a number of sulfonamide precursors have been selected as key building blocks for sultam scaffold development.[7] This strategy was recently demonstrated utilizing a number of different methods: Oxa-Michael and Baylis-Hillman,[8] aza-Michael,[3b] ring-closing metathesis (RCM),[9] and cascade metathesis (ROM-RCM-CM)[10] for generation of multiple, skeletally diverse sultams in rapid fashion.

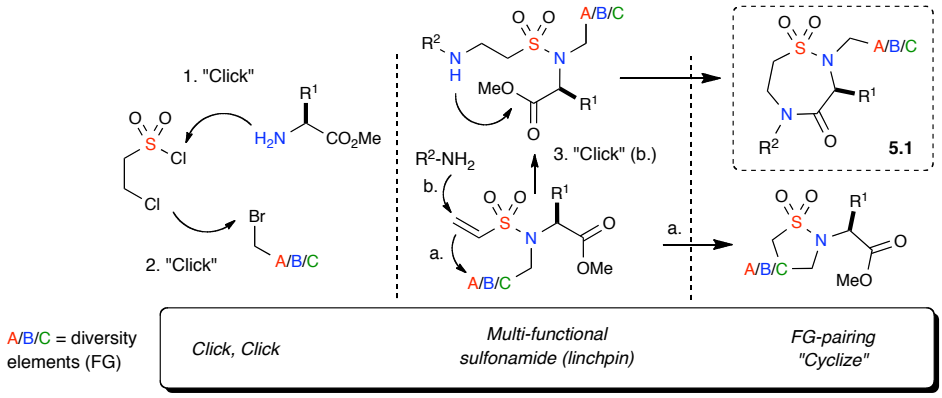

Figure 5.2 *Click/Click/Cyclize DOS strategy*

Until recently, the utility of this strategy had only previously been demonstrated for the generation of sultam scaffolds for small-scale (pilot) library production. This in part due to the majority of focus having been placed on new method development and pilot-scale library initiatives. However, with a collection of new methods in hand we

were then poised to further exploit these newly generated systems for larger-scale library production (100–300 compounds). In light of this new progression, we became interested in the development of a specific, thiadiazepin-1,1-dioxide-4-one (sultam) scaffold (**5.1**) for use in library production. Herein we describe efforts regarding the resynthesis, derivatization, and scaleup of this scaffold and its use in the production of a 225-member library using automated PASP and solution-phase protocols.

5.2 Results and Discussion

Having recently been synthesized in our group[3b], sultam motif **5.1** was of great interest in light of its similarity to other constrained peptidomimetic structures.[11] A very similar scaffold of this chemotype had previously been investigated by Liskamp[12] et. al. in the solid-phase synthesis of linear peptidosulfonamide libraries (Scheme 5.1). Interestingly, Liskamp makes note the amount of molecular diversity that can be achieved through the use of α- or β-substituted amino ethane sulfonamides as well as their facilitated synthesis by solid-phase (Merrifield) supports.

Scheme 5.1 *Solid-phase synthesis of cyclic peptidosulfonamides (sultams)*

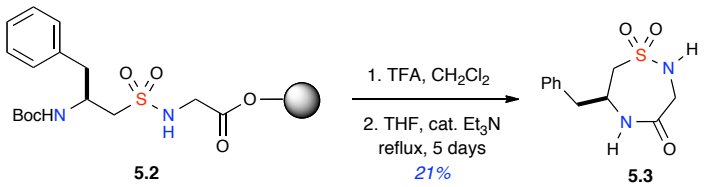

A number of seven-membered diazepinone-based scaffolds identified from literature have been shown to have interesting biological properties associated with

this core motif (Figure 5.3). These properties include inhibition of interleukin-1β (IL-1β)[13], modulatory activity of the follicle stimulating hormone receptor (FSHR)[14], as well as inhibition of the lymphocyte function-associated antigen-1 (LFA-1).[15]

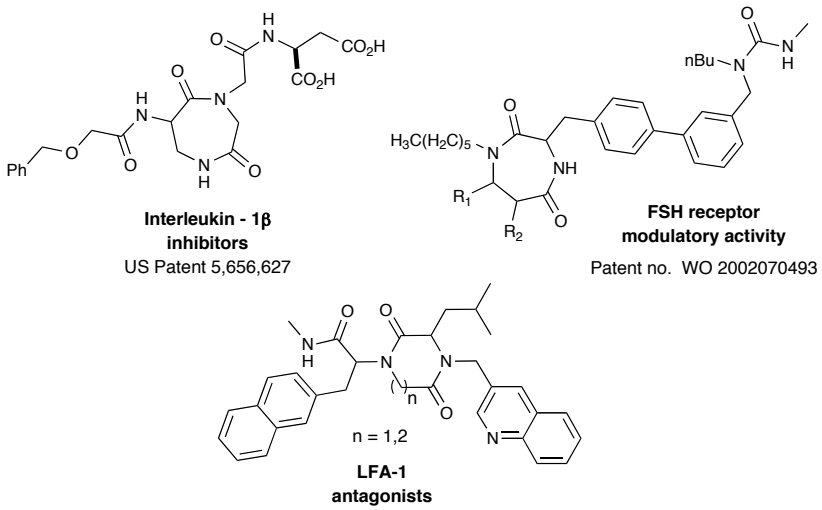

Figure 5.3 *Bioactive diazepinone-based structures*

Efforts to synthesize the general sultam motif (**5.1**) were next revisited to ensure the viablity of the current proceedure in regards to scale-up for library production (Scheme 5.2). Using conditions previously employed,[3b] sulfonylation of the *S*-valine methyl ester **5.4**{*2*} (ie. first "click reaction) was achieved using a masked vinyl sulfonyl chloride and DMAP to yield sulfonamide **5.5**{*2*}. This was then carried over without further purification and subjected to alkylation affording tertiary sulfonamide **5.6**{*2*}.

Scheme 5.2 *Scaffold resynthesis efforts*

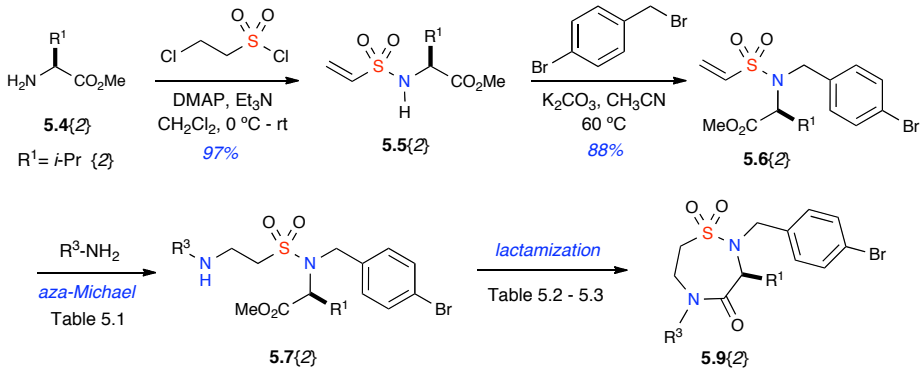

Previous efforts to facilitate the following aza-Michael addition (**5.6–5.7**) utilized a primary amine in a concentrated solution of MeOH (1M).[3b] However, due to complex mixtures and incomplete conversions w/ specific amines (Table 5.1, entry 1) at this stage we explored the use of catalytic amounts of DBU to aid the synthesis.[16] A noticeably longer reaction time was found using propargylamine as compared to isobutylamine. However, cleaner, more complete conversions were obtained for both using DBU as indicated by both TLC and GC analysis.

Table 5.1 *Aza-Michael optimization*

entry	R^3	amine equiv.	catalyst	equiv.	solvent	temp (°C)	time (h)	conv. (%)[a]
1	propargyl	1.1	x	x	MeOH	65	14	75
2	*i*-Bu	1.1	x	x	MeOH	65	3	88
3	*i*-Bu	1.1	DBU	0.5	CH_3CN	25	3	94
4	propargyl	1.1	DBU	0.5	CH_3CN	25	14	91
5	propargyl	1.2	DBU	0.5	CH_3CN	40	14	96

[a] Conversions (%) calculated by percent area using GC analysis.

We also explored a direct lactamization approach (Table 5.2) starting from tertiary sulfonamide **5.7**{*2*} to save an additional step in the synthesis as previous methods utilized a two-step hydrolysis/lactamization from **5.7–5.9**. With this notion, this

cyclization would also lend itself to the incorporation of more elements of diversity early in the synthesis without the need for aqueous acidic workups. A number of catalysts and conditions were tested at this stage (Table 5.2),[17] but despite several reports in the literature of similar transformations,[18] our efforts were met with little success.

Table 5.2 *Efforts towards a direct lactamization route via* ***5.7****{2}*

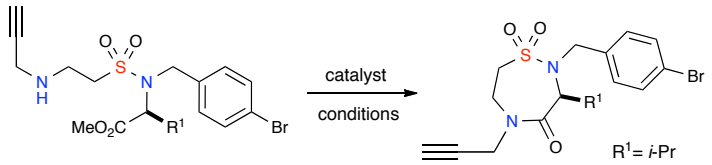

5.7{*2*} **5.9**{*2*}

entry	catalyst	equiv	additive	solvent	temp (ºC)	time (h)	yield (%)
1	$TiCl_4$	0.5	x	THF	25	24	NR
2	$TiCl_4$	1.0	x	DCE	150	24	NR
3	Et_3N	x	x	Et_3N	90	48	5
4	2-hydroxypyridine	0.5	x	toluene	120	24-48	20-27
5	2-hydroxypyridine	0.5	x	DCE	160	24-48	21
6	2-hydroxypyridine	0.2-0.5	x	DMF	160	24-48	39-56
7	2-hydroxypyridine	0.2	x	dioxane	μW 160	1	9
8	2-hydroxypyridine	0.2	x	toluene	μW 160	1	45
9	Otera's cat	0.05	x	toluene	μW 160	1	NR
10	AcOH	1	x	toluene	μW 160	1	NR
11	Zr(*t*-BuO)$_4$	1	x	toluene	μW 160	1	NR
12	Zr(*t*-BuO)$_4$	1	2-hydroxypyridine	toluene	μW 160	1	15
13	Zr(*t*-BuO)$_4$	1	HOAT	toluene	μW 160	1	NR

Despite having little success in a more direct synthetic route to the scaffold, we further pursued optimization of the current procedure involving lactamization via the sulfamido-amino acid. This was subsequently obtained via hydrolysis of amino-ester containing **5.7**{*2*} via aqueous LiOH to yield amino acid **5.8**{*2*} as a white-solid after neutralization (1M HCl). Due to its difficulty in separation from lithium salts, **5.8**{*2*}

was carried as a crude solid to the lactamization step. Cyclized product **5.9**{*2*} was obtained through the use of DCC as a coupling reagent, but was often contaminated with the urea byproduct as evident by ^{1}H-NMR. With this discovery, EDC was explored as an alternative coupling reagent for this step. Other reagents were also explored for lactamization (Table 5.3), including, but not limited to, oligomeric phosphorochloridate (OPC) and oligomeric dichlorotriazine (ODCT),[19] but each resulted in complete racemization of **5.9** as observed by optical rotation.

Table 5.3 *Continued efforts towards lactamization*

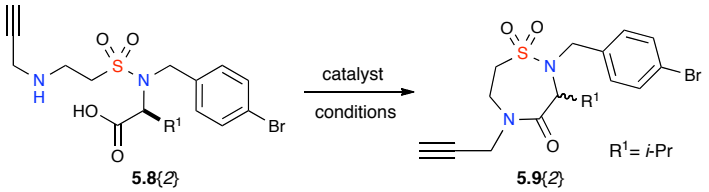

5.8{*2*} **5.9**{*2*}

entry	coupling reagent	base	solvent	temp (°C)	yield (%)	(±)[a]
1	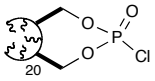	imidazole	CH_2Cl_2	25	95	√
2	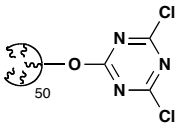	NMM	CH_2Cl_2	25	48	√
3	trichlorotriazine	NMM	CH_2Cl_2	25	99	√
4	phenyl dichlorophosphate	imidazole	CH_2Cl_2	25	90	√
5	DCC	NMM	CH_2Cl_2	25	84	
6	EDC/HOBt	NMM	CH_2Cl_2	25	90	

[a] (±) column displays complete racemization (√) as noted by optical rotation (α = 0.000) replicated x 3.

EDC was used with 10% HOBt to efficiently access **5.9**, but despite its reported use in the preservation of chirality, a degree of racemization was also observed by HPLC analysis late-stage in project development.[20] Racemization has been known to occur with the use of HOBt in certain circumstances as reported in the literature.[21] From a

library development perspective however, the need for providing enantiomerically pure material at this stage was not a major concern.

In the initial library planning stage, we envisaged installation of two functional group handles in regions **A**/**B** (Figure 5.4) on sultam scaffolds **5.9**{*1-3*} for the attachment of diverse appendages. With this notion, the Huisgen [3+2] cycloaddition[22,23] and Suzuki-Miyaura coupling reaction[24] were both chosen based upon their well-precedented efficiency[25] and use in library production.[26] This choice then renders the ability to efficiently link/exchange multiple fragments (azides and boronic acids) together selectively based upon potential bioactive lead structures that may arise in the future.

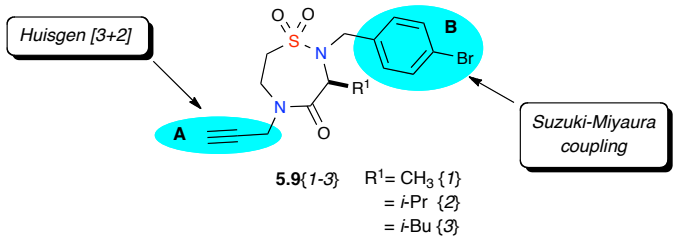

Figure 5.4 *Sultam scaffold design for appendage diversity*

Introduction of the propargyl group into region **A** prepared scaffolds **5.9**{*1-3*} for the preemptive formation of a 1,2,3-triazole linkage via copper-catalyzed Huisgen [3+2] cycloaddition. The bromophenyl functionality was employed in region **B** to provide the necessary functionality for the Suzuki-Miyaura coupling reaction. This group also renders the ability to perform several quick-change operations for alternative reaction processing including Buchwald-Hartwig coupling, Heck coupling, and other Pd-catalyzed transformations.[27] This strategy not only permits us

the flexibility to change either of these two appendages but also the functional group linkages (ie. handles) on each scaffold via future sulfonamide linchpin operations.

Each of the three sultam scaffolds (**5.9**{*1-3*}, Scheme 5.3) were accessed in which alanine **5.4**{*1*}, valine **5.4**{*2*}, and leucine **5.4**{*3*} underwent facile sulfonylation to provide vinyl linchpins **5.5**{*1-3*}. These were further exploited via alkylation to afford intermediates **5.6**{*1-3*}. Each were then subjected to the aza-Michael addition via propargylamine rendering sulfonamides **5.7**{*1-3*} in 39–52% yields over the three-step process. Scaffolds **5.9**{*1-3*} were formed via two-step hydrolysis/ lactamization[28] resulting in good overall yields (61–70%) and excellent purities. Using this newly optimized method, each of the three sultam scaffolds were scaled up prior to validation to a minimum quantity of 5 grams each resulting in high-quality material for library production.[29]

Scheme 5.3 *Synthesis of sultam scaffolds for library production*

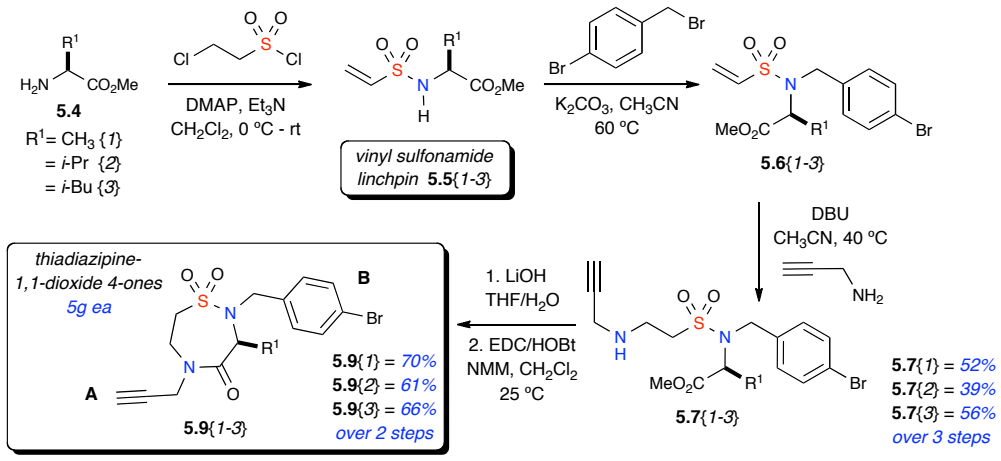

With each of the three scaffolds in hand we were poised to validate both regions **A**/**B** concerning the order of diversification. The most logical starting point relied on

the noted efficiency of the [3+2] cycloaddition for its preemptive use in region **A**. It was speculated that workup procedures for the Suzuki-Miyaura coupling reaction prior to the second diversification could prove costly in terms of transferred yields, and therefore region **A** was deemed as the initial starting point for diversification. In this regard, conditions employing Cu(I) catalyst (Table 5.4, entry 1) were first explored and found to be high-yielding but unfortunately afforded an undesirable mixture of regioisomers. The use of Cu(II) catalysts in *t*-BuOH/H_2O, however saw complete regioselectivity, but suffered from poorer yields (entry 2) presumably due to poor substrate solubility. The use of DCM (entry 3) or acetone (entries 4–6) as a co-solvent, however, resulted in near quantitative yields.

The use of lower catalyst/additive loadings was also explored in consideration to final library purification. It was determined that loadings could be reduced to as low as 10 mol% without risking a substantial loss in yield. Due to the efficient nature of this reaction, we were then motivated to explore the use of an immobilized source of copper (A-21•CuI)[30] that did not require a complex solvent mixture and/or aqueous workup. Conveniently, this bifunctional catalyst also acted as a supported base for the reaction wherein its primary functionality contains a tertiary amino group. These polymer-assisted efforts proved highly successful (entry 7) affording triazole-containing (±) sultam **5.10**{*1*} in excellent yield after SPE filtration.

Table 5.4 *Validation of Huisgen [3+2] cycloaddition*

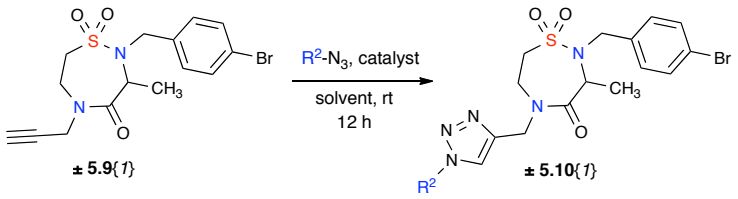

entry	catalyst	loading (mol%)	additive	equiv	solvent	yield (%)
1	CuI	10	2,6-lutidine	1.2	$CHCl_3$	88[a]
2	$CuSO_4$•$6H_2O$	10	Na ascorbate	0.1	*t*-BuOH/H_2O 1:2	45
3	$CuSO_4$•$6H_2O$	20	Na ascorbate	0.3	*t*-BuOH/H_2O/CH_2Cl_2 1:1:1	97
4	$CuSO_4$•$6H_2O$	20	Na ascorbate	0.3	*t*-BuOH/H_2O/acetone 3:4:1	96
5	$CuSO_4$•$6H_2O$	10	Na ascorbate	0.2	*t*-BuOH/H_2O/acetone 3:4:1	95
6	$CuSO_4$•$6H_2O$	5	Na ascorbate	0.1	*t*-BuOH/H_2O/acetone 3:4:1	78
7	A-21•CuI	20	none	-	CH_2Cl_2	90

[a] Resulted in a 4:1 mixture of regioisomers.

Initial efforts to validate conditions for the Suzuki-Miyaura coupling reaction (Table 5.5) were explored whereby use of Pd(dppf)Cl_2 as catalyst had previously been used for sultam diversification of this type (Ch. 3). Variation in Pd catalyst loadings were first explored starting from 1mol% up to 10 mol% (entries 1–3) resulting in only moderate yields. Due to similarity in Rf between starting material and product, monitoring reaction progression by TLC proved difficult, and as a result, reaction time was increased to 14 hours at 80 ºC using 5 mol% Pd. This resulted in high-yielding product formation (**5.11b,c**{*2-3*}) as evident in entries 4–5. Interest in compatibility/scope between substrates used in region **A** (ie. azides) and the Suzuki-Miyaura coupling reaction revealed that azide bearing esters (entries 6–9) were not good substrates for the library as each underwent base-catalyzed hydrolysis to give two products after the coupling event; each being separable by chromatography.

Table 5.5 *Initial validation of the Suzuki-Miyaura coupling reaction*

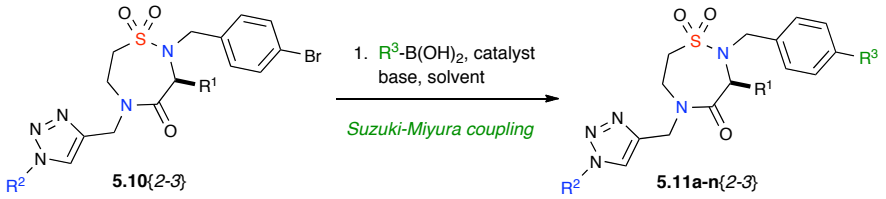

entry	R^1	R^2	R^3	catalyst loading (%)	base	temp (°C)	time (h)	yield (%)	pdt. **5.11**
1	*i*-Bu	*p*-Me-Bn	phenyl	1	Cs_2CO_3	70	8	46	**a**
2	*i*-Bu	*p*-Me-Bn	phenyl	5	Cs_2CO_3	70	8	51	**a**
3	*i*-Bu	*p*-Me-Bn	phenyl	10	Cs_2CO_3	70	8	68	**a**
4	*i*-Bu	Cyhex-Me	3-CN-Ph	5	K_2CO_3	80	14	97	**b**
5	*i*-Bu	Cyhex-Me	3-Ac-Ph	5	K_2CO_3	80	14	99	**c**
6	*i*-Bu	$(CH_2)_2OCOMe$	2,6 diMePh	5	K_2CO_3	80	14	38 (51)	**d**
7	*i*-Bu	$(CH_2)_2OCOMe$	3-CN-Ph	5	K_2CO_3	80	14	81 (19)	**e**
9	*i*-Bu	$(CH_2)_2OCOMe$	3-Ac-Ph	5	K_2CO_3	80	14	52 (30)	**f**
10	*i*-Pr	*p*-MeO-Bn	2,6 diMePh	5	K_2CO_3	80	14	88	**g**
11	*i*-Pr	*p*-MeO-Bn	2-thiophene	5	K_2CO_3	80	24	66	**h**
12	*i*-Pr	*p*-MeO-Bn	3-CN-Ph	5	K_2CO_3	80	14	73	**i**
13	*i*-Pr	*p*-MeO-Bn	3-Ac-Ph	5	K_2CO_3	80	14	87	**j**
14	*i*-Pr	furfuryl	2,6 diMePh	5	K_2CO_3	80	14	81	**k**
15	*i*-Pr	furfuryl	2-thiophene	5	K_2CO_3	80	24	76	**l**
16	*i*-Pr	furfuryl	3-CN-Ph	5	K_2CO_3	80	14	98	**m**
17	*i*-Pr	furfuryl	3-Ac-Ph	5	K_2CO_3	80	14	97	**n**

Entries 6–9: Yield (%) reported as coupled product X to hydrolyzed coupled product (X); each separately isolated. Product (pdt.) **d–f** refers to the non-hydrolyzed products.

A small substrate scope for the Suzuki-Miyaura coupling reaction was also performed under these conditions (entries 10–17) using both electron-rich and electron-deficient aryl boronic acids. Notably, the reactivity of 2-thiophene boronic acid was significantly lower than the other boronic acids and required longer reaction times to yield coupled product.

Initial attempts to validate these conditions on an automated platform *vide infra* unfortunately resulted in difficult emulsions and extended separation/workup times.

In light of this observation, we revisited these conditions (Table 5.6) having discovered that variations in the base and solvent affected overall workup times. It was revealed that the use of DME with cesium carbonate provided the most convenient workup while retaining reproducibly high product yields.

Table 5.6 *Validation of the Suzuki-Miyaura coupling reaction*

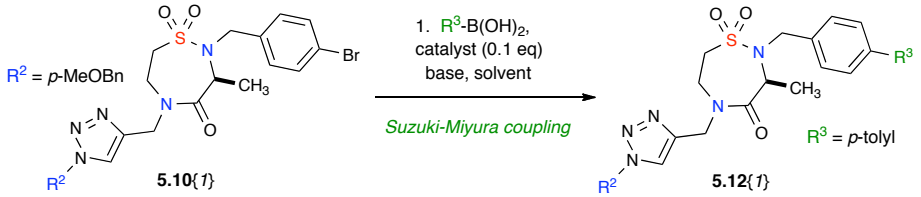

entry	catalyst	base	solvent	temp (°C)	time (h)	yield (%)
1	$Pd(dppf)Cl_2$	Cs_2CO_3	DMF/H_2O	70	14	85
2	$Pd(dppf)Cl_2$	Na_2CO_3	DMF/H_2O	70	14	10
3	$Pd(dppf)Cl_2$	K_3PO_4	DMF/H_2O	85	16	92
4	$Pd(dppf)Cl_2$	K_3PO_4	$Dioxane/H_2O$	90	16	90
5	$Pd(dppf)Cl_2$	Cs_2CO_3	$Dioxane/H_2O$	75	14	62
6	$Pd(dppf)Cl_2$	Cs_2CO_3	$Dioxane/H_2O$	90	16	94
7	$Pd(dppf)Cl_2$	Cs_2CO_3	DME/H_2O	85	16	89
8	$Pd(PPh_3)_4$	Cs_2CO_3	DME/H_2O	70	14	<5
9	$Pd(PPh_3)_4$	CsF	DME/H_2O	80	14	61

We also briefly explored the use of a resin-bound source of Pd (FibreCat®)[31] whereby reaction workup consisted of a simple SPE filtration event. Unfortunately, problems related to automation[32] quickly became apparent and the notion of using this reagent was disbanded. In the interest of time, no other Pd-functionalized resins were explored or tested for library use.

Based on the optimal conditions chosen for both reactions, we then explored combining both into a single-step sequence for ease of parallel synthesis (Scheme 5.4). Sultam **5.9**{*1*} was first reacted for 14 h with *p*-methoxybenzyl azide in the

presence of A-21•CuI, followed by filtration of the catalyst and concentration to yield crude, triazole-containing sultam **5.10**{*1*}. This material was then carried forward into the Suzuki-Miyaura coupling reaction without further purification. A basic workup was then necessary to remove excess boronic acid from the reaction followed by a liquid-liquid extraction using DCM. The resulting solution was then filtered via silica SPE and concentrated to afford sultam **5.12**{*1*} in excellent yield over the combined two-step sequence. Overall, this combined sequence was developed for its relevancy in the transfer of these chemistries to parallel methods, in which workup and purification are minimized.

Scheme 5.4 *Combined two-step diversification sequence*

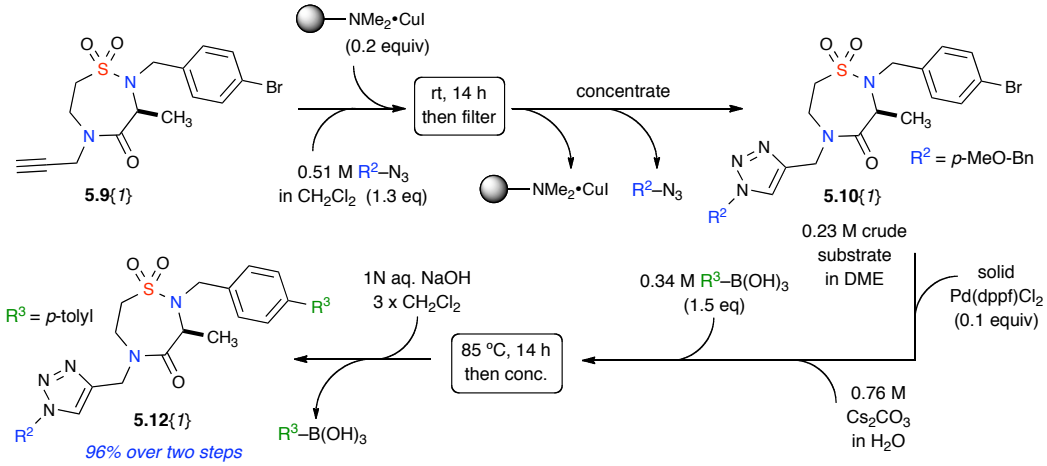

The combined two-step sequence was then envisaged on the Chemspeed Accelerator SLT-100® parallel synthesizer for library production (Figure 5.5).[33] The chemistry was first validated on this automated platform as a rehearsal 2 x 3 x 3 member library (Figure 5.6) for a total of 18 compounds.

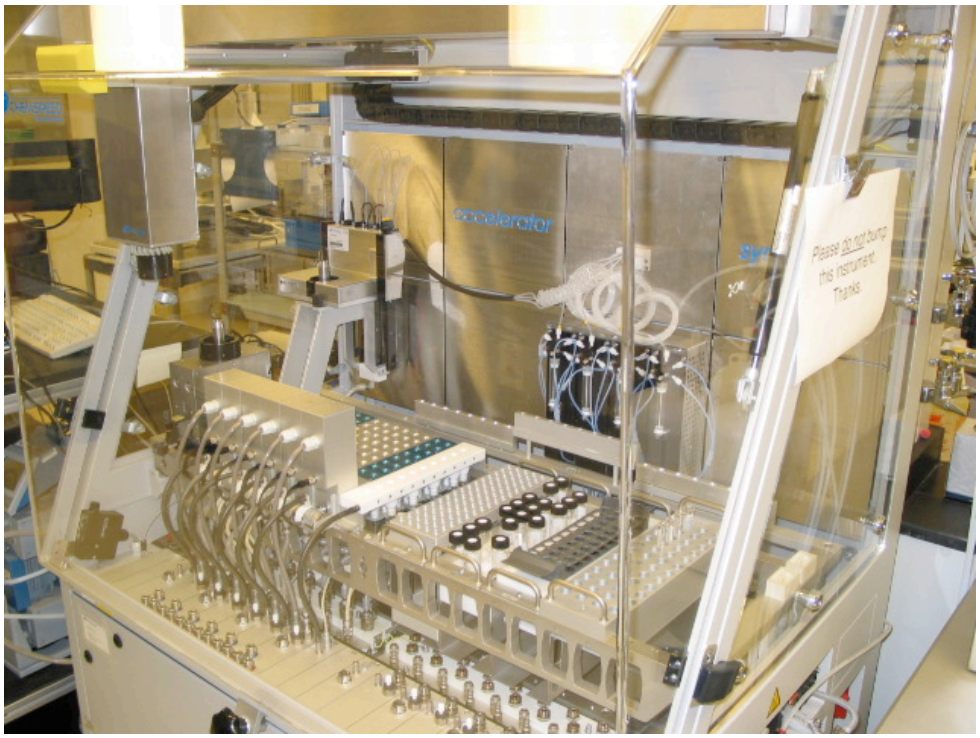

Figure 5.5 *Chemspeed Accellerator SLT-100 parallel synthesizer*

Azides 1-3 were chosen based upon members represented in the scope of the final library and a small substrate scope for the Suzuki-Miyaura coupling was also explored with the choice of electron-deficient and electron-rich phenyl, and alkyl boronic acids. With this information, the [3+2] cycloadditions were prepared and reacted in the Chemspeed for 14 h. Upon completion, the supernatant was removed and transferred to the next reaction leaving the catalyst behind in the reactors. The Suzuki-Miyaura coupling reaction was then conducted for 14 h at 85 ºC followed by the automated basic workup/extraction procedure. Silica SPE filtration was carried out prior to crude purity analysis and subsequent purification was achieved by HPLC/mass directed fractionation (MDF) methods.

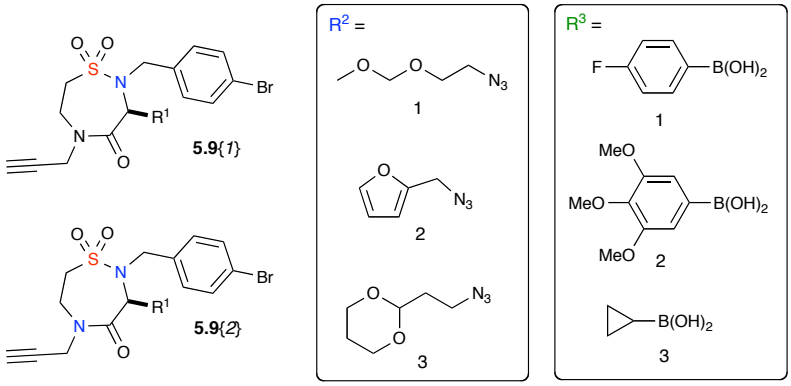

Figure 5.6 *Rehearsal 2 x 3 x 3 library building blocks*

Chart 5.1 displays the results of the validation efforts revealing an overall successful run for the combined two-step automated sequence. Product yields ranged from 23–49% over two-steps with final purities > 90% for 12 of the 18 compounds. Boronic acid {3} (cyclopropyl), however, notably revealed a significantly lower reactivity as compared to both phenyl boronic acids resulting in incomplete conversions for 6 out of the 18 total reactions.

Chart 5.1 *Chemspeed rehearsal 2 x 3 x 3 library of thiadiazepin-1,1-dioxide-4-ones*

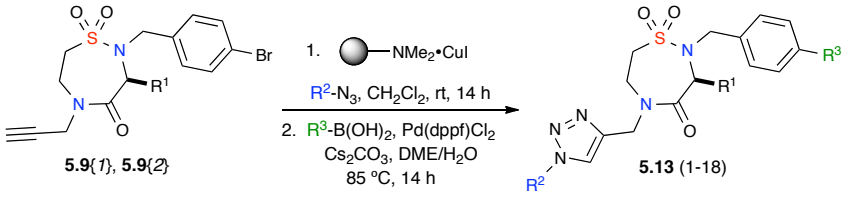

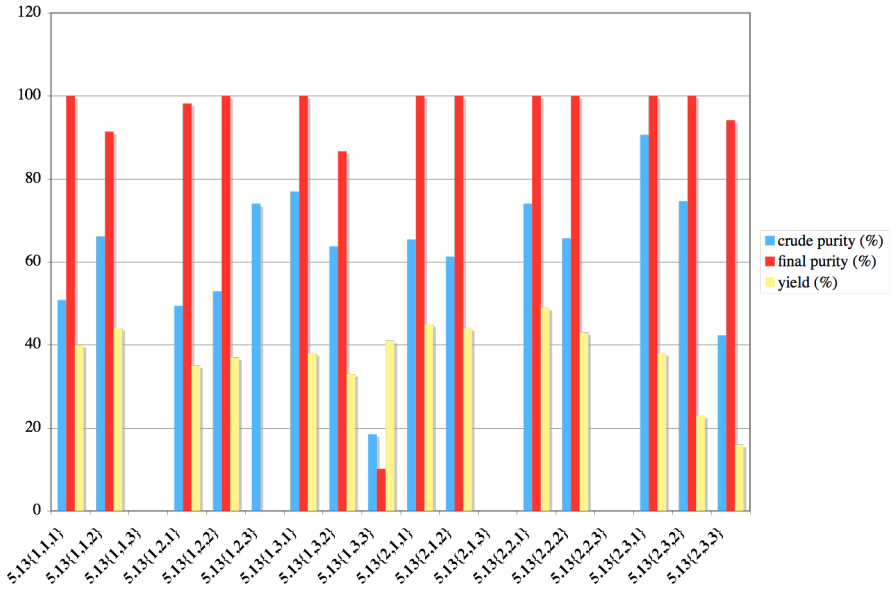

Purity determination is UV area percent from HPLC analysis.

With these results in hand, planning began for constructing the 225-member sultam library using the Chemspeed platform and the conditions set in place through the successful single-step validation sequence. A number of azides and boronic acids were chosen (Figure 5.7) based on various structure and polarity features desired in the final products and either purchased or synthesized for use in the final library. Based on results of previous validations, alkyl boronic acids and base-labile azides were excluded from the final library. The automated platform was then prepared for three sequential 75 compound runs for completion of a 3 x 5 x 15 member library. Using conditions previously validated, the library officially transitioned into the production phase.

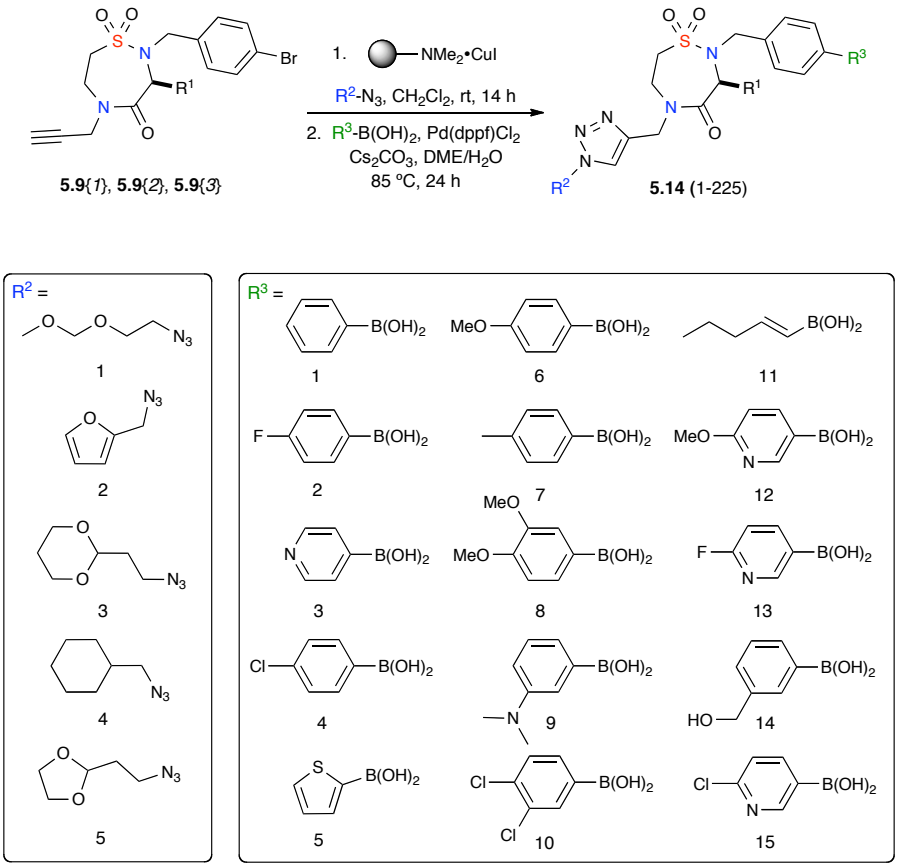

Figure 5.7 *Building blocks and conditions for the 3 x 5 x 15 library of thiadiazepin-1,1-dioxide-4-ones.*

After completion of the first run of 75 compounds on the Chemspeed, three random samples were chosen and subjected to UPLC/MS for crude purity analysis aside from standard MS analysis of the library. Product masses were confirmed for each of the three samples and crude purity analysis resulted in purities of 56%, 69%, and 78% - all on par with the rehearsal/validation library. With this information in hand, the remaining two 75 compound runs were prepared and reacted accordingly in the Chemspeed. After purification of the remaining 150 compounds, subsequent analysis revealed 166 compounds out of the 225 were obtained in greater than 90% purity with

average quantities ≥ 20 mg (using 0.150 mmol of sultams **5.9**{*1-3*}) and an average yield of 50% over the two-step sequence.[34] Further data analysis revealed no definitive trends in respect to yields between substrates and reagents, however, it was noted, that thiophene boronic acid (R^3 = 5) resulted in very low yields across the 15 reactions by which it was utilized.

5.3 Conclusions and Future Outlook

In conclusion we have successfully completed production of a 225 member library of thiadiazepin-1,1-dioxide-4-ones (sultams) utilizing a facile, two-step synthetic sequence performed on an automated platform. We have highlighted the use of a multi-functional linchpin and its use in efficiently generating diverse scaffolding for library production. The resulting compounds of this library are in the process of being relayed to a number of biological collaborators within the Molecular Libraries Screening Center Network (MLSCN) and future efforts will concentrate on targeted libraries of this and other related chemotypes as well as their anticipated biological evalution.

References

(1) (a) Omura, S., The Search for Bioactive Compounds from Microorganisms. Omura, S., Ed.; Springer, New York, N. Y., 1992; pp 1–352. (b) Kennedy, J. P.; Williams, L.; Bridges, T. M.; Daniels, R. N.; Weaver, D.; Lindsley, C. W., Application of Combinatorial Chemistry Science on Modern Drug Discovery. *J. Comb. Chem.* **2008**, *10*, 345–354.

(2) For reviews on Diversity-oriented synthesis (DOS) see: (a) Tan, D. S., Diversity-oriented synthesis: exploring the intersections between chemistry and biology. *Nat. Chem. Biol.* **2005**, *1*, 74–84. (b) Spandl, R. J.; Diaz-Gavilan, M.; O'Connell, K. M. G.; Thomas, G. L.; Spring, D. R., Diversity-oriented synthesis. *Chem. Rec.* **2008**, *8*, 129–142. (c) Schreiber, S. L., Target-oriented and diversity-oriented organic synthesis in drug discovery. *Science* **2000**, *287*, 1964–1969. (d) Arya, P.; Joseph, R.; Gan, Z.; Rakic, B. Exploring Chemical Space by Stereocontrolled Diversity-Oriented Synthesis. *Chem. Biol.* **2005**, *12*, 163–180.

(3) (a) Comer, E.; Rohan, E.; Deng, L.; Porco, J. A., An Approach to Skeletal Diversity Using Functional Group Pairing of Multifunctional Scaffolds *Org. Lett.* **2007**, *9*, 2123–2126. (b) Zhou, A.; Rayabarapu, D.; Hanson, P. R., "Click, click, cyclize": a DOS approach to sultams utilizing vinyl sulfonamide linchpins. *Org. Lett.* **2009**, *11*, 531–534. (c) Wipf, P.; Stephenson, C. R. J.; Walczak, M. A. A., Diversity-oriented synthesis of azaspirocycles. *Org. Lett.* **2004**, *6*, 3009–3012. (d) Santra, S.; Andreana, P. R., A One-Pot, Microwave-Influenced Synthesis of Diverse Small Molecules by Multicomponent Reaction Cascades. *Org. Lett.* **2007**, *9*, 5035–5038.

(4) Nielsen, T. E.; Schreiber, S. L., Towards the optimal screening collection. A synthesis strategy. *Angew. Chem. Int. Ed.* **2008**, *47*, 48–56.

(5) (a) Di Micco, S.; Vitale, R.; Pellecchia, M.; Rega, M. F.; Riva, R.; Basso, A.; Bifulco, G. Identification of Lead Compounds as Antagonists of Protein Bcl-xL with a Diversity-Oriented Multidisciplinary Approach. *J. Med. Chem.* **2009**, *52*, 7856–7867. (b) Tejedor, D.; Lopez-Tosco, S.; Gonzalez-Platas, J.; Garcia-Tellado, F., Tertiary Skipped Diynes: A Pluripotent Building Block for the Modular and Diversity-Oriented Synthesis of Nitrogen Heterocycles. *Chem-Eur. J.* **2010**, *16*, 3276–3280. (b) Diaz-Gavilan, M.; Galloway, W. R. J. D.; O'Connell, K. M. G.; Hodkingson, J. T.; Spring, D. R., Diversity-Oriented Synthesis of bicyclic and tricyclic alkaloids. *Chem. Comm.* **2010**, *46*, 776–778.

(6) Rolfe A.; Lushington, G. H.; Hanson, P. R., Reagent based DOS: A "Click, Click, Cyclize" strategy to probe chemical space. *Org. Biomol. Chem.* **2010**, *8*, 2198–2203.

(7) (a) Samarakoon, T. B.; Hur, M. Y.; Kurtz, R. D.; Hanson, P. R. A Formal [4+4] Complementary Ambiphile Pairing (CAP) Reaction: A New Cyclization Pathway for ortho-Quinone Methides. *Org. Lett.* **2010**, In Press. (b) Rolfe, A.; Samarakoon, T. B.; Hanson, P. R. Formal [4+3] Epoxide Cascade Reaction via a Complementary Ambiphilic Pairing Strategy. *Org. Lett.* **2010**, *12*, 1216–1219. (c) Rayabarapu, D.; Zhou, A.; Jeon, K. O.; Samarakoon, T.; Rolfe, A.; Siddiqui, H.; Hanson, P. R., α-Haloarylsulfonamides: Multiple Cyclization Pathways to Skeletally Diverse Benzofused Sultams. *Tetrahedron* **2009**, *65*, 3180–3188.

(8) Zhou, A.; Hanson, P. R., Synthesis of Sultam Scaffolds via Intramolecular Oxa-Michael and Diastereoselective Baylis - Hillman Reactions. *Org. Lett.* **2008**, *10*, 2951–2954.

(9) Jiménez-Hopkins, M.; Hanson, P. R., An RCM Strategy to Stereodiverse δ-Sultam Scaffolds. *Org. Lett.* **2008**, *10*, 2223–2226.

(10) Jeon, K. O.; Rayabarapu, D.; Rolfe, A.; Volp, K.; Omar, I.; Hanson, P. R., Metathesis Cascade Strategies (ROM-RCM-CM): A DOS Approach to Skeletally Diverse Sultams. *Tetrahedron* **2009**, *65*, 4992–5000.

(11) (a) Iden, H. S.; Lubell, W. D., 1,3,5-Tri- and 1,3,4,5-Tetra-Substituted 1,4-Diazepin-2-one Solid-Phase Synthesis. *J. Comb. Chem.* **2008**, *10*, 691–699. (b) Ramanathan, S. K.; Keeler, J.; Lee, H-L.; Reddy, D. S.; Lushington, G.; Aube, J., Modular Synthesis of Cyclic Peptidomimetics Inspired by γ - Turns. *Org. Lett.* **2005**, *7*, 1059–1062.

(12) de Bont, D. B. A.; Moree, W. J.; Liskamp, R. M. J., *Bioorgan. Med. Chem.* **1996**, *4*, 667–672.

(13) Bemis, G. W.; Golec, J. M. C.; Lauffer, D. J.; Mullican, M. D.; Murcko, M. A.; Livingston, D. J., Preparation of peptide inhibitors of interleukin-1β converting enzyme. **1998**, 106 pp., Cont.-in-part of U.S. 5,656,627.

(14) Guo, T.; Adang, A. E. P.; Dolle, R. E.; Dong, G.; Fitzpatrick, D.; Geng, P.; Ho, K-K.; Kultgen, S. G.; Liu, R.; McDonald, E.; McGuinness, B. F.; Saionz, K. W.; Valenzano, K. J.; van Straten, N. C. R.; Xie, D.; Webb, M. L., Small molecule biaryl FSH receptor agonists. Part 1. Lead discovery via encoded

combinatorial synthesis. *Bioorg. Med. Chem. Lett.* **2004**, *14*, 1713–1716.

(15) Wattanasin, S.; Kallen, J.; Myers, S.; Guo, Q.; Sabio, M.; Ehrhardt, C.; Albert, R.; Hommel, U.; Weckbecker, G.; Welzenbach, K.; Weitz-Schmidt, G. 1,4-Diazepane-2,5-diones as novel inhibitors of LFA-1. *Bioorg. Med. Chem. Lett.* **2005**, *15*, 1217–1220.

(16) Yeom, C-E.; Kim, M. J.; Kim, B. M., 1,8-Diazabicyclo[5.4.0]undec-7-ene (DBU)-promoted efficient and versatile aza-Michael addition *Tetrahedron* **2007**, *63*, 904–909.

(17) Several conditions were not reported due to a lack of reactivity.

(18) (a) Han, C.; Lee, J. P.; Lobkovsky, E.; Porco, J. A., Jr., Catalytic Ester-Amide Exchange Using Group (IV) Metal Alkoxide-Activator Complexes. *J. Am. Chem. Soc.* **2005**, *127*, 10039–10044. (b) Robins, M. J.; Sarker, S.; Xie, M.; Zhang, W.; Peterson, M. A., Nucleic acid related compounds. 90. Synthesis of 2',3'-fused (3.3.0) .gamma.-butyrolactone-nucleosides and coupling with amino-nucleosides to give amide-linked nucleotide-dimer analogs. *Tetrahedron Lett.* **1996**, *37*, 3921–3924. (c) Neogi, S.; Roy, A.; Naskar, D., One-Pot Synthesis of New Fused 4,5-Bridged 1,2,5-Triazepine-3,6-diones, 1,2,5-Triazepine-3,7-diones Heterocycles by Petasis Reaction. *J. Comb. Chem.* **2010**, *12*, 75–83. (d) Durow, A. C.; Long, G. C.; O'Connell, S. J.; Willis, C. L., Total synthesis of the chlorinated marine natural product dysamide B. *Org. Lett.* **2006**, *8*, 5401–5404.

(19) Rolfe, A.; Probst, D.; Volp, K.; Omar, I.; Flynn, D.; Hanson, P. R., High-load, Oligomeric dichlorotriazine (ODCT): A Versatile ROMP-derived Reagent and Scavenger. *J. Org. Chem.* **2008**, *73*, 8785–8790.

(20) HPLC analysis revealed enantiomeric excess ranging from 2%–17%. These values are currently being confirmed by analysis of racemic material.

(21) Sieber, P.; Kamber, B.; Hartmann, A.; Joehl, A.; Riniker, B.; Rittel, W., Total synthesis of human insulin. IV. Description of the final steps. *Helv. Chim. Acta.* **1977**, *60*, 27–37.

(22) Kolb, H. C.; Finn, M. G.; Sharpless, K. B., Click chemistry: diverse chemical function from a few good reactions. *Angew. Chem. Int. Ed.* **2001**, *40*, 2004–2021.

(23) (a) Huisgen, R.; Knorr, R.; Moebius, L.; Szeimies, G., 1,3-Dipolar cycloadditions. XXIII. Addition of organic azides to C-C triple bonds. *Chem. Ber.* **1965**, *98*, 4014–4021. (b) Huisgen, R.; Szeimies, G.; Moebius, L., 1,3-Dipolar cycloadditions. XXXII. *Chem. Ber.* **1967**, *100*, 2494–2507.

(24) Miyaura, N.; Yanagi, T. Suzuki, A. *Synth. Commun.* The palladium-catalyzed cross-coupling reaction of phenylboronic acid with haloarenes in the presence of bases. **1981**, *11*, 513–519.

(25) (a) Miyaura, N. Introduction to cross-coupling reactions. *Top. Curr. Chem.* **2002**, *219*, 1–9. (b) Kotha, S.; Lahiri, K.; Kashinath, D., Recent applications of the Suzuki-Miyaura cross-coupling reaction in organic synthesis. *Tetrahedron* **2002**, *58*, 9633–9695. (c) Franzen, R., The Suzuki, the Heck, and the Stille reaction; three versatile methods for the introduction of new C-C bonds on solid support. *Can. J. Chem.* **2000**, *78*, 957–962. (d) Sasaki, M.; Fuwa, H., Palladium-catalyzed carbonylation of lactone-derived enol phosphates: stereoselective construction of functionalized cyclic ethers from lactones. *Synlett* **2004**, 1851–1874. (e) Stanforth, S. P., Catalytic cross-coupling reactions in biaryl synthesis. *Tetrahedron* **1998**, *54*, 263–303.

(26) (a) Cho, C.-H.; Neuenswander, B.; Larock, R. C., Diverse Methyl Sulfone-Containing Benzo[b]thiophene Library via Iodocyclization and Palladium-Catalyzed Coupling. *J. Comb. Chem.* **2010**, *12*, 278–285. (b) Zhou, H.; Zhang, W.; Yan, B., Use of Cyclohexylisocyanide and Methyl 2-Isocyanoacetate as Convertible Isocyanides for Microwave-Assisted Fluorous Synthesis of 1,4-Benzodiazepine-2,5-dione Library. *J. Comb. Chem.* **2010**, *12*, 206–214. (c) Jeges, G.; Nagy, T.; Meszaros, T.; Kovacs, J.; Dorman, G.; Kowalczyk, A.; Goodnow, R. A., Practical Synthesis of 5-Aryl-3-alkylsulfonyl-phenol and 5-Aryl-3-arylsulfonyl-phenol Libraries. *J. Comb. Chem.* **2009**, *11*, 327–334. (d) Agarkov, A.; Gilbertson, S. R., Preparation of a Library of Unsymmetrical Ureas Based on 8-Azabicyclo[3.2.1]Octane Scaffold. *J. Comb. Chem.* **2008**, *10*, 655–657. (e) Tan, L. P.; W., Hao; Yang, P.-Y.; Kalesh, K. A.; Zhang, X.; Hu, M.; Srinivasan, R.; Yao, S. Q., High-Throughput Discovery of Mycobacterium tuberculosis Protein Tyrosine Phosphatase B (MptpB) Inhibitors Using Click Chemistry. *Org. Lett.* **2009**, *11*, 5102–5105. (e) Rogers, S. A.; Melander, C., Construction and screening of a 2-aminoimidazole library identifies a small molecule capable of inhibiting and dispersing bacterial biofilms across order, class, and phylum. *Angew. Chem. Int. Ed.* **2008**, *47*, 5229–5231. (f) Pagliai, F; Pirali, T; Del Grosso, E; Di Brisco, R.; Tron, G. C.; Sorba, G.; Genazzani, A. A., Rapid Synthesis of Triazole-Modified Resveratrol Analogues via Click Chemistry. *J. Med. Chem.* **2006**, *49*, 467–470.

(27) Kürti, L.; Czakó, B. In *Strategic Applications of Named Reactions in Organic Synthesis*: Hayhurst, J., Ed.; Elsevier: Massachusetts, 2005; pp.71, 197, 258, 424, 436–439.

(28) Ho, G.-J.; Emerson, K. M.; Mathre, D. J.; Shuman, R. F.; Grabowski, E. J. J., Carbodiimide-Mediated Amide Formation in a Two-Phase System. A High-Yield and Low-Racemization Procedure for Peptide Synthesis. *J. Org. Chem.* **1995**, *60*, *3569–3570*.

(29) All three scaffolds were a crystalline white foam with purity > 95% as determined by ^{1}H NMR.

(30) Girard, C.; Onen, E.; Aufort, M.; Beauviere, S.; Samson, E.; Herscovici, J., Reusable Polymer-Supported Catalyst for the [3+2] Huisgen Cycloaddition in Automation Protocols. *Org. Lett.* **2006**, *8*, 1689–1692.

(31) Colacot, T. J.; Carole, W. A.; Neide, B. A.; Harad, N., Tunable Palladium-FibreCats for Aryl Chloride Suzuki Coupling with Minimal Metal Leaching. *Organometallics* **2008**, *27*, 5605–5611.

(32) Due to the fibrous nature of this reagent its delivery and separation via Chemspeed platform proved difficult.

(33) Chemspeed Technologies Home Page. http://www.chemspeed.com/ (accessed April, 10, 2010.

(34) The standards for compound purity and quantity are based upon those requested for the National Institutes of Health's Molecular Libraries Small Molecule Repository (http://mlsmr.glpg.com/MLSMR_HomePage/submitcompounds.html). The compound purities were determined by reverse-phase HPLC with peak area (UV) at 214 nm.

Chapter 6

Experimentals

General Experimental

All air- and moisture-sensitive reactions were carried out in flame- or oven-dried glassware under argon atmosphere using standard gastight syringes, canellas, and septa. THF, CH_2Cl_2, toluene, CH_3CN, and Et_2O were purified by passage through a Solv-Tek (www.solvtek.com) purification system employing activated Al_2O_2 (Grubbs, R. H.; Rosen, R. K.; Timmers, F. J. Organometallics **1996**, *15*, 1518–1520). $CHCl_3$ was passed through basic alumina and dried over molecular sieves. All other solvents were purchased commercially. Flash column chromatography was performed with SiO_2 (Sorbent Technologies 30930M-25, Silica Gel 60 Å, 40-63 μm). Automated flash column chromatography was performed using a Biotage SP1 purification system. SPE purification was performed with SiO_2 purchased from Sorbent Technology (30930M-25, Silica Gel 60A, 40-63 μm) and 6 mL empty cartridges were purchased from Silicycle Inc. Thin layer chromatography was performed on silica gel 60F 254 plates. Visualization of TLC spots was effected using $KMnO_4$ stain. ^1H and ^{13}C NMR spectra were recorded on a Bruker DRX-400 NMR spectrometer operating at 400 and 100 MHz respectively as well as a Bruker DRX-500 spectrometer operating at 500 MHz, 126 MHz respectively. Gas chromatography (GC) was performed using an Agilent Technologies 6890N with data processing on a Dell desktop. GC/mass spectrometry was performed using a Quattro micro GC (Micromass UK Limited). High-resolution mass spectrometry (HRMS) was recorded on a LCT Premier Spectrometer (Micromass UK Limited) operating on ESI (MeOH). Bohdan® block assemblies and a Chemspeed Accelerator SLT-100® was used for

library preparation and production. Nanoparticles were analyzed by FTIR spectroscopy (1% in KBr using a Tensor 27 Spectrometer, Bruker Optics equipped with a diffuse reflectance accessory, DiffusIR™, Pike Technologies), atom absorption spectroscopy (Varian SpectrAA 220FS), elemental microanalysis (LECO CHN-900), transmission electron microscopy (CM30 ST-Philips, LaB_6 cathode, operated at 300 kV point resolution ~ 4 Å), scanning electron microscopy (Hitachi S-2700 equipped with a quartz PCI digital capture) and magnetic hysteresis susceptibility (vibrating sample magnetometer, VSM, Princeton Measurements Corporation, model 3900). FTIR spectroscopy on soluble compounds was performed using a Shimadzu FTIR-8400S instrument. Grubbs catalysts (**1G**, **2G**, and **3G**) were generously provided by Materia Inc. and used without further purification. Azide bearing nanoparticles were prepared at ETH Zurich. Deuterated solvents were purchased from Cambridge Isotope laboratories. Observed rotations at 589 nm, 20 ºC were measured using an AUTOPOL IV Model automatic polarimeter. HPLC was performed using a Chiracel AD column with 95:5 hexanes:IPA with UV monitoring at 254 nm.

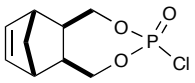

5-norbornene-2-*exo*, 3-*exo*-dimethyl phosphorochloridate (2.26)

To a flame-dried 250 mL RB flask under argon atmosphere was added the *exo*-norbornene dimethanol **2.25** (1.0 g, 6.5 mmol) as solution in CH_2Cl_2 or neat followed by addition of CH_2Cl_2 (33 mL), Et_3N (20 mmol) and anhydrous *N*-methylimidazole (NMI) (0.65 mmol). This was then cooled to 0 ºC and allowed to stir for 10 min. To this was added freshly distilled $POCl_3$ (7.1 mmol) drop-wise over several minutes w/ noticeable gas evolution and salt formation. The reaction was then promptly removed from the cooling bath and allowed to stir at rt for 2.5 – 3 hrs monitoring by TLC (2:1 Hexanes:EtOAc). Upon completion, the reaction was concentrated by ~ ¾ volume and 50 – 75 mL anhydrous THF was added to the flask to precipitate the $Et_3NH^+Cl^-$ salts. This mixture was filtered through a glass frit under vacuum containing celite with a minimal amount of dry silica and rinsed several times with fresh anhydrous THF (3 x 20 mL). This was then subjected to a short silica plug (3.5 in) (4:1 Hexanes:EtOAc up to 1:2 Hexanes:EtOAc) to afford phosphorochloridate **2.26** (808 mg, 3.4 mmol, 53% yield) as a distinctly smelling white solid and inseparable mixture of *P*-diastereomers (*dr* = 11:1).

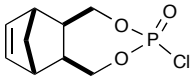

5-norbornene-2-*exo*, 3-*exo*-dimethyl phosphorochloridate (2.26)

^{1}H NMR ($CDCl_3$, 400 MHz) δ ppm 6.26 (s, 2H), 4.39 (dd, J = 12.4, 4.2, 1H), 4.31 (dd, J = 12.4, 4.2, 1H), 4.23 – 4.06 (m, 2H), 2.68 – 2.54 (m, 2H), 2.27 – 2.17 (m, J = 7.6, 5.8, 4.0, 2H), 1.50 – 1.37 (m, 2H); **^{13}C NMR** ($CDCl_3$, 125 MHz) δ ppm 137.3, 70.6 (d, J_{COP} = 36.0 Hz), 44.7, 43.5, 41.6; **^{31}P NMR** ($CDCl_3$, 162 MHz) δ ppm 7.25, 2.81 (*dr* = 11:1); **FTIR** (thin film) 3076, 2978, 1299, 1253, 1045 cm^{-1}; **HRMS** calculated for $C_9H_{12}ClO_3PNa$ $(M+Na)^+$ = 257.0110; found 257.0116 (TOF MS ES+)

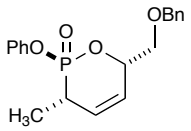

(2*S*,3*S*,6*S*)-6-((benzyloxy)methyl)-3-methyl-2-phenoxy-3,6-dihydro-2H-1,2-oxa phosphinine 2-oxide (2.50)

A 1.0 M solution of CuCN•2LiCl was prepared in dry THF and sealed under argon. 0.46 mL of this solution (0.46 mmol) was transferred via cannula to a flame-dried 5 mL RB flask and cooled to -78 ºC. To this was added Me_2Zn (0.38 mL, 0.46 mmol) in drop-wise manner via syringe w/ stirring and allowed to slowly warm to -30 ºC. This mixture was then added drop-wise via cannulation to a solution of oligomeric-bound **2.48** (25 mg, 0.046 mmol) in THF (0.2 M) at -30 ºC and allowed to slowly warm to rt overnight. Notable sequestration of the copper salt byproducts was noted after several hours. After such time, the reaction was quenched with 10% HCl, extracted w/ EtOAc (3 x 8 mL), and dried over $MgSO_4$. This was then passed through a silica SPE to yield the product **2.50** (9.8 mg, 0.028 mmol, 62 %) as a clear oil.

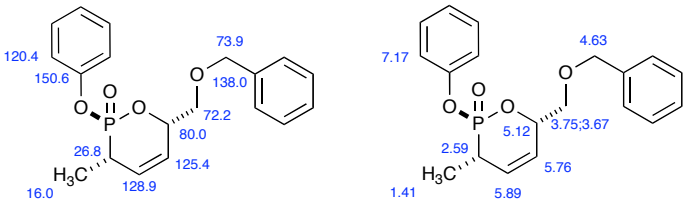

(2*S*,3*S*,6*S*)-6-((benzyloxy)methyl)-3-methyl-2-phenoxy-3,6-dihydro-2H-1,2-oxa phosphinine 2-oxide (2.50)

$[\alpha]^{20}_{D}$ = -8.0 ° (c = 0.46, CH_2Cl_2); **^{1}H NMR** (500 MHz, $CDCl_3$) δ ppm 7.39 – 7.28 (m, 7H), 7.23 (dd, *J* = 7.7, 0.9 Hz, 2H), 7.17 (t, *J* = 7.4 Hz, 1H), 5.89 (dddd, *J* = 29.5, 10.6, 5.8, 2.2 Hz, 1H), 5.76 (ddd, *J* = 10.6, 3.6, 1.9 Hz, 1H), 5.16 – 5.08 (m, 1H), 4.65 – 4.59 (m, 2H), 3.75 (ddd, *J* = 10.3, 5.6, 1.6 Hz, 1H), 3.67 (ddd, *J* = 10.3, 5.2, 1.6 Hz, 1H), 2.65 – 2.52 (m, 2H), 1.41 (dd, *J* = 18.9, 7.5 Hz, 3H); **^{13}C NMR** (126 MHz, $CDCl_3$) δ ppm 150.6 (d, J_{COP} = 8.1 Hz), 138.0, 130.1, 128.9 (d, $^{2}J_{CP}$ = 7.6 Hz), 128.7, 128.0, 127.9, 125.4 (d, J_{CCOP} = 15.1 Hz), 125.2, 120.4 (d, J_{CCOP} = 4.6 Hz), 80.0 (d, J_{COP} = 8.3 Hz), 73.9, 72.2 (d, J_{CCOP} = 7.6 Hz), 26.8 (d, $^{1}J_{CP}$ = 133.1 Hz), 16.0 (d, $^{2}J_{CP}$ = 4.3 Hz); **^{31}P NMR** (162 MHz, $CDCl_3$) δ ppm 21.9; **FTIR** (thin film) 3030, 2930, 1720, 1593, 1491, 1454, 1207, 926 cm^{-1}; **HRMS** calculated for $C_{19}H_{21}O_4PNa$ $(M+Na)^+$ = 367.1075; found 367.1078 (TOF MS ES+).

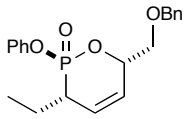

(2*S*,3*S*,6*S*)-6-((benzyloxy)methyl)-3-ethyl-2-phenoxy-3,6-dihydro-2H-1,2-oxa phosphinine 2-oxide (2.51)

A 1.0 M solution of CuCN•2LiCl was prepared in dry THF and sealed under argon. 0.46 mL of this solution (0.46 mmol) was transferred via cannula to a flame-dried 5 mL RB flask and cooled to -78 ºC. To this was added Et_2Zn (0.46 mL, 0.46 mmol) in drop-wise manner via syringe w/ stirring and allowed to slowly warm to -30 ºC. This mixture was then added drop-wise via cannulation to a solution of oligomeric-bound **2.48** (25 mg, 0.046 mmol) in THF (0.2 M) at -30 ºC and allowed to slowly warm to rt overnight. Notable sequestration of the copper salt byproducts was noted after several hours. After such time, the reaction was quenched with 10% HCl, extracted w/ EtOAc (3 x 8 mL), and dried over $MgSO_4$. This was then passed through a silica SPE to yield the product **2.51** (11.2 mg, 0.031 mmol, 68 %) as a clear oil.

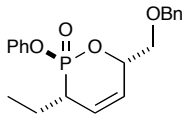

(2*S*,3*S*,6*S*)-6-((benzyloxy)methyl)-3-ethyl-2-phenoxy-3,6-dihydro-2H-1,2-oxa phosphinine 2-oxide (2.51)

$[\alpha]^{20}_{D}$ = -13.6 º (c = 0.46, CH_2Cl_2); **^{1}H NMR** (400 MHz, $CDCl_3$) δ 7.40 – 7.28 (m, 6H), 7.28 – 7.20 (m, 3H), 7.17 (td, *J* = 7.4, 0.7 Hz, 1H), 5.95 – 5.82 (m, 1H), 5.85 – 5.83 (m, 1H), 5.11 (td, *J* = 5.2, 2.5 Hz, 1H), 4.60 – 4.55 (m, 2H), 3.74 (ddd, *J* = 10.3, 5.7, 1.5 Hz, 1H), 3.66 (ddd, *J* = 10.3, 5.3, 1.6 Hz, 1H), 2.56 – 2.41 (m, 1H), 2.02 – 1.86 (m, 1H), 1.79 (ddd, *J* = 21.2, 14.0, 7.3 Hz, 1H), 1.13 – 0.99 (t, *J* = 7.4 Hz, 3H).; **^{13}C NMR** (126 MHz, $CDCl_3$) δ ppm 150.5 (d, J_{COP} = 8.1 Hz), 137.9, 130.0, 128.7, 128.0, 127.9, 126.9 (d, $^2J_{CP}$ = 7.3 Hz), 126.4 (d, J_{CCOP} = 15.3 Hz), 125.1, 120.3 (d, J_{CCOP} = 4.6 Hz), 79.5 (d, J_{CP} = 8.2 Hz), 73.9, 72.0 (d, J_{CP} = 7.5 Hz), 33.8, 32.8, 29.9, 23.8 (d, J_{CP} = 3.0 Hz), 11.8 (d, J_{CP} = 9.8 Hz); **^{31}P NMR** (162 MHz, $CDCl_3$) δ ppm 20.9; **FTIR** (thin film) 3029, 2922, 1591, 1491, 1454, 1207, 922 cm^{-1}; **HRMS** calculated for $C_{20}H_{24}O_4P$ $(M+H)^+$ = 359.1412; found 359.1414 (TOF MS ES+).

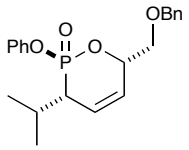

(2*S*,3*S*,6*S*)-6-((benzyloxy)methyl)-3-isopropyl-2-phenoxy-3,6-dihydro-2H-1,2-oxaphosphinine 2-oxide (2.52)

A 1.0 M solution of CuCN•2LiCl was prepared in dry THF and sealed under argon. 0.51 mL of this solution (0.51 mmol) was transferred via cannula to a flame-dried 5 mL RB flask and cooled to -78 ºC. To this was added *i*-Pr_2Zn (0.51 mL, 0.51 mmol) in drop-wise manner via syringe w/ stirring and allowed to slowly warm to -30 ºC. This mixture was then added drop-wise via cannulation to a solution of oligomeric-bound **2.48** (25 mg, 0.046 mmol) in THF (0.2 M) at -30 ºC and allowed to slowly warm to rt overnight. Notable sequestration of the copper salt byproducts was observed after several hours. After such time, the reaction was quenched with 10% HCl, extracted w/ EtOAc (3 x 8 mL), and dried over $MgSO_4$. This was then passed through a silica SPE to yield the product (9.5 mg, 0.026 mmol, 50 %) as a clear oil.

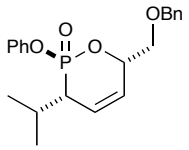

(2*S*,3*S*,6*S*)-6-((benzyloxy)methyl)-3-isopropyl-2-phenoxy-3,6-dihydro-2H-1,2-oxaphosphinine 2-oxide (2.52)

$[\alpha]^{20}_{D}$ = -13.6 º (c = 0.46, CH_2Cl_2); **^{1}H NMR** (500 MHz, $CDCl_3$) δ ppm 7.39 – 7.26 (m, 7H), 7.25 – 7.21 (m, 2H), 7.16 (t, *J* = 7.3 Hz, 1H), 5.95 – 5.89 (m, 1H), 5.88 – 5.76 (m, 1H), 5.13 – 5.08 (m, 1H), 4.65 – 4.54 (m, 2H), 3.78 – 3.69 (m, 1H), 3.65 (ddd, *J* = 10.2, 5.5, 1.6 Hz, 1H), 2.56 – 2.47 (m, 1H), 2.41 – 2.28 (m, 1H), 1.09 (dd, *J* = 9.3, 7.5 Hz, 6H).; **^{13}C NMR** (126 MHz, $CDCl_3$) δ ppm 150.6 (d, *J* = 8.4 Hz), 137.9, 130.0, 128.6, 128.0, 127.9, 127.7 (d, J_{CCOP} = 15.5 Hz), 125.0, 124.3 (d, $^2J_{CP}$ = 7.8 Hz), 120.3 (d, J_{CCOP} = 4.2 Hz), 79.5 (d, J_{COP} = 8.2 Hz), 73.9, 72.3 (d, J_{CCOP} = 7.5 Hz), 38.5 (d, $^1J_{CP}$ = 129.2 Hz) 28.7, 21.0 (d, $^2J_{CP}$ = 13.9 Hz); **^{31}P NMR** (162 MHz, $CDCl_3$) δ ppm 20.2; **FTIR** (thin film) 3032, 2961, 1722, 1591, 1491, 1454, 1205, 924 cm^{-1}; **HRMS** calculated for $C_{21}H_{25}O_4PNa$ $(M+Na)^+$ = 395.1388; found 395.1373 (TOF MS ES+).

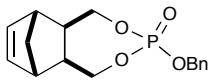

Procedure for formation of 5-norbornene-2-*exo*, 3-*exo*-dimethyl benzyl phosphate (2.61) (OBP monomer) and substituted analogues (2.61a, e–l)

To a flame-dried 25 mL RB flask under argon atmosphere was added benzyl alcohol (0.88 mL, 8.5 mmol) via syringe followed by addition of DCM (8.5 mL) and anhydrous NMI (0.97 mmol). To this mixture was added phosphorochloridate **2.26** in several portions (1.0 g, 4.3 mmol) with stirring. The reaction turned light yellow in color and was complete by TLC in 2-3 hours. The reaction was then concentrated *in vacuo* and purified by flash chromatography (4:1 Hexanes: EtOAc up to 1:2 Hexanes to EtOAc) to afford OBP monomer **2.61** (1.1 g, 3.6 mmol, 85% yield) as a white solid. **^{1}H NMR** ($CDCl_3$, 400 MHz) δ ppm 7.44 – 7.36 (m, 5H), 6.21 (s, 2H), 5.12 (d, J = 7.8 Hz, 2H), 4.16 (dd, J = 12.1, 3.9 Hz, 1H), 4.10 (dd, J = 12.1, 4.0 Hz, 1H), 4.02 – 3.96 (m, 2H), 2.51 (m, 2H), 2.18 – 2.09 (m, 2H), 1.32 (s, 2H); **^{13}C NMR** ($CDCl_3$, 125 MHz) δ ppm 137.4, 135.7, 128.7, 128.1, 69.1 (d, J_{COP} = 7.9 Hz), 68.7 (d, J_{COP} = 5.1 Hz), 44.7, 43.5, 41.9; **^{31}P NMR** ($CDCl_3$, 162 MHz) δ ppm 7.26, 1.07 (*dr* = 33:1); **FTIR** (thin film) 2962, 2927, 1461, 1274, 1255, 1056, 1006, 975 cm^{-1}; **HRMS** calculated for $C_{16}H_{19}O_4PNa$ $(M+Na)^+$ = 329.0919; found 329.0914 (TOF MS ES+)

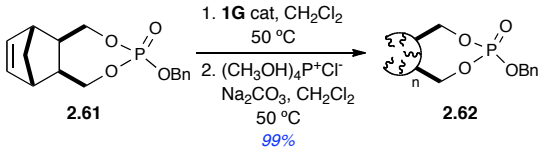

Procedure for formation of OBP_{20} (2.62) and substituted analogs (2.62e–l)

To a flame-dried 250 mL RB flask under argon was added 3.1 g (9.8 mmol) of OBP monomer **2.61** and solubilized in 100 mL of anhydrous, degassed DCM. To this was added 404 mg (0.48 mmol) of cat **1G** with water-cooled condenser and immediately placed at 50 ºC in an oil bath and allowed to stir for 2-3 hours while monitored via TLC (100 % EtOAc, R_f = 0). Upon completion, the reaction was allowed to cool below reflux followed by the addition of 0.5 mL ethyl vinyl ether (5.0 mmol) and allowed to stir for 0.5 hr. After such time was added Na_2CO_3 (1.1 g, 10 mmol) followed by drop-wise addition of tetrakis(hydroxymethyl) phosphonium chloride (THPC) (1.4 mL, 10 mmol) 80% in H_2O while stirring. Noticeable gas evolution occurred during the addition. The reaction was refluxed until complete disappearance of the purple color was observed. After which time the reaction was cooled to room temperature and washed with deionized water (2 x 30 mL) and brine (1 x 30 mL). The organic layer was then dried over $MgSO_4$, filtered through a celite plug, and concentrated *in vacuo* until slight viscosity of the solution is observed. The resulting solution was precipitated drop-wise in Et_2O (1 L) with stirring. Stirring was continued for 10 minutes after which time the oligomer was filtered through a 200 mL medium-sintered glass frit and dried *in vacuo* to yield the desired oligomeric benzyl phosphate (OBP) **2.62** as a white powder in quantitative yield. Subsequent

solubility tests (Table 6.1) confirmed the appropriate solvents to use for the benzylation reaction sequence.

Table 6.1 *Solubility profile of* OBP_{20} **2.62**

solvent	conditions	results
CH_2Cl_2	RT w/ stirring	soluble
$CHCl_3$	RT w/ stirring	soluble
THF	reflux w/ stirring	soluble
DME	reflux w/ stirring	miscible
1,3 dioxane	reflux w/ stirring	soluble
DMF	RT w/ stirring	soluble
Toluene	reflux w/ stirring	insoluble
CH_3CN	reflux w/ stirring	insoluble

General procedure for benzylation using OBP_{20} (2.62) and substituted analogs (2.62e–l)

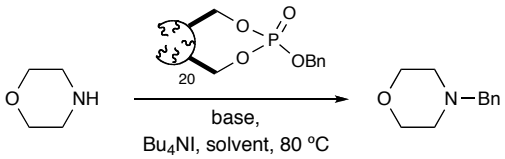

To a 1-dram vial w/ teflon cap was added OBP_{20} **2.62** (1.3–3.0* equiv) followed by addition of tetrabutylammonium iodide (0.1 – 0.2 equiv), K_2CO_3 or Cs_2CO_3 (3 equiv), and solvent ($CHCl_3$ or THF) (0.3M). The mixture was stirred rapidly until the oligomer dissolved (< 30 s) followed by subsequent addition of amine nucleophile. The reaction was sealed under argon and heated to 80 ºC w/ stirring. Reaction time varied between nucleophiles (2–24 hrs) after which time noticeable precipitation of the monoanionic oligomeric phosphate occurred. After such time the reaction was cooled to rt and transferred via 1 mL syringe to a 25 mL RB flask containing approx. 200 mg SiO_2 and then concentrated *in vacuo*. Alternatively the reaction was precipitated into 8–10 mL of diethyl ether with stirring. The crude mixture of either case was then filtered via SiO_2 packed 6 mL SPE and rinsed several times with a mixture of hexanes:EtOAc (50% up to 100%). The resulting eluent was then concentrated *in vacuo* to yield the benzylated products in good to excellent yields and purities. *3.0 equiv. was only used for the dibenzylation of piperazine. All other monobenzylations were performed with 1.3–1.5 equiv. of OBP_{20} or analogs thereof.

Representative Procedure for benzylation of benzothiaoxazepine-1,1-dioxides

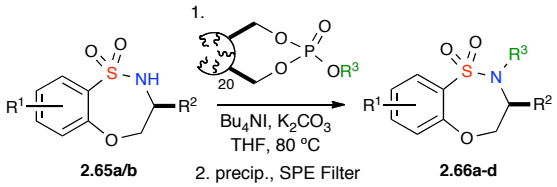

To a flame-dried pressure tube (2.0–5.0 mL) charged with (*S*)-7-bromo-3-phenyl-3,4-dihydro-2H-benzo[b][1,4,5]oxathiazepine 1,1-dioxide **2.65a** (50 mg, 0.14 mmol) was added K_2CO_3 (59 mg, 0.42 mmol), Bu_4NI (10 mg, 0.042 mmol), OBP_{20} (86mg, 0.28 mmol) and THF (1.4 mL, 0.1 M). The reaction vessel was sealed and stirred at 80 ºC overnight. The reaction was then allowed to cool to rt and 4:1 hexane: EtOAc (3 mL) was added, stirred for an additional 10 minutes and the reaction mixture was filtered through a silica SPE cartridge. Evaporation of solvent under reduced pressure afforded (*S*)-2-benzyl-7-bromo-3-phenyl-3,4-dihydro-2H-benzo[b][1,4,5] oxathiazepine 1,1-dioxide **2.66a** as a white solid (54 mg, 99%).

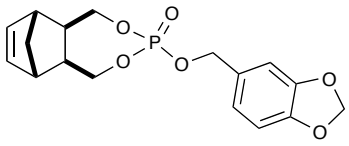

5-norbornene-2-*exo*, 3-*exo*-dimethyl (3,4-(methylenedioxy)benzyl) phosphate (2.61a) (major *P*-diastereomer)

^{1}H NMR ($CDCl_3$, 400 MHz) δ ppm 6.87 (s, 1H), 6.82 – 6.77 (m, 2H), 6.22 (m, 2H), 5.96 (s, 2H), 4.43 (s, 2H), 4.23 – 4.16 (m, 4H), 2.55 (s, 2H), 2.16 – 2.06 (m, 2H), 1.48 (d, J = 9.2 Hz, 1H), 1.35 (d, J = 7.7 Hz, 1H); **^{13}C NMR** ($CDCl_3$, 125 MHz) δ ppm 147.7, 147.1, 137.3, 134.9, 132.0, 121.4, 108.5, 108.0, 100.9, 71.6, 68.8 (J_{COP} = 6.1 Hz), 44.8, 43.7, 42.1; **^{31}P NMR** ($CDCl_3$, 162 MHz) δ ppm 2.25, -3.67 (*dr* = 12:1); **FTIR** (thin film) 2964, 2902, 2358, 1490, 1442, 1251, 1118, 1039, 1010, 975 cm^{-1}; **HRMS** calculated for $C_{17}H_{19}O_6PNa$ $(M+Na)^+$ = 373.0817; found 373.0820 (TOF MS ES+).

***Analogs 2.61a-d were not utilized or polymerized due to their instability**

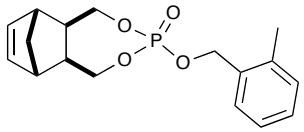

5-norbornene-2-*exo*, 3-*exo*-dimethyl (2-methylbenzyl) phosphate (2.61e) (major *P*-diastereomer)

^{1}H NMR ($CDCl_3$, 400 MHz) δ ppm 7.39 (d, *J* = 7.1, 1H), 7.28 (d, *J* = 7.3, 1H), 7.23 (t, *J* = 6.9, 2H), 6.22 – 6.18 (m, 2H), 5.16 (d, *J* = 6.9, 2H), 4.15 (dd, *J* = 12.1, 4.0, 1H), 4.10 (dd, *J* = 12.1, 4.0, 1H), 4.02 – 3.92 (m, 2H), 2.51 (s, 2H), 2.42 (s, 3H), 2.18 – 2.06 (m, 2H), 1.31 (s, 2H).; **^{13}C NMR** ($CDCl_3$, 125 MHz) δ ppm δ 137.4, 136.8, 133.8, 130.5, 128.9, 126.1, 69.1 (d, J_{COP} = 7.9 Hz), 67.0 (d, J_{COP} = 5.0 Hz), 44.7, 43.5, 41.9, 18.8; **^{31}P NMR** ($CDCl_3$, 162 MHz) δ ppm 2.59, -3.58 (*dr* = 5:1); **FTIR** (thin film) 2964, 1317, 1292, 1257, 1091, 1064, 1010 cm^{-1}; **HRMS** calculated for $C_{17}H_{21}O_4PNa$ $(M+Na)^+$ = 343.1075; found 343.1076 (TOF MS ES+).

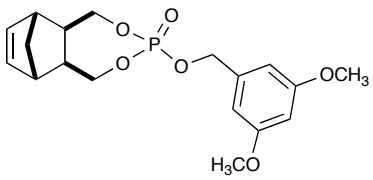

5-norbornene-2-*exo*, 3-*exo*-dimethyl (3,5-dimethoxybenzyl) phosphate (2.61f) (major *P*-diastereomer)

^{1}H NMR ($CDCl_3$, 400 MHz) δ ppm 6.56 (d, *J* = 2.2 Hz, 2H), 6.45 (t, *J* = 2.2 Hz, 1H), 6.22 – 6.19 (m, 2H), 5.05 (dd, *J* = 7.6, 2.7 Hz, 2H), 4.23 – 4.16 (m, 1H), 4.13 (dd, *J* = 12.1, 4.1 Hz, 1H), 4.07 – 4.00 (m, 2H), 3.82 (s, 6H), 2.56 – 2.48 (m, 2H), 2.14 (d, *J* = 12.0 Hz, 2H), 1.36 – 1.31 (m, 2H); **^{13}C NMR** ($CDCl_3$, 125 MHz) δ ppm 161.2, 138.1, 137.6, 106.0, 105.6, 100.6, 69.4 (d, J_{COP} = 7.7 Hz), 68.8 (d, J_{COP} = 4.7 Hz), 55.6, 45.0, 43.7, 42.1; **^{31}P NMR** ($CDCl_3$, 162 MHz) δ ppm 2.49, -3.65 (*dr* = 5:1); **FTIR** (thin film) 2966, 2904, 1596, 1460, 1431, 1325, 1292, 1205, 1153, 1058, 1012 cm^{-1}; **HRMS** calculated for $C_{18}H_{23}O_6PNa$ $(M+Na)^+$ = 389.1130; found 389.1136 (TOF MS ES+).

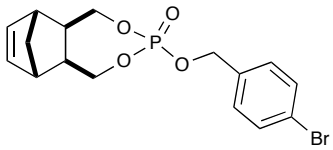

5-norbornene-2-*exo*, 3-*exo*-dimethyl (4-bromobenzyl) phosphate (2.61g) (major *P*-diastereomer)

^{1}H NMR ($CDCl_3$, 400 MHz) δ ppm 7.51 (d, J = 8.4 Hz, 2H), 7.30 (d, J = 8.3 Hz, 2H), 6.20 – 6.17 (m, 2H), 5.05 (d, J = 8.2 Hz, 2H), 4.18 – 4.14 (m, 1H), 4.13 – 4.08 (m, 1H), 4.04 – 3.93 (m, 2H), 2.54 – 2.48 (m, 2H), 2.17 – 2.07 (m, 2H), 1.31 (s, 2H); **^{13}C NMR** ($CDCl_3$, 125 MHz) δ ppm 137.3, 134.6, 131.7, 129.7, 122.7, 69.1 (d, J_{COP} = 8.0 Hz), 67.9 (d, J_{COP} = 5.2 Hz), 44.7, 43.5, 41.8; **^{31}P NMR** ($CDCl_3$, 162 MHz) δ ppm 2.56, -3.75 (*dr* = 7.5:1); **FTIR** (thin film) 3060, 2966, 2879, 1488, 1290, 1253, 1116, 1066, 1033, 1008, 975 cm^{-1}; **HRMS** calculated for $C_{16}H_{18}O_4BrPNa$ $(M+Na)^+$ = 407.0024; found 407.0025 (TOF MS ES+).

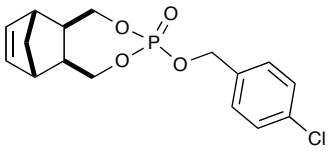

5-norbornene-2-*exo*, 3-*exo*-dimethyl (4-chlorobenzyl) phosphate (2.61h) (major *P*-diastereomer)

^{1}H NMR ($CDCl_3$, 400 MHz) δ ppm 7.37 (s, 4H), 6.22 – 6.20 (m, 2H), 5.08 (d, J = 8.2 Hz, 2H), 4.18 (dd, J = 4.0, 12.1 Hz, 1H), 4.11 (dd, J = 4.1, 12.1 Hz, 1H), 4.04 – 3.93 (m, 2H), 2.55 – 2.48 (m, 2H), 2.19 – 2.09 (m, 2H), 1.34 (s, 2H); **^{13}C NMR** ($CDCl_3$, 125 MHz) δ ppm 137.3, 134.7, 134.2, 129.6, 128.9, 69.2 (d, J_{COP} = 7.9 Hz) 68.1 (d, J_{COP} = 5.0 Hz), 44.8, 43.6, 41.9; **^{31}P NMR** ($CDCl_3$, 162 MHz) δ ppm 2.65, -3.79 (*dr* = 6.5:1); **FTIR** (thin film) 3061, 2966, 1493, 1292, 1065, 1032, 1011, 976, 849, 714 cm^{-1}; **HRMS** calculated for $C_{16}H_{18}ClO_4PNa$ $(M+Na)^+$ = 363.0529; found = 363.0521 (TOF MS ES+).

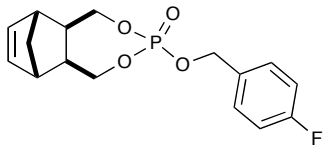

5-norbornene-2-*exo*, 3-*exo*-dimethyl (4-fluorobenzyl) phosphate (2.61i) (major *P*-diastereomer)

^{1}H NMR ($CDCl_3$, 400 MHz) δ ppm 7.44 – 7.38 (m, 2H), 7.10 – 7.05 (m, 2H), 6.21 – 6.17 (m, 2H), 5.08 (d, J = 8.3 Hz, 2H), 4.17 (dd, J = 12.1, 4.1 Hz, 1H), 4.10 (dd, J = 12.1, 4.1 Hz, 1H), 4.03 – 3.92 (m, 2H), 2.54 – 2.47 (m, 2H), 2.17 – 2.05 (m, 2H), 1.32 (s, 2H); **^{13}C NMR** ($CDCl_3$, 125 MHz) δ ppm 162.9 (d, $^{1}J_{CF}$ = 248 Hz) 137.3, 131.5 (q, $^{4}J_{CF}$ = 3.3 Hz), 130.3 (d, $^{3}J_{CF}$ = 8.4 Hz), 115.6 (d, $^{2}J_{CF}$ = 21.7 Hz), 69.1 (d, J_{COP} = 8.1 Hz), 68.0 (d, J_{COP} = 5.1 Hz), 44.8, 43.5, 41.9; **^{31}P NMR** ($CDCl_3$, 162 MHz) δ ppm 2.57, -3.69 (*dr* = 8:1); **FTIR** (thin film) 3064, 2976, 2907, 1494, 1463, 1291, 1253, 1061, 1010, 975 cm^{-1}; **HRMS** calculated for $C_{16}H_{18}O_4FPNa$ $(M+Na)^+$ = 347.0824; found 347.0826 (TOF MS ES+).

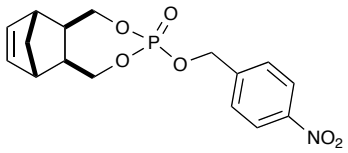

5-norbornene-2-*exo*, 3-*exo*-dimethyl (4-nitrobenzyl) phosphate (2.61j) (major *P*-diastereomer)

^{1}H NMR ($CDCl_3$, 400 MHz) δ ppm δ 8.28 – 8.24 (m, 2H), 7.60 (d, *J* = 8.8 Hz, 2H), 6.28 – 6.17 (m, 2H), 5.20 (d, *J* = 8.0 Hz, 2H), 4.25 (dd, *J* = 12.1, 4.0 Hz, 1H), 4.20 (dd, *J* = 12.1, 4.0 Hz, 1H), 4.10 – 4.02 (m, 2H), 2.58 – 2.53 (m, 2H), 2.16 (m, 2H), 1.36 – 1.34 (m, 2H); **^{13}C NMR** ($CDCl_3$, 125 MHz) δ ppm 147.9, 142.8, 137.3, 134.9, 128.2, 123.9, 69.4 (d, J_{COP} = 8.1 Hz), 67.1 (d, J_{COP} = 4.7 Hz), 44.8, 43.5, 41.9; **^{31}P NMR** ($CDCl_3$, 162 MHz) δ ppm 2.65, -3.88 (*dr* = 42:1); **FTIR** (thin film) 3396, 2968, 1606, 1517, 1346, 1286, 1178, 1116, 1035, 1012 cm^{-1}; **HRMS** calculated for $C_{16}H_{18}O_6NPNa$ $(M+Na)^+$ = 374.0769; found 374.0770 (TOF MS ES+).

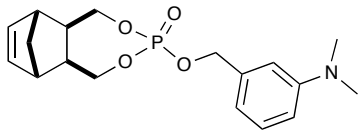

5-norbornene-2-*exo*, 3-*exo*-dimethyl (3-dimethylaminobenzyl) phosphate (2.61k) (major *P*-diastereomer)

^{1}H NMR ($CDCl_3$, 400 MHz) δ ppm 7.30 – 7.23 (m, 1H), 6.81 – 6.71 (m, 3H), 6.23 – 6.19 (m, 2H), 5.08 (d, J = 7.5 Hz, 2H), 4.19 (dd, J = 12.2, 3.9 Hz, 1H), 4.12 (dd, J = 12.1, 4.1 Hz, 1H), 4.06 – 3.98 (m, 2H), 2.98 (s, 6H), 2.52 (m, 2H), 2.17 – 2.09 (m, 2H), 1.35 – 1.29 (m, 2H); **^{13}C NMR** ($CDCl_3$, 125 MHz) δ ppm 150.6, 137.4, 136.4, 129.3, 116.0, 112.6, 112.0, 69.3 (d, J_{COP} = 8.4 Hz), 69.0 (d, J_{COP} = 5.2 Hz), 44.7, 43.4, 42.3, 40.4; **^{31}P NMR** ($CDCl_3$, 162 MHz) δ ppm 2.44, -3.49 (*dr* = 6:1); **FTIR** (thin film) 2962, 2900, 2804, 1606, 1502, 1353, 1292, 1253, 1118, 1064, 1010 cm^{-1}; **HRMS** calculated for $C_{18}H_{24}NO_4PNa$ $(M+Na)^+$ = 372.1341; found 372.1327 (TOF MS ES+).

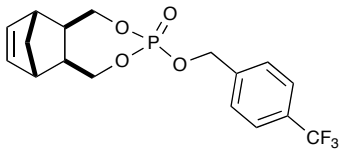

5-norbornene-2-*exo*, 3-*exo*-dimethyl (3-trifluoromethylbenzyl) phosphate (2.61l) (major *P*-diastereomer)

^{1}H NMR ($CDCl_3$, 400 MHz) δ ppm 7.67 (d, J = 8.1 Hz, 2H), 7.55 (d, J = 8.0 Hz, 2H), 6.23 – 6.21 (m, 2H), 5.17 (d, J = 7.9 Hz, 2H), 4.22 (dd, J = 12.0, 4.0 Hz, 1H), 4.17 (dd, J = 12.1, 4.1 Hz 1H), 4.08 – 3.99 (m, 2H), 2.58 – 2.52 (m, 2H), 2.19 – 2.14 (m, 2H), 1.37 – 1.34 (m, 2H); **^{13}C NMR** ($CDCl_3$, 125 MHz) δ ppm 139.9 (d, $^{3}J_{CF}$ = 7.3 Hz), 137.5, 131.0 (q, $^{2}J_{CF}$ = 32.5 Hz), 128.5, 125.9 (q, $^{4}J_{CF}$ = 3.7 Hz), 123.8 (q, $^{1}J_{CF}$ = 272 Hz), 69.5 (d, J_{COP} = 8.0 Hz), 67.9 (d, J_{COP} = 4.9 Hz), 45.0, 43.8, 42.1; **^{31}P NMR** ($CDCl_3$, 162 MHz) δ ppm 2.72, -3.81 (*dr* = 8:1); **FTIR** (thin film) 3068, 2968, 1622, 1421, 1327, 1285, 1165, 1117, 1067, 1041, 1012, 976, 903, 852, 712 cm^{-1}; **HRMS** calculated for $C_{17}H_{18}F_3O_4PNa$ $(M+Na)^+$ = 397.0792; found 397.0790 (TOF MS ES+).

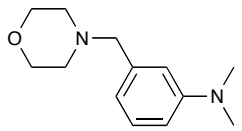

***N*,*N*-dimethyl-3-(morpholinomethyl)aniline (2.64k)**

^{1}H NMR ($CDCl_3$, 500 MHz) δ ppm 7.21 – 7.18 (m, 1H), 6.74 – 6.70 (m, 2H), 6.66 (dd, *J* = 8.1, 2.3 Hz, 1H), 3.77 – 3.70 (m, 4H), 3.48 (s, 2 H), 2.96 (s, 6H), 2.47 (s, 4H); **^{13}C NMR** ($CDCl_3$, 125 MHz) δ ppm 149.0, 136.9, 127.2, 115.9, 111.7, 109.7, 65.4, 62.3, 52.0, 39.0; **FTIR** (thin film) 2924, 2802, 1659, 1605, 1497, 1454, 1532, 1117, 1001, 868, 771, 694 cm^{-1}; **HRMS** calculated for $C_{13}H_{21}N_2O$ $(M+H)^+$ = 221.1654; found 221.1648 (TOF MS ES+).

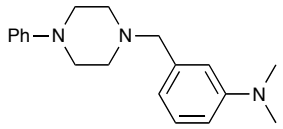

***N*,*N*-dimethyl-3-((4-phenylpiperazin-1-yl)methyl)aniline (2.64k′)**

^{1}H NMR ($CDCl_3$, 400 MHz) δ ppm 7.34 – 7.29 (m, 3H), 7.04 – 7.00 (m, 2H), 6.93 (t, *J* = 7.3, 1H), 6.90 – 6.80 (m, 2H), 6.75 (dd, *J* = 7.8, 2.1 Hz, 1H), 3.62 (s, 2H), 3.34 – 3.25 (m, 4H), 3.04 (s, 6H), 2.75 – 2.67 (m, 4H); **^{13}C NMR** ($CDCl_3$, 125 MHz) δ ppm 151.6, 150.9, 129.3, 129.1, 119.7, 117.9, 116.2, 113.6, 111.7 63.7, 53.3, 49.3, 40.9; **FTIR** (thin film) 2877, 2810, 1601, 1501, 1452, 1350, 1229, 758, 692 cm^{-1}; **HRMS** calculated for $C_{19}H_{26}N_3$ $(M+H)^+$ = 296.2127; found 296.2124 (TOF MS ES+)

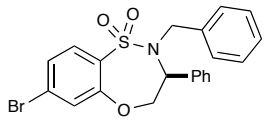

(*S*)-2-benzyl-7-bromo-3-phenyl-3,4-dihydro-2H-benzo[b][1,4,5]oxathiazepine 1,1-dioxide (2.66a)

$[\alpha]_D^{20}$ = + 48.0 (c = 1.7, $CHCl_3$); **^{1}H NMR** (500 MHz, $CDCl_3$) δ ppm 7.78 (d, *J* = 8.5 Hz, 1H), 7.35 (dd, *J* = 7.5, 2.0 Hz, 2H), 7.32 – 7.27 (m, 4H), 7.21 (d, *J* = 1.8 Hz, 1H), 7.20 – 7.14 (m, 3H), 7.07 – 7.03 (m, 2H), 5.26 – 5.18 (m, 1H), 4.91 (dd, *J* = 10.7, 3.9 Hz, 1H), 4.66 (d, *J* = 15.2 Hz, 1H), 4.56 (dd, *J* = 13.5, 4.1 Hz, 1H), 4.18 (d, *J* = 15.2 Hz, 1H); **^{13}C NMR** (126 MHz, $CDCl_3$) δ 155.4, 135.4, 134.7, 131.0, 129.2, 128.7, 128.6, 128.5, 128.4, 127.9, 127.9, 127.2, 125.9, 124.3, 73.3, 63.8, 53.2; **FTIR** (thin film) 3051, 2980, 1598, 1355, 1340, 1164 cm^{-1}; **HRMS** calculated for $C_{21}H_{18}BrNO_3SNa$ $(M+Na)^+$ = 466.0088: found 464.0084 (TOF MS ES+).

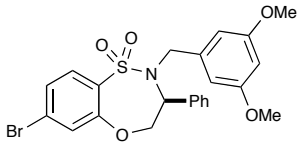

(*S*)-7-bromo-2-(3,5-dimethoxybenzyl)-3-phenyl-3,4-dihydro-2*H* benzo[*b*] [1,4,5]oxathiazepine 1,1-dioxide (2.66b)

$[\alpha]_D^{20}$ = + 17.2 (c = 1.18, $CHCl_3$); **^{1}H NMR** (500 MHz, $CDCl_3$) δ ppm 7.80 (d, *J* = 8.5 Hz, 1H), 7.43 (dd, *J* = 7.8, 1.4 Hz, 2H), 7.36 – 7.30 (m, 3H), 7.30 – 7.26 (m, 1H), 7.22 (d, *J* = 1.9 Hz, 1H), 6.29 (t, *J* = 2.3 Hz, 1H), 6.17 (d, *J* = 2.2 Hz, 2H), 5.31 (dd, *J* = 15.7, 8.8 Hz, 1H), 4.85 (dd, *J* = 10.9, 4.1 Hz, 1H), 4.70 (d, *J* = 15.4 Hz, 1H), 4.52 (dd, *J* = 13.6, 4.2 Hz, 1H), 4.09 (d, *J* = 15.4 Hz, 1H), 3.56 (s, 6H); **^{13}C NMR** (126 MHz, $CDCl_3$) δ ppm 160.7, 155.3, 137.7, 134.7, 130.8, 129.0, 128.7, 128.5, 128.0, 127.1, 125.7, 124.2, 106.0, 100.3, 73.4, 63.9, 55.1, 53.5; **FTIR** (thin film) 3057, 2955, 1600, 1358, 1339, 1164 cm^{-1}; **HRMS** calculated for $C_{23}H_{22}BrNO_5SNa$ $(M+Na)^+$ = 503.0402; found 503.0405 (TOF MS ES+).

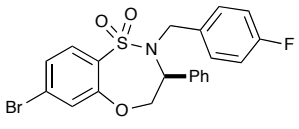

(*S*)-7-bromo-2-(4-fluorobenzyl)-3-phenyl-3,4-dihydro-2H-benzo[b][1,4,5] oxa thiazepine 1,1-dioxide (2.66c)

$[\alpha]_D^{20}$ = 88.2 (c = 1.04, $CHCl_3$); **^{1}H NMR** (500 MHz, $CDCl_3$) δ ppm 7.77 (d, *J* = 8.5 Hz, 1H), 7.35 – 7.31 (m, 3H), 7.31 – 7.27 (m, 4H), 7.24 (d, *J* = 1.9 Hz, 1H), 7.01 (dd, *J* = 8.6, 5.3 Hz, 2H), 6.84 (ddd, *J* = 10.7, 5.9, 2.5 Hz, 2H), 5.19 – 5.11 (m, 1H), 4.94 (d, *J* = 7.0 Hz, 1H), 4.60 (dd, *J* = 12.9, 3.4 Hz, 1H), 4.58 (s, 1H), 4.15 (d, *J* = 15.3 Hz, 1H); **^{13}C NMR** (126 MHz, $CDCl_3$) δ ppm 162.3 (d, $^1J_{CF}$ = 247 Hz), 134.6, 131.3 (d, $^4J_{CF}$ = 1.7 Hz), 130.2 (d, $^3J_{CF}$ = 8.3 Hz), 130.1, 129.3, 128.7, 128.6, 127.9, 127.4, 126.1, 124.6, 115.3, 115.1, (d, $^2J_{CF}$ = 21.5 Hz), 73.2, 63.9, 52.2; **FTIR** (thin film) 3057, 2955, 1600, 1358, 1339, 1164 cm^{-1}; **HRMS** calculated for $C_{21}H_{17}BrFNO_3SNa$ $(M+Na)^+$ = 483.9994; found 483.9989 (TOF MS ES+).

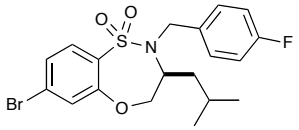

(*S*)-7-bromo-2-(4-fluorobenzyl)-3-isobutyl-3,4-dihydro-2H-benzo[b][1,4,5] oxathiazepine 1,1-dioxide (2.66d)

$[\alpha]_D^{20}$ = + 40.3 (c = 2.25, $CHCl_3$); **^{1}H NMR** (500 MHz, $CDCl_3$) δ ppm 7.70 (d, *J* = 8.4 Hz, 1H), 7.36 – 7.30 (m, 3H), 7.23 (d, *J* = 1.8 Hz, 1H), 7.04 – 6.98 (m, 2H), 4.60 (t, *J* = 11.9 Hz, 1H), 4.39 (d, *J* = 14.7 Hz, 1H), 4.31 (dd, *J* = 13.2, 4.5 Hz, 1H), 4.05 (d, *J* = 14.8 Hz, 1H), 3.81 (s, 1H), 1.55 (d, *J* = 8.5 Hz, 2H), 1.34 (td, *J* = 13.3, 6.6 Hz, 1H), 1.29 – 1.22 (m, 1H), 0.65 (dd, *J* = 18.7, 6.5 Hz, 6H); **^{13}C NMR** (126 MHz, $CDCl_3$) δ ppm 162.6 (d, $^1J_{CF}$ = 247 Hz), 156.1, 131.7 (d, $^4J_{CF}$ = 3.1 Hz), 131.1, 130.6 (d, $^3J_{CF}$ = 8.2 Hz), 130.2 127.3 126.7, 124.9, 115.4 (d, $^2J_{CF}$ = 21.5 Hz) 74.4, 59.6, 39.5, 30.9, 24.7, 22.3, 22.1; **FTIR** (thin film) 3045, 2970, 1605, 1365, 1335, 1164 cm^{-1}; **HRMS** calculated for $C_{19}H_{21}BrFNO_3SNa$ $(M+Na)^+$ = 464.0307; found 464.0308 (TOF MS ES+).

General procedure for palladium-catalyzed reductive Heck and *in situ* ROMP

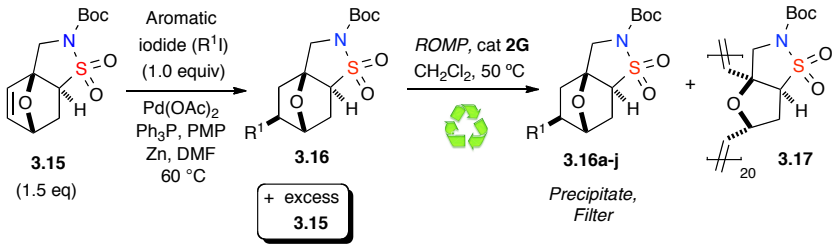

To a 25 mL round-bottom flask, sultam **3.15** (50 mg, 0.174 mmol, 1.5 equiv.), aryl iodide (28.3 mg, 0.12 mmol, 1.0 equiv.), $Pd(OAc)_2$ (4 mg, 0.017 mmol, 15 mol%), PPh_3 (9 mg, 0.036 mmol, 30 mol%), PMP (9.3 mg, 0.06 mmol, 0.5 equiv.), Zn (227 mg, 3.48 mmol, 10 equiv.) and HCO_2H (0.00856 mL, 0.12 mmol, 1.0 equiv.) were added under argon and followed by addition of dry DMF (6 mL). The resulting mixture was heated w/ stirring at 60 ºC for 14 hours until the iodide was consumed as indicated by TLC. The reaction mixture was allowed to cool to room temperature and DMF was evaporated, followed by the addition of 4:1 EtOAc/hexanes (30 mL). This mixture was extracted 4 times with brine using 5 mL each. The organic layer was separated and dried over $MgSO_4$ and filtered through a pad of Celite. The filtrate was concentrated *in vacuo* and the crude product was treated with catalyst **2G** (2.43 mg, 0.00287 mmol) in deoxygenated CH_2Cl_2 (0.1 M) at 50 ºC overnight in a round-bottom flask under argon w/ water condenser. The reaction mixture was allowed to cool to rt and 0.1 mL of ethyl vinyl ether (EVE) was added and stirred at room temperature for 30 min. The reaction mixture was concentrated *in vacuo* until slight viscosity is observed and precipitated drop-wise into Et_2O (40 mL). Simple filtration through a medium glass frit afforded the dry (reclaimed) oligomer **3.17**. The filtrate was concentrated *in vacuo* and filtered through a SiO_2 SPE with 50% EtOAc/hexanes to afford reductive Heck products **3.16a–j**.

General procedure for Suzuki-coupling (reclaimed scaffold) and Vanishing Support Protocol (VSP)

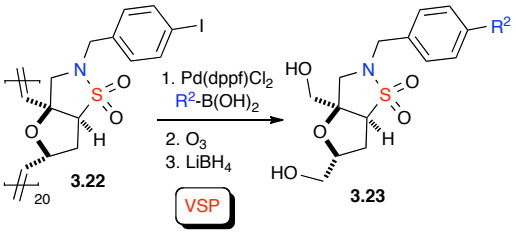

In a 15–20 mL round bottom flask w/ condenser under argon was added oligomeric-bound sultam **3.22** (100 mg, 0.25 mmol, 20-*mer*), Cs_2CO_3 (155 mg, 1 mmol), $Pd(dppf)Cl_2$ (37 mg, 50 μmol), boronic acid (155 mg, 1 mmol), and dry THF:DMF (5:1 v/v, 2.5 mL, 0.1 M). The reaction was stirred at 70 ºC for 14-16 hours and allowed to return to 25 ºC. The reaction was quenched via addition of aqueous NaOH (5 mL, 2.5 M) and stirred for 30-45 min. The reaction was washed w/ additional aqueous NaOH (3 x 5 ml, 2.5 M), dried ($MgSO_4$), and rinsed through a pad of Celite w/ multiple portions of CH_2Cl_2. The oligomeric-containing filtrate was concentrated *in vacuo* until slightly viscous and precipitated drop-wise into Et_2O (200 mL). Filtration through medium glass frit and wash w/ Et_2O yields a light grey, powdered oligomer in excellent yield. This was added to a 50 mL round bottom flask, dissolved in CH_2Cl_2, and cooled to -78 ºC. This solution was then subjected to ozonolysis via bubbling ozone gently through the solution in the open flask. After a period of 1 hour the solution was allowed to warm to -30 ºC while being purged with an argon-filled balloon and 4 in. needle. Excess solid $LiBH_4$ was added to the flask at -30 ºC w/ stir and the flask was sealed over argon. The resulting solution was stirred and allowed to return to room temperature overnight. The reaction was quenched with water over 1 hour, extracted w/ chloroform (3 x 5 mL), and concentrated *in vacuo* to yield the pure dimethanolic sultam product **3.23** in good yields over the three-step process (30-48%). No further purification was carried out.

Procedure for Dihydroxylation and *in-situ* ROMP

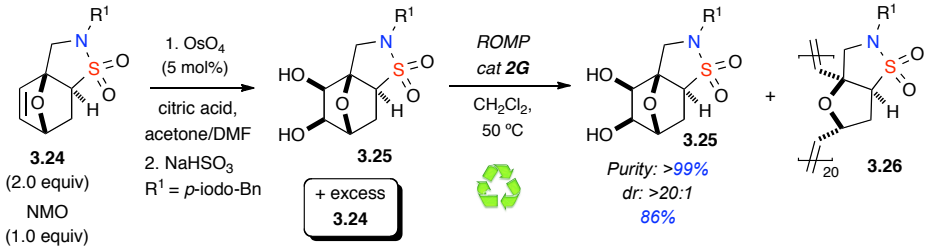

To a 10 mL round bottom flask was added sultam **3.24** (100 mg, 0.25 mmol), citric acid (40 mg, 0.19 mmol), *N*-methyl morpholine *N*-oxide (22 mg, 0.125 mmol), OsO_4 (5% in H_2O) (5 % by weight, 64 μL), and acetone:DMF (3:1 v/v, 2.5 mL, 0.1 M). This mixture was then stirred at RT over argon. After monitoring over 6 hours via TLC, the reaction was quenched with sodium bisulfite ($NaHSO_3$) and stirred at RT for an additional 30 min. This mixture was extracted with $CHCl_3$ (3 x 7 mL), dried ($MgSO_4$), and filtered through a pad of Celite. The filtrate was then concentrated *in vacuo* and reconstituted in deoxygenated CH_2Cl_2 followed by transfer into a 5 mL Kimex pressure tube. To this was added catalyst **2G** (5 mol%, 0.1 M), assuming an initial 50% conversion of the dihydroxylated product, and placed over argon w/ stirring at 50 ºC for 2 hours. The reaction was allowed to cool to rt followed by the addition of EVE (0.1 mL). This was allowed to stir for an additional 15–20 min. The white, crystalline product **3.25** precipitated out during the ROM polymerization event and was collected by filtration via Büchner funnel with repeated rinsing (CH_2Cl_2) and dried under vacuum to yield (47 mg, 0.11 mmol, 86 %). The oligomeric-containing filtrate (reclaimed) was then concentrated *in vacuo* until slightly viscous followed by drop-wise precipitation in Et_2O (100 mL). Filtration through medium glass frit yielded the reclaimed oligomeric scaffold **3.26** (50 mg), which was dried *in vacuo* for 20 min. No further purification was needed.

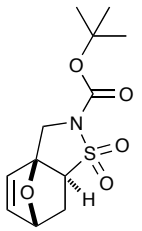

(±) tert-butyl3,6,7,7a-tetrahydro-2H-3a,6-epoxybenzo[d] isothiazole-2-carboxylate 1,1-dioxide (3.15)

^{1}H NMR (500 MHz, $CDCl_3$) δ ppm 6.55 (dd, *J* = 5.8, 1.7 Hz, 1H), 6.27 (d, *J* = 6.0 Hz, 1H), 5.20 (dd, *J* = 4.7, 1.6 Hz, 1H), 4.20 (q, *J* = 12.3 Hz, 2H), 3.30 (dd, *J* = 7.6, 3.2 Hz, 1H), 2.66 (ddd, *J* = 12.5, 4.6, 3.2 Hz, 1H), 1.81 (dd, *J* = 12.5, 7.7 Hz, 1H), 1.48 (s, 9H); **^{13}C NMR** (126 MHz, $CDCl_3$) δ ppm 149.7, 140.5, 132.7, 88.1, 84.4, 79.5, 62.2, 47.1, 30.1, 28.0; **FTIR** (neat) 1720, 1330, 1170, 1135, 983 cm^{-1}; **HRMS** calculated for $C_{12}H_{17}NO_5SNa$ $(M+Na)^+$ = 310.0725; found 310.0698 (TOF MS ES+).

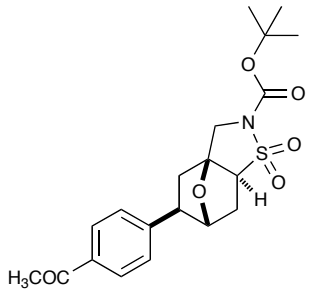

(±) tert-butyl-5-(4-acetylphenyl)hexahydro-2H-3a,6-epoxybenzo[d]isothiazole-2-carboxylate 1,1-dioxide (3.16a)

^{1}H NMR (500 MHz, $CDCl_3$) δ ppm 7.93 (d, *J* = 8.2 Hz, 2H); 7.40 (d, *J* = 8.2 Hz, 2H), 4.76 (d, *J* = 5.4 Hz, 1H), 4.35 (d, *J* = 12.3 Hz, 1H), 3.98 (d, *J* = 12.3 Hz, 1H), 3.70 (dd, *J* = 8.5, 4.1 Hz, 1H), 3.17 (dd, *J* = 8.7, 5.2 Hz, 1H), 2.78 (dt, *J* = 13.3, 4.7 Hz, 1H), 2.62 (s, 3 H), 2.45 (dd, *J* = 12.6, 8.8 Hz, 1H), 2.31 (dd, *J* = 13.4, 8.3 Hz, 1H), 1.91 (dd, *J* = 12.8, 5.2 Hz, 1H), 1.58 (s, 9H); **^{13}C NMR** (126 MHz, $CDCl_3$) δ ppm 197.5, 149.6, 149.3, 135.9, 128.9, 127.2, 85.7, 84.5, 83.4, 65.2, 48.2, 46.6, 41.9, 35.3, 28.0, 26.6; **FTIR** (neat) 1720, 1679, 1332, 1309, 1135 cm^{-1}; **HRMS** calculated for $C_{20}H_{25}NO_6SNa$ $(M+Na)^+$ = 430.1300; found 430.1296 (TOF MS ES+).

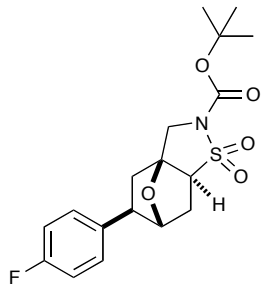

(±) tert-butyl-5-(4-acetylphenyl)hexahydro-2H-3a,6-epoxybenzo[d]isothiazole-2-carboxylate 1,1-dioxide (3.16b)

^{1}H NMR (500 MHz, $CDCl_3$) δ ppm 7.16 (dd, *J* = 8.7, 5.2 Hz, 2H), 6.92 (dd, *J* = 8.5, 4.4 Hz, 2H), 4.62 (d, *J* = 5.0 Hz, 1H), 3.87 (d, *J* = 12.3 Hz, 1H), 3.58 (dd, *J* = 8.5, 4.1 Hz, 1H), 2.99 (dd, *J* = 8.8, 5.4 Hz, 1H), 2.65 (ddd, *J* = 13.2, 4.9, 4.6 Hz, 1 H), 2.33 (dd, *J* = 12.8, 8.7 Hz, 1H), 2.18 (dd, *J* = 13.4, 8.4 Hz, 1H), 1.77 (dd, *J* = 12.8, 5.2 Hz, 1H), 1.49 (s, 9H); **^{13}C NMR** (126 MHz, $CDCl_3$) δ ppm 161.8 (d, $^{1}J_{CF}$ = 246 Hz), 160.8, 149.7, 139.9 (d, $^{4}J_{CF}$ = 3.8 Hz), 128.5 (d, $^{3}J_{CF}$ = 7.6 Hz), 115.6 (d, $^{2}J_{CF}$ = 20.2 Hz), 85.6, 84.5, 83.8, 47.5, 46.6, 42.2, 35.3, 28.0; **FTIR** (neat) 2983, 1720, 1330, 1309, 1157, 1132 cm^{-1}; **HRMS** calculated for $C_{18}H_{22}FNO_5SNa$ $(M+Na)^+$ = 406.1100; found 406.0997 (TOF MS ES+).

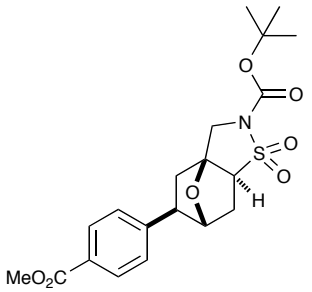

(±) tert-butyl 5-(4-(methoxycarbonyl)phenyl)hexahydro-2H-3a,6-epoxybenzo [d]isothiazole-2-carboxylate 1,1-dioxide (3.16c)

^{1}H NMR (500 MHz, $CDCl_3$) δ ppm 8.00 (d, *J* = 8.5 Hz, 2H), 7.34-7.40 (m, 2H), 4.76 (d, *J* = 5.0 Hz, 1H), 4.35 (d, *J* = 12.0 Hz, 1H), 3.94-4.01 (m, 1H), 3.93 (s, 3H), 3.70 (dd, *J* = 8.5, 4.1 Hz, 1H), 3.16 (dd, *J* = 8.8, 5.4 Hz, 1H), 2.77 (d, *J* = 13.2 Hz, 1H), 2.45 (dd, *J* = 12.9, 8.8 Hz, 1H), 2.30 (dd, *J* = 13.4, 8.4 Hz, 1H), 1.91 (dd, *J* = 12.9, 5.4 Hz, 1 H), 1.58 (s, 9H); **^{13}C NMR** (126 MHz, $CDCl_3$) δ ppm 166.7, 149.6, 149.1, 130.1, 128.9, 127.0, 85.7, 84.5, 83.4, 65.2, 52.1, 48.2, 46.6, 41.9, 35.3, 28.0; **FTIR** (neat) 1720, 1332, 1280, 1166, 985 cm^{-1}; **HRMS** calculated for $C_{20}H_{25}NO_7SNa$ $(M+Na)^+$ = 446.1249; found 446.1235 (TOF MS ES+).

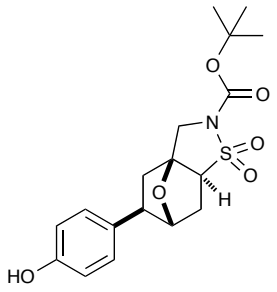

(±)-tert-butyl-5-(4-hydroxyphenyl)hexahydro-2H-3a,6-epoxybenzo[d]isothiazole-2-carboxylate 1,1-dioxide (3.16d)

^{1}H NMR (500 MHz, $CDCl_3$) δ ppm 7.06 (d, *J* = 8.5 Hz, 2H), 6.70 (d, *J* = 8.5 Hz, 2H), 4.60 (s, 1 H), 4.23 (d, *J* = 12.3 Hz, 1H), 3.86 (d, *J* = 12.3 Hz, 1H), 3.57 (dd, *J* = 8.4, 3.9 Hz, 1H), 2.94 (dd, *J* = 8.7, 5.2 Hz, 1H), 2.63 (dt, *J* = 13.3, 4.7 Hz, 1H), 2.29 (dd, *J* = 12.6, 8.8 Hz, 1H), 2.16 (dd, *J* = 13.2, 8.5 Hz, 1H), 1.77 (dd, *J* = 12.9, 5.0 Hz, 1H), 1.48 (s, 9H); **^{13}C NMR** (126 MHz, $CDCl_3$) δ ppm 154.4, 149.7, 136.5, 128.2, 115.5, 85.6, 84.5, 83.9, 65.4, 47.5, 46.7, 42.2, 35.3, 28.0; **FTIR** (neat) 2979, 1722, 1515, 1371, 1290, 1238 cm^{-1}; **HRMS** calculated for $C_{18}H_{23}NO_6SNa$ $(M+Na)^+$ = 404.1144; found 404.1120 (TOF MS ES+).

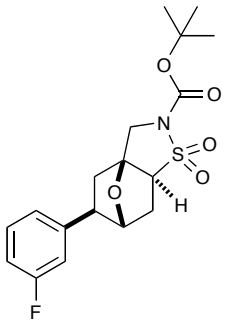

(±) tert-butyl-5-(3-fluorophenyl) hexahydro-2H-3a,6-epoxybenzo[d]isothiazole-2-carboxylate 1,1-dioxide (3.16e)

^{1}H NMR (500 MHz, $CDCl_3$) δ ppm 7.29 – 7.25 (m, 3H), 7.02 (ddd, *J* = 10.1, 8.8, 4.7 Hz, 3H), 6.94 (td, *J* = 8.4, 2.2 Hz, 1H), 4.73 (d, *J* = 5.2 Hz, 1H), 4.32 (d, *J* = 12.1 Hz, 1H), 3.94 (t, *J* = 9.9 Hz, 1H), 3.66 (dd, *J* = 8.4, 4.0 Hz, 1H), 3.08 (dd, *J* = 8.7, 5.2 Hz, 1H), 2.77 – 2.69 (m, 1H), 2.41 (dd, *J* = 12.8, 8.8 Hz, 1H), 2.26 (dd, *J* = 13.4, 8.4 Hz, 2H), 1.88 (dd, *J* = 12.8, 5.2 Hz, 1H), 1.56 (d, *J* = 7.3 Hz, 12H), 1.50 (s, 1H); **^{13}C NMR** (126 MHz, $CDCl_3$) δ ppm 163.2 (d, $^{1}J_{CF}$ = 247 Hz), 149.9, 146.7 (d, $^{2}J_{CF}$ = 7.2 Hz), 130.5 (d, $^{2}J_{CF}$ = 8.3 Hz), 122.9 (d, $^{4}J_{CF}$ = 2.7 Hz), 114.2 (d, $^{3}J_{CF}$ = 6.2 Hz), 114.1 (d, $^{3}J_{CF}$ = 5.4 Hz), 85.8, 84.7, 83.7, 48.1, 46.8, 42.2, 35.3, 28.2; **FTIR** (thin film) 2978, 1720, 1371, 1329,1310, 1242, 1138, 984, 735 cm^{-1}; **HRMS** calculated for $C_{18}H_{22}FNO_5SNa$ $(M+Na)^+$ 406.1100; found 406.1101 (0.2 ppm).

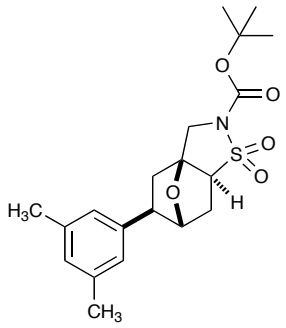

(±) tert-butyl 5-(3,5-dimethylphenyl) hexahydro-2H-3a,6 epoxybenzo [d]iso thiazole-2-carboxylate 1,1-dioxide (3.16f)

^{1}H NMR (500 MHz, $CDCl_3$) δ ppm 7.22 – 7.07 (m, 4H), 4.70 (d, *J* = 5.2 Hz, 1H), 4.31 (d, *J* = 12.1 Hz, 1H), 3.94 (d, *J* = 12.1 Hz, 1H), 3.66 (dd, *J* = 8.4, 4.1 Hz, 1H), 3.04 (dd, *J* = 8.7, 5.3 Hz, 1H), 2.78 – 2.63 (m, 1H), 2.38 (dd, *J* = 12.7, 8.8 Hz, 1H), 2.33 (s, 3H), 2.29 – 2.21 (m, 1H), 1.88 (dd, *J* = 12.8, 5.2 Hz, 1H), 1.56 (s, 9H); **^{13}C NMR** (126 MHz, $CDCl_3$) δ ppm 149.7, 144.0, 138.3, 128.5, 124.7, 85.6, 84.4, 83.7, 65.4, 48.1, 46.7, 41.9, 35.4, 28.0, 28.0, 21.3; **FTIR** (thin film) 2980, 1724, 1345, 1310, 1259, 1138, 845, 735 cm^{-1}; **HRMS** calculated for $C_{20}H_{27}NO_5SNa$ $(M+Na)^+$ = 416.1508; found 416.1510 (0.5 ppm).

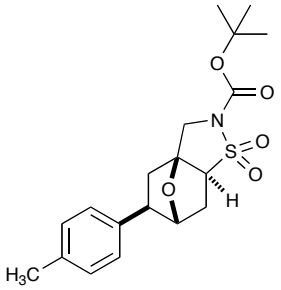

(±) *tert*-butyl-5-(*p*-tolyl) hexahydro-2*H*-3a,6-epoxybenzo[*d*]isothiazole-2-carboxylate 1,1-dioxide (3.16g)

^{1}H NMR (500 MHz, $CDCl_3$) δ ppm 7.20 – 7.09 (m, 4H), 4.70 (d, *J* = 5.2 Hz, 1H), 4.31 (d, *J* = 12.1 Hz, 1H), 3.94 (d, *J* = 12.1 Hz, 1H), 3.65 (dt, *J* = 17.6, 8.8 Hz, 1H), 3.04 (dd, *J* = 8.7, 5.3 Hz, 1H), 2.77 – 2.66 (m, 1H), 2.38 (dd, *J* = 12.7, 8.8 Hz, 1H), 2.33 (s, 3H), 2.25 (dd, *J* = 13.3, 8.4 Hz, 1H), 1.88 (dd, *J* = 12.8, 5.2 Hz, 1H); **^{13}C NMR** (126 MHz, $CDCl_3$) δ ppm 149.8, 141.1, 136.6, 129.4, 126.8, 85.6, 84.4, 83.9, 65.4, 47.8, 46.7, 42.1, 35.4, 28.0, 21.0; **FTIR** (thin film) 2982, 1722, 1333, 1167, 1136, 735 cm^{-1}; **HRMS** calculated for $C_{19}H_{25}NO_5SNa$ $(M+Na)^+$ = 402.1351; found 402.1357 (1.5 ppm).

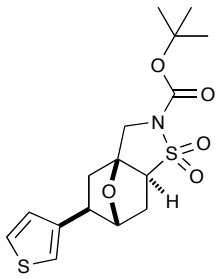

(±) tert-butyl-5-(4-(thiophen-3-yl)phenyl) hexahydro-2H-3a,6-epoxybenzo [d]iso-thiazole-2-carboxylate 1,1-dioxide (3.16h)

^{1}H NMR (500 MHz, $CDCl_3$) δ ppm 7.29 (dd, *J* = 5.0, 3.0 Hz, 1H), 7.06 – 7.00 (m, 2H), 4.71 (d, *J* = 5.2 Hz, 1H), 4.28 (d, *J* = 12.1 Hz, 1H), 3.95 – 3.90 (m, 1H), 3.67 – 3.60 (m, 1H), 3.24 (dd, *J* = 8.6, 5.0 Hz, 1H), 2.75 – 2.69 (m, 1H), 2.38 – 2.32 (m, 1H), 2.23 (dt, *J* = 20.7 Hz, 10.4, 1H), 1.89 – 1.82 (m, 1H), 1.56 (d, *J* = 4.8 Hz, 9H); **^{13}C NMR** (126 MHz, $CDCl_3$) δ ppm 144.6, 126.5, 126.4, 120.2, 85.7, 84.4, 83.3, 65.3, 46.7, 43.5, 41.3, 35.5, 34.9, 30.6, 29.3, 28.0, 27.9; **FTIR** (thin film) 2980, 1722, 1333, 1136, 735 cm^{-1}; **HRMS** calculated for $C_{16}H_{21}NO_5S_2Na$ $(M+Na)^+$ = 394.0759; found 394.0750 (2.3 ppm).

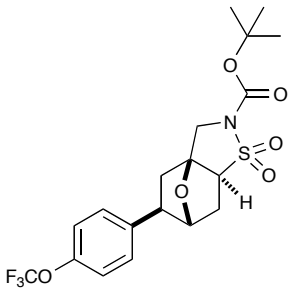

(±) tert-butyl-5-(4-(trifluoromethoxy)phenyl) hexahydro-2H-3a,6-epoxybenzo [d] isothiazole -2-carboxylate 1,1-dioxide (3.16i)

^{1}H NMR (500 MHz, $CDCl_3$) δ ppm 7.32 – 7.29 (m, 2H), 7.16 (d, *J* = 8.0 Hz, 2H), 4.72 (d, *J* = 5.2 Hz, 1H), 4.31 (d, *J* = 12.1 Hz, 1H), 3.95 (d, *J* = 12.2 Hz, 1H), 3.66 (dt, *J* = 8.5, 4.3 Hz, 1H), 3.10 (dd, *J* = 8.7, 5.2 Hz, 1H), 2.77 – 2.71 (m, 1H), 2.42 (dd, *J* = 12.8, 8.8 Hz, 1H), 2.27 (dd, *J* = 13.4, 8.4 Hz, 1H), 1.88 – 1.83 (m, 1H), 1.56 (s, 9H); **^{13}C NMR** (126 MHz, $CDCl_3$) δ ppm 149.1 (d, $^{1}J_{CF}$ = 200 Hz), 143.1, 128.6, 121.5, 85.9, 84.8, 83.8, 65.5, 47.8, 42.4, 35.5, 28.3 cm^{-1}; **HRMS** calculated for $C_{19}H_{22}F_3NO_6SNa$ $(M+Na)^+$ = 472.1018; found 472.1023 (1.1 ppm).

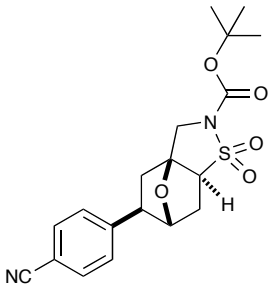

(±) tert-butyl-5-(4-cyanophenyl) hexahydro-2H-3a,6-epoxybenzo[d]isothiazole-2-carboxylate 1,1-dioxide (3.16j)

^{1}H NMR (500 MHz, $CDCl_3$) δ ppm 7.62 (d, *J* = 8.2 Hz, 2H), 7.40 (d, *J* = 8.3 Hz, 2H), 4.73 (d, *J* = 5.2 Hz, 1H), 4.32 (d, *J* = 12.2 Hz, 1H), 3.96 (d, *J* = 12.2 Hz, 1H), 3.69 – 3.65 (m, 1H), 3.14 (dd, *J* = 8.6, 5.2 Hz, 1H), 2.79 – 2.73 (m, 1H), 2.45 (dd, *J* = 12.9, 8.8 Hz, 1H), 2.29 (dt, *J* = 13.5, 6.1 Hz, 1H), 1.87 (dd, *J* = 12.9, 5.1 Hz, 1H), 1.57 (s, 9H); **^{13}C NMR** (126 MHz, $CDCl_3$) δ ppm 149.5, 132.9, 129.1, 128.1, 118.9, 111.3, 86.0, 84.9, 83.5, 65.4, 48.5, 46.7, 42.2, 35.5, 29.9, 28.3, 28.2; **FTIR** (thin film) 2928, 2359, 1722, 1606, 1332, 1138, 835 cm^{-1}; **HRMS**; calculated for $C_{19}H_{22}N_2O_5SNa$ $(M+Na)^+$ = 413.1147; found 413.1147 (0.0 ppm).

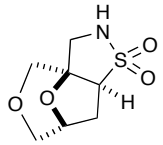

(±) hexahydro-2H-3a,7-epoxyoxepino[3,4-d]isothiazole 1,1-dioxide (3.19)

^{1}H NMR (500 MHz, $CDCl_3$) δ ppm 4.63 (br s, 1H); 4.47 (d, *J* = 6.3 Hz, 1H), 3.80 (dd, *J* = 9.3, 4.6 Hz, 1H), 3.75 (d, *J* = 11.7 Hz, 1H), 3.66 (t, *J* = 11.0 Hz, 1H), 3.61 (t, *J* = 11.2 Hz, 1H), 3.51 (d, *J* = 11.7 Hz, 1H), 3.23 (dd, *J* = 13.7, 5.8 Hz, 1H), 3.09 (t, *J* = 11.3 Hz, 1H), 2.63 (dt, *J* = 12.6, 6.3 Hz, 1H), 2.44 (dd, *J* = 13.4, 9.6 Hz, 1H); **^{13}C NMR** (126 MHz, $CDCl_3$) δ ppm 93.3, 78.4, 70.1, 69.9, 64.3, 44.8, 33.2; **FTIR** (neat) 1771, 1615, 1460, 1371, 1312 cm^{-1}; **HRMS** calculated for $C_7H_{11}NO_4SNa$ (M+Na) = 228.0306; found 228.0291 (TOF MS ES+); Purity calculated by GC 93%.

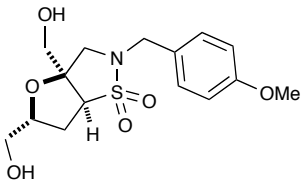

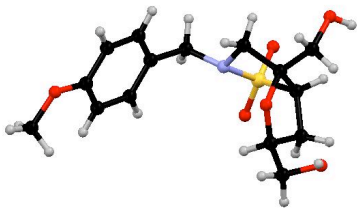

X-Ray Crystal Structure

(±)-3a,5-bis(hydroxymethyl)-2-(4-methoxybenzyl)hexahydrofuro[2,3-d]isothiazole 1,1-dioxide (3.21)

^{1}H NMR (400 MHz, $CO(CD_3)_2$) δ ppm 7.28 (d, *J* = 8.7 Hz, 2H), 6.92 (d, *J* = 8.7 Hz, 2H), 4.33 (dddd, *J* = 9.5, 6.4, 3.4, 3.4 Hz, 1H), 4.25 (t, *J* = 4.7 Hz, 1H), 4.24 (d, *J* = 13.2 Hz, 1H), 3.91 (t, *J* = 4.7 Hz, 1H), 3.89 (d, *J* = 14.1 Hz, 1H), 3.79 (s, 3H), 3.75 (d, *J* = 7.9 Hz, 1H), 3.64 (dd, *J* = 11.7, 4.7 Hz, 1H), 3.51 – 3.59 (m, 2H), 2.98 (dd, *J* = 13.1, 10.7 Hz, 2H), 2.87 (s, 1H), 2.47 (ddd, *J* = 13.6, 5.9, 1.4 Hz, 1H), 2.36 (ddd, *J* = 13.7, 10.0, 9.4 Hz, 1H); **^{13}C NMR** (125 MHz, $CO(CD_3)_2$) δ ppm 159.5, 129.8, 127.5, 113.9, 87.7, 81.6, 65.4, 63.2, 62.4, 54.7, 53.3, 46.3, 30.8; **FTIR** (neat) 3344, 2918, 1770, 1720, 1612, 1514, 1445, 1304, 1250, 1151, 1028, 822 cm^{-1}; **HRMS** calculated for $C_{15}H_{22}NO_6S$ $(M+H)^+$ = 344.1168; found 344.1170 (TOF MS ES+).

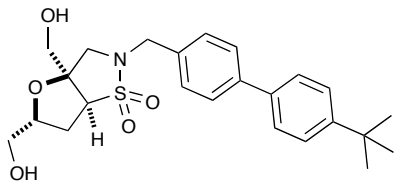

(±) 2-((4'-(tert-butyl)-[1,1'-biphenyl]-4-yl)methyl)-3a,5-bis(hydroxymethyl) hexa-hydrofuro[2,3-d]isothiazole 1,1-dioxide (3.23a)

^{1}H NMR (400 MHz, $CDCl_3$) δ ppm 7.65 – 7.43 (m, 6H), 7.36 (d, 7.4 Hz, 2H), 4.46 (s, 1H), 4.38 (d, *J* = 13.8 Hz, 1H), 4.07 (d, *J* = 13.7 Hz, 1H), 3.93 (d, *J* = 9.6 Hz, 1H), 3.83 (d, 6.9 Hz, 1 H), 3.78 – 3.45 (m, 3H), 3.10 (d, *J* = 10.0 Hz, 1H), 2.92 (d, *J* = 10.2 Hz, 1 H), 2.63 – 2.48 (m, 2H), 1.37 (s, 9H); **^{13}C NMR** (125 MHz, $CDCl_3$) 150.6, 141.0, 137.5, 133.3, 128.9, 127.4, 126.7, 125.8, 87.7, 81.2, 66.2, 63.6, 62.4, 53.4, 47.0, 34.6, 30.4, 29.7; **FTIR** (neat) 3377, 2960, 2924, 2866, 1772, 1612, 1499, 1460, 1439, 1364, 1310, 1150, 1057, 951, 816, 758 cm^{-1}; **HRMS** calculated for $C_{24}H_{31}NO_5SNa$ $(M+Na)^+$ = 468.1821; found 468.1801 (TOF MS ES+).

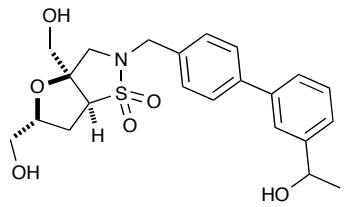

(±) 2-((3'-(1-hydroxyethyl)-[1,1'-biphenyl]-4-yl)methyl)-3a,5-bis(hydroxymethyl) hexa-hydrofuro[2,3-d]isothiazole 1,1-dioxide (3.23b) – mixture of diastereomers

^{1}H NMR (500 MHz, $CDCl_3$) δ ppm 7.60 – 7.53 (m, 3H), 7.47 (d, *J* = 7.4 Hz, 1H), 7.41 (t, *J* = 7.6 Hz, 1H), 7.33 (d, *J* = 6.8 Hz, 3H) 4.94 (q, *J* = 6.2 Hz, 1H), 4.40 – 4.25 (m, 1H), 4.32 (d, *J* = 14.0 Hz, 1H), 4.00 (d, *J* = 14.0 Hz, 1H), 3.95 (s, 1H), 3.9 (d, *J* = 12.0 Hz, 1H), 3.73 (d, *J* = 9.2 Hz, 1H), 3.65 (d, *J* = 11.7 Hz, 1H), 3.56 (d, *J* = 12.1 Hz, 1H), 3.51 (d, *J* = 12.1 Hz, 1H), 3.36 (s, 1H), 3.01 (d, *J* = 10.7 Hz, 1 H), 2.87 (d, *J* = 10.8 Hz, 1 H), 2.68 (s, 1 H), 2.5 (dd, *J* = 13.6, 5.5 Hz, 1H), 2.40 – 2.31 (m, 1H), 1.52 (d, *J* = 6.4 Hz, 3H); **^{13}C NMR** (125 MHz, $CDCl_3$) δ ppm 146.4, 141.0, 140.9, 140.6, 133.8, 130.7, 129.1, 129.0, 127.6, 126.2, 124.7, 87.6, 81.2, 70.4, 65.9, 63.4, 62.2, 61.3, 53.3, 46.9, 30.3, 25.3; **FTIR** (neat) 3381, 2966, 2924, 2854, 1439, 1306, 1150, 1076, 797, 752, 706 cm^{-1}; **HRMS** calculated for $C_{22}H_{28}NO_6S$ (M+H) = 434.1639; found 434.1621 (TOF MS ES+).

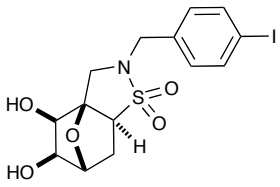

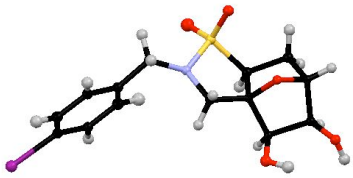

X-Ray Crystal Structure

(±) 4,5-dihydroxy-2-(4-iodobenzyl)hexahydro-2H-3a,6-epoxybenzo[d]isothiazole 1,1-dioxide (3.25)

^{1}H NMR (400 MHz, MeOD) δ ppm 7.70 (d, *J* = 10.7 Hz, 2H), 7.18 (d, *J* = 8.3 Hz, 2H), 4.40 (d, *J* = 5.4 Hz, 1H), 4.20 (s, 1 H), 3.98 (d, *J* = 5.9 Hz, 1H), 3.92 (d, *J* = 5.9 Hz, 1H), 3.50 (t, *J* = 4.7 Hz, 1H), 3.48 (d, *J* = 11.4 Hz, 1H) 3.32 (d, MeOD overlap, 1 H) 2.22 (dt, *J* = 5.2, 13.1 Hz, 1H), 2.02 (dd, *J* = 8.5, 13.1 Hz, 1H); **^{13}C NMR** (125 MHz, MeOD) δ ppm 137.5, 135.7, 130.2, 92.6, 90.0, 83.3, 74.2, 72.6, 47.7, 46.1, 28.9; **FTIR** (KBr) 3443, 2181, 2131, 2089, 1607, 1398, 1150, 997, 968, 630 cm^{-1}; **HRMS** calculated for $C_{28}H_{36}I_2N_3O_{10}S_2$ $(2M+NH_4)^+$ = 891.9931; found 891.9932 (TOF MS ES+)

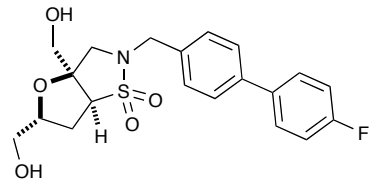

(±) 2-((4'-fluoro-[1,1'-biphenyl]-4-yl)methyl)-3a,5-bis(hydroxymethyl)hexahydro furo[2,3-d]isothiazole 1,1-dioxide (3.28a)

^{1}H NMR (400 MHz, $CDCl_3$) δ ppm 7.55 – 7.48 (m, 4H), 7.35 (d, *J* = 8.0 Hz, 2H), 7.11 (t, *J* = 8.6 Hz, 2H), 4.47 – 4.38 (m, 1H), 4.35 (d, *J* = 13.9 Hz, 1H), 4.15 (d, *J* = 13.9 Hz, 1H), 3.91 (d, *J* = 11.1 Hz, 1H), 3.79 (d, *J* = 8.5 Hz, 1H), 3.78 – 3.48 (m, 3H), 3.06 (d, *J* = 10.7 Hz, 1H), 2.91 (d, *J* = 10.7 Hz, 1H), 2.54 (dd, *J* = 13.1, 5.3 Hz, 1H), 2.50 – 2.38 (m, 1H); **^{13}C NMR** (125 MHz, $CDCl_3$) δ ppm 162.6 (d, $^{1}J_{CF}$ = 247 Hz), 140.1, 136.6 (d, $^{4}J_{CF}$ = 3.4 Hz), 133.7, 129.0, 128.6 (d, $^{3}J_{CF}$ = 8.1 Hz), 127.4, 115.7 (d, $^{2}J_{CF}$ = 21.6 Hz); **FTIR** (neat) 3381, 2953, 2918, 2849, 1603, 1499, 1308, 1232, 1150, 1059, 947, 822, 756 cm^{-1}; **HRMS** calculated for $C_{20}H_{22}FNO_5SNa$ $(M+Na)^+$ = 430.1100; found 430.1104 (TOF MS ES+).

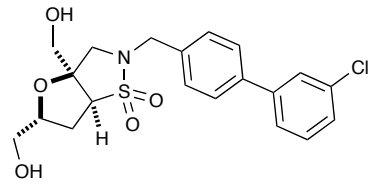

(±) 2-((3'-chloro-[1,1'-biphenyl]-4-yl)methyl)-3a,5-bis(hydroxymethyl) hexahydrofuro[2,3-d]isothiazole 1,1-dioxide (3.28b)

^{1}H NMR (400 MHz, $CDCl_3$) δ ppm 7.55 (dd, *J* = 8.9, 2.0 Hz, 3H), 7.46 (dt, *J* = 7.4, 1.5 Hz, 1H), 7.42 – 7.32 (m, 4H), 4.49 – 4.42 (m, 1H), 4.38 (d, *J* = 14.0 Hz, 1H), 4.06 (d, *J* = 14.0 Hz, 1H), 3.95 (d, *J* = 11.9 Hz, 1H), 3.82 (d, *J* = 8.9 Hz, 1H), 3.73 (d, *J* = 11.7 Hz, 1H), 3.68 – 3.57 (m, 2H), 3.07 (d, *J* = 10.7 Hz, 1H), 2.93 (d, *J* = 10.7 Hz, 1H), 2.58 (dd, *J* = 13.0, 6.0 Hz, 1H), 2.47 (dt, *J* = 13.8, 9.6 Hz, 1H); **^{13}C NMR** (125 MHz, $CDCl_3$) 142.2, 139.7, 134.7, 134.3, 130.1, 129.1, 127.2, 125.18, 87.6, 81.2, 66.1, 63.5, 62.3, 53.3, 46.9, 30.4; **FTIR** (neat) 3354, 2924, 1664, 1595, 1440, 1396, 1308, 1150, 1037, 787 cm^{-1}; **HRMS** calculated for $C_{20}H_{22}ClNO_5SNa$ $(M+Na)^+$ = 446.0805; found 446.0812 (TOF MS ES+).

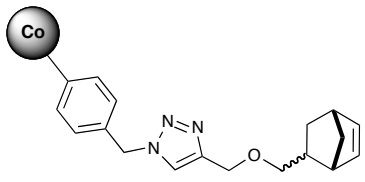

Norbornene-tagged Co/C-nanoparticles (4.8)

The azide-tagged carbon coated cobalt nanoparticles **4.6** (400 mg; 0.1 mmol/g azide-loading) were suspended in degassed toluene (3 mL) by the use of an ultrasonic bath (Sonorex RK 255 H-R, Bandelin) before propargylated bicyclo[2.2.1]hept-5-en-2-ylmethanol **4.7** (130 mg, 0.8 mmol), triethylamine (20 μL, 0.12 mmol) and CuI (5 mg, 0.03 mmol) were added. The resulting slurry was sonicated for 48 hr at ambient temperature under an argon atmosphere. The nanoparticles were recovered from the reaction mixture with the aid of a neodymium based magnet (N48, W-12-N, Webcraft GmbH, side length 12 mm) and washed with toluene (6 x 5 mL). Each washing step consisted of suspending the particles in the solvent, ultrasonication (5 min) and retracting the particles from the solvent by the aid of the magnet. After the last washing step the particles were dried *in vacuo* to yield 430 mg of **4.8**. IR (ν/cm^{-1}): 2928, 2817, 2097, 1693, 1598, 1505, 1404, 1377, 1253, 1214, 1175, 1096, 1013, 824, 71681; elemental microanalysis: 13.57% C, 0.69% H, 1.18% N.

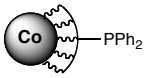

PPh_3-functionalized Co/C-ROMPgel (4.10)

200 mg (0.02 mmol) of norbornene-tagged Co/C-nanoparticles **4.8** were dispersed in CH_2Cl_2 (2 mL) by sonication in a sealed microwave reaction vessel under argon atmosphere (30 min). A solution of catalyst **2G** (17 mg, 0.02 mmol) in CH_2Cl_2 (1 mL) was injected and the ultrasound bath tempered to 60 °C while sonication of the reaction mixture continued (30 min). (4-*exo*-(bicyclo[2.2.1]hept-5-en-2-yl)phenyl) diphenyl phosphine **4.9** (353 mg, 1.0 mmol) was added and the dispersion was subjected to sonication at 60 °C for 2 hrs. Within 50 min the formation of voluminous black gel was observed. After 2 hrs the reaction was quenched and a single, jelly-like lump was removed from the reaction vessel, crushed and dried *in vacuo* to yield 490 mg of **4.10**. IR (ν/cm^{-1}): 2929, 2859, 1644, 1584, 1475, 1432, 1400, 1303, 1259, 1177, 1089, 1064, 962, 894, 852, 760, 691, 655; elemental microanalysis: 55.95% C; 4.59% H, 0.47% N, 3.45% P.

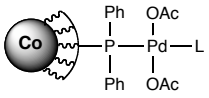

Pd-PPh_3-functionalized Co/C-ROMPgel (4.11)

200 mg of PPh_3-functionalized Co/C-ROMPgel **4.10** was allowed to swell in CH_2Cl_2 (2 mL) under sonication at 60°C under an atmosphere of argon (30 min) before $Pd(OAc)_2$ (40 mg, 0.18 mmol) was added to the reaction vessel. Sonication was maintained for additional 2 hrs before the magnetic ROMPgel was isolated from the reaction mixture by the aid of an external magnet and dried *in vacuo* to yield 212 mg of **4.11**. IR (ν/cm^{-1}): 2982, 2360, 2155, 1053, 1033, 1014, 696, 674, 664, 652; elemental microanalysis: 49.23% C; 4.06% H; 0.43% N.

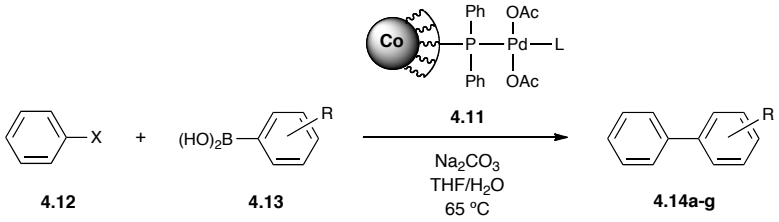

General procedure for the Suzuki-Miyaura cross-coupling reactions catalyzed by 4.11:

11 mg of Pd-PPh_3-functionalized Co/C-ROMPgel **4.11** (0.48 mmol/g Pd-loading, 1.1 mol%) was placed in a reaction vessel equipped with a magnetic stir bar and THF was added (1 mL). The particles were allowed to swell while stirring (30 min). Na_2CO_3 (160 mg, 1.5 mmol) dissolved in H_2O (2 mL), phenylboronic acid (0.55 mmol) and phenylhalide (0.5 mmol) were added subsequently and the reaction mixture was heated to 65 °C in an oil bath while stirring (1500 rpm) continued until the reaction was completed (TLC). The reaction mixture was magnetically decanted and the retained material washed with Et_2O (5 x 5 mL). Each washing step consisted of suspending the particles in the solvent, ultrasonication (5 min) and decanting the solvent from the particles with magnetic assist. The Et_2O portions were extracted against the decanted THF/water-mixture and the combined organic layers were dried over $MgSO_4$ and concentrated. These were subjected to silica SPE filtration using a 3:1 mixture of hexanes:EtOAc affording biaryl coupled products **4.14a-g** in excellent yields and purities. The recovered nanocatalyst **4.11** was washed with H_2O (3 x 5 mL) as described above and subjected to the next reaction.

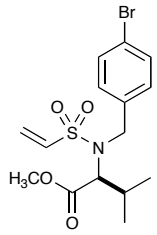

(*S*)-methyl 2-(*N*-(4-bromobenzyl)vinylsulfonamido)-3-methylbutanoate 5.6{*2*}

$[\alpha]^{20}_{D}$ = -32.0 º (c = 1.0, CH_2Cl_2); **^{1}H NMR** (500 MHz, $CDCl_3$) δ ppm 7.46 – 7.43 (m, 2H), 7.35 – 7.32 (m, 2H), 6.38 (dd, *J* = 16.5, 9.9 Hz, 1H), 6.19 (d, *J* = 16.5 Hz, 1H), 5.89 (d, *J* = 9.9 Hz, 1H), 4.45 – 4.37 (m, 2H), 4.07 (d, *J* = 10.6 Hz, 1H), 3.70 (s, 3H), 2.05 – 1.93 (m, 1H), 0.86 (d, *J* = 6.6 Hz, 3H), 0.81 (d, *J* = 6.6 Hz, 3H); **^{13}C NMR** (126 MHz, $CDCl_3$) δ ppm 171.3, 136.2, 135.1, 131.6, 131.0, 127.1, 122.0, 66.5, 51.9, 48.3, 28.5, 19.7, 19.7; **FTIR** (thin film) cm^{-1} 2966, 1740, 1489, 1342, 1142, 760; **HRMS** calculated for $C_{15}H_{20}BrNO_4SNa$ $(M+H)^+$ = 390.0375; found 390.0369 (TOF MS ES+). To a 250 mL RB flask containing crude vinyl sulfonamide linchpin **5.5**{*2*} (1.14 g, 5.15 mmol) was added 4-bromobenzyl bromide (1.50 g, 6.18 mmol), K_2CO_3 (1.40 g, 10.3 mmol) in CH_3CN (51 mL, 0.1 M). This was allowed to stir at 60 ºC for 12 – 14 hrs over argon and monitored by TLC. After which time the reaction was cooled to rt and filtered through a pad of celite to afford the crude tertiary sulfonamide **5.6**{*2*} as a dark orange oil.

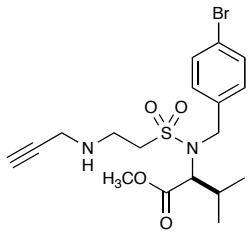

(*S*)-methyl 2-(*N*-(4-bromobenzyl)-2-(prop-2-yn-1-ylamino)ethylsulfonamido)-3-methylbutanoate 5.7{*2*}

$[\alpha]^{20}_{D}$ = -22.4 ° (c = 1.10, CH_2Cl_2); **^{1}H NMR** (500 MHz, $CDCl_3$) δ ppm 7.49 – 7.44 (m, 2H), 7.33 (d, *J* = 8.4 Hz, 2H), 4.56 (d, *J* = 15.4 Hz, 1H), 4.40 (d, *J* = 15.4 Hz, 1H), 4.11 (d, *J* = 10.7 Hz, 1H), 3.77 (s, 3H), 3.41 (d, *J* = 2.3 Hz, 2H), 3.11 – 3.07 (m, 2H), 3.04 – 2.95 (m, 2H), 2.24 (t, *J* = 2.4 Hz, 1H), 2.10 – 1.99 (m, 1H), 1.77 (s, 1H), 0.88 (d, *J* = 6.5 Hz, 3H), 0.85 (d, *J* = 6.7 Hz, 3H).; **^{13}C NMR** (126 MHz, $CDCl_3$) δ ppm 171.3, 135.9, 131.6, 131.0, 122.0, 81.3, 72.0, 66.3, 53.3, 52.1, 48.1, 42.5, 38.0, 28.2, 19.5, 19.3; **FTIR** (thin film) 3290, 2966, 1738, 1489, 1335, 1138 cm^{-1}; **HRMS** calculated for $C_{18}H_{25}BrN_2O_4SNa$ $(M+Na)^+$ = 467.0616; found 467.0634 (TOF MS ES+). To a 100 mL RB flask containing the crude tertiary sulfonamide **5.6**{*2*} (1.91 g, 4.89 mmol) was added 5 mL CH_3CN and DBU (373 mg, 2.45 mmol) followed by addition of propargylamine (404 mg, 7.34 mmol). This mixture was allowed to stir for 12 hrs over argon at 40 ºC. After such time, the reaction was concentrated *in vacuo* and subjected to silica column chromatography using 1:3 hexanes to EtOAc up to 100% EtOAc affording the amino ester-containing sulfonamide **5.7**{*2*} as clear, yellowish oil (1.15 g, 2.57 mmol, 50 % over three steps).

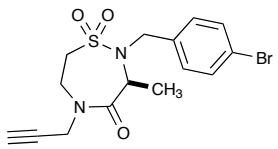

(*S*)-2-(4-bromobenzyl)-3-methyl-5-(prop-2-yn-1-yl)-1,2,5-thiadiazepin-1,1-dioxide-4-one 5.9{*1*}

ee = 2%; $[\alpha]^{20}_{D}$ = -18.5 º (c = 0.6, CH_2Cl_2); **^{1}H NMR** (400 MHz, $CDCl_3$) δ ppm 7.45 (d, *J* = 8.0 Hz, 2H), 7.27 (d, *J* = 7.8 Hz, 2H), 4.74 (m, 2H), 4.44 (d, *J* = 16.4 Hz, 1H), 4.13 (dd, *J* = 16.4, 11.3 Hz, 1H), 3.98 (d, *J* = 17.7 Hz, 1H), 3.93 (d, *J* = 16.5 Hz, 1H), 3.81 (dd, *J* = 16.7, 4.3 Hz, 1H), 3.31 (dd, *J* = 14.4, 5.2 Hz, 1H), 3.25 (m, 1H), 2.35 (t, *J* = 2.5 Hz, 1H), 1.24 (d, *J* = 6.7 Hz, 3H); **^{13}C NMR** (126 MHz, $CDCl_3$) δ ppm 171.5, 136.9, 131.7, 129.4, 121.6, 78.2, 73.5, 54.7, 50.0, 47.9, 43.4, 37.5, 16.3; **FTIR** (thin film) 3292, 2988, 2937, 1663, 1337, 1142 cm^{-1}; **HRMS** calculated for $C_{15}H_{17}BrN_2O_3SNa$ $(M+Na)^+$ = 407.0041; found 407.0045 (TOF MS ES+).

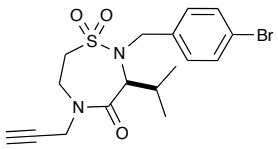

(*S*)-2-(4-bromobenzyl)-3-isopropyl-5-(prop-2-yn-1-yl)-1,2,5-thiadiazepin-1,1-dioxide-4-one 5.9{*2*}

ee = 17%; $[\alpha]^{20}_{D}$ = +2.5 ° (c = 0.5, CH_2Cl_2); **^{1}H NMR** (400 MHz, $CDCl_3$) δ ppm 7.45 (d, *J* = 8.5 Hz, 2H), 7.35 (d, *J* = 8.4 Hz, 2H), 4.77 (dd, *J* = 17.4, 2.4 Hz, 1H), 4.38 (d, *J* = 15.5 Hz, 1H), 4.13 (dd, *J* = 16.7, 11.2 Hz, 1H), 4.03 (d, *J* = 10.6 Hz, 1H), 3.93 (d, *J* = 15.6 Hz, 1H), 3.89 (dd, *J* = 17.6, 2.4 Hz, 1H), 3.76 (dd, *J* = 16.9, 3.5 Hz, 1H), 3.26 (ddd, *J* = 14.5, 5.2, 1.1 Hz, 1H), 3.16 (ddd, *J* = 14.3, 11.4, 2.1 Hz, 1H), 2.30 (t, *J* = 2.5 Hz, 1H), 2.05 (m, 1H), 0.89 (d, *J* = 6.3 Hz, 3H), 0.70 (d, *J* = 6.7 Hz, 3H); **^{13}C NMR** (126 MHz, $CDCl_3$) δ ppm 169.9, 135.5, 131.7, 131.4, 122.3, 78.3, 73.4, 65.2, 50.0, 48.5, 43.7, 37.0, 27.1, 20.6, 19.1; **FTIR** (thin film) 3296, 2964, 1661, 1339, 1142 cm^{-1}; **HRMS** calculated for $C_{17}H_{21}BrN_2O_3SNa$ $(M+Na)^+$ = 435.0354; found 435.0373 (TOF MS ES+). To a 10 mL RB was added the amino ester-containing sulfonamide **5.7**{*2*} (575 mg, 1.29 mmol) in 0.5 mL of THF. To this was added LiOH•H_2O (217 mg, 5.20 mmol) with 0.5 mL deionized H_2O and was allowed to stir rapidly at rt for 12 hrs. After such time, THF was removed in vacuo and the reaction was transferred a separatory funnel containing 10 mL DCM and 5 mL of deionized H_2O. The upper aqueous layer was then neutralized with 10% HCl. Upon reaching a pH value near neutral, a white precipitate formed and was collected by vacuum filtration and dried at 70 ºC under vacuum. This crude sulfonamide amino acid **5.8**{*2*} (620 mg) (likely containing residual Li salts) was then placed in a 100 mL RB under argon containing 30 mL DCM (0.05 M). To this was added EDC•HCl (550 mg, 2.87 mmol) and HOBt (20 mg, 0.14 mmol) along with NMM (632 μL, 5.75 mmol). Upon addition of NMM, the reaction became completely homogeneous and was allowed to stir for 3 – 4 hours with monitoring by TLC. After such time the reaction was concentrated and passed through a short silica plug with a 1:1 mixture of hexanes:EtOAc and concentrated to afford the cyclized product **5.9**{*2*} as a white crystalline foam (375 mg, 0.91 mmol, 70% over two steps).

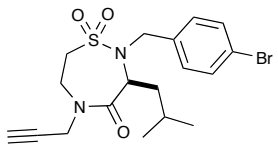

(*S*)-2-(4-bromobenzyl)-3-isobutyl-5-(prop-2-yn-1-yl)-1,2,5-thiadiazepin-1,1-dioxide-4-one 5.9{*3*}

ee = 9% $[\alpha]^{20}_{D}$ = -75.0 º (c = 0.6, CH_2Cl_2); **^{1}H NMR** (400 MHz, $CDCl_3$) δ ppm 7.45 (d, *J* = 8.3 Hz, 2H), 7.29 (d, *J* = 8.3 Hz, 2H), 4.72 (dd, *J* = 17.5, 2.2 Hz, 1H), 4.57 (dd, *J* = 9.9, 4.6 Hz, 1H), 4.41 (d, *J* = 15.9 Hz, 1H), 4.12 (dd, *J* = 16.7, 11.4 Hz, 1H), 3.94 (dd, *J* = 17.5, 2.1 Hz, 1H), 3.85 (d, *J* = 15.9 Hz, 1H), 3.78 (dd, *J* = 16.9, 4.0 Hz, 1H), 3.30 (dd, *J* = 14.3, 5.0 Hz, 1H), 3.22 (m, 1H), 2.35 (t, *J* = 2.4 Hz, 1H), 1.54 (dt, *J* = 10.3, 3.0 Hz, 1H), 1.40 (m, 2H), 0.87 (d, *J* = 6.2 Hz, 3 H), 0.57 (d, *J* = 6.4 Hz, 3 H); **^{13}C NMR** (126 MHz, $CDCl_3$) δ ppm 171.5, 136.4, 131.7, 130.3, 121.9, 78.3, 73.5, 57.3, 50.0, 48.3, 43.6, 37.7, 37.4, 23.6, 22.8, 21.4; **FTIR** (thin film) 3292, 2957, 2868, 1663, 1339, 1144 cm^{-1}; **HRMS** calculated for $C_{18}H_{23}BrN_2O_3SNa$ $(M+Na)^+$ = 449.0510; found 449.0522 (TOF MS ES+).

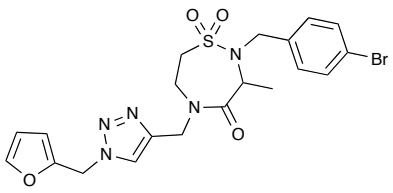

(±) 2-(4-bromobenzyl)-5-((1-(furan-2-ylmethyl)-1H-1,2,3-triazol-4-yl)methyl)-3-methyl-1,2,5-thiadiazepin-1,1-dioxide 4-one 5.10{*l*}

^{1}H NMR (400 MHz, $CDCl_3$) δ ppm 7.62 (d, *J* = 4.5 Hz, 1H), 7.45 – 7.40 (m, 2H), 7.38 (dt, *J* = 4.7, 2.4 Hz, 1H), 7.19 (d, *J* = 8.4 Hz, 2H), 6.50 – 6.45 (m, 1H), 6.40 – 6.34 (m, 1H), 5.53 (q, *J* = 15.4 Hz, 2H), 4.89 (d, *J* = 14.9 Hz, 1H), 4.73 (q, *J* = 6.8 Hz, 1H), 4.50 (d, *J* = 14.9 Hz, 1H), 4.21 (dd, *J* = 14.8, 9.6 Hz, 1H), 4.17 – 4.08 (m, 1H), 3.98 – 3.88 (m, 1H), 3.68 – 3.56 (m, 1H), 3.27 – 3.11 (m, 2H), 1.17 (d, *J* = 6.9 Hz, 3H); **^{13}C NMR** (126 MHz, $CDCl_3$) δ ppm 172.7, 147.9, 144.9, 144.7, 138.1, 132.5, 130.2, 123.7, 122.4, 112.0, 111.6, 55.6, 50.5, 48.7, 47.9, 45.7, 45.2, 17.2; **FTIR** (thin film) 3142, 2988, 1659, 1487, 1337, 1142, 735 cm^{-1}; **HRMS** calculated for $C_{20}H_{22}BrN_5O_4SNa$ $(M+Na)^+$ = 530.0474; found 530.0474 (TOF MS ES+).

General procedure for initial solution-phase Suzuki-Miyaura coupling validation

To 1 dram vials were added 50 mg ea of the corresponding sultams **5.10**{*1-3*} followed by the addition of $Pd(dppf)Cl_2$ (4.0 mg, 4.4 μmol) and anhydrous K_2CO_3 (24.0 mg, 0.17 mmol) as solids. To each were added DMF (500 μL) and stirred until soluble. The corresponding boronic acids were each prepared as stock solutions in DMF (450 μL) and added to the vials followed by subsequent addition of H_2O (190 μL) to each (0.08 M total). Reactions were then sealed over Ar atmosphere and allowed to react for 14 – 16 hours at 80 ºC on a carousel plate. After such time the reactions were cooled to rt, concentrated and re-constituted in EtOAc/ H_2O and washed with 1N (aq) NaOH (1 x 5 mL) and deionized water (2 x 5 mL) and separated. The organic layer was passed through a 6 mL silica SPE cartridge (400 mg) using a Fisher vacuum filtration box. A two-stage flush was performed: 2:1 hexanes:EtOAc (2 x 5 mL) – discarded, followed by addition of 100% EtOAc to afford the Suzuki-coupled sultams **5.11a-n**{*2-3*} in good to excellent yields and purities (Table 5.5).

Combined two-step reaction sequence – Library validation and production of thiadiazepin-1,1-dioxide-4-ones on the Chemspeed Accelerator platform

In the appropriate reactor position in the Chemspeed Accelerator SLT100® (3S x 5A x 5B = 75 members) was added 25.0 mg of Amberlyst-21 bound CuI (0.03 mmol), 0.824 mL of a 0.182 M (0.150 mmol) solution in methylene chloride of the sultam (S) and 0.824 mL of a 0.362 M (0.300 mmol) solution in methylene chloride of the azide (A), and the reaction mixture was vortexed at rt for 14 hours. The vortexing was ceased and the reaction solution was transferred (without Amberlyst-21 bound CuI) to the appropriate adjacent reactor via syringe. The remaining Amberlyst-21 bound CuI was washed with methylene chloride (2 x 0.824 mL) and again the solution was transferred to the appropriate adjacent reactor. The reaction mixture was then concentrated and 0.824 mL of 1,2-dimethoxyethane was added to the crude triazole product. $Pd(dppf)Cl_2$ (11.0 mg) was added to the reaction solution using the solid-dispensing unit.. This was then followed by addition 0.412 mL of a 0.728 M (0.300 mmol) solution of cesium carbonate in water and 0.824 mL of a 0.273 M (0.225 mmol) solution of the boronic acid (B) in 1,2-dimethoxyethane. The reaction mixture was then vortex shaken at 85 °C for 24 hours over argon. The reaction mixtures were concentrated and 2 mL of 1N NaOH was added to the resulting residue. The mixture was vortexed and extracted with methylene chloride (3 x 1.5 mL) and the extracts were gravity filtered through a silica SPE plug into CCT tubes followed by washing the SPE with ethyl acetate (2 mL). The solutions were concentrated and the resulting residues were purified by mass-directed HPLC. This process was repeated 3 times for a total of 225 compounds.

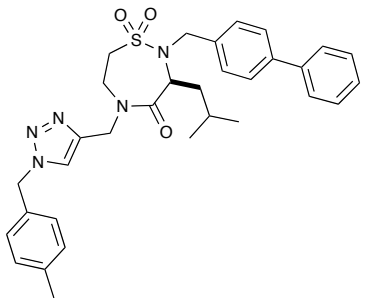

(*S*)-2-([1,1'-biphenyl]-4-ylmethyl)-3-isobutyl-5-((1-(4-methylbenzyl)-1H-1,2,3-triazol-4-yl)methyl)-1,2,5-thiadiazepin-4-one 1,1-dioxide 5.11a{*3*}

$[\alpha]^{20}_{D}$ = -3.2 ° (c = 0.41, CH_2Cl_2); **^{1}H NMR** (400 MHz, $CDCl_3$) δ 7.58 (d, *J* = 7.5 Hz, 2H), 7.52 (d, *J* = 8.9 Hz, 3H), 7.45 (t, *J* = 7.5 Hz, 2H), 7.36 (d, *J* = 8.0 Hz, 3H), 7.14 (dd, *J* = 19.4, 7.9 Hz, 4H), 5.54 (d, *J* = 14.6 Hz, 1H), 5.38 (d, *J* = 14.6 Hz, 1H), 4.93 (d, *J* = 14.8 Hz, 1H), 4.56 (dd, *J* = 10.1, 4.4 Hz, 1H), 4.44 (d, *J* = 14.8 Hz, 1H), 4.28 – 4.07 (m, 2H), 3.95 (dd, *J* = 16.5, 4.0 Hz, 1H), 3.51 (d, *J* = 15.7 Hz, 1H), 3.24 (dd, *J* = 14.4, 5.1 Hz, 1H), 3.11 – 3.00 (m, 1H), 2.23 (s, 3H), 1.60 – 1.49 (m, 1H), 1.48 – 1.34 (m, *J* = 6.4 Hz, 1H), 1.32 – 1.20 (m, 1H), 0.83 (d, *J* = 6.4 Hz, 3H), 0.48 (d, *J* = 6.6 Hz, 3H); **^{13}C NMR** (126 MHz, $CDCl_3$) δ 171.8, 144.0, 140.9, 140.6, 139.2, 136.5, 131.4, 130.1, 129.0, 129.0, 128.3, 127.5, 127.2, 127.1, 122.8, 57.3, 54.3, 49.7, 48.4, 44.9, 44.3, 37.7, 23.5, 22.8, 21.4, 21.2; **FTIR** (thin film) 3055, 2955, 1657, 1336, 1144, 758 cm^{-1}; **HRMS** calculated for $C_{32}H_{37}N_5O_3SNa$ $(M+Na)^+$ = 594.2515; found 594.2517 (TOF MS ES+).

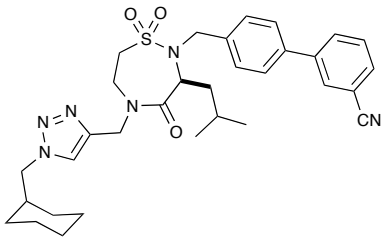

(*S*)-4'-((5-((1-(cyclohexylmethyl)-1H-1,2,3-triazol-4-yl)methyl)-3-isobutyl-1,1-dioxido-4-oxo-1,2,5-thiadiazepin-2-yl)methyl)-[1,1'-biphenyl]-3-carbonitrile 5.11b{*3*}

[a]$^{20}_{D}$ = -32.2° (c = 1.00, CH_2Cl_2); **^{1}H NMR** (400 MHz, $CDCl_3$) δ ppm 7.83 (s, 1H), 7.78 (d, *J* = 8.0 Hz, 1H), 7.61 (d, *J* = 7.8 Hz, 1H), 7.57 (s, 1H), 7.52 (t, *J* = 7.8 Hz, 1H), 7.47 (q, *J* = 8.2 Hz, 4H), 4.92 (d, *J* = 14.9 Hz, 1H), 4.59 (dd, *J* = 9.9, 4.5 Hz, 1H), 4.52 (d, *J* = 14.9 Hz, 1H), 4.37 (d, *J* = 15.9 Hz, 1H), 4.21 – 4.11 (m, 3H), 3.97 (dt, *J* = 15.6, 3.3 Hz, 1H), 3.66 (d, *J* = 15.9 Hz, 1H), 3.31 – 3.25 (m, 2H), 1.91 – 0.93 (m, 14H), 0.83 (d, *J* = 6.3 Hz, 3H), 0.49 (d, *J* = 6.6 Hz, 3H); **^{13}C NMR** (126 MHz, $CDCl_3$) δ ppm 171.5, 143.0, 141.8, 138.0, 137.8, 131.3, 130.7, 130.5, 129.6, 128.9, 126.9, 123.2, 118.7, 112.8, 57.2, 56.5, 53.4, 49.4, 48.2, 44.8, 44.2, 38.6, 37.6, 30.4, 30.4, 25.9, 25.3, 23.4, 22.5, 21.2; **FTIR** (thin film) 2928, 2853, 1655, 1337, 1144, 1049, 793, 768, 735 cm^{-1}; **HRMS** calculated for $C_{32}H_{40}N_6O_3SNa$ $(M+Na)^+$ = 611.2780; found 611.2780 (TOF MS ES+).

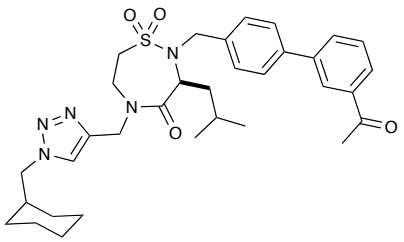

(S)-2-((3'-acetyl-[1,1'-biphenyl]-4-yl)methyl)-5-((1-(cyclohexylmethyl)-1H-1,2,3-triazol-4-yl)methyl)-3-isobutyl-1,2,5-thiadiazepin-1,1-dioxide 4-one 5.11c{*3*}

[a]$^{20}_{D}$ = -31.8° (c = 1.00, CH_2Cl_2); **^{1}H NMR** (400 MHz, $CDCl_3$) δ ppm 8.14 (s, 1H), 7.91 (d, *J* = 7.7 Hz, 1H), 7.75 (d, *J* = 7.7 Hz, 1H), 7.56 – 7.50 (m, 4H), 7.44 (d, *J* = 8.0 Hz, 2H), 4.89 (d, *J* = 14.9 Hz, 1H), 4.59 (dd, *J* = 9.9, 4.5 Hz, 1H), 4.52 (d, *J* = 14.9 Hz, 1H), 4.37 (d, *J* = 15.9 Hz, 1H), 4.21 – 4.11 (m, 3H), 3.96 (dt, *J* = 17.2, 3.3 Hz, 1H), 3.68 (d, *J* = 15.9 Hz, 1H), 3.27 – 3.24 (m, 2H), 2.64 (s, 3H), 1.88 – 0.93 (m, 14H), 0.84 (d, *J* = 6.4 Hz, 3H), 0.51 (d, *J* = 6.6 Hz, 3H); **^{13}C NMR** (126 MHz, $CDCl_3$) δ ppm 198.0, 171.6, 143.0, 141.1, 139.3, 137.5, 137.1, 131.6, 129.0, 128.9, 127.2, 126.9, 126.6, 123.2, 57.2, 56.5, 53.4, 49.4, 48.3, 44.7, 44.1, 38.6, 37.6, 30.4, 30.4, 26.7, 25.9, 25.3, 23.4, 22.6, 21.2; **FTIR** (thin film) 2928, 2853, 1682, 1657, 1337, 1144, 1049, 797, 768, 735 cm^{-1}; **HRMS** calculated for $C_{33}H_{43}N_5O_4SNa$ $(M+Na)^+$ = 628.2933; found 628.2920 (TOF MS ES+).

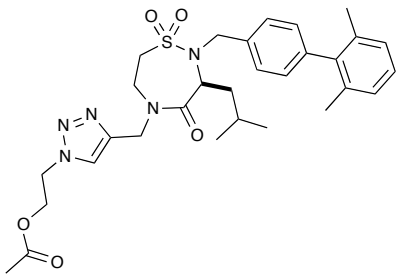

(*S*)-2-(4-((2-((2',6'-dimethyl-[1,1'-biphenyl]-4-yl)methyl)-3-isobutyl-1,1-dioxido-4-oxo-1,2,5-thiadiazepin-5-yl)methyl)-1*H*-1,2,3-triazol-1-yl)ethyl acetate 5.11d{*3*}

[a]$^{20}_{D}$ = -34.6° (c = 1.00, CH_2Cl_2); **^{1}H NMR** (400 MHz, $CDCl_3$) δ ppm 7.70 (s, 1H), 7.46 (d, *J* = 7.9 Hz, 2H), 7.17 – 7.09 (m, 5H), 4.86 (d, *J* = 14.8 Hz, 1H), 4.64 – 4.61 (m, 4H), 4.51 – 4.48 (m, 3H), 4.18 (dd, *J* = 16.6, 11.2 Hz, 1H), 4.00 (ddd, *J* = 16.6, 4.8, 1.8 Hz, 1H), 3.65 (d, *J* = 15.6 Hz, 1H), 3.35 – 3.20 (m, 2H), 2.04 (s, 3H), 2.00 (s, 6H), 1.68 – 1.63 (m, 1H), 1.50 – 1.40 (m, 1H), 1.32 – 1.28 (m, 1H), 0.86 (d, *J* = 6.5 Hz, 3H), 0.54 (d, *J* = 6.5 Hz, 3H); **^{13}C NMR** (126 MHz, $CDCl_3$) δ ppm 172.0, 170.3, 143.6, 141.3, 140.4, 135.9, 135.8, 129.0, 128.5, 127.2, 127.0, 123.4, 62.2, 57.4, 49.5, 49.3, 48.6, 44.7, 44.0, 37.6, 23.2, 22.9, 21.0, 20.8, 20.6; **FTIR** (thin film) 2955, 2926, 2868, 1744, 1655, 1366, 1337, 1231, 1144, 771 cm^{-1}; **HRMS** calculated for $C_{30}H_{39}N_5O_5SNa$ $(M+Na)^+$ = 604.2570; found 604.2545 (TOF MS ES+)

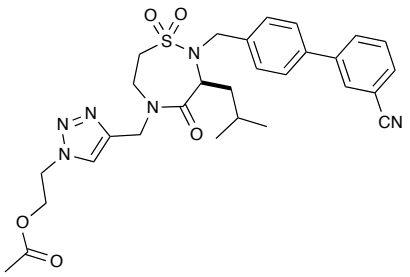

(*S*)-2-(4-((2-((3'-cyano-[1,1'-biphenyl]-4-yl)methyl)-3-isobutyl-1,1-dioxido-4-oxo-1,2,5-thiadiazepin-5-yl)methyl)-1H-1,2,3-triazol-1-yl)ethyl acetate 5.11e{*3*}

[a]$^{20}_{D}$ = -33.7° (c = 1.00, CH_2Cl_2); **^{1}H NMR** (400 MHz, $CDCl_3$) δ ppm 7.61 (s, 1H), 7.57 (d, *J* = 7.3 Hz, 1H), 7.47 (s, 1H), 7.40 (d, *J* = 7.3 Hz, 1H), 7.33 – 7.25 (m, 4H), 4.68 (d, *J* = 14.9 Hz, 1H), 4.44 – 4.37 (m, 4H), 4.26 – 4.20 (m, 3H), 3.98-3.82 (m, 1H), 3.76 (d, *J* = 17.0 Hz, 1H), 3.49 (d, *J* = 16.0 Hz, 1H), 3.09 – 3.02 (m, 2H), 1.82 (s, 3H), 1.35 – 1.30 (m, 1H), 1.27 – 1.20 (m, 1H), 1.15 – 1.09 (m, 1H), 0.63 (d, *J* = 6.5 Hz, 3H), 0.29 (d, *J* = 6.5 Hz, 3H); **^{13}C NMR** (126 MHz, $CDCl_3$) δ ppm 171.7, 170.3, 143.5, 141.8, 138.0, 137.9, 131.3, 130.7, 130.5, 129.6, 128.9, 126.9, 123.4, 118.8, 112.8, 62.1, 57.2, 49.4, 49.2, 48.3, 44.6, 44.0, 37.6, 36.4, 31.3, 29.6, 23.4, 22.6, 21.2, 20.6; **FTIR** (thin film) 2957, 2934, 1744, 1657, 1366, 1337, 1231, 1144, 735 cm^{-1}; **HRMS** calculated for $C_{29}H_{34}N_6O_5SNa$ $(M+Na)^+$ = 601.2209; found 601.2191 (TOF MS ES+).

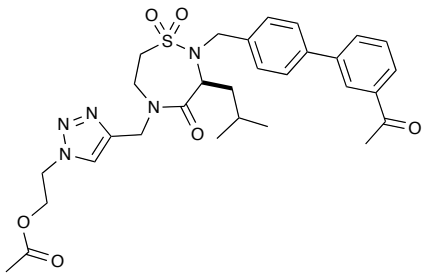

(*S*)-2-(4-((2-((3'-acetyl-[1,1'-biphenyl]-4-yl)methyl)-3-isobutyl-1,1-dioxido-4-oxo-1,2,5-thiadiazepin-5-yl)methyl)-1H-1,2,3-triazol-1-yl)ethyl acetate 5.11f{*3*}

[a]$^{20}_{D}$ = -36.0° (c = 1.00, CH_2Cl_2); **^{1}H NMR** (400 MHz, $CDCl_3$) δ ppm 8.15 (s, 1H), 7.92 (d, *J* = 7.7 Hz, 1H), 7.77 (d, *J* = 7.7 Hz, 1H), 7.68 (s, 1H), 7.58 – 7.47 (m, 5H), 4.86 (d, *J* = 14.9 Hz, 1H), 4.63 – 4.57 (m, 4H), 4.47 – 4.41 (m, 3H), 4.19 – 4.14 (m, 1H), 3.98 (d, *J* = 15.0 Hz, 1H), 3.73 (d, *J* = 15.9 Hz, 1H), 3.29 – 3.21 (m, 2H), 2.64 (s, 3H), 2.02 (s, 3H), 1.61 – 1.56 (m, 1H), 1.51 – 1.45 (m, 1H), 1.38 – 1.33 (m, 1H), 0.85 (d, *J* = 6.5 Hz, 3H), 0.53 (d, *J* = 6.5 Hz, 3H); **^{13}C NMR** (126 MHz, $CDCl_3$) δ ppm 198.1, 171.8, 170.3, 143.6, 141.1, 139.4, 137.6, 137.1, 131.6, 129.0, 128.9, 127.3, 127.0, 126.7, 123.4, 62.2, 57.2, 49.4, 49.3, 48.3, 44.6, 44.0, 37.6, 26.8, 23.4, 22.6, 21.2, 20.6; **FTIR** (thin film) 2957, 2928, 1744, 1682, 1657, 1362, 1337, 1234, 1144, 735 cm^{-1}; **HRMS** calculated for $C_{30}H_{37}N_5O_6SNa$ $(M+Na)^+$ = 618.2362; found 618.2360 (TOF MS ES+).

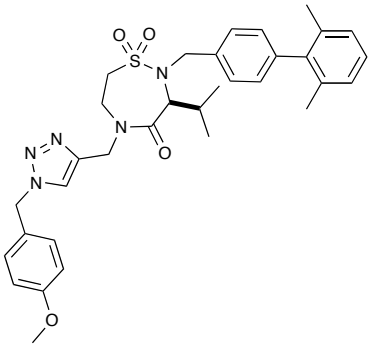

(*S*)-2-((2',6'-dimethyl-[1,1'-biphenyl]-4-yl)methyl)-3-isopropyl-5-((1-(4-methoxy benzyl)-1*H*-1,2,3-triazol-4-yl)methyl)-1,2,5-thiadiazepin-1,1-dioxide-4-one 5.11g{*2*}

$[\alpha]^{20}_{D}$ = -70.9 ° (c = 2.3, CH_2Cl_2); **^{1}H NMR** (500 MHz, $CDCl_3$) δ 7.54 (s, 1H), 7.41 (d, *J* = 8.0 Hz, 2H), 7.22 – 7.18 (m, 2H), 7.16 (dd, *J* = 8.4, 6.5 Hz, 1H), 7.09 (dd, *J* = 12.4, 7.8 Hz, 4H), 6.80 (m, 2H), 5.52 (d, *J* = 14.6 Hz, 1H), 5.37 (d, *J* = 14.6 Hz, 1H), 5.00 (d, *J* = 14.8 Hz, 1H), 4.38 (d, *J* = 14.8 Hz, 1H), 4.23 – 4.14 (m, 2H), 4.02 (d, *J* = 10.7 Hz, 1H), 3.93 (dd, *J* = 16.8, 3.9 Hz, 1H), 3.69 (s, 3H), 3.47 (d, *J* = 15.1 Hz, 1H), 3.21 (dd, *J* = 14.5, 5.1 Hz, 1H), 3.00 (t, *J* = 12.4 Hz, 1H), 2.00 (s, 6H), 2.00 (s, 1H), 0.85 (d, *J* = 6.4 Hz, 3H), 0.58 (d, *J* = 6.6 Hz, 3H); **^{13}C NMR** (126 MHz, $CDCl_3$) δ 170.1, 160.2, 144.1, 141.6, 140.8, 136.1, 135.3, 129.7, 129.7, 129.1, 127.4, 127.2, 126.4, 122.8, 114.8, 65.3, 55.4, 54.1, 49.7, 48.7, 45.3, 44.4, 27.2, 20.9, 20.7, 18.9; **FTIR** (thin film) 2960, 1659, 1514, 1337, 1252, 1153, 733 cm^{-1}; **HRMS** calculated for $C_{33}H_{39}N_5O_4SNa$ $(M+Na)^+$ = 624.2620; found 624.2620 (TOF MS ES+).

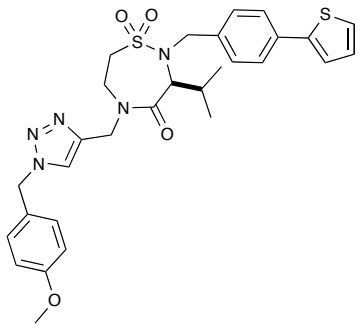

(*S*)-3-isopropyl-5-((1-(4-methoxybenzyl)-1H-1,2,3-triazol-4-yl)methyl)-2-(4-(thiophen-2-yl)benzyl)-1,2,5-thiadiazepin-1,1-dioxide-4-one 5.11h{*2*}

$[\alpha]^{20}_D$ = -40.0 ° (c = 1.7, CH_2Cl_2); **^{1}H NMR** (500 MHz, $CDCl_3$) δ 7.52 (d, *J* = 7.9 Hz, 3H), 7.33 (dd, *J* = 3.6, 0.9 Hz, 1H), 7.17 (d, *J* = 8.5 Hz, 2H), 7.08 (dd, *J* = 5.0, 3.7 Hz, 1H), 6.76 (d, *J* = 8.5 Hz, 2H), 5.51 (d, *J* = 14.6 Hz, 1H), 5.33 (d, *J* = 14.6 Hz, 1H), 5.03 (d, *J* = 14.8 Hz, 1H), 4.32 (d, *J* = 14.8 Hz, 1H), 4.18 (dd, *J* = 16.6, 11.8 Hz, 1H), 4.00 (dd, *J* = 12.5, 9.7 Hz, 2H), 3.92 (dd, *J* = 16.5, 4.4 Hz, 1H), 3.61 (s, 3H), 3.42 (d, *J* = 15.4 Hz, 1H), 3.19 (dd, *J* = 14.5, 5.2 Hz, 1H), 2.98 (t, *J* = 12.9 Hz, 1H), 1.97 (tt, *J* = 12.8, 6.5 Hz, 1H), 0.85 (d, *J* = 6.3 Hz, 3H), 0.63 (d, *J* = 6.6 Hz, 3H); **^{13}C NMR** (126 MHz, $CDCl_3$) δ 170.1, 160.2, 144.1, 141.6, 140.8, 136.1, 135.3, 129.7, 129.7, 129.1, 127.4, 127.2, 126.4, 122.8, 114.8, 65.3, 55.4, 54.1, 49.7, 48.7, 45.3, 44.4, 27.2, 20.9, 20.7, 18.9; **FTIR** (thin film) 3140, 2961, 1655, 1514, 1335, 1252, 1153, 1032, 735 cm^{-1}; **HRMS** calculated for $C_{29}H_{33}N_5O_4S_2Na$ $(M+Na)^+$ = 602.1872; found 602.1888 (TOF MS ES+).

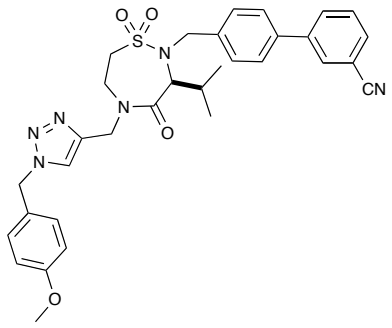

(*S*)-4'-((3-isopropyl-5-((1-(4-methoxybenzyl)-1H-1,2,3-triazol-4-yl)methyl)-1,1-dioxido-4-oxo-1,2,5-thiadiazepin-2-yl)methyl)-[1,1'-biphenyl]-3-carbonitrile 5.11i{*3*}

$[\alpha]^{20}_{D}$ = -65.8 ° (c = 1.9, CH_2Cl_2); **^{1}H NMR** (500 MHz, $CDCl_3$) δ 7.86 (s, 1H), 7.81 (dd, *J* = 7.9, 1.0 Hz, 1H), 7.62 (dd, *J* = 7.7, 1.1 Hz, 1H), 7.58 – 7.50 (m, 2H), 7.47 (d, *J* = 8.1 Hz, 2H), 7.38 (d, *J* = 8.1 Hz, 2H), 7.18 (d, *J* = 8.5 Hz, 2H), 6.76 (d, *J* = 8.6 Hz, 2H), 5.52 (d, *J* = 14.6 Hz, 1H), 5.34 (d, *J* = 14.6 Hz, 1H), 5.04 (d, *J* = 14.8 Hz, 1H), 4.34 (d, *J* = 14.9 Hz, 1H), 4.19 (dd, *J* = 17.3, 11.1 Hz, 1H), 4.07 (d, *J* = 15.4 Hz, 1H), 4.01 (d, *J* = 10.6 Hz, 1H), 3.93 (dd, *J* = 16.3, 4.1 Hz, 1H), 3.61 (s, 3H), 3.45 (d, *J* = 15.4 Hz, 1H), 3.21 (dd, *J* = 14.5, 5.1 Hz, 1H), 3.11 – 3.02 (m, 1H), 1.93 (dq, *J* = 18.8, 6.2 Hz, 1H), 0.84 (d, *J* = 6.3 Hz, 3H), 0.62 (d, *J* = 6.5 Hz, 3H). **^{13}C NMR** (126 MHz, CDCl3) δ 170.0, 160.1, 144.1, 142.0, 138.2, 137.2, 131.5, 130.9, 130.7, 130.0, 129.8, 129.7, 127.0, 126.4, 122.7, 119.0, 114.7, 113.1, 65.3, 55.3, 54.0, 49.5, 48.3, 45.4, 44.5, 27.1, 20.5, 19.1. **FTIR** (thin film) 2928, 2228, 1651, 1514, 1333, 1153, 789 cm^{-1}; **HRMS** calculated for $C_{32}H_{34}N_6O_4SNa$ $(M+Na)^+$ = 621.2260; found 621.2276 (TOF MS ES+).

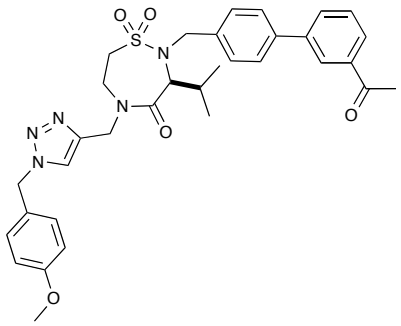

(*S*)-2-((3'-acetyl-[1,1'-biphenyl]-4-yl)methyl)-3-isopropyl-5-((1-(4-methoxybenzyl) -1H-1,2,3-triazol-4-yl)methyl)-1,2,5-thiadiazepin-1,1-dioxide-4-one 5.11j{*2*}

$[\alpha]^{20}_{D}$ = -63.8 ° (c = 2.4, CH_2Cl_2); **^{1}H NMR** (500 MHz, $CDCl_3$) δ 8.20 – 8.15 (m, *J* = 1.6, 1H), 7.98 – 7.89 (m, 1H), 7.82 – 7.74 (m, 1H), 7.54 (dd, *J* = 8.2, 6.6, 4H), 7.38 (d, *J* = 8.1, 2H), 7.18 (d, *J* = 8.6, 2H), 6.76 (d, *J* = 8.6, 2H), 5.52 (d, *J* = 14.6, 1H), 5.34 (d, *J* = 14.6, 1H), 5.03 (d, *J* = 14.8, 1H), 4.35 (d, *J* = 14.8, 1H), 4.19 (dd, *J* = 16.6, 11.8, 1H), 4.07 (d, *J* = 15.4, 1H), 4.01 (d, *J* = 10.6, 1H), 3.93 (dd, *J* = 16.7, 3.9, 1H), 3.61 (s, 3H), 3.47 (d, *J* = 15.4, 1H), 3.20 (dd, *J* = 14.5, 5.1, 1H), 3.04 (t, *J* = 13.1, 1H), 2.66 (s, 3H), 1.97 (dq, *J* = 18.9, 6.4, 1H), 0.85 (d, *J* = 6.4, 3H), 0.64 (d, *J* = 6.6, 3H); **^{13}C NMR** (126 MHz, CDCl3) δ 198.3, 170.1, 160.1, 144.1, 141.3, 139.6, 137.8, 136.47, 131.8, 129.9, 129.7, 129.3, 127.5, 127.1, 126.9, 126.4, 122.8, 114.7, 65.3, 55.3, 54.1, 49.5, 48.4, 45.3, 44.5, 27.1, 27.0, 20.6, 19.1; **FTIR** (thin film) 2959, 1682, 1651, 1333, 1151, 783 cm^{-1}; **HRMS** calculated for $C_{33}H_{37}N_5O_5SNa$ $(M+Na)^+$ = 638.2413; found 638.2403 (TOF MS ES+).

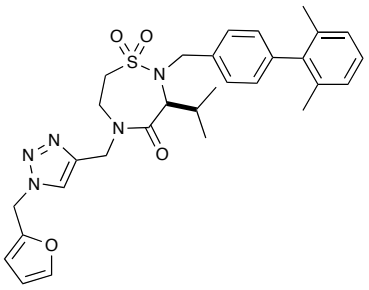

(*S*)-2-((2',6'-dimethyl-[1,1'-biphenyl]-4-yl)methyl)-5-((1-(furan-2-ylmethyl)-1H-1,2,3-triazol-4-yl)methyl)-3-isopropyl-1,2,5-thiadiazepin-1,1-dioxide-4-one 5.11k{*2*}

$[\alpha]^{20}_{D}$ = -2.71 ° (c = 2.1, CH_2Cl_2); **^{1}H NMR** (500 MHz, $CDCl_3$) δ 7.68 (s, 1H), 7.45 (d, *J* = 8.0 Hz, 2H), 7.27 (dd, *J* = 1.9, 0.7 Hz, 1H), 7.16 (dd, *J* = 8.4, 6.5 Hz, 1H), 7.09 (dd, *J* = 9.5, 7.9 Hz, 4H), 6.44 (dd, *J* = 3.3, 0.5 Hz, 1H), 6.29 (dd, *J* = 3.3, 1.9 Hz, 1H), 5.57 (d, *J* = 15.5 Hz, 1H), 5.48 (d, *J* = 15.5 Hz, 1H), 5.00 (d, *J* = 14.8 Hz, 1H), 4.43 (d, *J* = 14.8 Hz, 1H), 4.26 (d, *J* = 15.1 Hz, 1H), 4.19 (dd, *J* = 16.7, 11.7 Hz, 1H), 4.04 (d, *J* = 10.7 Hz, 1H), 3.93 (dd, *J* = 16.8, 3.6 Hz, 1H), 3.54 (d, *J* = 15.1 Hz, 1H), 3.22 (dd, *J* = 14.4, 4.9 Hz, 1H), 3.11 – 3.02 (m, 1H), 2.09 – 2.02 (m, 1H), 1.99 (s, 6H), 0.87 (d, *J* = 6.3, Hz, 3H), 0.61 (d, *J* = 6.6 Hz, 3H); **^{13}C NMR** (126 MHz, $CDCl_3$) δ 170.3, 147.1, 144.1, 144.0, 141.6, 140.8, 136.1, 135.3, 129.8, 129.1, 127.4, 127.3, 123.0, 111.0, 110.6, 65.3, 49.6, 48.8, 47.0, 45.3, 44.4, 27.2, 20.9, 20.7, 18.9; **FTIR** (thin film) 2961, 1650, 1331, 1151, 735 cm^{-1}; **HRMS** calculated for $C_{30}H_{35}N_5O_4SNa$ $(M+Na)^+$ = 584.2307; found 584.2304 (TOF MS ES+).

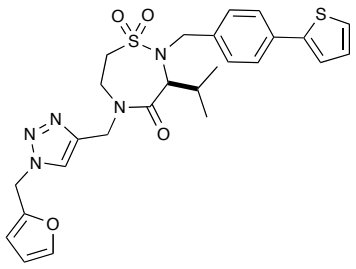

(*S*)-5-((1-(furan-2-ylmethyl)-1H-1,2,3-triazol-4-yl)methyl)-3-isopropyl-2-(4-(thiophen-2-yl)benzyl)-1,2,5-thiadiazepin-1,1-dioxide-4-one 5.11l{*2*}

$[\alpha]^{20}_{D}$ = -2.0 º (c = 1.9, CH_2Cl_2); **^{1}H NMR** (500 MHz, $CDCl_3$) δ 7.63 (s, 1H), 7.54 (d, *J* = 8.3 Hz, 2H), 7.38 (d, *J* = 8.2 Hz, 2H), 7.32 (dd, *J* = 3.6 Hz, 1.1, 1H), 7.29 – 7.27 (m, 2H), 7.08 (dd, *J* = 5.1, 3.6 Hz, 1H), 6.44 – 6.41 (m, 1H), 6.30 (dd, *J* = 3.3 Hz, 1.9, 1H), 5.54 (d, *J* = 15.5 Hz, 1H), 5.45 (d, *J* = 15.5 Hz, 1H), 4.97 (d, *J* = 15.1 Hz, 1H), 4.40 (d, *J* = 14.8, 1H), 4.14 (d, *J* = 15.5, 2H), 4.00 (d, *J* = 10.5, 1H), 3.91 (dd, 1H), 3.59 (d, *J* = 15.4, 1H), 3.19 (dd, *J* = 14.5, 5.0, 1H), 3.09 – 2.95 (m, 1H), 2.07 – 1.98 (m, 1H), 0.87 (d, *J* = 6.3, 3H), 0.66 (d, *J* = 6.6, 3H); **^{13}C NMR** (126 MHz, CDCl3) δ 170.3, 147.1, 144.0, 135.9, 134.0, 131.5, 131.2, 130.1, 128.2, 125.8, 125.1, 123.4, 122.9, 111.0, 110.6, 65.2, 49.6, 48.5, 47.0, 45.1, 44.2, 27.1, 20.6, 19.2; **FTIR** (thin film) 2962, 1651, 1331, 1151, 739 cm^{-1}; **HRMS** calculated for $C_{26}H_{29}N_5O_4S_2Na$ $(M+Na)^+$ = 562.1559; found 562.1550 (TOF MS ES+).

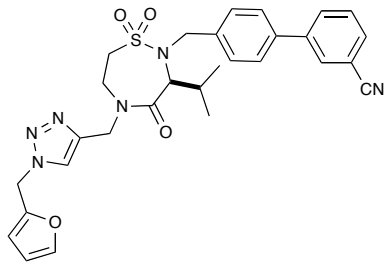

(*S*)-4'-((5-((1-(furan-2-ylmethyl)-1H-1,2,3-triazol-4-yl)methyl)-3-isopropyl-1,1-dioxido-4-oxo-1,2,5-thiadiazepin-2-yl)methyl)-[1,1'-biphenyl]-3-carbonitrile 5.11m{*2*}

$[\alpha]^{20}_{D}$ = -2.0 ° (c = 1.9, CH_2Cl_2); **^{1}H NMR** (500 MHz, $CDCl_3$) δ 7.86 (t, *J* = 1.5 Hz, 1H), 7.83 – 7.79 (m, 1H), 7.66 (s, 1H), 7.62 (dt, *J* = 7.7, 1.3 Hz, 1H), 7.54 (t, *J* = 7.8 Hz, 1H), 7.51 – 7.46 (m, 4H), 7.29 (dd, *J* = 1.8, 0.7 Hz, 1H), 6.44 (dd, *J* = 3.3, 0.5 Hz, 1H), 6.31 (dd, *J* = 3.2, 1.9 Hz, 1H), 5.56 (d, *J* = 15.5 Hz, 1H), 5.48 (d, *J* = 15.5 Hz, 1H), 5.01 (d, *J* = 14.9 Hz, 1H), 4.42 (d, *J* = 14.9 Hz, 1H), 4.25 – 4.15 (m, *J* = 14.1 Hz, 2H), 4.04 (d, *J* = 10.6 Hz, 1H), 3.93 (dd, *J* = 16.8, 3.6 Hz, 1H), 3.62 (d, *J* = 15.5 Hz, 1H), 3.21 (dd, *J* = 14.5, 4.8 Hz, 1H), 3.15 – 3.06 (m, 1H), 2.03 – 1.95 (m, 1H), 0.87 (d, *J* = 6.4 Hz, 3H), 0.65 (d, *J* = 6.6 Hz, 3H).; **^{13}C NMR** (126 MHz, $CDCl_3$) δ 170.1, 147.1, 144.0, 144.0, 142.0, 138.3, 137.3, 131.6, 130.9, 130.8, 130.1, 129.8, 127.0, 122.9, 119.0, 113.1, 111.0, 110.7, 65.3, 49.5, 48.5, 47.0, 45.2, 44.3, 27.2, 20.6, 19.2; **FTIR** (thin film) 2961, 2228, 1651, 1478, 1333, 1153, 733 cm^{-1}; **HRMS** calculated for $C_{29}H_{30}N_6O_4SNa$ $(M+Na)^+$ = 581.1947; found 581.1946 (TOF MS ES+).

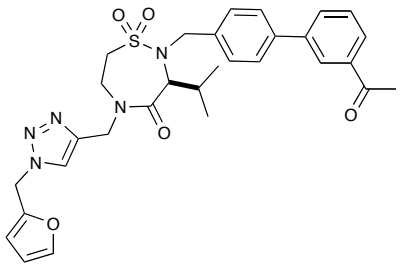

(*S*)-2-((3'-acetyl-[1,1'-biphenyl]-4-yl)methyl)-5-((1-(furan-2-ylmethyl)-1H-1,2,3-triazol-4-yl)methyl)-3-isopropyl-1,2,5-thiadiazepin-1,1-dioxide-4-one 5.11n{*2*}

$[\alpha]^{20}_D$ = -2.9 ° (c = 2.6, CH_2Cl_2); **^{1}H NMR** (500 MHz, $CDCl_3$) δ 8.17 (t, *J* = 1.7 Hz, 1H), 7.94 – 7.89 (m, 1H), 7.78 (ddd, *J* = 7.7, 1.7, 1.1 Hz, 1H), 7.65 (s, 1H), 7.53 (dd, *J* = 14.5, 8.0 Hz, 4H), 7.46 (d, *J* = 8.2 Hz, 2H), 7.28 (dd, *J* = 1.8, 0.7 Hz, 1H), 6.43 (dd, *J* = 3.3, 0.5 Hz, 1H), 6.30 (dd, *J* = 3.3, 1.9 Hz, 1H), 5.55 (d, *J* = 15.5 Hz, 1H), 5.47 (d, *J* = 15.5 Hz, 1H), 4.99 (d, *J* = 14.9 Hz, 1H), 4.42 (d, *J* = 14.9 Hz, 1H), 4.23 – 4.14 (m, 2H), 4.03 (d, *J* = 10.6 Hz, 1H), 3.62 (d, *J* = 15.4 Hz, 1H), 3.20 (dd, *J* = 14.5, 4.9 Hz, 1H), 3.11 – 3.03 (m, 1H), 2.65 (s, 3H), 2.07 – 1.97 (m, 1H), 0.87 (d, *J* = 6.4 Hz, 3H), 0.66 (d, *J* = 6.6 Hz, 3H); **^{13}C NMR** (126 MHz, $CDCl_3$) δ 198.3, 170.2, 147.0, 144.0, 141.2, 139.6, 137.8, 136.5, 131.8, 130.0, 129.2, 127.5, 127.1, 126.9, 122.9, 111.0, 110.6, 65.3, 49.5, 48.5, 47.0, 45.2, 44.3, 27.2, 27.0, 20.6, 19.2; **FTIR** (thin film) 2961, 2228, 1651, 1478, 1333, 1153, 733 cm^{-1}; **HRMS** calculated for $C_{30}H_{33}N_5O_5SNa$ $(M+Na)^+$ = 598.2100; found 598.2098 (TOF MS ES+).

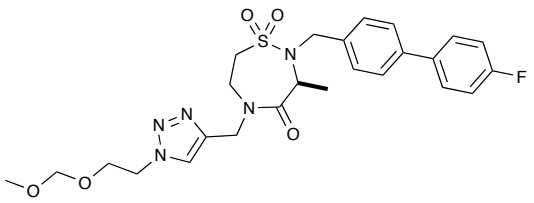

(*S*)-2-((4'-fluoro-[1,1'-biphenyl]-4-yl)methyl)-5-((1-(2-(methoxymethoxy)ethyl)-1*H*-1,2,3-triazol-4-yl)methyl)-3-methyl-1,2,5-thiadiazepin-1,1-dioxide-4-one 5.13{*1,1,1*}

$[\alpha]^{20}_{D}$ = -15.3 ° (c = 0.60, CH_2Cl_2); **^{1}H NMR** (500 MHz, $CDCl_3$) δ 7.74 (s, 1H), 7.56 – 7.50 (m, 2H), 7.50 – 7.46 (m, 2H), 7.41 (d, *J* = 8.3, 2H), 7.15 – 7.08 (m, 2H), 4.87 (d, *J* = 14.9, 1H), 4.77 (q, *J* = 6.8, 1H), 4.63 – 4.54 (m, 5H), 4.40 (t, *J* = 11.3, 1H), 4.13 (dd, *J* = 16.6, 10.4, 1H), 3.97 (ddd, *J* = 17.0, 5.1, 2.2, 1H), 3.92 (t, *J* = 5.1, 2H), 3.82 (d, *J* = 16.4, 1H), 3.75 (ddd, *J* = 6.6, 3.4, 1.6, 1H), 3.27 (s, 3H), 3.24 – 3.16 (m, 2H), 1.25 (d, *J* = 6.9, 3H).; **^{13}C NMR** (126 MHz, $CDCl_3$) δ 171.8, 162.5 (d, $^1J_{CF}$ = 246.3 Hz), 143.23, 139.34, 137.0, 136.8 (d, $^4J_{CF}$ = 3.2 Hz), 128.59 (d, $^3J_{CF}$ = 8.0 Hz), 127.93, 126.96, 123.81, 115.62 (d, $^2J_{CF}$ = 21.4 Hz), 96.48, 65.73, 55.49, 54.64, 50.51, 49.51, 47.97, 44.45, 44.04, 16.26; **FTIR** (thin film) 3142, 2941, 1659, 1499, 1337, 1142, 766 cm^{-1}; **HRMS** calculated for $C_{25}H_{31}FN_5O_5S$ $(M+H)^+$ = 532.2024; found 532.2023 (+ESI).

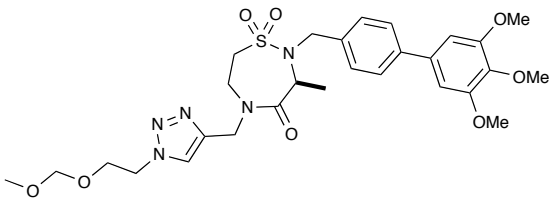

(*S*)-5-((1-(2-(methoxymethoxy)ethyl)-1H-1,2,3-triazol-4-yl)methyl)-3-methyl-2-((3',4',5'-trimethoxy-[1,1'-biphenyl]-4-yl)methyl)-1,2,5-thiadiazepin-1,1-dioxide 4-one 5.13{*1,1,2*}

$[\alpha]^{20}_{D}$ = -13.8 ° (c = 0.73, CH_2Cl_2); **^{1}H NMR** (500 MHz, $CDCl_3$) δ ppm 7.74 (s, 1H), 7.52 – 7.48 (m, 2H), 7.41 (d, *J* = 8.3 Hz, 2H), 6.76 (s, 2H), 4.88 (d, *J* = 14.9 Hz, 1H), 4.77 (q, *J* = 6.8 Hz, 1H), 4.63 – 4.55 (m, 5H), 4.40 (d, *J* = 10.9 Hz, 1H), 4.18 – 4.10 (m, 1H), 4.01 – 3.94 (m, 1H), 3.94 – 3.91 (m, 9H), 3.89 (s, 3H), 3.83 (d, *J* = 16.4 Hz, 1H), 3.28 (s, 3H), 3.24 – 3.22 (m, 1H), 1.26 (d, *J* = 6.9 Hz, 3H); **^{13}C NMR** (126 MHz, $CDCl_3$) δ ppm 172.0, 153.6, 143.4, 140.7, 137.8, 137.3, 136.9, 128.0, 127.3, 124.0, 104.5, 96.7, 65.9, 61.2, 56.4, 55.7, 54.9, 50.7, 49.7, 48.2, 44.7, 44.2, 16.5; **FTIR** (thin film) 3138, 2939, 1659, 1589, 1499, 1340, 1126, 766, 733 cm^{-1}; **HRMS** calculated for $C_{29}H_{34}N_5O_7S$ $(M+H)^+$ = 604.2436; found 604.2434 (+ESI).

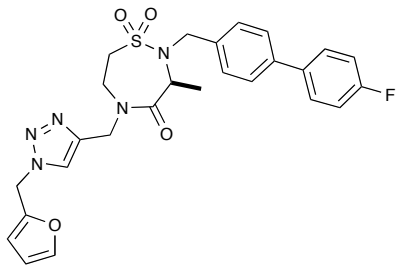

(*S*)-2-((4'-fluoro-[1,1'-biphenyl]-4-yl)methyl)-5-((1-(furan-2-ylmethyl)-1*H*-1,2,3-triazol-4-yl)methyl)-3-methyl-1,2,5-thiadiazepin-1,1-dioxide-4-one 5.13{*1,2,1*}

$[\alpha]^{20}_{D}$ = -12.4 ° (c = 0.75, CH_2Cl_2); **^{1}H NMR** (500 MHz, $CDCl_3$) δ 7.63 (s, 1H), 7.57 – 7.50 (m, 2H), 7.50 – 7.46 (m, 2H), 7.42 – 7.34 (m, 3H), 7.16 – 7.08 (m, 2H), 6.47 (dd, *J* = 3.3, 0.6 Hz, 1H), 6.37 (dd, *J* = 3.3, 1.9 Hz, 1H), 5.53 (q, *J* = 15.5, 23.2 Hz, 2H), 4.87 (d, *J* = 12.1 Hz, 1H), 4.75 (q, *J* = 6.8, 13.6 Hz, 1H), 4.55 (d, *J* = 14.9 Hz, 1H), 4.33 (d, *J* = 16.4 Hz, 1H), 4.12 (dd, *J* = 24.8, 12.3 Hz, 1H), 3.98 – 3.91 (m, 1H), 3.29 – 3.11 (m, 2H), 1.23 (d, *J* = 6.9 Hz, 3H); **^{13}C NMR** (126 MHz, $CDCl_3$) δ 172.0, 162.65 (d, $^1J_{CF}$ = 246.4 Hz), 147.1, 144.1, 143.9, 139.5, 137.2, 137.0 (d, $^4J_{CF}$ = 3.3 Hz), 128.8 (d, $^3J_{CF}$ = 8.1 Hz) 128.1, 127.1, 122.8, 115.8 (d, $^2J_{CF}$ = 21.4 Hz), 111.1, 110.7, 54.8, 49.7, 48.1, 47.0, 44.8, 44.3, 16.4; **FTIR** (thin film) 3140, 2940, 1659, 1500, 1337, 1142, 766 cm^{-1}; **HRMS** calculated for $C_{26}H_{27}FN_5O_4S$ $(M+H)^+$ = 524.1762; found 524.1758 (+ESI).

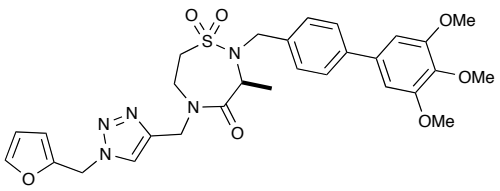

(*S*)-5-((1-(furan-2-ylmethyl)-1H-1,2,3-triazol-4-yl)methyl)-3-methyl-2-((3',4',5'-trimethoxy-[1,1'-biphenyl]-4-yl)methyl)-1,2,5-thiadiazepin-1,1-dioxide 4-one 5.13{*1,2,2*}

$[\alpha]^{20}_{D}$ = -13.1 º (c = 0.84, CH_2Cl_2); **^{1}H NMR** (500 MHz, $CDCl_3$) δ ppm 7.62 (s, 1H), 7.52 – 7.47 (m, 2H), 7.39 (dt, *J* = 8.5, 4.4 Hz, 3H), 6.77 (s, 2H), 6.48 (dd, *J* = 3.2, 0.5 Hz, 1H), 6.38 (dd, *J* = 3.3, 1.9 Hz, 1H), 5.53 (q, *J* = 15.5 Hz, 2H), 4.87 (d, *J* = 14.9 Hz, 1H), 4.76 (q, *J* = 6.7 Hz, 1H), 4.55 (d, *J* = 14.9 Hz, 1H), 4.37 – 4.30 (m, 1H), 4.13 (dd, *J* = 16.6, 11.0 Hz, 1H), 3.97 (dd, *J* = 5.2, 1.8 Hz, 1H), 3.93 (s, 6H), 3.89 (s, 3H), 3.78 (s, 1H), 3.27 – 3.20 (m, 1H), 3.20 – 3.11 (m, 1H), 1.24 (d, *J* = 6.8 Hz, 3H); **^{13}C NMR** (126 MHz, $CDCl_3$) δ ppm 172.0, 153.6, 147.1, 144.1, 140.7, 137.8, 137.2, 136.9, 128.1, 127.2, 122.8, 111.1, 110.8, 104.5, 61.2, 56.4, 54.8, 49.7, 48.1, 47.0, 44.8, 44.3, 16.4; **FTIR** (thin film) 3140, 2937, 1659, 1589, 1499, 1340, 1126, 766, 735 cm^{-1}; **HRMS** calculated for $C_{29}H_{34}N_5O_7S$ $(M+H)^+$ = 596.2173; found 596.2169 (+ESI).

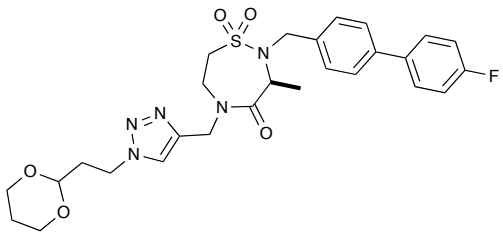

(*S*)-5-((1-(2-(1,3-dioxan-2-yl)ethyl)-1H-1,2,3-triazol-4-yl)methyl)-2-((4'-fluoro-[1,1'-biphenyl]-4-yl)methyl)-3-methyl-1,2,5-thiadiazepin-1,1-dioxide 4-one 5.13{*1,3,1*}

$[\alpha]^{20}_{D}$ = -23.6 º (c = 0.70, CH_2Cl_2); **^{1}H NMR** (500 MHz, $CDCl_3$) δ ppm 7.57 (d, *J* = 4.5 Hz, 1H), 7.53 – 7.47 (m, 2H), 7.47 – 7.43 (m, 2H), 7.37 (d, *J* = 8.3 Hz, 2H), 7.11 – 7.05 (m, 2H), 4.79 (d, *J* = 14.9 Hz, 1H), 4.73 (q, *J* = 6.8 Hz, 1H), 4.56 (d, *J* = 16.5 Hz, 1 H), 4.56 – 4.53 (m, 1H), 4.45 (td, *J* = 7.0, 2.2 Hz, 2H), 4.35 (d, *J* = 16.4 Hz, 1H), 4.13 – 4.08 (m, 1H), 4.08 – 4.03 (m, 2H), 3.98 – 3.90 (m, 1H), 3.78 (d, *J* = 16.4 Hz, 1H), 3.69 (ddd, *J* = 12.4, 3.9, 2.5 Hz, 2H), 3.24 – 3.18 (m, 2H), 2.19 – 2.12 (m, 2H), 2.03 (qt, *J* = 12.5, 5.0 Hz, 1H), 1.31 (dm, 1H), 1.22 (d, *J* = 6.9 Hz, 3H); **^{13}C NMR** (126 MHz, $CDCl_3$) δ ppm 172.1, 162.7 (d, $^1J_{CF}$ = 246 Hz), 143.3, 139.53, 136.8 (d, $^4J_{CF}$ = 3.0 Hz), 128.8 (d, $^3J_{CF}$ = 8.1 Hz), 128.1, 127.2, 123.3, 115.8 (d, $^2J_{CF}$ = 21.4 Hz) 99.1, 67.1, 54.8, 49.7, 48.2, 45.7, 44.7, 44.3, 35.6, 25.8, 16.5; **FTIR** (thin film) 3138, 2939, 1659, 1589, 1499, 1340, 1126, 766, 733 cm^{-1}; **HRMS** calculated for $C_{27}H_{33}N_5O_5S$ $(M+H)^+$ = 558.2181; found 558.2176 (+ESI).

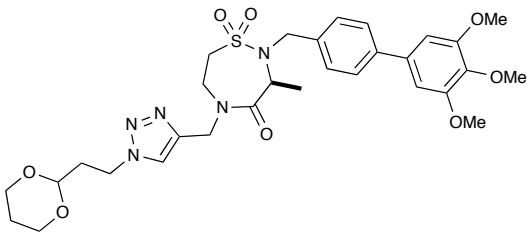

(*S*)-5-((1-(2-(1,3-dioxan-2-yl)ethyl)-1H-1,2,3-triazol-4-yl)methyl)-3-methyl-2-((3',4',5'-trimethoxy-[1,1'-biphenyl]-4-yl)methyl)-1,2,5-thiadiazepin-1,1-dioxide 4-one 5.13{*1,3,2*}

$[\alpha]^{20}_{D}$ = -15.4 ° (c = 0.68, CH_2Cl_2); **^{1}H NMR** (500 MHz, $CDCl_3$) δ ppm 7.61 (s, 1H), 7.52 – 7.48 (m, 2H), 7.40 (d, *J* = 8.3 Hz, 2H), 6.76 (s, 2H), 4.83 (d, *J* = 14.9 Hz, 1H), 4.77 (q, *J* = 6.6 Hz, 1H), 4.60 (d, *J* = 14.5 Hz, 1H), 4.57 (d, *J* = 4.7 Hz, 1H), 4.49 (td, *J* = 7.0, 2.2 Hz, 2H), 4.39 (d, *J* = 16.4 Hz, 1H), 4.09 (ddd, *J* = 11.8, 4.9, 1.1 Hz, 3H), 4.01 – 3.94 (m, 1H), 3.92 (s, 6H), 3.89 (s, 3H), 3.82 (d, *J* = 16.4 Hz, 1H), 3.77 – 3.69 (m, 1H), 3.25 (dd, *J* = 6.1, 3.9 Hz, 1H), 2.22 – 2.16 (m, 2H), 2.06 (qt, *J* = 12.5, 5.0 Hz, 1H), 1.39 – 1.32 (m, 1H), 1.26 (d, *J* = 6.8 Hz, 3H); **^{13}C NMR** (126 MHz, $CDCl_3$) δ ppm 172.1, 153.6, 143.3, 140.7, 137.8, 137.2, 136.9, 128.0, 127.3, 123.3, 104.5, 99.1, 67.1, 67.1, 61.2, 56.4, 54.9, 49.7, 48.2, 45.7, 44.7, 44.3, 35.6, 25.8, 16.5; **FTIR** (thin film) 3138, 2939, 1659 1589, 1499, 1340, 1126, 766, 733 cm^{-1}; **HRMS** calculated for $C_{30}H_{40}N_5O_8S$ $(M+H)^+$ = 630.2592; found 630.2591 (+ESI).

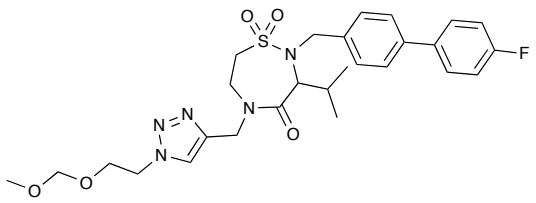

(±)-2-((4'-fluoro-[1,1'-biphenyl]-4-yl)methyl)-3-isopropyl-5-((1-(2-(methoxy methoxy)ethyl)-1H-1,2,3-triazol-4-yl)methyl)-1,2,5-thiadiazepin-1,1-dioxide 4-one 5.13{*2,1,1*}

^{1}H NMR (500 MHz, $CDCl_3$) δ ppm 7.75 (s, 1H), 7.57 – 7.52 (m, 2H), 7.48 (s, 4H), 7.15 – 7.09 (m, 2H), 4.96 (d, *J* = 14.9 Hz, 1H), 4.55 (q, *J* = 10.1 Hz, 5.1 Hz, 2H), 4.53 (s, 2H), 4.50 (d, *J* = 14.9 Hz, 2H), 4.28 (d, *J* = 15.4 Hz, 1H), 4.18 (dd, *J* = 16.6, 11.6 Hz, 1H), 4.05 (d, *J* = 10.6 Hz, 1H), 3.99 – 3.92 (m, 1H), 3.90 (t, *J* = 5.1 Hz, 2H), 3.74 (d, *J* = 15.4 Hz, 1H), 3.24 (s, 3H), 3.21 (dd, *J* = 14.5, 4.9 Hz, 1H), 3.13 – 3.04 (m, 1H), 2.07 (qt, *J* = 12.4, 6.2 Hz, 1H), 0.90 (d, *J* = 6.4 Hz, 3H), 0.69 (d, *J* = 6.6 Hz, 3H); **^{13}C NMR** (126 MHz, $CDCl_3$) δ ppm 170.3, 162.7 (d, $^{1}J_{CF}$ = 247 Hz), 143.6, 139.8, 136.9 (d, $^{4}J_{CF}$ = 3.2 Hz), 135.9, 130.0, 128.8 (d, $^{3}J_{CF}$ = 8.1 Hz), 127.0, 124.1, 115.9 (d, $^{2}J_{CF}$ = 21.5 Hz), 96.7, 65.9, 65.4, 55.7, 50.7, 49.6, 48.6, 45.0, 44.1, 27.2, 20.7, 19.2; **FTIR** (thin film) 3142, 2955, 1657, 1499, 1337, 1155, 735 cm^{-1}; **HRMS** calculated for $C_{27}H_{34}N_5O_5S$ $(M+H)^+$ = 560.2337; found 560.2331 (+ESI).

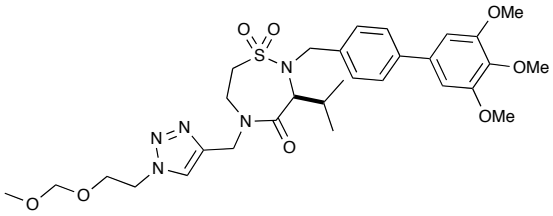

(*S*)-3-isopropyl-5-((1-(2-(methoxymethoxy)ethyl)-1*H*-1,2,3-triazol-4-yl)methyl)-2-((3',4',5'-trimethoxy-[1,1'-biphenyl]-4-yl)methyl)-1,2,5-thiadiazepin-1,1-dioxide 4-one 5.13{*2,1,2*}

$[\alpha]^{20}_{D}$ = +1.6 ° (c = 0.84, CH_2Cl_2); **^{1}H NMR** (500 MHz, $CDCl_3$) δ ppm 7.75 (s, 1H), 7.49 (q, *J* = 13.0, 8.1 Hz, 4H), 6.78 (s, 2H), 4.97 (d, *J* = 14.9 Hz, 1H), 4.61 – 4.46 (m, 5H), 4.28 (d, *J* = 15.6 Hz, 1H), 4.18 (dd, *J* = 16.3, 11.8 Hz, 1H), 4.05 (d, *J* = 10.5 Hz, 1H), 3.96 (m, 1H), 3.93 (s, 6H), 3.90 (m, 1H), 3.88 (s, 3H), 3.75 (d, *J* = 15.4 Hz, 1H), 3.25 (s, 3H), 3.22 – 3.18 (m, 1H), 3.09 (t, *J* = 12.8 Hz, 1H), 2.16 – 2.01 (m, 1H), 0.91 (d, *J* = 6.2 Hz, 3H), 0.68 (t, *J* = 14.6 Hz, 3H); **^{13}C NMR** (126 MHz, $CDCl_3$) δ ppm 170.3, 153.7, 143.6, 140.9, 137.9, 136.7, 135.9, 129.9, 127.0, 124.0, 104.5, 96.6, 65.9, 65.4, 61.2, 56.4, 55.7, 50.7, 49.6, 48.6, 45.0, 44.0, 27.2, 20.7, 19.3; **FTIR** (thin film) 3138, 2957, 1657, 1589, 1499, 1342, 1155, 1126, 731 cm^{-1}; **HRMS** calculated for $C_{30}H_{42}N_5O_8S$ $(M+H)^+$ = 632.2749; found 632.2746 (+ESI).

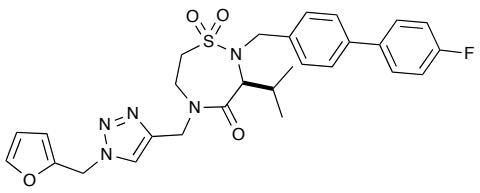

(*S*)-2-((4'-fluoro-[1,1'-biphenyl]-4-yl)methyl)-5-((1-(furan-2-ylmethyl)-1H-1,2,3-triazol-4-yl)methyl)-3-isopropyl-1,2,5-thiadiazepin-1,1-dioxide 4-one 5.13{*2,2,1*}

$[\alpha]^{20}_{D}$ = -0.30 º (c = 1.0, CH_2Cl_2); **^{1}H NMR** (500 MHz, $CDCl_3$) δ ppm 7.64 (s, 1H), 7.57 – 7.52 (m, 2H), 7.50 – 7.46 (m, 2H), 7.44 (d, *J* = 8.3 Hz, 2H), 7.29 (dd, *J* = 1.8, 0.7 Hz, 1H), 7.15 – 7.10 (m, 2H), 6.44 (dd, *J* = 3.2, 0.5 Hz, 1H), 6.31 (dd, *J* = 3.2, 1.9 Hz, 1H), 5.55 (d, *J* = 15.5 Hz, 1H), 5.47 (d, *J* = 15.5 Hz, 1H), 4.97 (d, *J* = 14.9 Hz, 1H), 4.43 (d, *J* = 14.9 Hz, 1H), 4.23 – 4.13 (m, 2H), 4.03 (d, *J* = 10.6 Hz, 1H), 3.96 – 3.88 (m, 1H), 3.63 (d, *J* = 15.4 Hz, 1H), 3.20 (dd, *J* = 14.5, 4.9 Hz, 1H), 3.09 – 3.02 (m, 1H), 2.09 – 1.99 (m, 1H), 0.88 (d, *J* = 6.4 Hz, 3H), 0.67 (d, *J* = 6.6 Hz, 3H); **^{13}C NMR** (126 MHz, $CDCl_3$) δ ppm 170.3, 162.7 (d, $^1J_{CF}$ = 247 Hz), 147.1, 144.1, 139.7, 136.9, 136.9, 135.9, 130.0, 128.8 (d, $^4J_{CF}$ = 8.0 Hz), 126.90, 122.92, 115.9 (d, $^3J_{CF}$ = 21.4 Hz), 110.9 (d, $^2J_{CF}$ = 48.8 Hz) 65.3, 49.6, 48.5, 47.0, 45.2, 44.3, 27.2, 20.7, 19.2; **FTIR** (thin film) 3142, 2955, 1657, 1499, 1337, 1155, 1138, 735 cm^{-1}; **HRMS** calculated for $C_{28}H_{31}FN_5O_4S$ $(M+H)^+$ = 552.2075; found 552.2072 (+ESI).

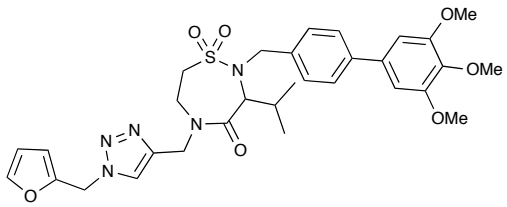

(±)-5-((1-(furan-2-ylmethyl)-1H-1,2,3-triazol-4-yl)methyl)-3-isopropyl-2-((3',4',5'-trimethoxy-[1,1'-biphenyl]-4-yl)methyl)-1,2,5-thiadiazepin-1,1-dioxide 4-one 5.13{*2,2,2*}

^{1}H NMR (500 MHz, $CDCl_3$) δ ppm 7.64 (s, 1H), 7.51 – 7.48 (m, 2H), 7.44 (d, *J* = 8.2 Hz, 2H), 7.30 (dd, *J* = 1.8, 0.7 Hz, 1H), 6.78 (s, 2H), 6.44 (dd, *J* = 3.3, 0.5 Hz, 1H), 6.31 (dd, *J* = 3.2, 1.9 Hz, 1H), 5.55 (d, *J* = 15.5 Hz, 1H), 5.47 (d, *J* = 15.5 Hz, 1H), 4.98 (d, *J* = 14.9 Hz, 1H), 4.43 (d, *J* = 14.9 Hz, 1H), 4.18 (dd, *J* = 16.0, 11.6 Hz, 2H), 4.06 – 4.00 (m, 1H), 3.94 (s, 7H), 3.90 (d, *J* = 10.0 Hz, 4H), 3.65 (d, *J* = 15.4 Hz, 1H), 3.20 (dd, *J* = 14.5, 5.0 Hz, 1H), 3.10 – 3.02 (m, 1H), 2.11 – 2.00 (m, 1H), 0.89 (d, *J* = 6.4 Hz, 3H), 0.69 (d, *J* = 6.6 Hz, 3H); **^{13}C NMR** (126 MHz, $CDCl_3$) δ ppm 170.3, 153.7, 147.1, 144.1, 144.1, 140.8, 137.9, 136.7, 135.9, 129.9, 127.0, 122.9, 111.1, 110.7, 104.5, 65.3, 61.2, 56.4, 49.6, 48.6, 47.0, 45.2, 44.3, 27.2, 20.7, 19.2; **FTIR** (thin film) 3142, 2962, 1655, 1589, 1499, 1342, 1153, 1126, 733 cm^{-1}; **HRMS** calculated for $C_{31}H_{38}N_5O_7S$ $(M+H)^+$ = 624.2486; found 624.2484 (+ESI).

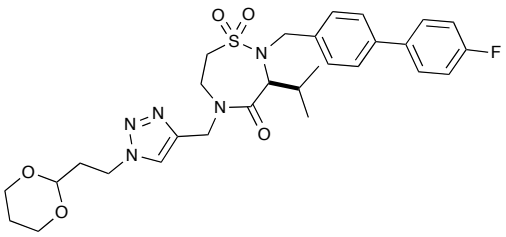

(*S*)-5-((1-(2-(1,3-dioxan-2-yl)ethyl)-1H-1,2,3-triazol-4-yl)methyl)-2-((4'-fluoro-[1,1'-biphenyl]-4-yl)methyl)-3-isopropyl-1,2,5-thiadiazepin-1,1-dioxide 4-one 5.13{*2,3,1*}

$[\alpha]^{20}_{D}$ = -2.3 ° (c = 0.49, CH_2Cl_2); **^{1}H NMR** (500 MHz, $CDCl_3$) δ ppm 7.60 (s, 1H), 7.57 – 7.52 (m, 2H), 7.51 – 7.46 (m, 4H), 7.15 – 7.09 (m, 2H), 4.89 (d, *J* = 14.9 Hz, 1H), 4.53 (t, *J* = 4.8 Hz, 1H), 4.51 (d, *J* = 15.1 Hz, 1H), 4.48 (td, *J* = 7.0, 1.5 Hz, 2H), 4.29 (d, *J* = 15.4 Hz, 1H), 4.21 – 4.13 (m, 1H), 4.08 (ddd, *J* = 8.4, 4.5, 2.5 Hz, 1H), 4.07 – 4.03 (m, 2H), 3.98 – 3.91 (m, 1H), 3.76 (d, *J* = 8.2 Hz, 1H), 3.70 (tt, *J* = 12.2, 2.6 Hz, 2H), 3.26 – 3.19 (m, 1H), 3.18 – 3.10 (m, 1H), 2.20 – 2.14 (m, 2H), 2.12 – 1.99 (m, 2H), 1.36 – 1.29 (dm, 1H), 0.91 (d, *J* = 6.4 Hz, 3H), 0.70 (d, *J* = 6.6 Hz, 3H); **^{13}C NMR** (126 MHz, $CDCl_3$) δ ppm 170.4, 162.7 (d, $^1J_{CF}$ = 247 Hz), 143.5, 139.8, 136.9 (d, $^4J_{CF}$ = 3.2 Hz), 135.8, 130.0, 128.8 (d, $^3J_{CF}$ = 8.0 Hz), 127.0, 123.3, 115.9 (d, $^2J_{CF}$ = 21.4, Hz), 99.1, 67.1, 65.3, 49.7, 48.7, 45.7, 45.0, 44.0, 35.6, 27.2, 25.7, 20.8, 19.2; **FTIR** (thin film) 3140, 2964, 1657, 1499, 1337, 1155, 735 cm^{-1}; **HRMS** calculated for $C_{29}H_{37}FN_5O_5S$ $(M+H)^+$ = 586.2494; found 586.2493 (+ESI).

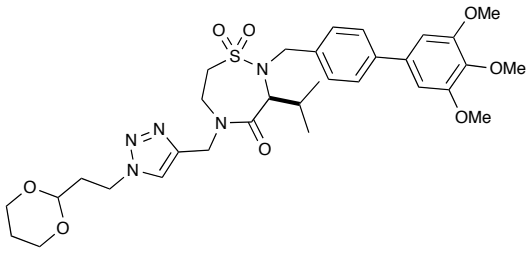

(S)-5-((1-(2-(1,3-dioxan-2-yl)ethyl)-1H-1,2,3-triazol-4-yl)methyl)-3-isopropyl-2-((3',4',5'-trimethoxy-[1,1'-biphenyl]-4-yl)methyl)-1,2,5-thiadiazepin-1,1-dioxide 4-one 5.13{*2,3,2*}

$[\alpha]^{20}_{D}$ = +4.1 ° (c = 0.52, CH_2Cl_2); **^{1}H NMR** (500 MHz, $CDCl_3$) δ ppm 7.61 (s, 1H), 7.52 – 7.46 (m, 4H), 6.78 (s, 2H), 4.90 (d, *J* = 14.9 Hz, 1H), 4.55 – 4.50 (m, 2H), 4.48 (td, *J* = 7.0, 1.2 Hz, 2H), 4.29 (d, *J* = 15.4 Hz, 1H), 4.17 (dd, *J* = 16.6, 11.3 Hz, 1H), 4.11 – 4.03 (m, 3H), 3.98 – 3.95 (m, 1H), 3.94 (s, 6H), 3.89 (s, 3H), 3.78 – 3.73 (m, 1H), 3.70 (tt, *J* = 12.2, 2.5 Hz, 2H), 3.23 (dd, *J* = 14.4, 4.4 Hz, 1H), 3.19 – 3.12 (m, 1H), 2.20 – 2.14 (m, 2H), 2.13 – 1.99 (m, 2H), 1.36 – 1.30 (m, 1H), 0.91 (d, *J* = 6.3 Hz, 3H), 0.71 (d, *J* = 6.6 Hz, 3H); **^{13}C NMR** (126 MHz, $CDCl_3$) δ ppm 170.4, 153.7, 143.5, 140.8, 137.9, 136.7, 135.9, 129.9, 127.0, 123.3, 104.5, 99.1, 67.1, 65.4, 61.2, 56.4, 49.6, 48.7, 45.7, 45.0, 44.0, 35.6, 27.2, 25.8, 20.8, 19.3; **FTIR** (thin film) 3140, 2963, 1655, 1589, 1340, 1126, 731 cm^{-1}; **HRMS** calculated for $C_{32}H_{44}N_5O_8S$ $(M+H)^+$ = 658.2905; found 658.2903 (+ESI).

Table 6.1 *Final Library Data Set – Thiadiazepin-1,1-dioxide 4-ones*

entry	compound	actual yield (mg)	actual yield (%)	final purity (%)
1	**5.14**{*1*,*1*,*1*}	34.6	44.9	98.5
2	**5.14**{*1*,*2*,*1*}	31.6	41.7	100.0
3	**5.14**{*1*,*3*,*1*}	35.5	43.9	100.0
4	**5.14**{*1*,*4*,*1*}	37.2	46.3	100.0
5	**5.14**{*1*,*5*,*1*}	35.8	45.4	97.7
6	**5.14**{*2*,*1*,*1*}	34.3	42.2	100.0
7	**5.14**{*2*,*2*,*1*}	29.0	36.2	100.0
8	**5.14**{*2*,*3*,*1*}	31.0	36.4	100.0
9	**5.14**{*2*,*4*,*1*}	32.4	38.3	100.0
10	**5.14**{*2*,*5*,*1*}	33.6	40.5	100.0
11	**5.14**{*3*,*1*,*1*}	35.7	42.8	100.0
12	**5.14**{*3*,*2*,*1*}	43.0	52.3	100.0
13	**5.14**{*3*,*3*,*1*}	38.3	43.9	100.0
14	**5.14**{*3*,*4*,*1*}	0.0	0.0	0.0
15	**5.14**{*3*,*5*,*1*}	68.9	80.9	100.0
16	**5.14**{*1*,*1*,*2*}	36.3	45.5	98.2
17	**5.14**{*1*,*2*,*2*}	10.1	12.9	100.0
18	**5.14**{*1*,*3*,*2*}	24.4	29.2	100.0
19	**5.14**{*1*,*4*,*2*}	34.2	41.2	100.0
20	**5.14**{*1*,*5*,*2*}	19.9	24.4	98.3
21	**5.14**{*2*,*1*,*2*}	21.0	25.0	100.0
22	**5.14**{*2*,*2*,*2*}	23.8	28.8	100.0
23	**5.14**{*2*,*3*,*2*}	21.1	24.0	100.0
24	**5.14**{*2*,*4*,*2*}	33.3	38.2	97.3
25	**5.14**{*2*,*5*,*2*}	25.7	30.0	100.0
26	**5.14**{*3*,*1*,*2*}	30.1	35.0	100.0
27	**5.14**{*3*,*2*,*2*}	19.5	23.0	94.8
28	**5.14**{*3*,*3*,*2*}	28.8	32.0	100.0
29	**5.14**{*3*,*4*,*2*}	25.9	29.0	88.8
30	**5.14**{*3*,*5*,*2*}	26.1	29.7	100.0
31	**5.14**{*1*,*1*,*3*}	18.3	23.7	100.0
32	**5.14**{*1*,*2*,*3*}	42.2	55.5	100.0
33	**5.14**{*1*,*3*,*3*}	25.8	31.8	100.0
34	**5.14**{*1*,*4*,*3*}	39.9	49.6	93.3
35	**5.14**{*1*,*5*,*3*}	23.7	30.0	100.0
36	**5.14**{*2*,*1*,*3*}	38.9	47.8	100.0
37	**5.14**{*2*,*2*,*3*}	31.0	38.7	100.0
38	**5.14**{*2*,*3*,*3*}	26.1	30.6	100.0
39	**5.14**{*2*,*4*,*3*}	31.7	37.4	98.9
40	**5.14**{*2*,*5*,*3*}	30.5	36.7	100.0
41	**5.14**{*3*,*1*,*3*}	31.4	37.6	100.0
42	**5.14**{*3*,*2*,*3*}	39.2	47.6	100.0

43	**5.14**{*3,3,3*}	43.3	49.5	100.0
44	**5.14**{*3,4,3*}	34.5	39.7	100.0
45	**5.14**{*3,5,3*}	42.4	49.7	100.0
46	**5.14**{*1,1,4*}	37.3	45.4	100.0
47	**5.14**{*1,2,4*}	26.8	33.1	100.0
48	**5.14**{*1,3,4*}	51.0	59.2	100.0
49	**5.14**{*1,4,4*}	41.8	48.9	100.0
50	**5.14**{*1,5,4*}	47.1	56.1	100.0
51	**5.14**{*2,1,4*}	36.9	42.7	100.0
52	**5.14**{*2,2,4*}	39.1	45.9	100.0
53	**5.14**{*2,3,4*}	28.2	31.2	100.0
54	**5.14**{*2,4,4*}	38.6	43.0	100.0
55	**5.14**{*2,5,4*}	31.8	36.0	100.0
56	**5.14**{*3,1,4*}	50.6	57.2	100.0
57	**5.14**{*3,2,4*}	44.4	50.8	100.0
58	**5.14**{*3,3,4*}	54.5	59.0	100.0
59	**5.14**{*3,4,4*}	36.0	39.2	95.8
60	**5.14**{*3,5,4*}	38.7	42.8	99.3
61	**5.14**{*1,1,5*}	7.6	9.8	25.3
62	**5.14**{*1,2,5*}	4.9	6.4	100.0
63	**5.14**{*1,3,5*}	7.0	8.6	26.7
64	**5.14**{*1,4,5*}	2.9	3.6	100.0
65	**5.14**{*1,5,5*}	6.0	7.5	27.5
66	**5.14**{*2,1,5*}	2.4	2.9	100.0
67	**5.14**{*2,2,5*}	3.5	4.3	92.0
68	**5.14**{*2,3,5*}	3.4	4.0	100.0
69	**5.14**{*2,4,5*}	4.2	4.9	27.2
70	**8.14**{*2,5,5*}	3.8	4.5	100.0
71	**8.14**{*3,1,5*}	2.7	3.2	100.0
72	**8.14**{*3,2,5*}	3.0	3.6	31.1
73	**8.14**{*3,3,5*}	4.8	5.4	67.9
74	**8.14**{*3,4,5*}	4.0	4.6	86.7
75	**8.14**{*3,5,5*}	3.4	4.0	74.2
76	**8.14**{*1,1,6*}	66.0	80.9	98.3
77	**8.14**{*1,2,6*}	53.1	66.1	100.0
78	**8.14**{*1,3,6*}	70.4	82.4	100.0
79	**8.14**{*1,4,6*}	44.9	52.9	94.0
80	**8.14**{*1,5,6*}	9.1	10.9	96.7
81	**8.14**{*2,1,6*}	56.2	65.5	100.0
82	**8.14**{*2,2,6*}	63.9	75.6	99.0
83	**8.14**{*2,3,6*}	12.9	14.4	73.2
84	**8.14**{*2,4,6*}	64.4	72.3	95.6
85	**8.14**{*2,5,6*}	51.3	58.6	100.0
86	**8.14**{*3,1,6*}	66.3	75.5	99.0
87	**8.14**{*3,2,6*}	52.2	60.2	93.1
88	**8.14**{*3,3,6*}	17.1	18.6	21.7
89	**8.14**{*3,4,6*}	49.9	54.7	95.6

90	**5.14**{*3,5,6*}	13.8	15.4	75.9
91	**5.14**{*1,1,7*}	57.2	72.3	100.0
92	**5.14**{*1,2,7*}	45.2	58.0	100.0
93	**5.14**{*1,3,7*}	59.9	72.1	100.0
94	**5.14**{*1,4,7*}	43.2	52.4	100.0
95	**5.14**{*1,5,7*}	54.4	67.2	99.6
96	**5.14**{*2,1,7*}	53.8	64.5	100.0
97	**5.14**{*2,2,7*}	18.4	22.4	100.0
98	**5.14**{*2,3,7*}	53.2	61.0	100.0
99	**5.14**{*2,4,7*}	41.1	47.4	100.0
100	**5.14**{*2,5,7*}	46.3	54.4	100.0
101	**5.14**{*3,1,7*}	39.0	45.6	100.0
102	**5.14**{*3,2,7*}	38.0	45.1	100.0
103	**5.14**{*3,3,7*}	59.9	67.0	100.0
104	**5.14**{*3,4,7*}	42.4	47.8	97.4
105	**5.14**{*3,5,7*}	55.5	63.6	100.0
106	**5.14**{*1,1,8*}	32.7	38.0	100.0
107	**5.14**{*1,2,8*}	59.7	70.4	85.8
108	**5.14**{*1,3,8*}	69.4	77.1	99.7
109	**5.14**{*1,4,8*}	0.0	0.0	0.0
110	**5.14**{*1,5,8*}	56.1	63.9	100.0
111	**5.14**{*2,1,8*}	62.6	69.4	88.0
112	**5.14**{*2,2,8*}	60.1	67.5	100.0
113	**5.14**{*2,3,8*}	61.9	65.7	93.5
114	**5.14**{*2,4,8*}	42.1	45.0	100.0
115	**5.14**{*2,5,8*}	59.1	64.2	90.4
116	**5.14**{*3,1,8*}	68.3	73.9	93.1
117	**5.14**{*3,2,8*}	48.7	53.4	99.4
118	**5.14**{*3,3,8*}	26.0	27.0	99.1
119	**5.14**{*3,4,8*}	21.3	22.3	100.0
120	**5.14**{*3,5,8*}	56.8	60.3	98.9
121	**5.14**{*1,1,9*}	51.7	61.9	94.9
122	**5.14**{*1,2,9*}	52.8	64.2	94.5
123	**5.14**{*1,3,9*}	57.2	65.4	95.0
124	**5.14**{*1,4,9*}	48.2	55.5	89.9
125	**5.14**{*1,5,9*}	46.6	54.6	93.3
126	**5.14**{*2,1,9*}	52.9	60.3	95.5
127	**5.14**{*2,2,9*}	63.1	72.9	90.9
128	**5.14**{*2,3,9*}	48.0	52.4	92.9
129	**5.14**{*2,4,9*}	52.6	57.8	84.4
130	**5.14**{*2,5,9*}	51.1	57.1	94.2
131	**5.14**{*3,1,9*}	49.9	55.6	92.4
132	**5.14**{*3,2,9*}	56.6	63.9	90.6
133	**5.14**{*3,3,9*}	57.3	61.1	91.6
134	**5.14**{*3,4,9*}	38.3	41.1	82.7
135	**5.14**{*3,5,9*}	50.9	55.6	91.3
136	**5.14**{*1,1,10*}	45.7	52.3	100.0

137	**5.14**{*1,2,10*}	5.9	6.8	99.8
138	**5.14**{*1,3,10*}	64.9	71.1	100.0
139	**5.14**{*1,4,10*}	48.8	53.8	100.0
140	**5.14**{*1,5,10*}	41.1	46.1	100.0
141	**5.14**{*2,1,10*}	52.6	57.4	100.0
142	**5.14**{*2,2,10*}	59.0	65.3	100.0
143	**5.14**{*2,3,10*}	46.7	48.9	100.0
144	**5.14**{*2,4,10*}	0.0	0.0	0.0
145	**5.14**{*2,5,10*}	56.0	60.0	100.0
146	**5.14**{*3,1,10*}	0.0	0.0	0.0
147	**5.14**{*3,2,10*}	45.0	48.7	100.0
148	**5.14**{*3,3,10*}	42.8	43.9	100.0
149	**5.14**{*3,4,10*}	7.0	7.2	99.8
150	**5.14**{*3,5,10*}	56.3	59.0	100.0
151	**5.14**{*1,1,11*}	41.5	54.7	100.0
152	**5.14**{*1,2,11*}	38.2	51.2	100.0
153	**5.14**{*1,3,11*}	13.5	16.9	96.4
154	**5.14**{*1,4,11*}	36.8	46.5	100.0
155	**5.14**{*1,5,11*}	26.2	33.7	100.0
156	**5.14**{*2,1,11*}	50.6	63.2	100.0
157	**5.14**{*2,2,11*}	30.7	38.9	100.0
158	**5.14**{*2,3,11*}	47.1	56.1	100.0
159	**5.14**{*2,4,11*}	45.0	54.0	100.0
160	**5.14**{*2,5,11*}	37.6	45.9	100.0
161	**5.14**{*3,1,11*}	50.2	61.1	100.0
162	**5.14**{*3,2,11*}	29.1	35.9	100.0
163	**5.14**{*3,3,11*}	56.3	65.4	100.0
164	**5.14**{*3,4,11*}	23.4	27.4	100.0
165	**5.14**{*3,5,11*}	31.0	36.9	100.0
166	**5.14**{*1,1,12*}	45.8	56.1	100.0
167	**5.14**{*1,2,12*}	53.1	66.0	87.9
168	**5.14**{*1,3,12*}	44.1	51.5	88.0
169	**5.14**{*1,4,12*}	34.3	40.3	78.9
170	**5.14**{*1,5,12*}	41.9	50.2	100.0
171	**5.14**{*2,1,12*}	52.6	61.2	96.9
172	**5.14**{*2,2,12*}	54.8	64.7	98.5
173	**5.14**{*2,3,12*}	41.4	46.1	100.0
174	**5.14**{*2,4,12*}	20.3	22.8	93.1
175	**5.14**{*2,5,12*}	32.0	36.5	93.6
176	**5.14**{*3,1,12*}	36.5	41.5	57.1
177	**5.14**{*3,2,12*}	38.1	43.9	55.0
178	**5.14**{*3,3,12*}	28.1	30.6	69.9
179	**5.14**{*3,4,12*}	10.1	11.1	94.7
180	**5.14**{*3,5,12*}	0.0	0.0	0.0
181	**5.14**{*1,1,13*}	53.2	66.6	98.8
182	**5.14**{*1,2,13*}	47.6	60.5	100.0
183	**5.14**{*1,3,13*}	41.3	49.3	100.0

184	**5.14**{*1,4,13*}	51.3	61.7	98.6
185	**5.14**{*1,5,13*}	37.4	45.8	100.0
186	**5.14**{*2,1,13*}	55.6	66.1	99.4
187	**5.14**{*2,2,13*}	34.9	42.1	100.0
188	**5.14**{*2,3,13*}	44.8	50.9	96.1
189	**5.14**{*2,4,13*}	35.7	40.8	100.0
190	**5.14**{*2,5,13*}	37.6	43.8	93.4
191	**5.14**{*3,1,13*}	42.6	49.4	96.5
192	**5.14**{*3,2,13*}	36.1	42.5	100.0
193	**5.14**{*3,3,13*}	23.9	26.5	100.0
194	**5.14**{*3,4,13*}	14.2	15.9	100.0
195	**5.14**{*3,5,13*}	12.7	14.4	100.0
196	**5.14**{*1,1,14*}	53.0	65.0	100.0
197	**5.14**{*1,2,14*}	52.0	64.7	100.0
198	**5.14**{*1,3,14*}	62.8	73.5	100.0
199	**5.14**{*1,4,14*}	42.0	49.5	98.8
200	**5.14**{*1,5,14*}	46.0	55.2	99.2
201	**5.14**{*2,1,14*}	47.0	54.8	100.0
202	**5.14**{*2,2,14*}	0.0	0.0	0.0
203	**5.14**{*2,3,14*}	50.1	55.9	99.6
204	**5.14**{*2,4,14*}	42.7	47.9	100.0
205	**5.14**{*2,5,14*}	41.1	46.9	100.0
206	**5.14**{*3,1,14*}	48.9	55.7	100.0
207	**5.14**{*3,2,14*}	44.5	51.4	98.1
208	**5.14**{*3,3,14*}	19.2	20.9	97.2
209	**5.14**{*3,4,14*}	31.8	34.9	100.0
210	**5.14**{*3,5,14*}	9.0	10.0	100.0
211	**5.14**{*1,1,15*}	51.5	62.5	100.0
212	**5.14**{*1,2,15*}	43.8	54.0	83.9
213	**5.14**{*1,3,15*}	61.8	71.6	97.0
214	**5.14**{*1,4,15*}	40.4	47.2	69.7
215	**5.14**{*1,5,15*}	42.1	50.0	100.0
216	**5.14**{*2,1,15*}	13.7	15.8	100.0
217	**5.14**{*2,2,15*}	60.3	70.6	92.1
218	**5.14**{*2,3,15*}	42.6	47.1	89.6
219	**5.14**{*2,4,15*}	41.9	46.6	90.8
220	**5.14**{*2,5,15*}	37.7	42.7	19.1
221	**5.14**{*3,1,15*}	44.5	50.2	97.9
222	**5.14**{*3,2,15*}	34.1	39.0	19.7
223	**5.14**{*3,3,15*}	44.6	48.2	89.8
224	**5.14**{*3,4,15*}	6.8	7.4	30.0
225	**5.14**{*3,5,15*}	28.7	31.7	76.9

Appendix A

NMR Spectra

***Exo* carbic anhydride (2.24)**

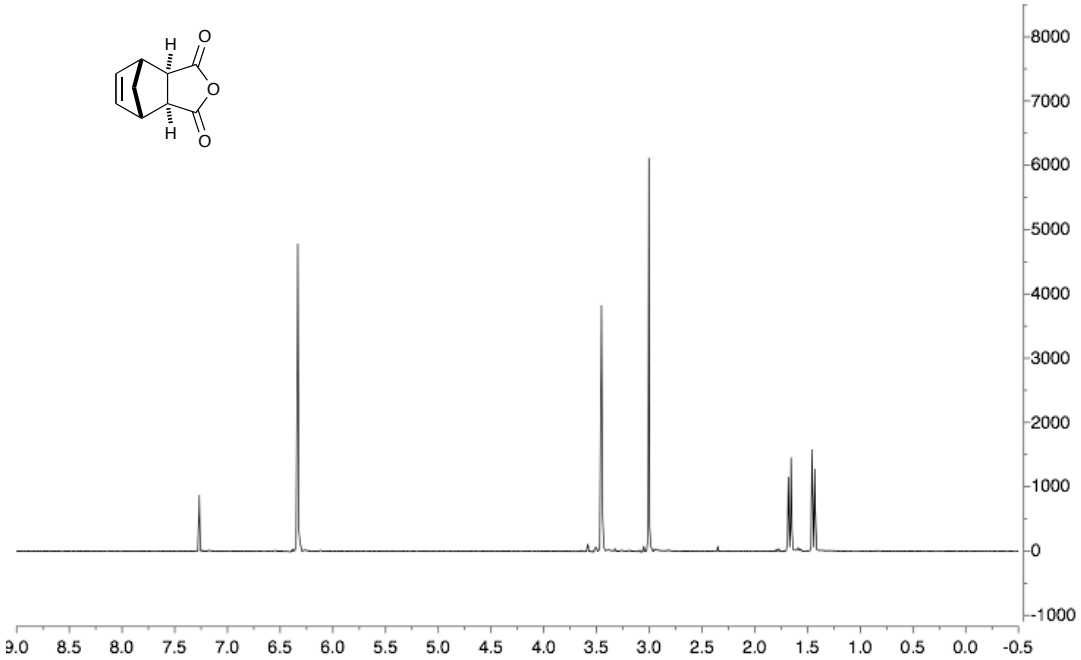

5-Norbornene-2-*exo*, 3-*exo*-dimethanol (2.25)

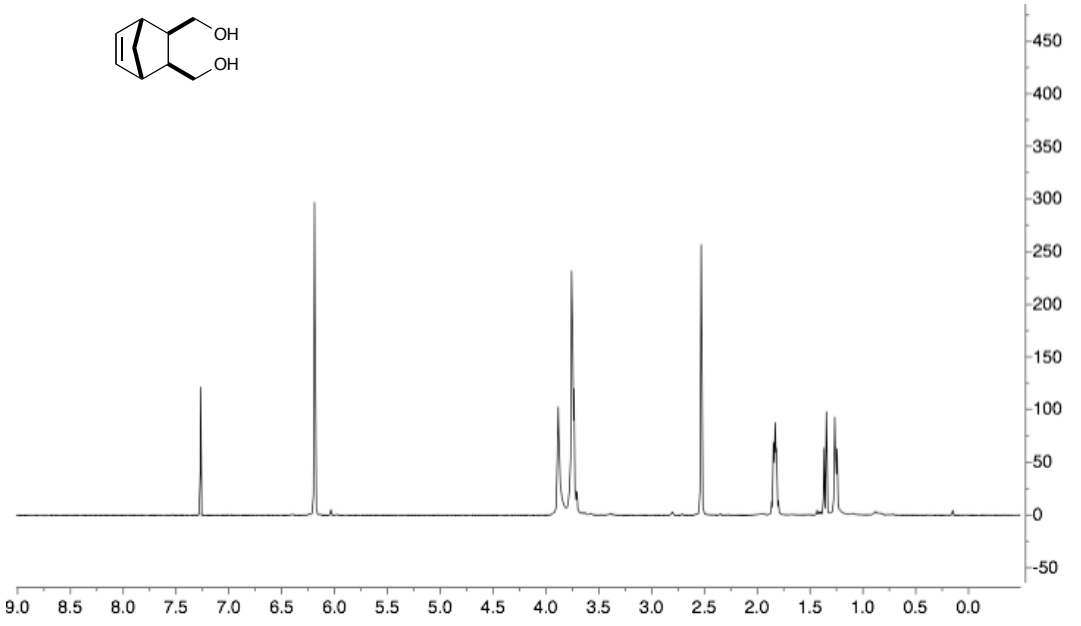

5-norbornene-2-*exo*, 3-*exo*-dimethyl phosphorochloridate (2.26) (major *P*-diastereomer)

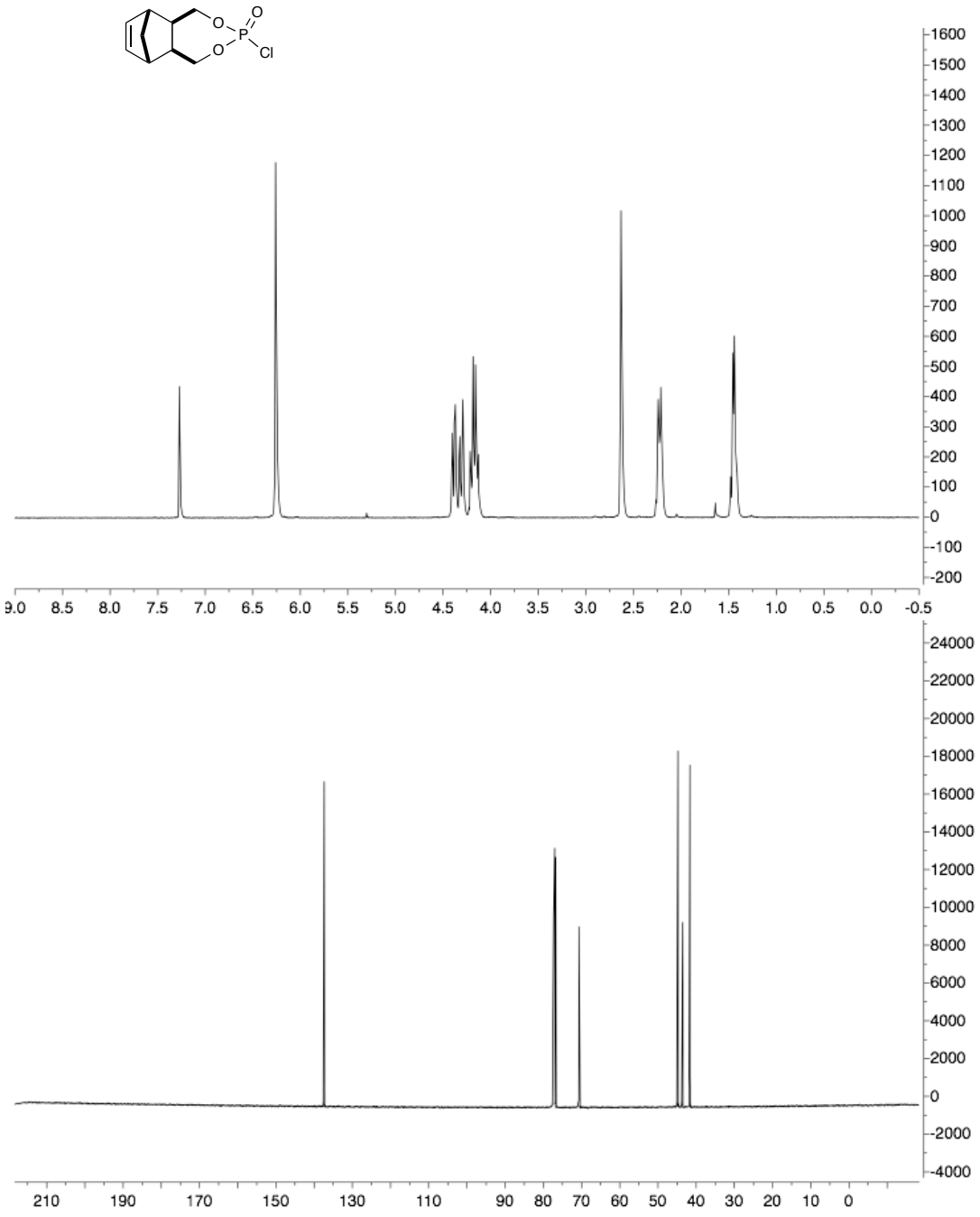

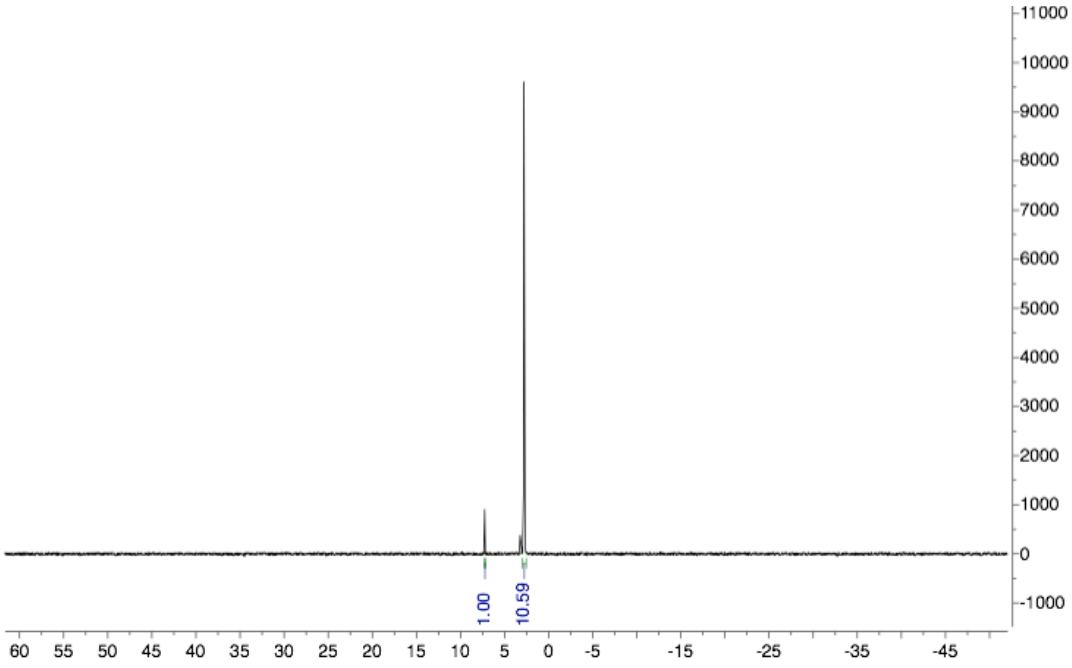

(2*S*,3*S*,6*S*)-6-((benzyloxy)methyl)-3-methyl-2-phenoxy-3,6-dihydro-2H-1,2-oxaphosphinine 2-oxide (2.50)

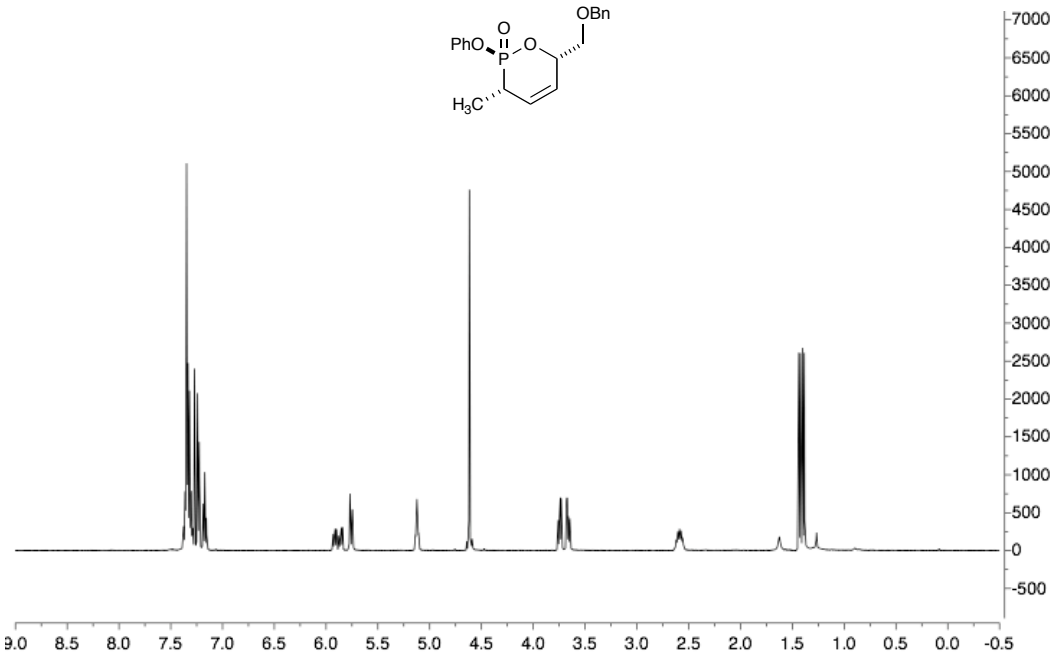

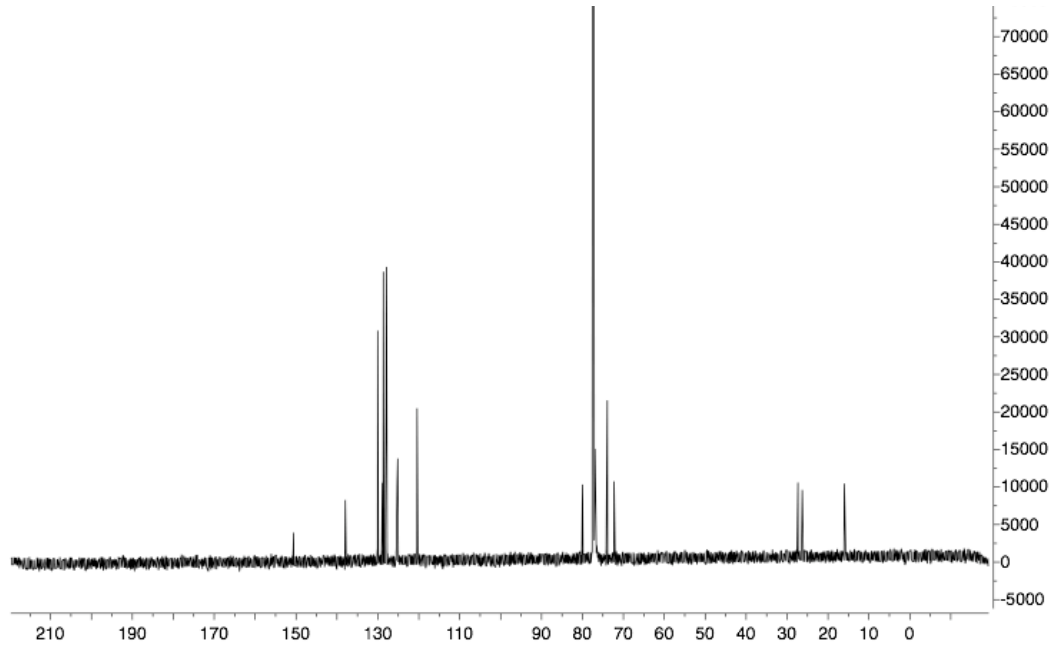
70000
65000
60000
55000
50000
45000
40000
35000
30000
25000
20000
15000
10000
5000
0
-5000
210
190
170
150
130
110
90
80
70
60
50
40
30
20
10
0

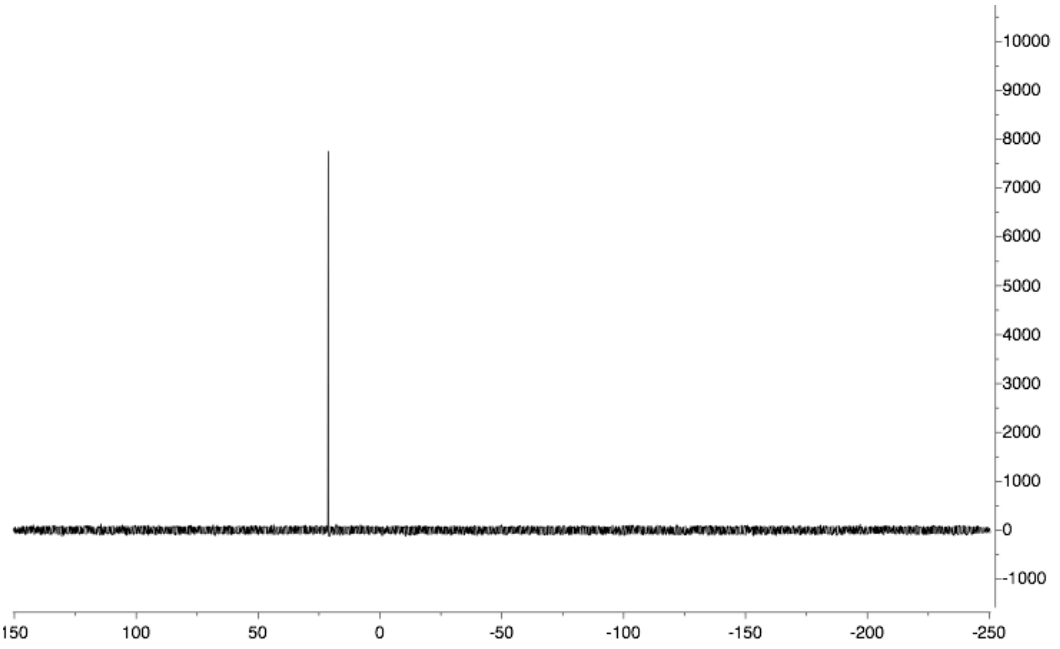
10000
9000
8000
7000
6000
5000
4000
3000
2000
1000
0
-1000
150
100
50
0
-50
-100
-150
-200
-250

(2*S*,3*S*,6*S*)-6-((benzyloxy)methyl)-3-ethyl-2-phenoxy-3,6-dihydro-2H-1,2-oxa phosphinine 2-oxide (2.51)

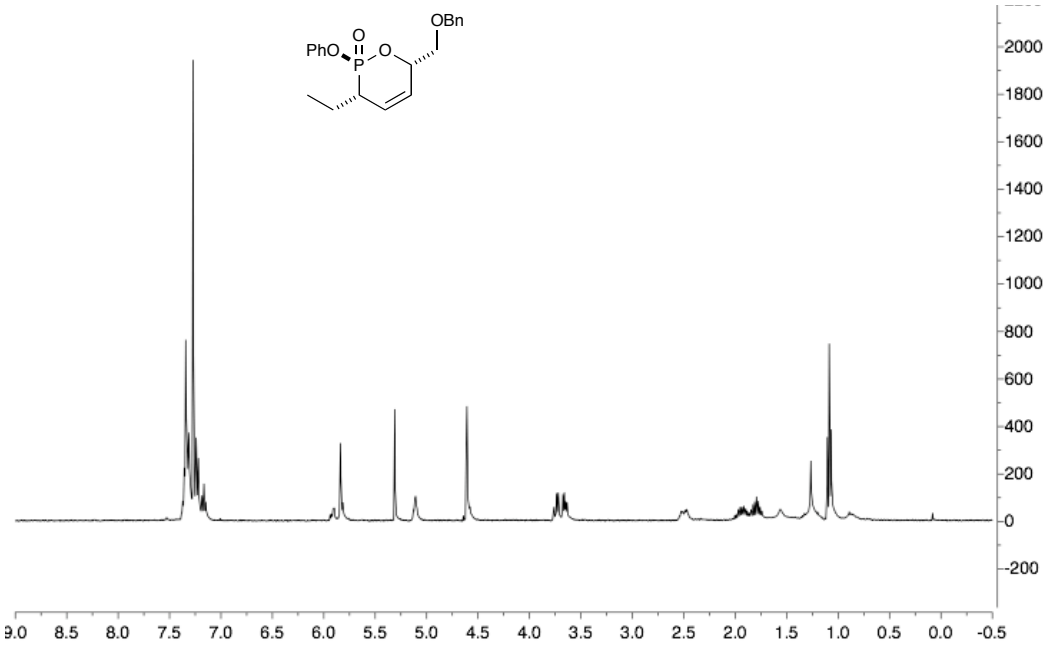

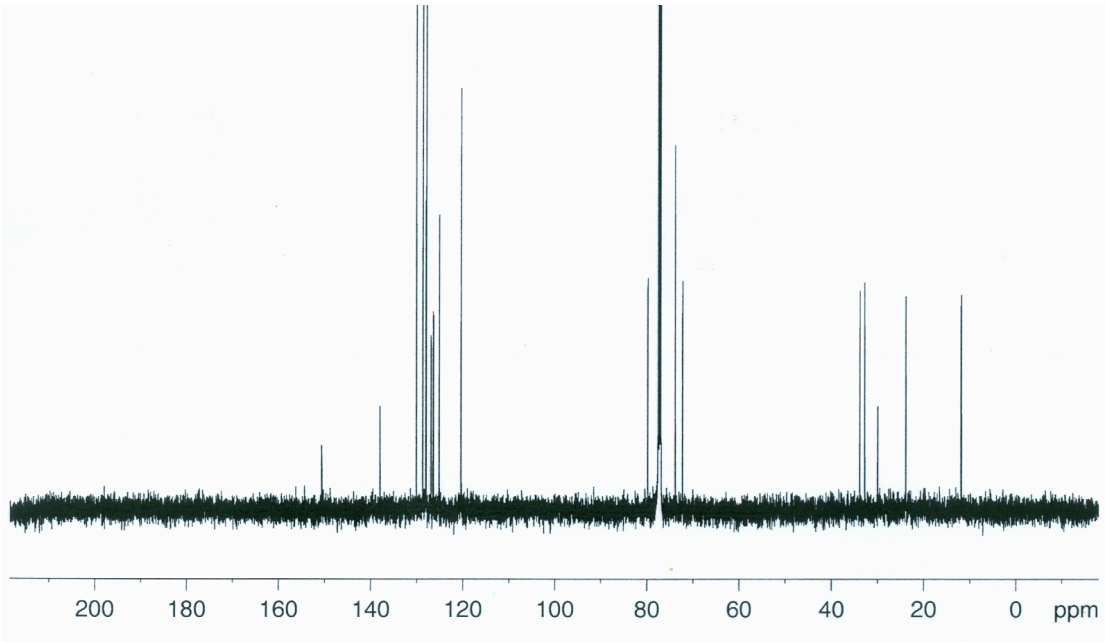

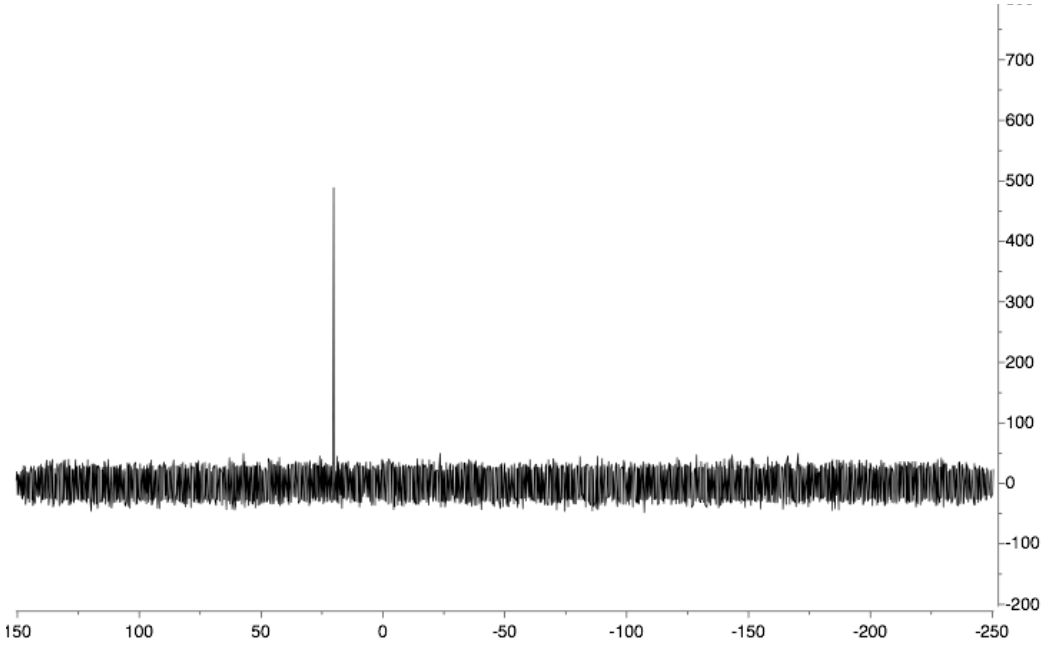

(2*S*,3*S*,6*S*)-6-((benzyloxy)methyl)-3-isopropyl-2-phenoxy-3,6-dihydro-2H-1,2-oxaphosphinine 2-oxide (2.52)

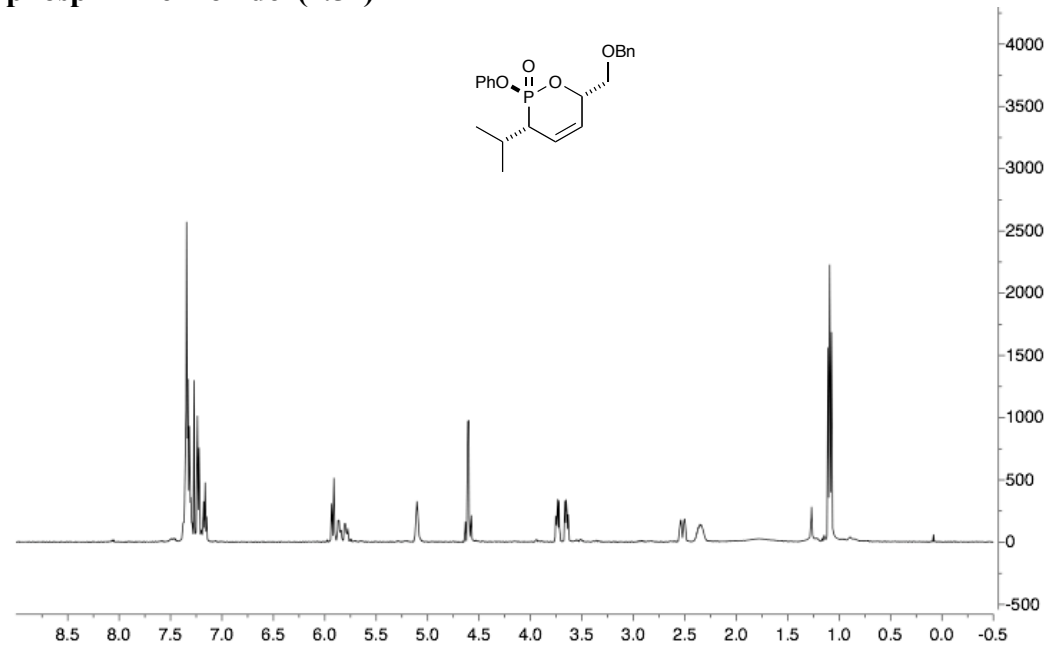

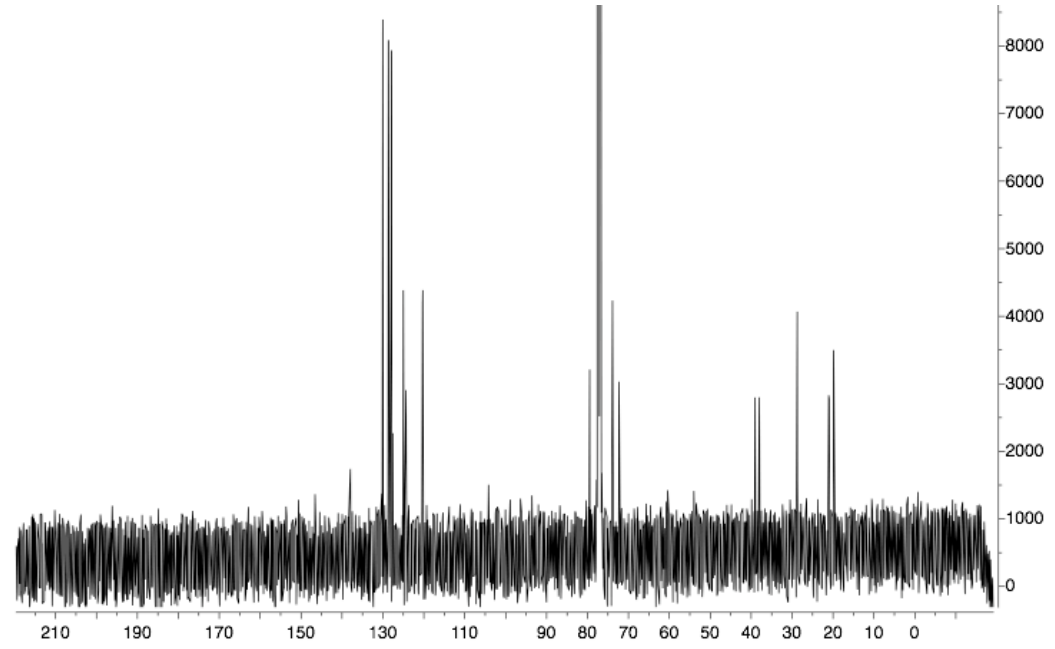
8000
7000
6000
5000
4000
3000
2000
1000
0
210
190
170
150
130
110
90
80
70
60
50
40
30
20
10
0

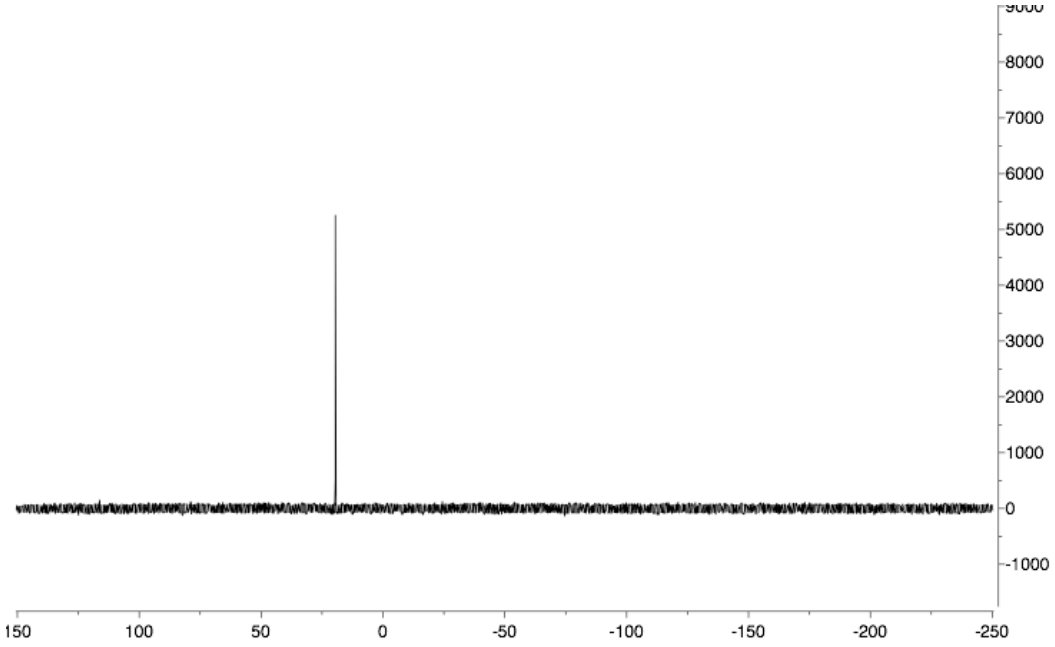
8000
7000
6000
5000
4000
3000
2000
1000
0
-1000
150
100
50
0
-50
-100
-150
-200
-250

5-norbornene-2-*exo*, 3-*exo*-dimethyl benzylphosphate (2.61) (major *P*-diastereomer)

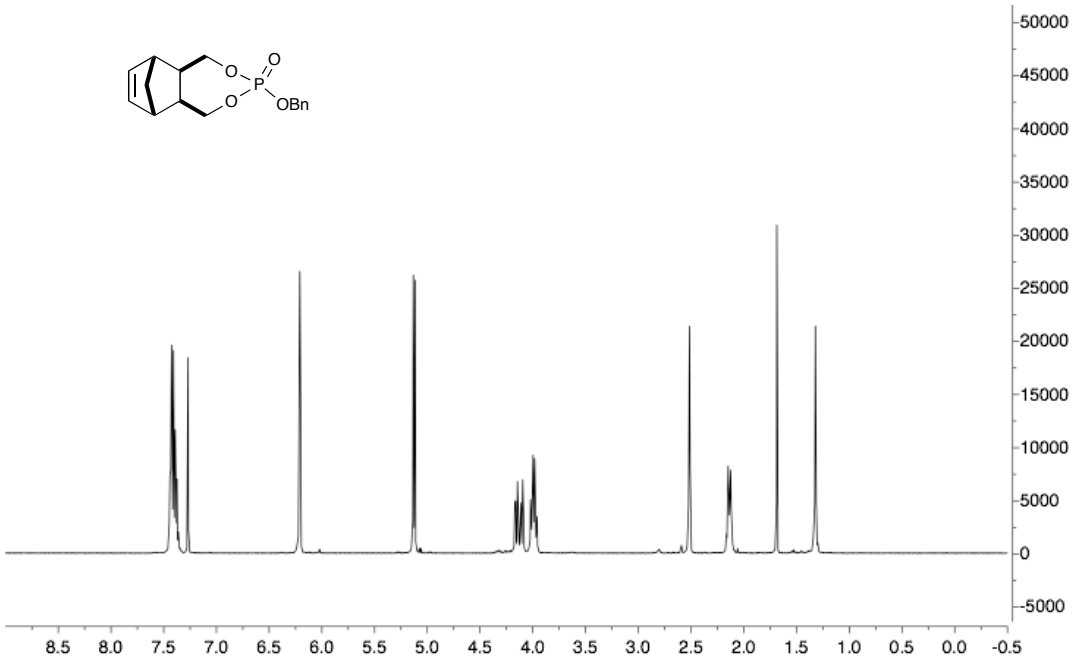

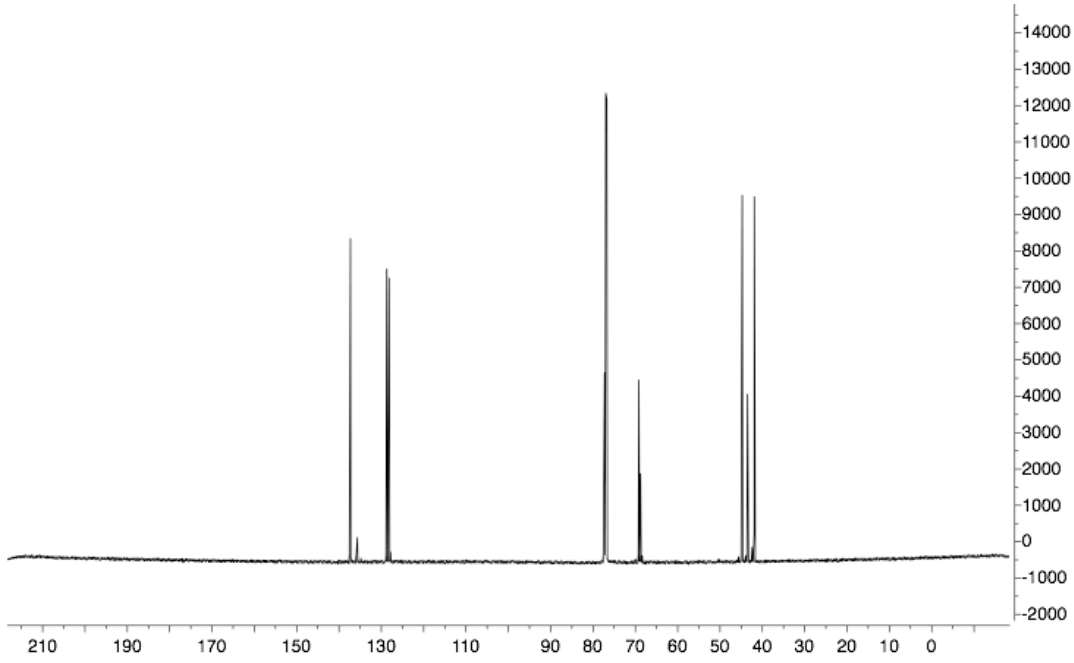
14000
13000
12000
11000
10000
9000
8000
7000
6000
5000
4000
3000
2000
1000
0
-1000
-2000
210
190
170
150
130
110
90
80
70
60
50
40
30
20
10
0

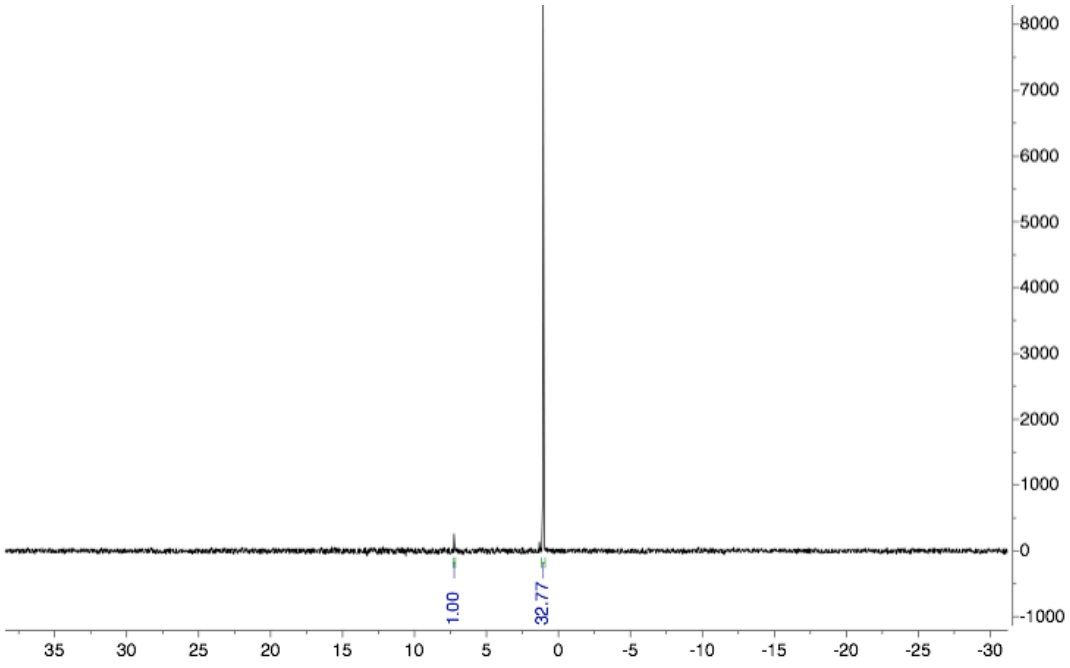
8000
7000
6000
5000
4000
3000
2000
1000
0
-1000
1.00
32.77
35
30
25
20
15
10
5
0
-5
-10
-15
-20
-25
-30

Oligomeric benzylphosphate 20mer (OBP_{20}) (2.62)

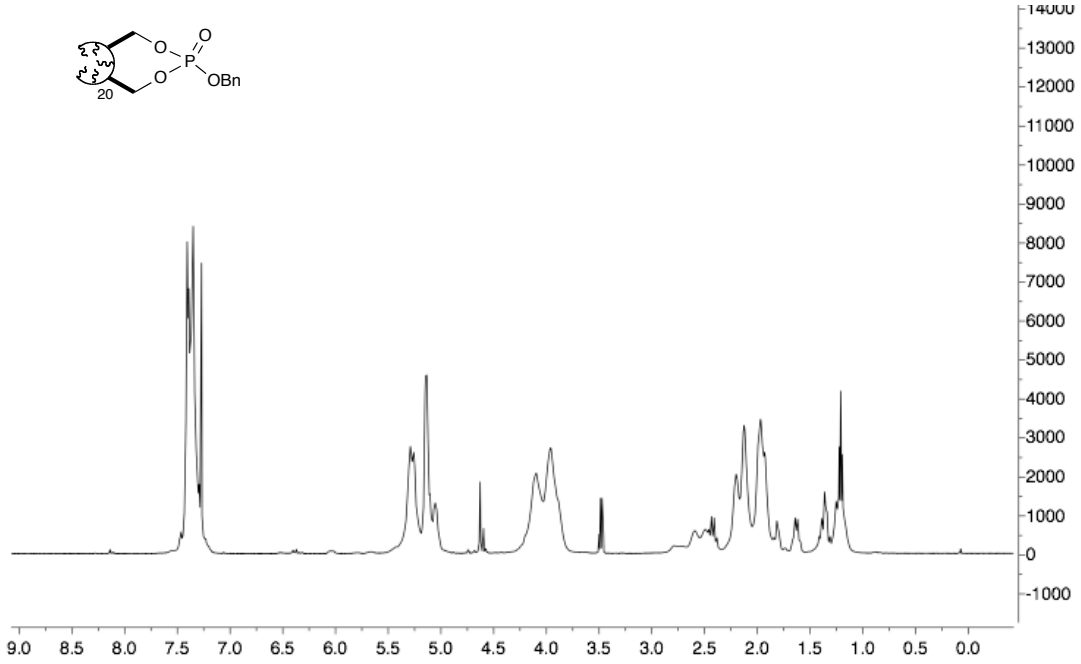

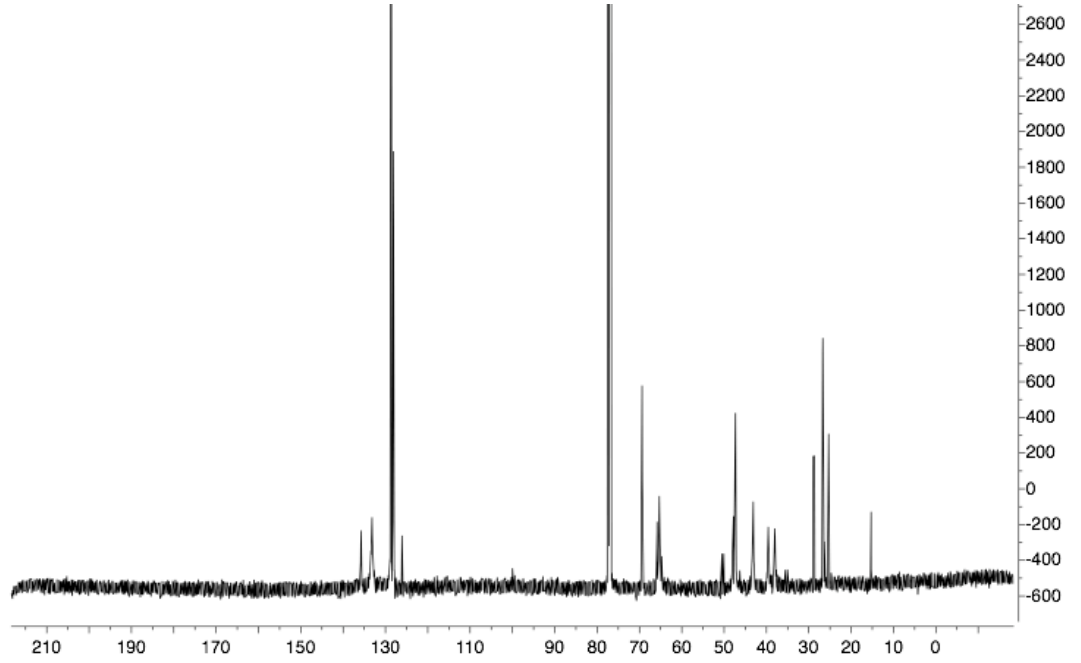

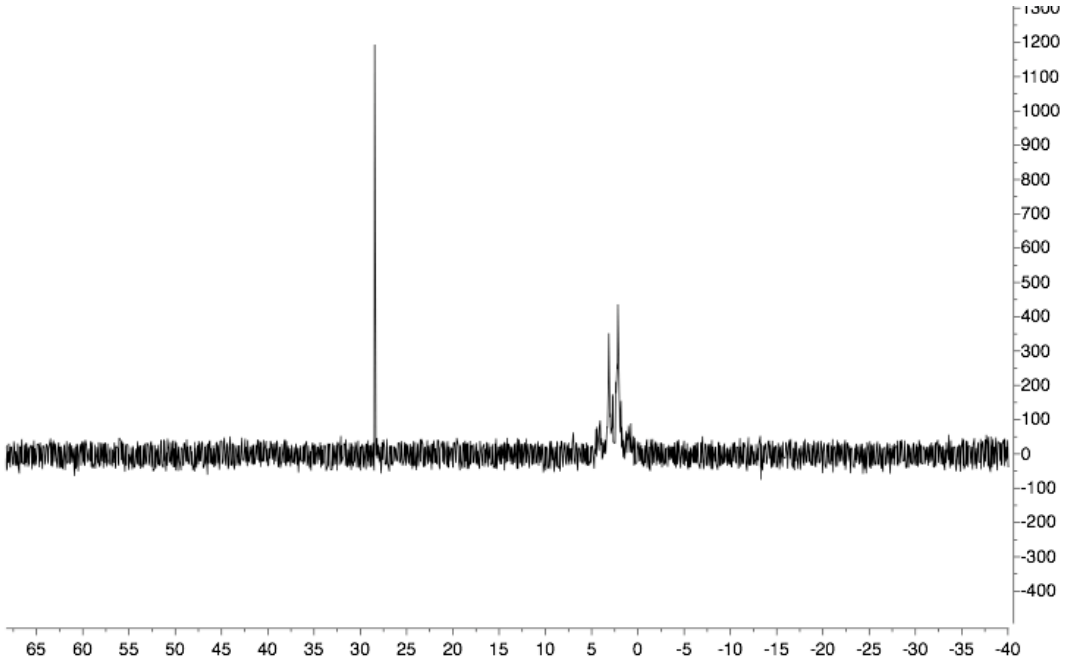

5-norbornene-2-*exo*, 3-*exo*-dimethyl (3,4-(Methylenedioxy)benzyl) phosphate (2.61a) (major *P*-diastereomer)

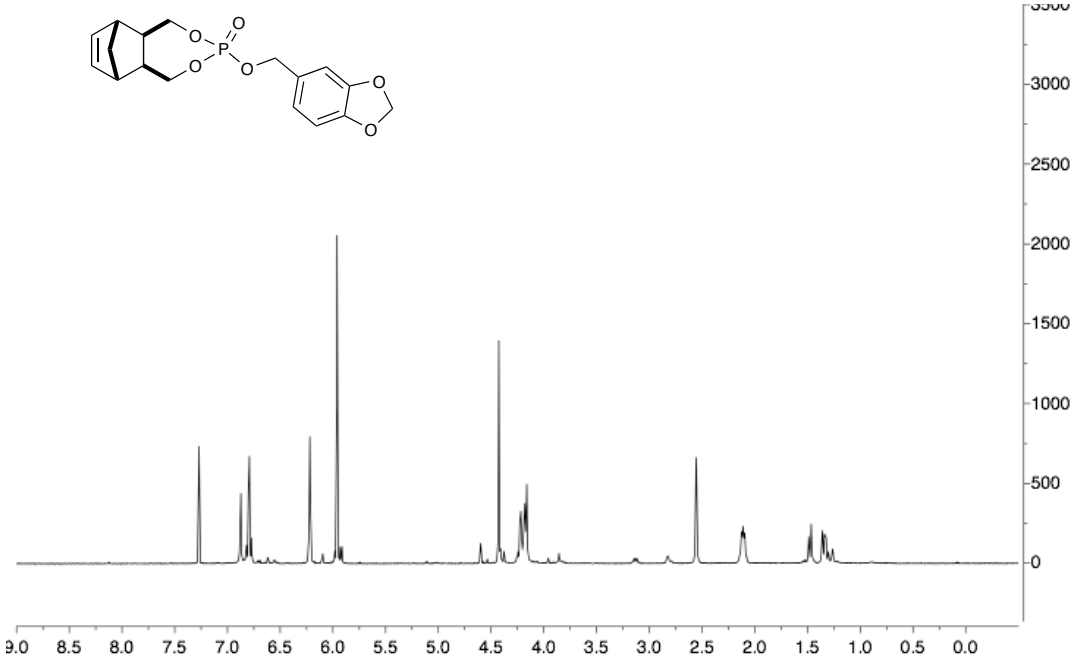

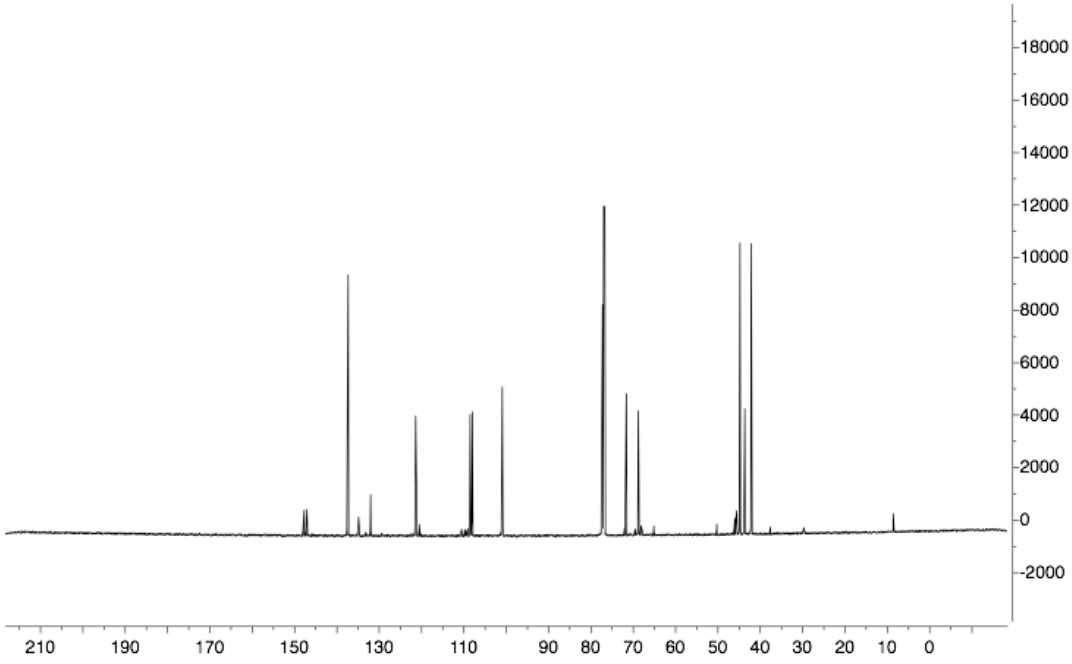
18000
16000
14000
12000
10000
8000
6000
4000
2000
0
-2000
210
190
170
150
130
110
90
80
70
60
50
40
30
20
10
0

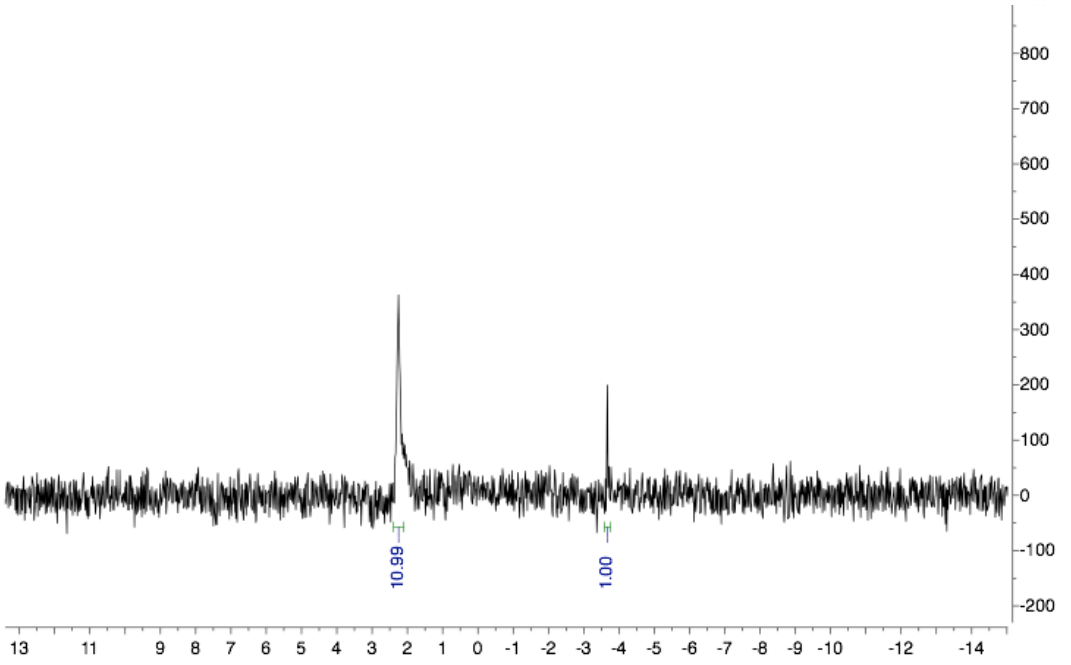
800
700
600
500
400
300
200
100
0
-100
-200
10.99
1.00
13
11
9
8
7
6
5
4
3
2
1
0
-1
-2
-3
-4
-5
-6
-7
-8
-9
-10
-12
-14

5-norbornene-2-*exo*, 3-*exo*-dimethyl (2-methyl benzyl) phosphate (2.61e) (major *P*-diastereomer)

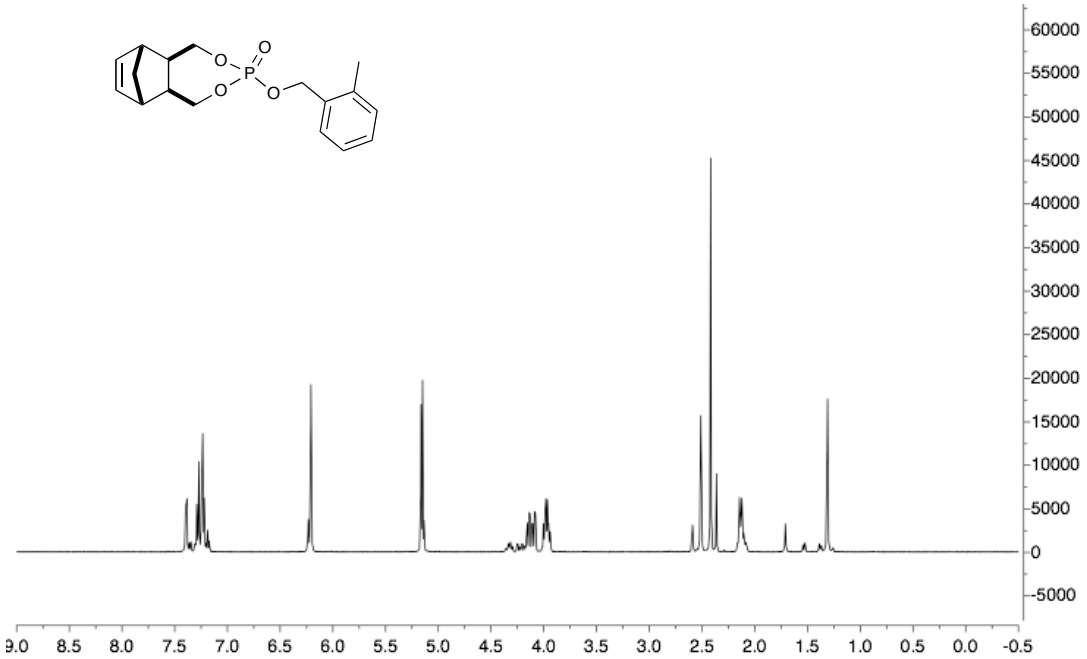

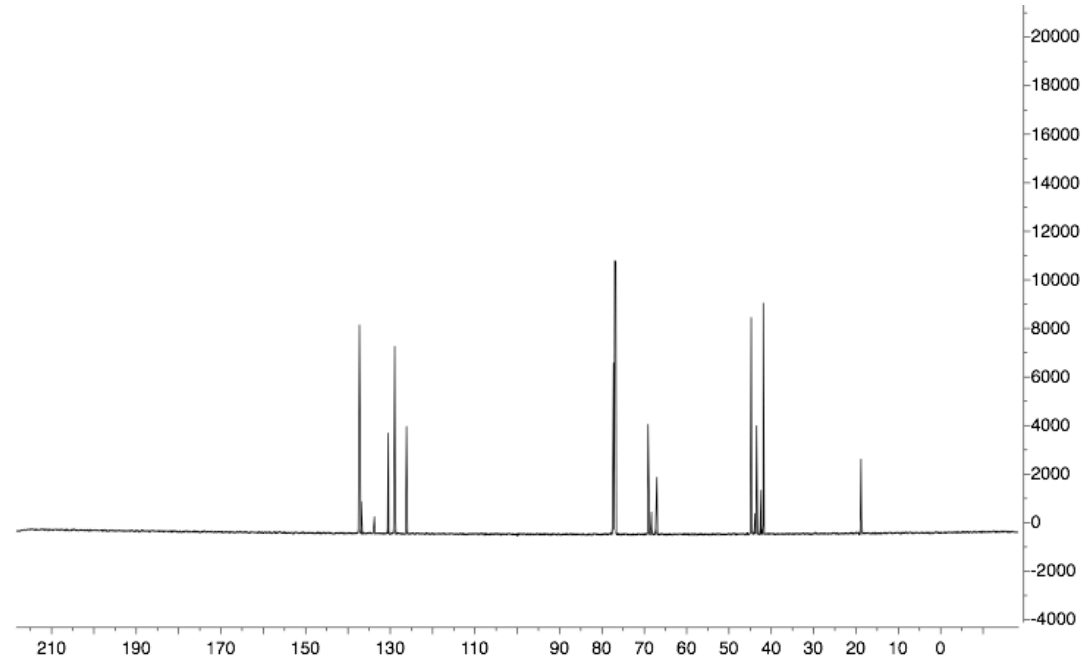

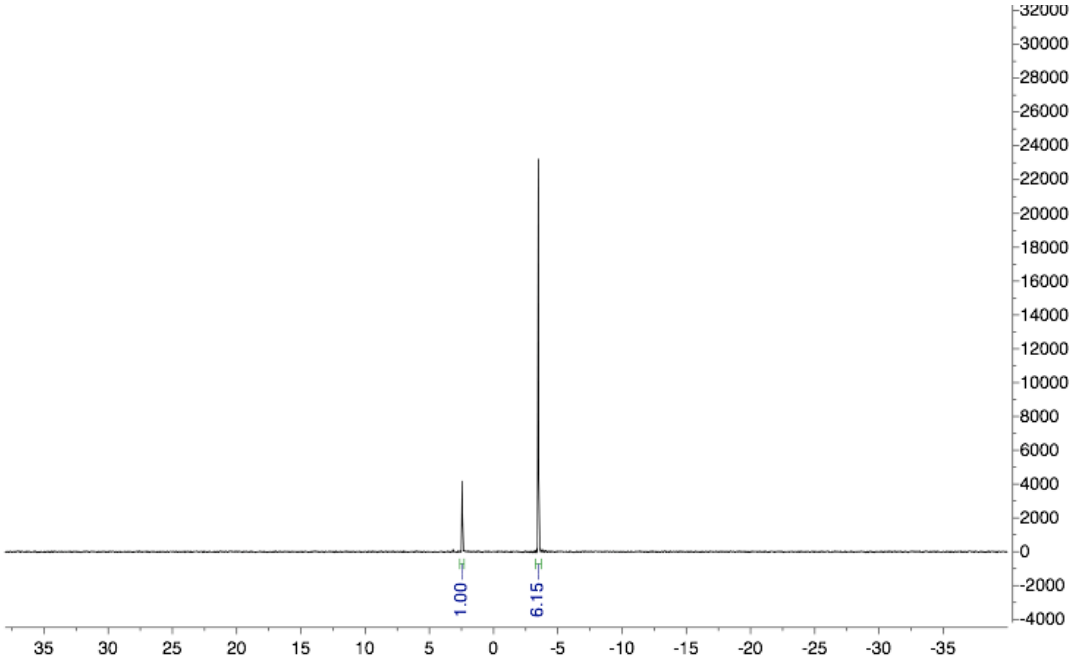

5-norbornene-2-*exo*, 3-*exo*-dimethyl (3,5-dimethoxy benzyl) phosphate (2.61f) (major *P*-diastereomer)

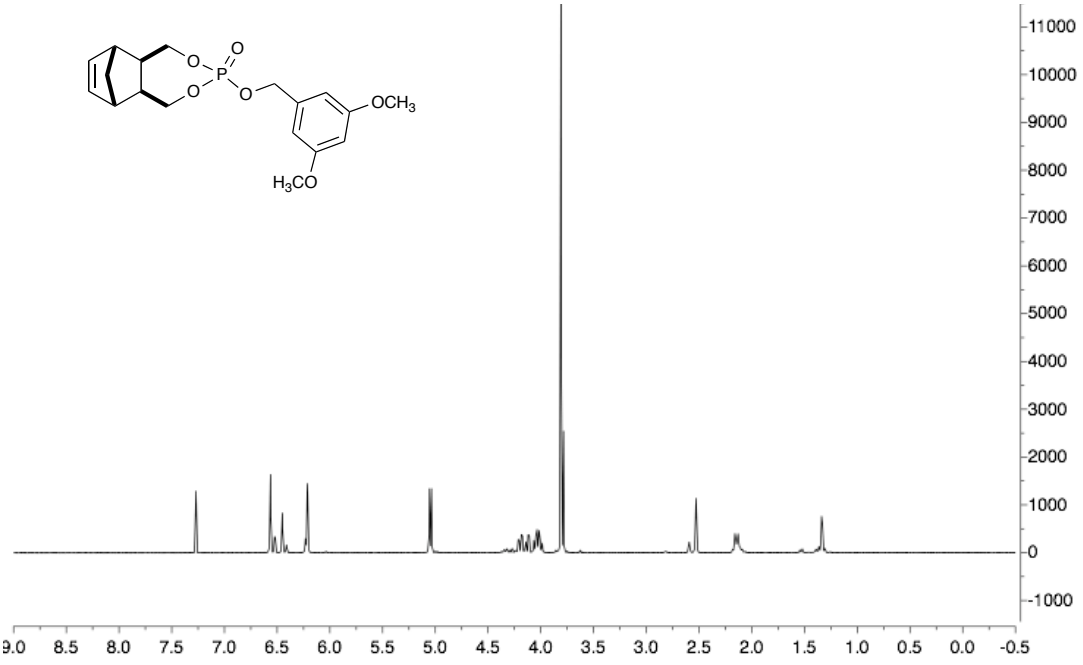

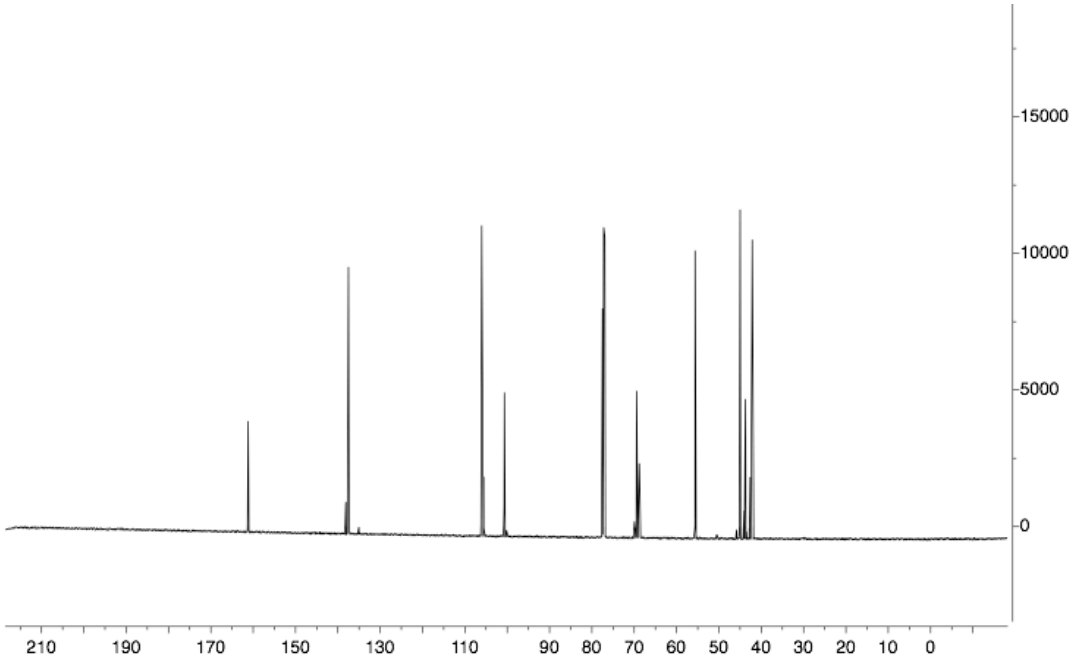
15000
10000
5000
0
210
190
170
150
130
110
90
80
70
60
50
40
30
20
10
0

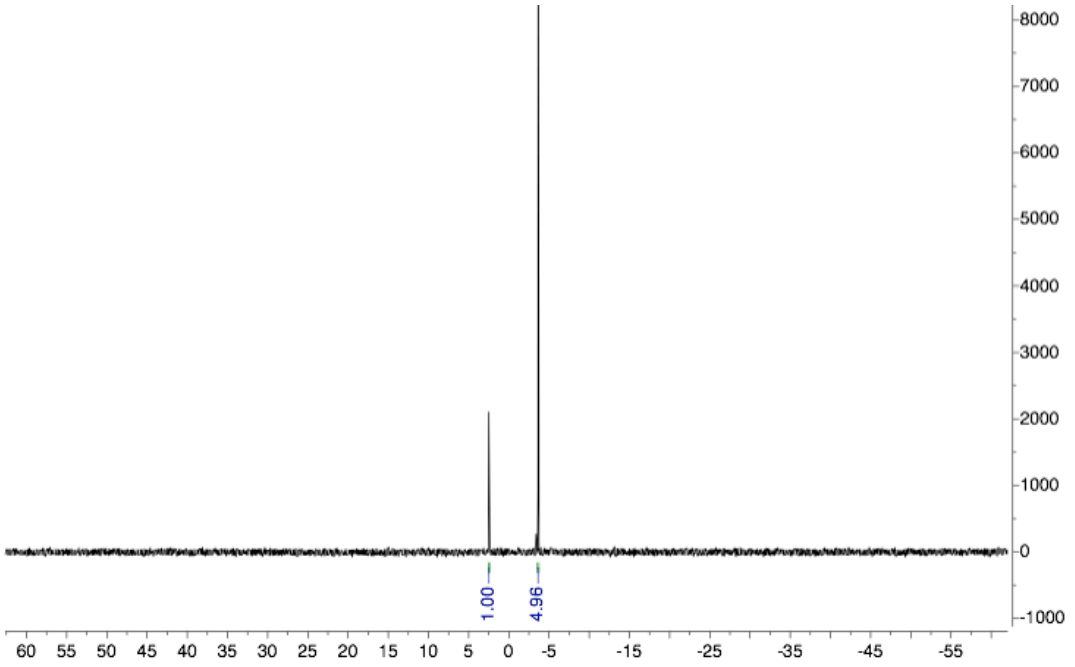
8000
7000
6000
5000
4000
3000
2000
1000
0
-1000
1.00
4.96
60
55
50
45
40
35
30
25
20
15
10
5
0
-5
-15
-25
-35
-45
-55

5-norbornene-2-*exo*, 3-*exo*-dimethyl (4-bromo-benzyl) phosphate (2.61g) (major *P*-diastereomer)

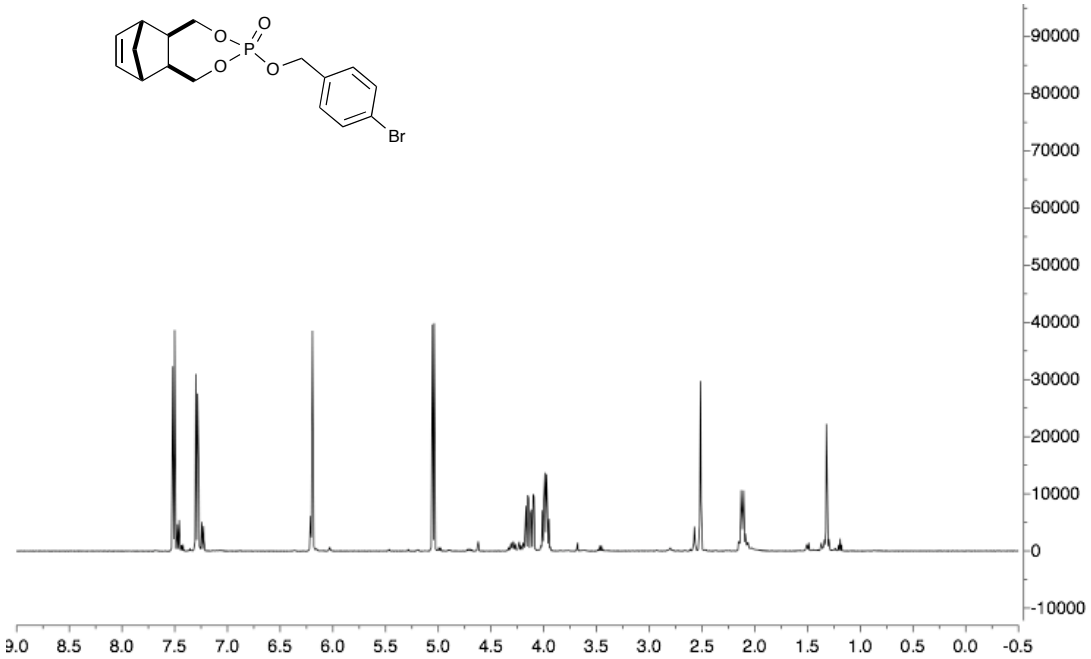

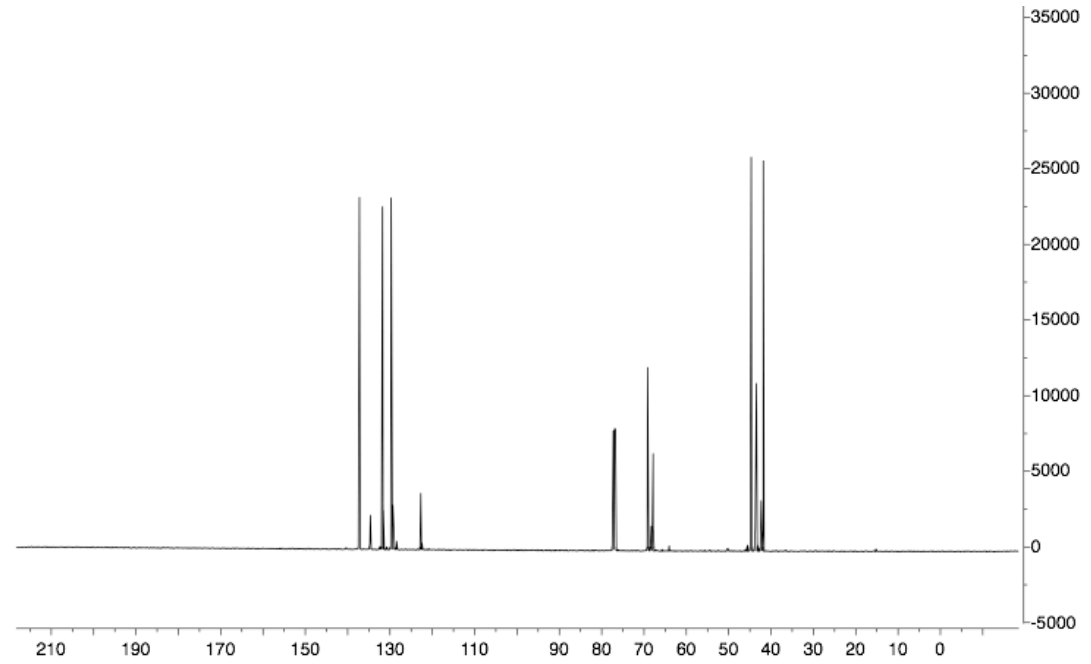

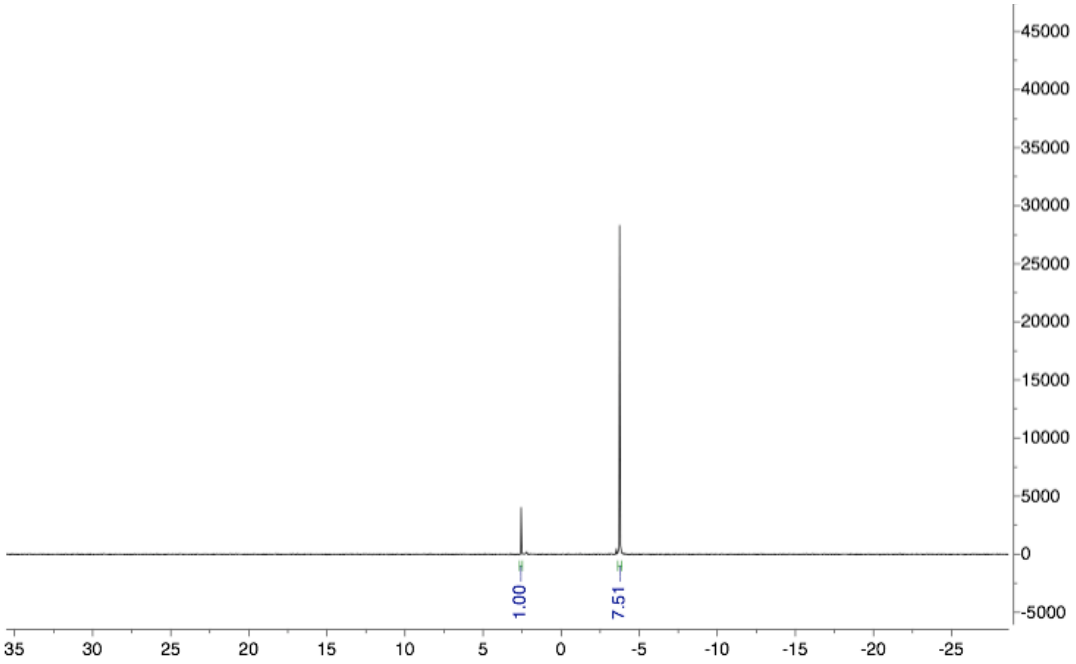

5-norbornene-2-*exo*, 3-*exo*-dimethyl (4-chloro-benzyl) phosphate (2.61h) (major *P*-diastereomer)

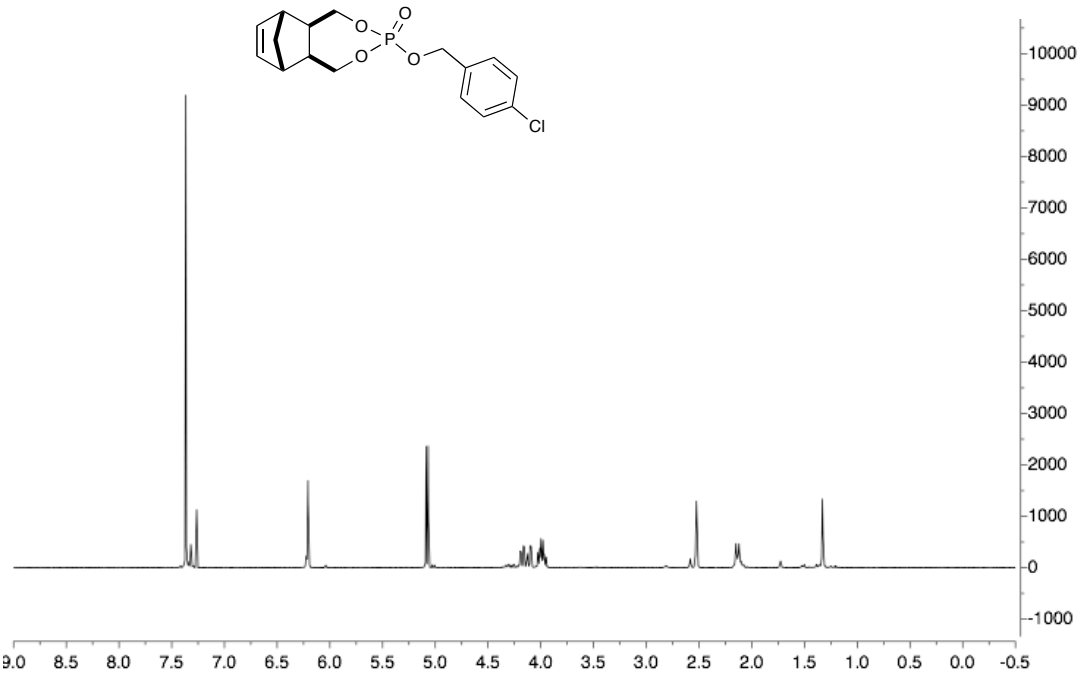

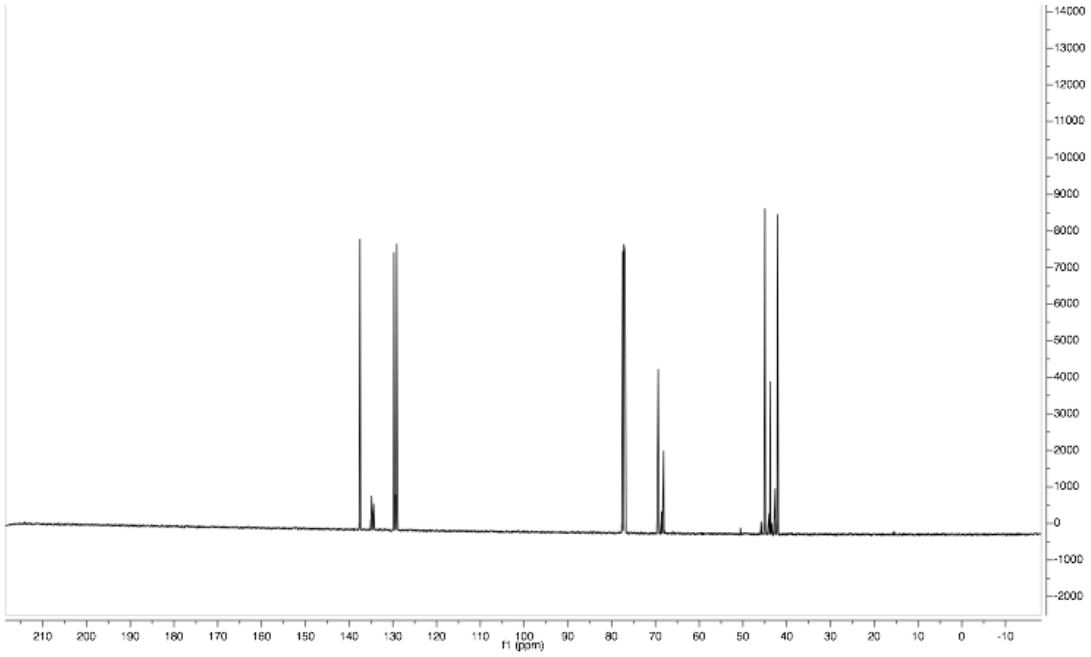
f1 (ppm)

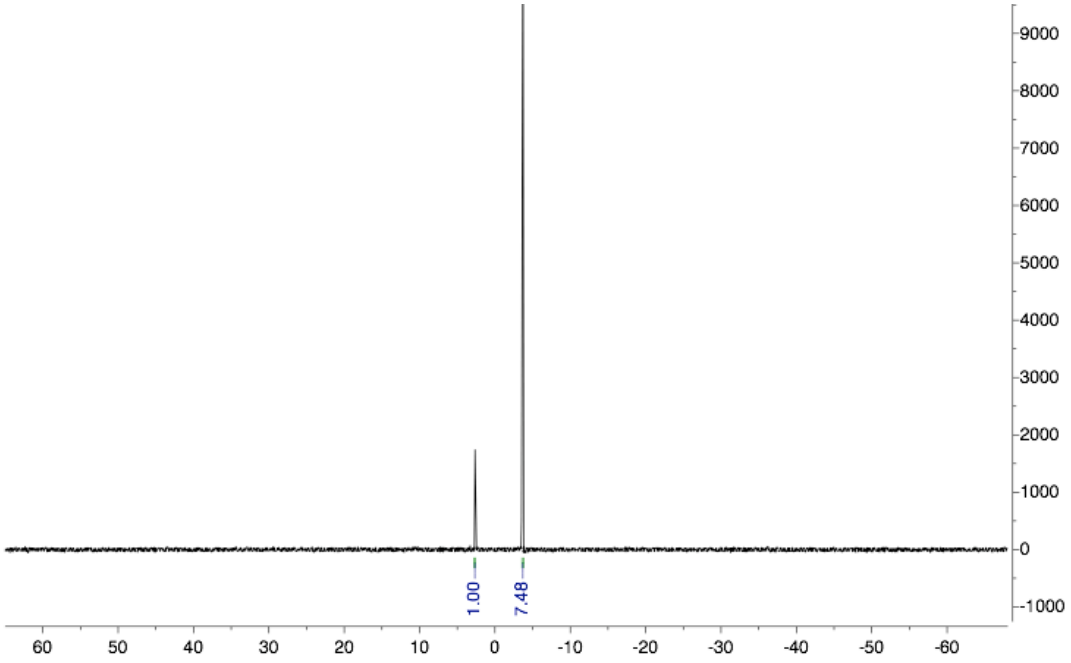
1.00
7.48

5-norbornene-2-*exo*, 3-*exo*-dimethyl (4-fluoro-benzyl) phosphate (2.61i) (major *P*-diastereomer)

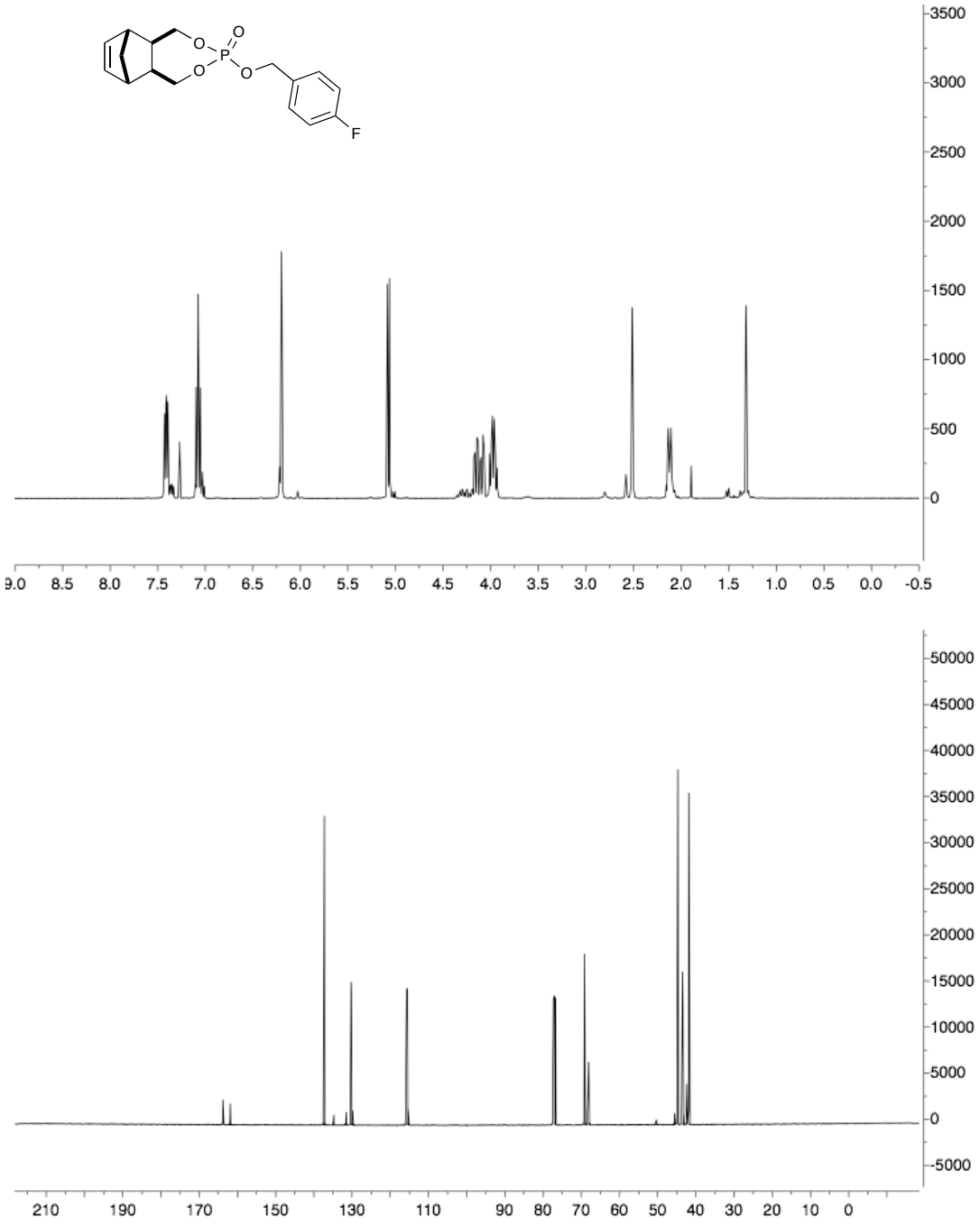

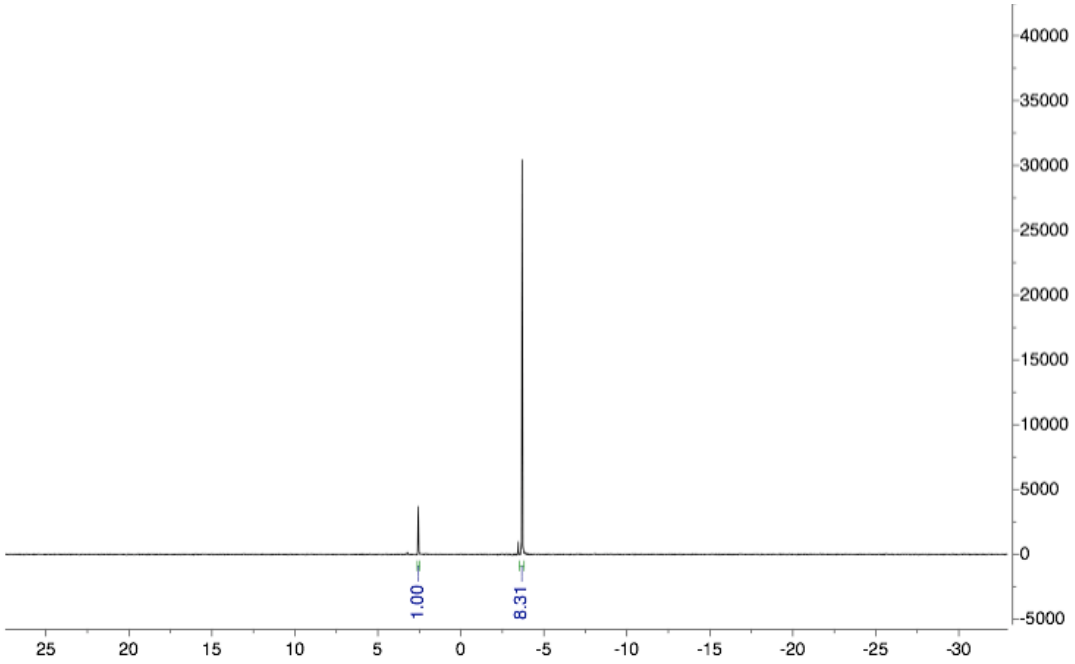

5-norbornene-2-*exo*, 3-*exo*-dimethyl (4-nitro-benzyl) phosphate (2.61j) (major *P*-diastereomer)

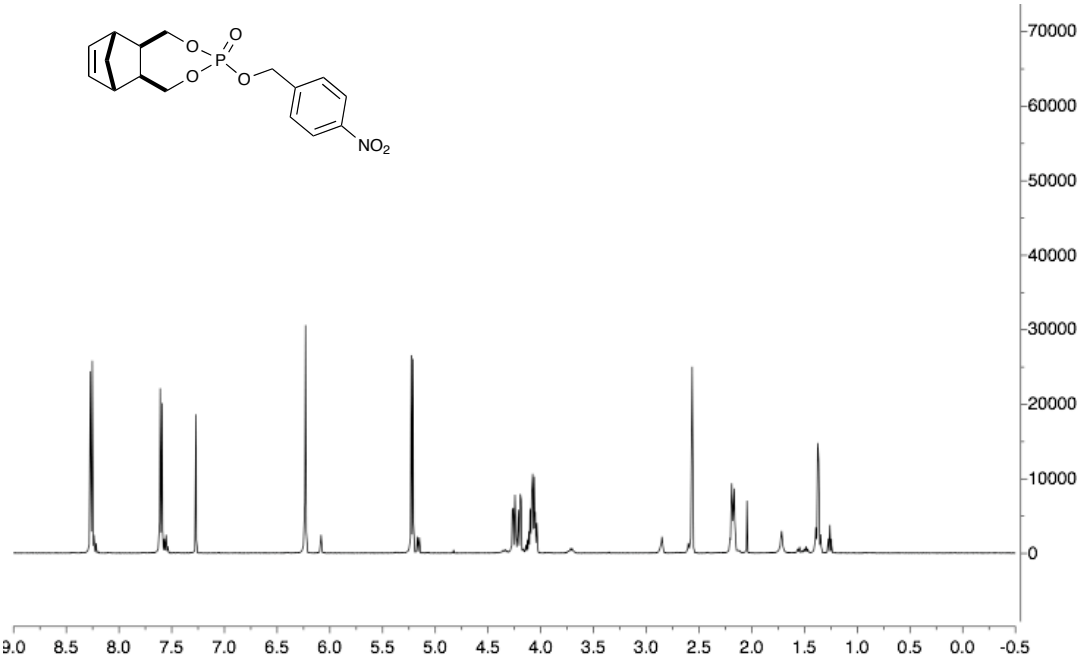

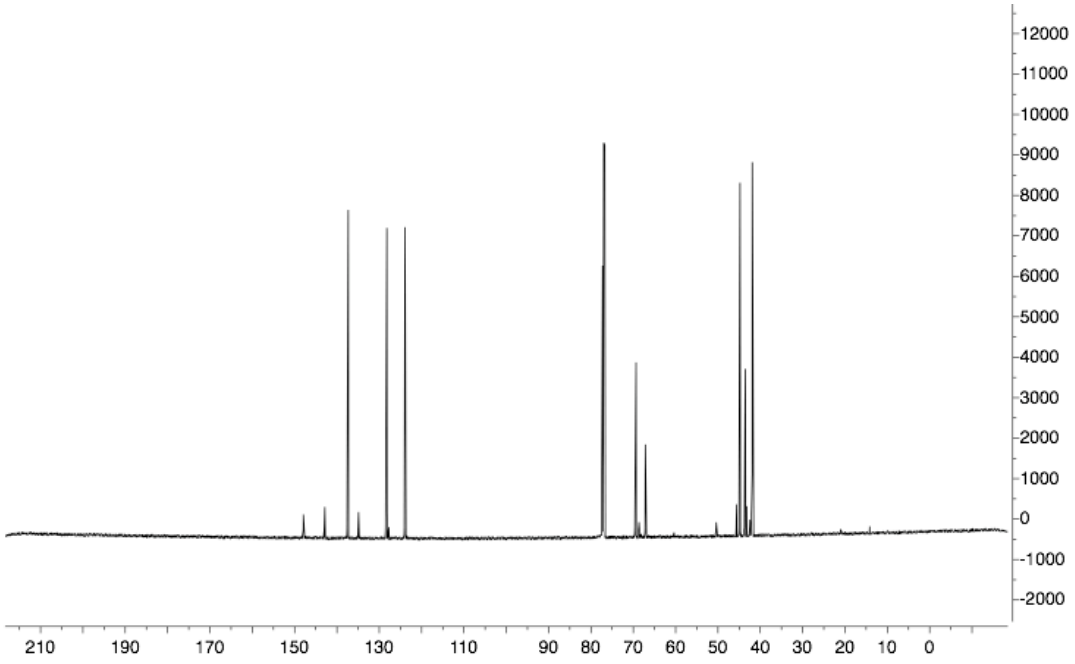
12000
11000
10000
9000
8000
7000
6000
5000
4000
3000
2000
1000
0
-1000
-2000
210
190
170
150
130
110
90
80
70
60
50
40
30
20
10
0

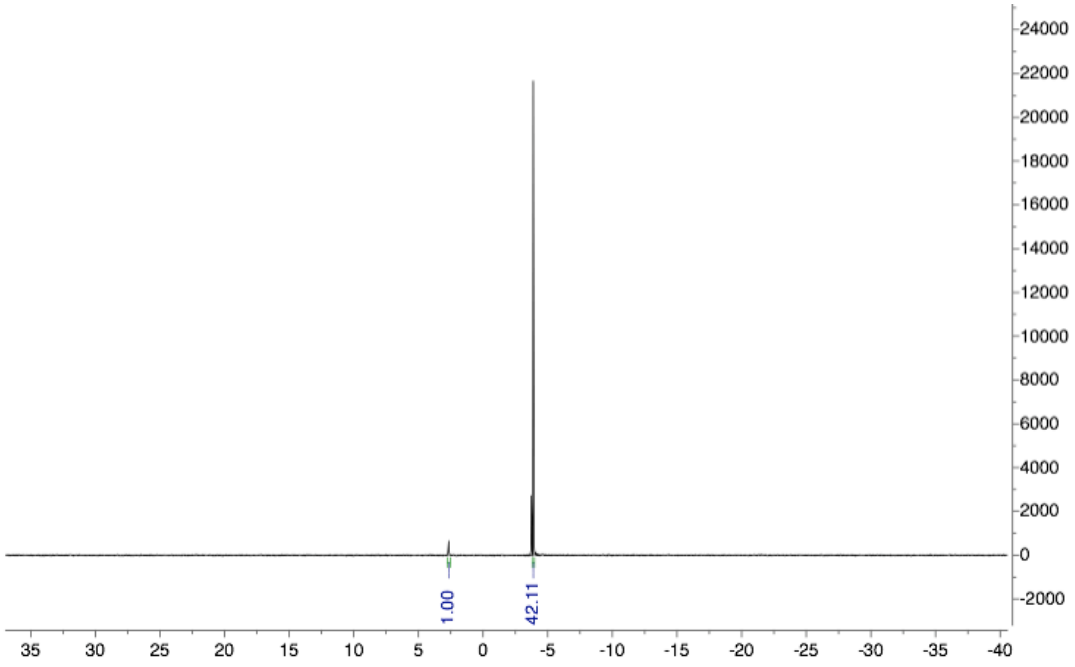
24000
22000
20000
18000
16000
14000
12000
10000
8000
6000
4000
2000
0
-2000
1.00
42.11
35
30
25
20
15
10
5
0
-5
-10
-15
-20
-25
-30
-35
-40

5-norbornene-2-*exo*, 3-*exo*-dimethyl (3-dimethylamino benzyl) phosphate (2.61k) (major *P*-diastereomer)

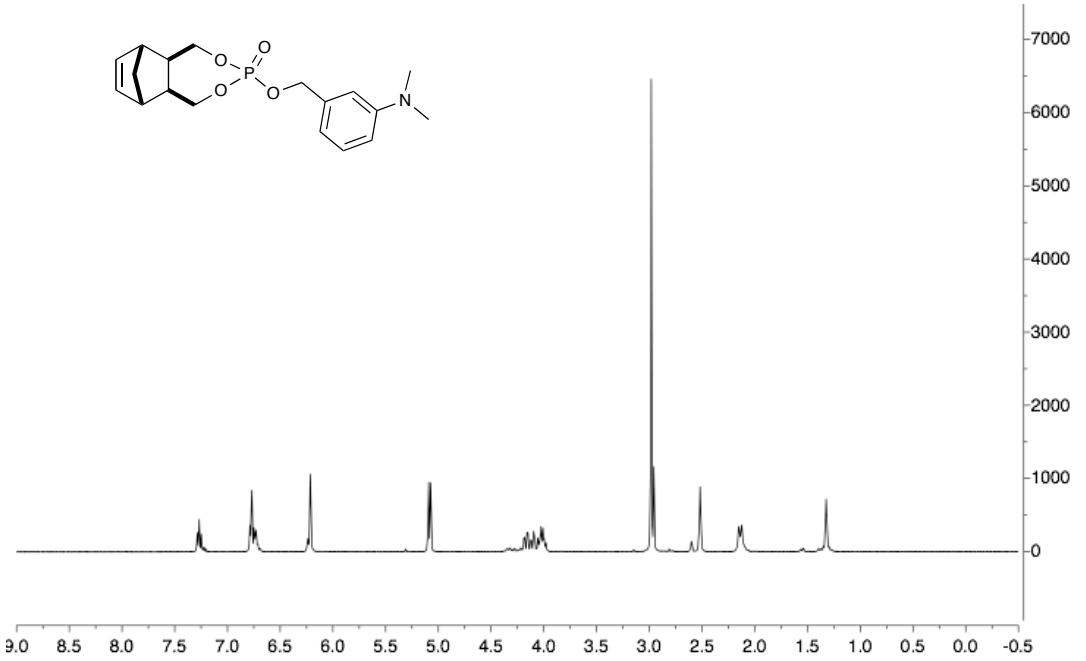

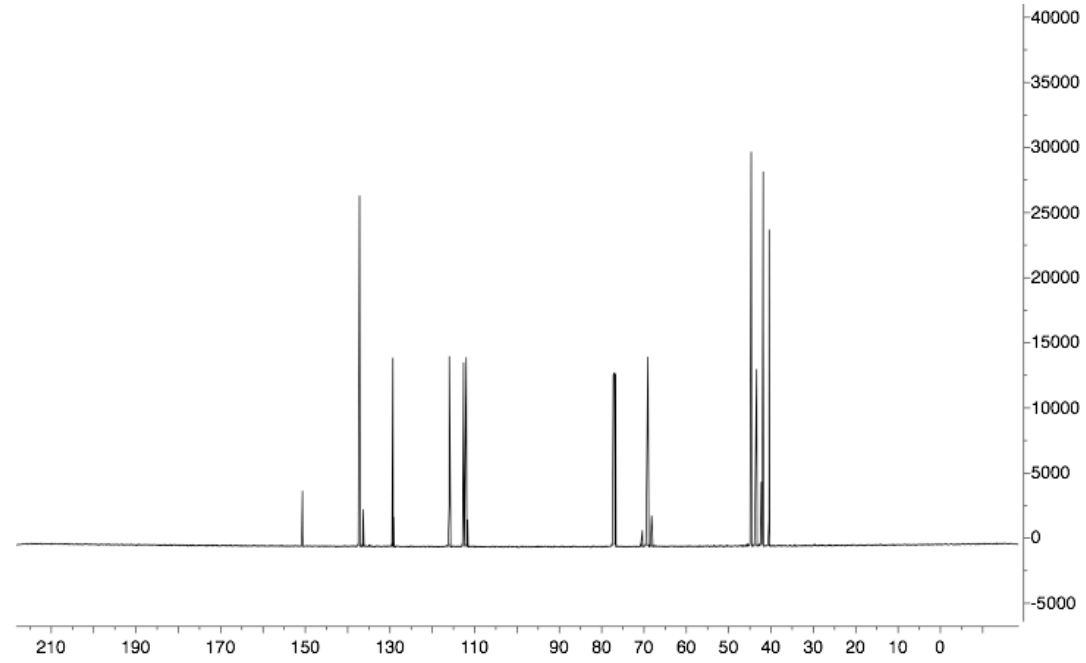

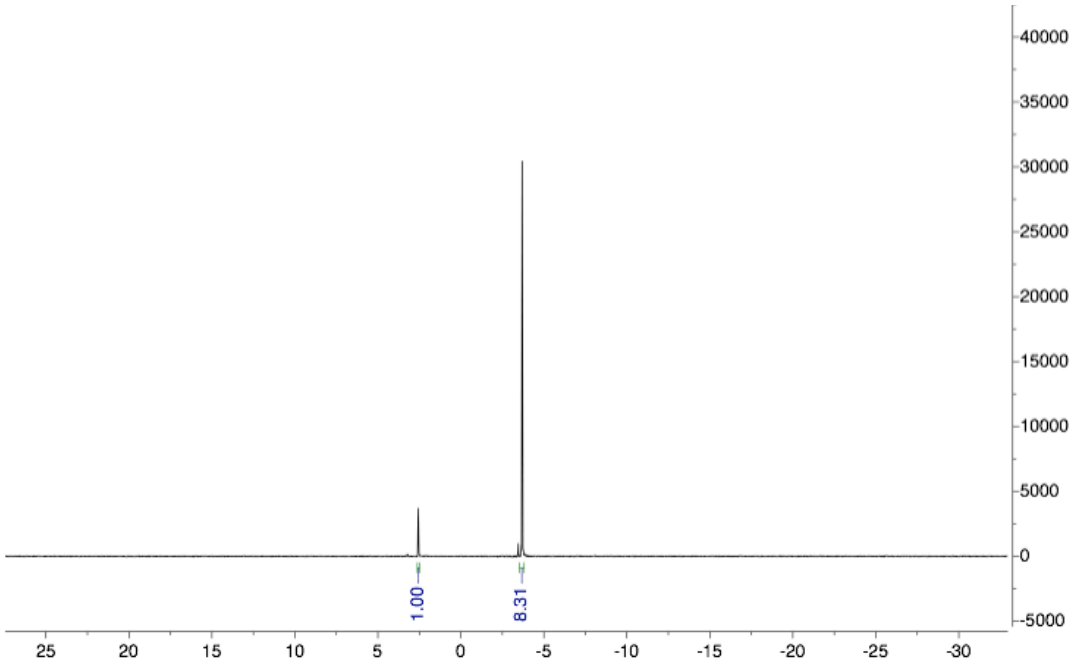

5-norbornene-2-*exo*, 3-*exo*-dimethyl (3-trifluoromethylbenzyl) phosphate (2.61l) (*P*-diastereomer)

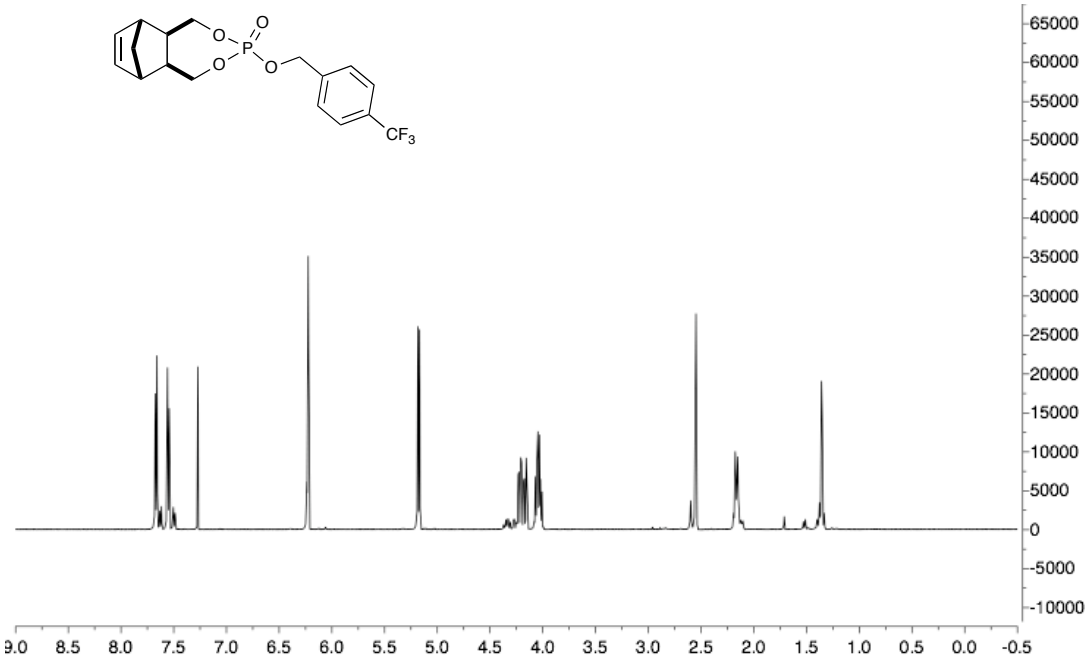

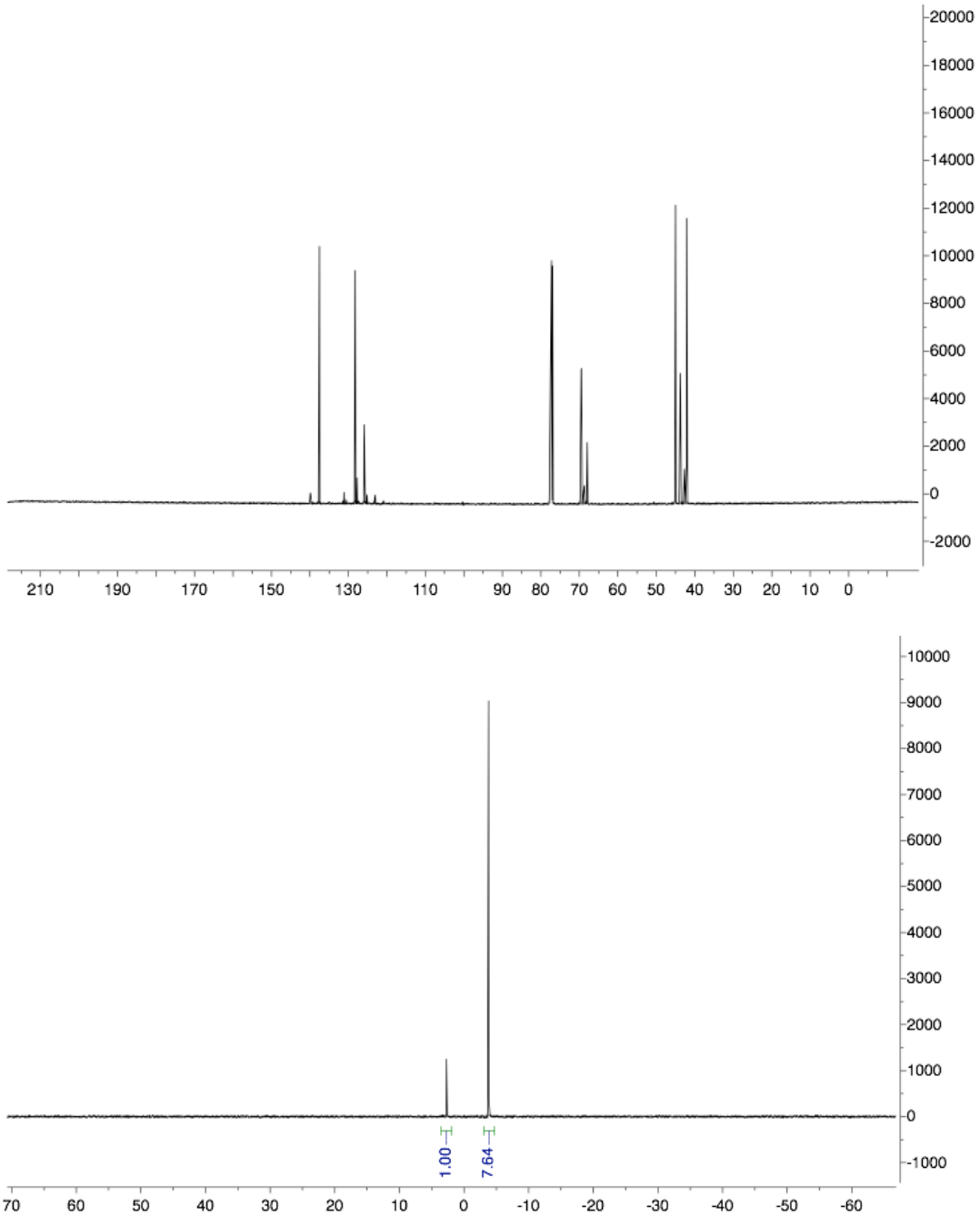
20000
18000
16000
14000
12000
10000
8000
6000
4000
2000
0
-2000
210
190
170
150
130
110
90
80
70
60
50
40
30
20
10
0
10000
9000
8000
7000
6000
5000
4000
3000
2000
1000
0
-1000
1.00
7.64
70
60
50
40
30
20
10
0
-10
-20
-30
-40
-50
-60

***N*,*N*-dimethyl-3-(morpholinomethyl)aniline (2.64k)**

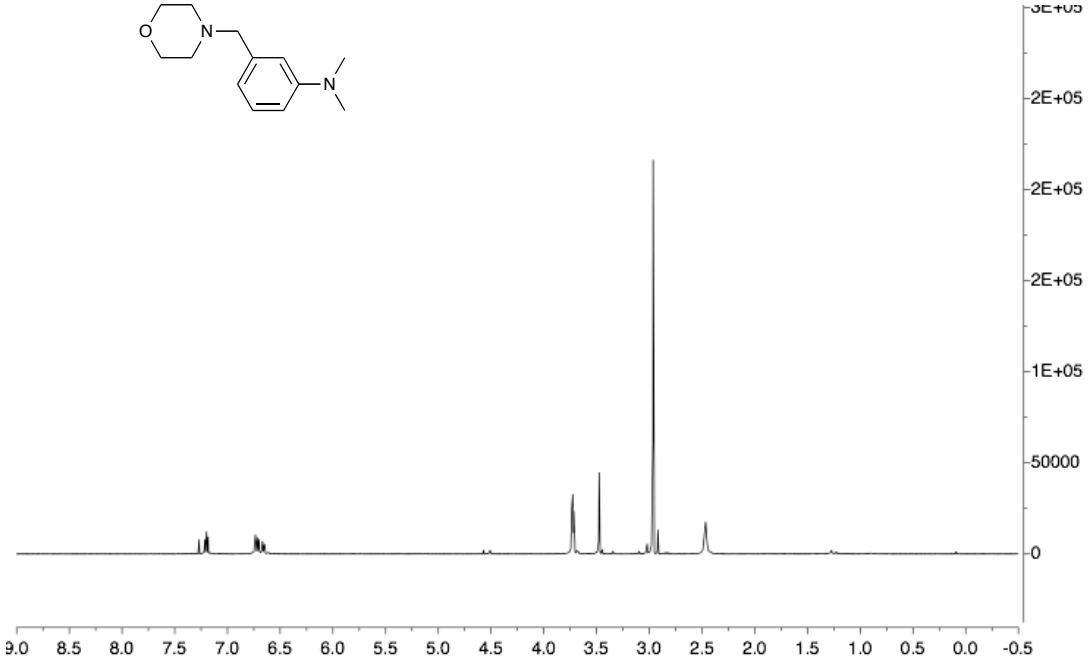

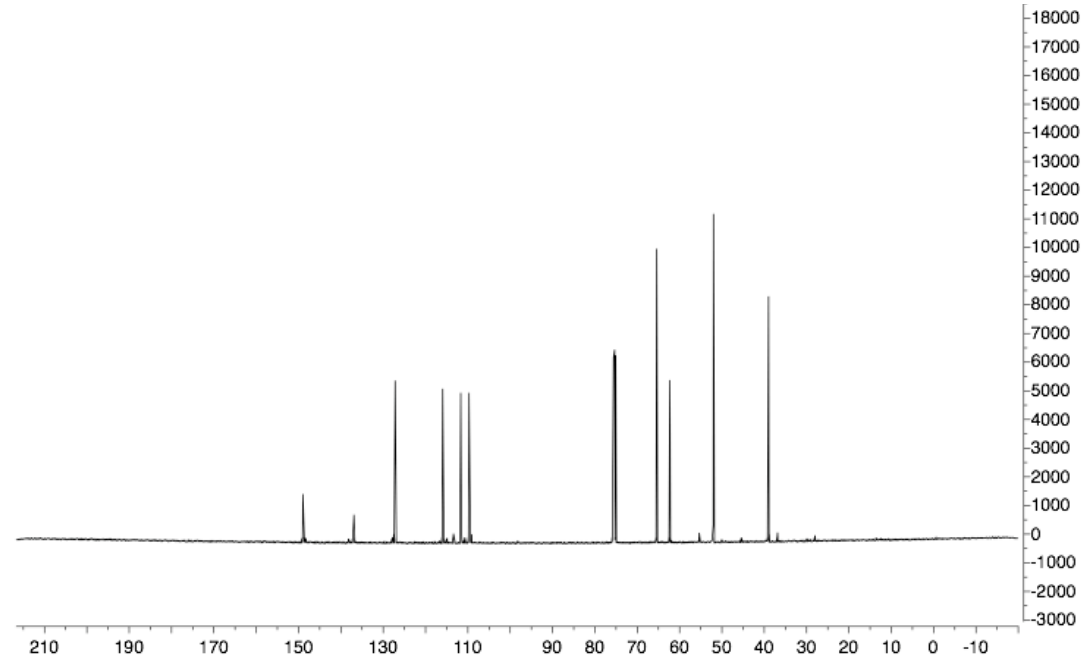

***N*,*N*-dimethyl-3-((4-phenylpiperazin-1-yl)methyl)aniline (2.64k′)**

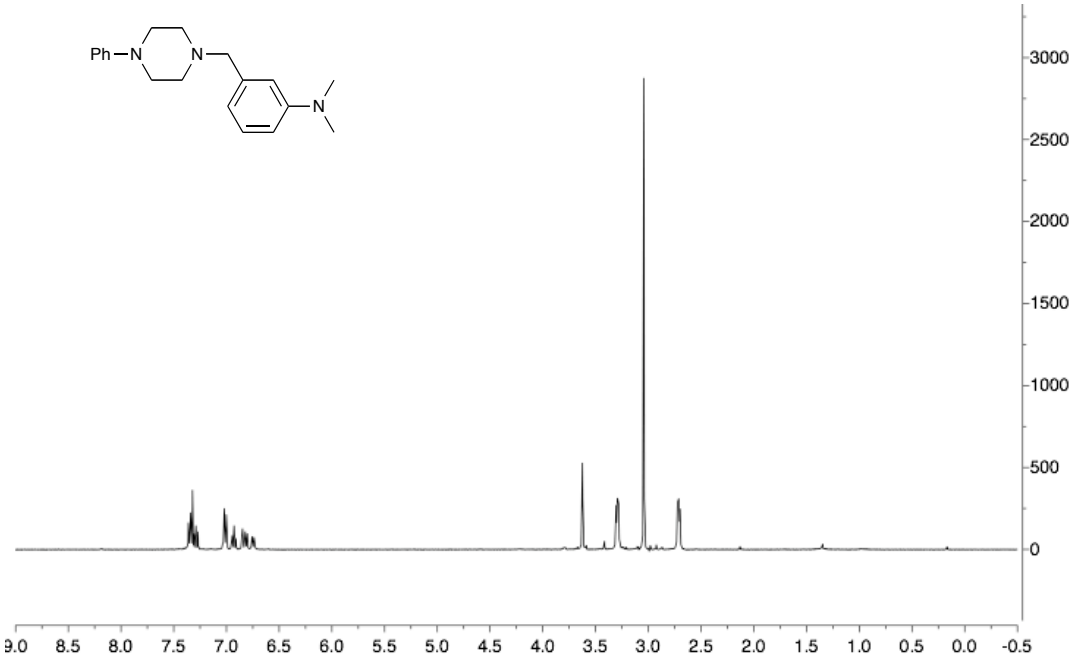

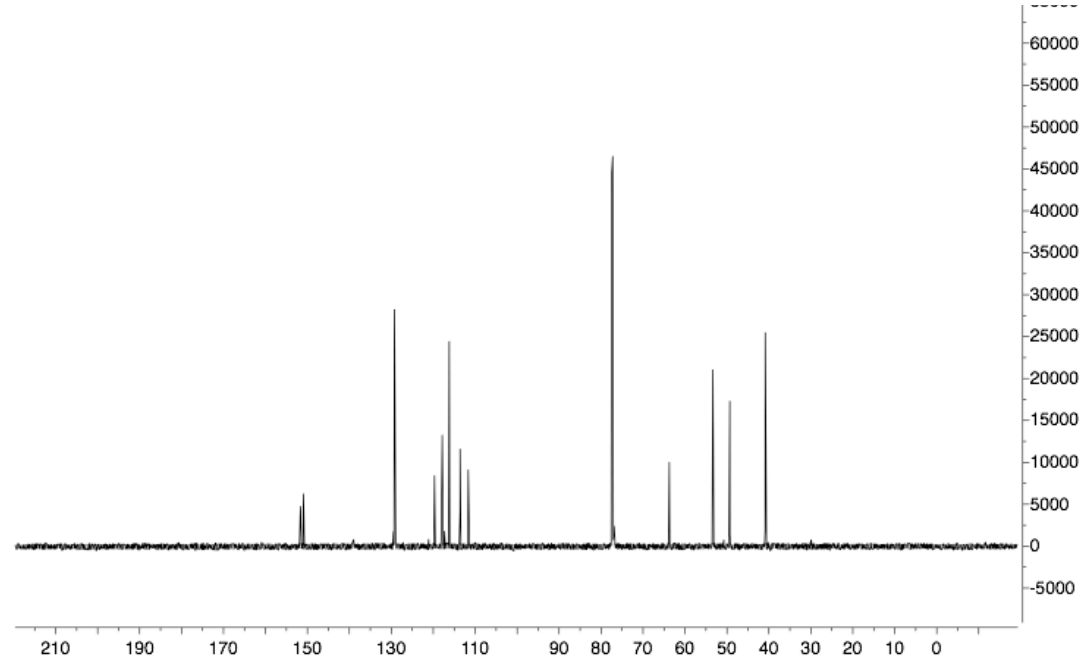

(*S*)-2-benzyl-7-bromo-3-phenyl-3,4-dihydro-2H-benzo[b][1,4,5]oxathiazepine 1,1-dioxide (2.66a)

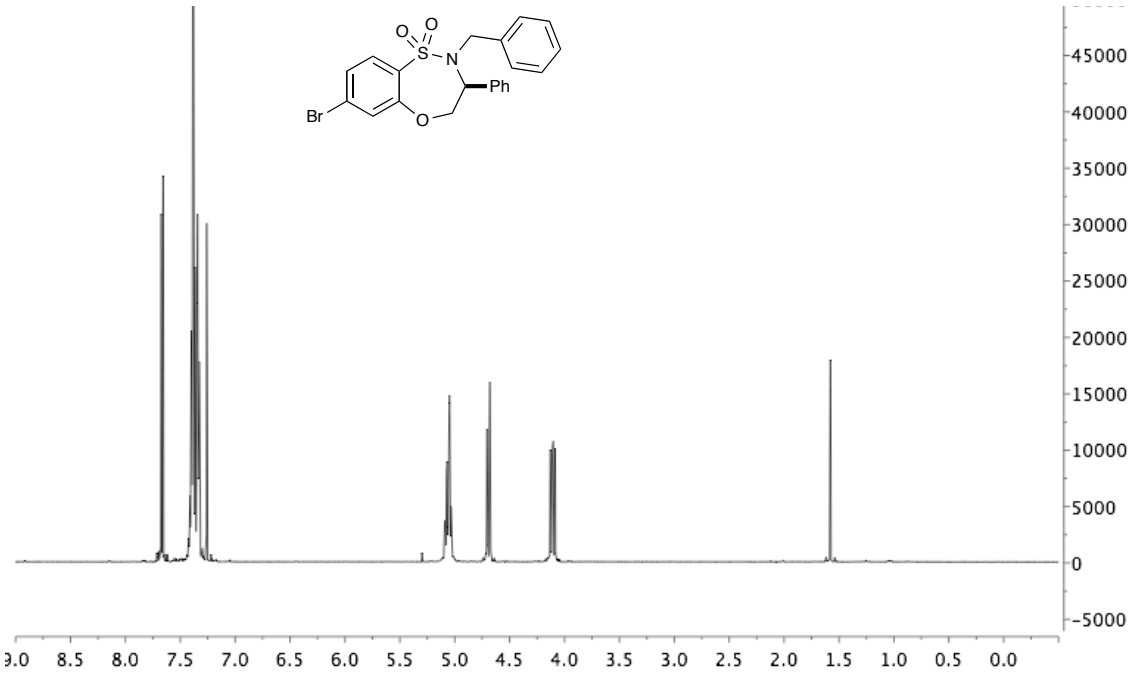

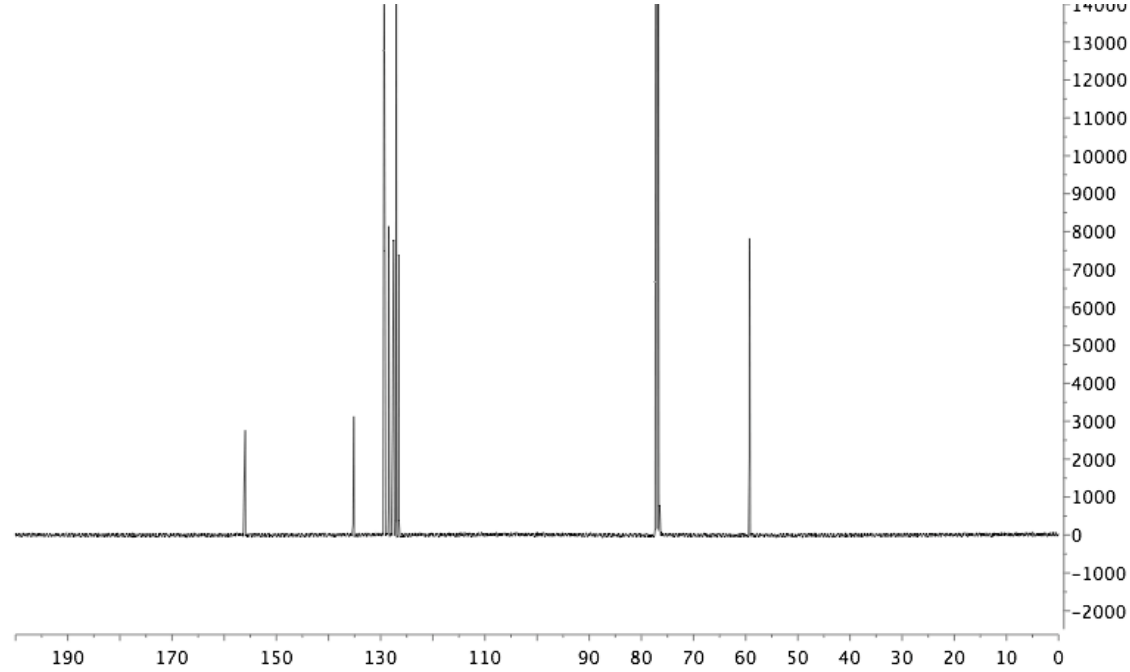

(*S*)-7-bromo-2-(3,5-dimethoxybenzyl)-3-phenyl-3,4-dihydro-2*H* benzo[*b*] [1,4,5]oxathiazepine 1,1-dioxide (2.66b)

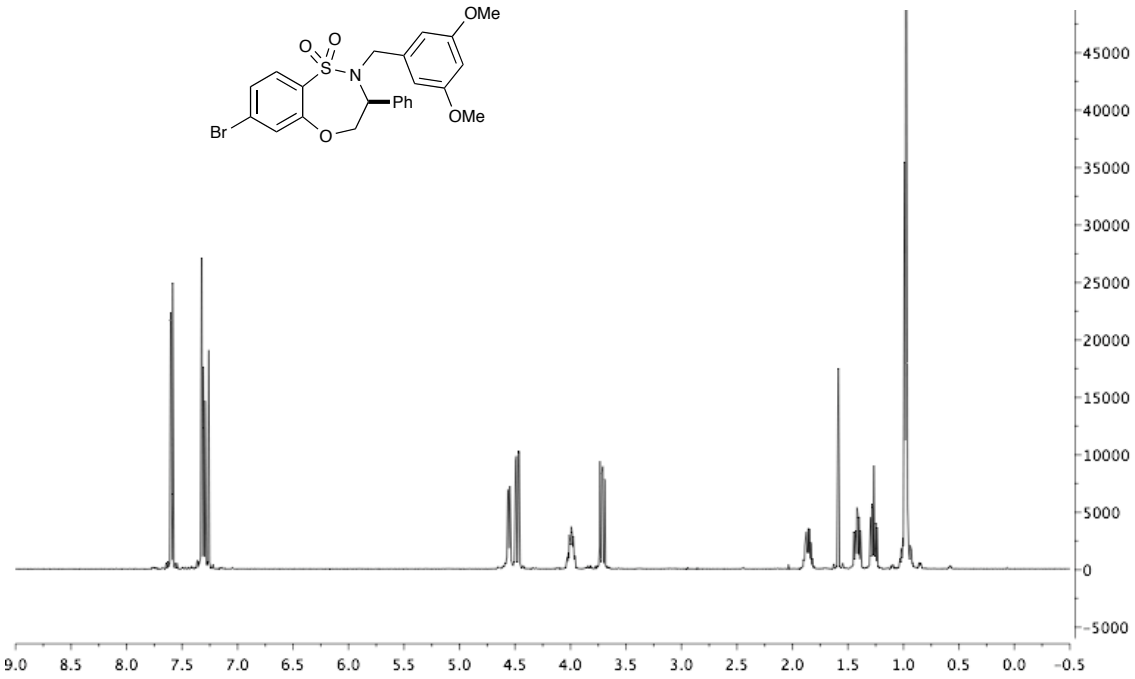

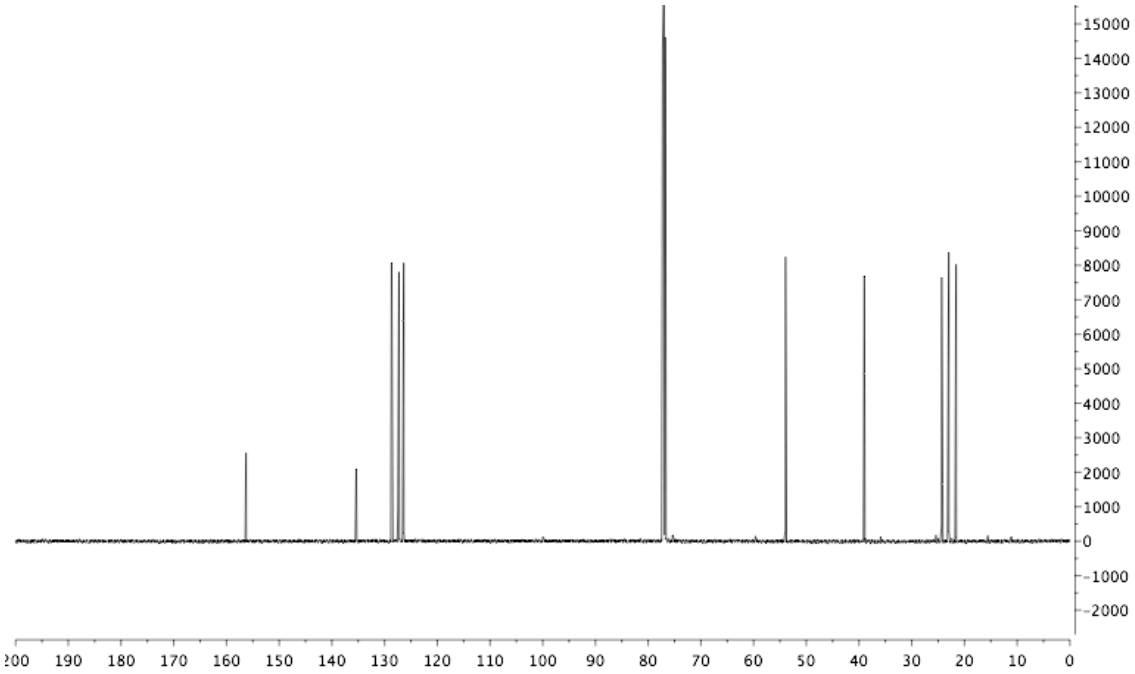

(*S*)-7-bromo-2-(4-fluorobenzyl)-3-phenyl-3,4-dihydro-2H-benzo[b][1,4,5] oxa thiazepine 1,1-dioxide (2.66c)

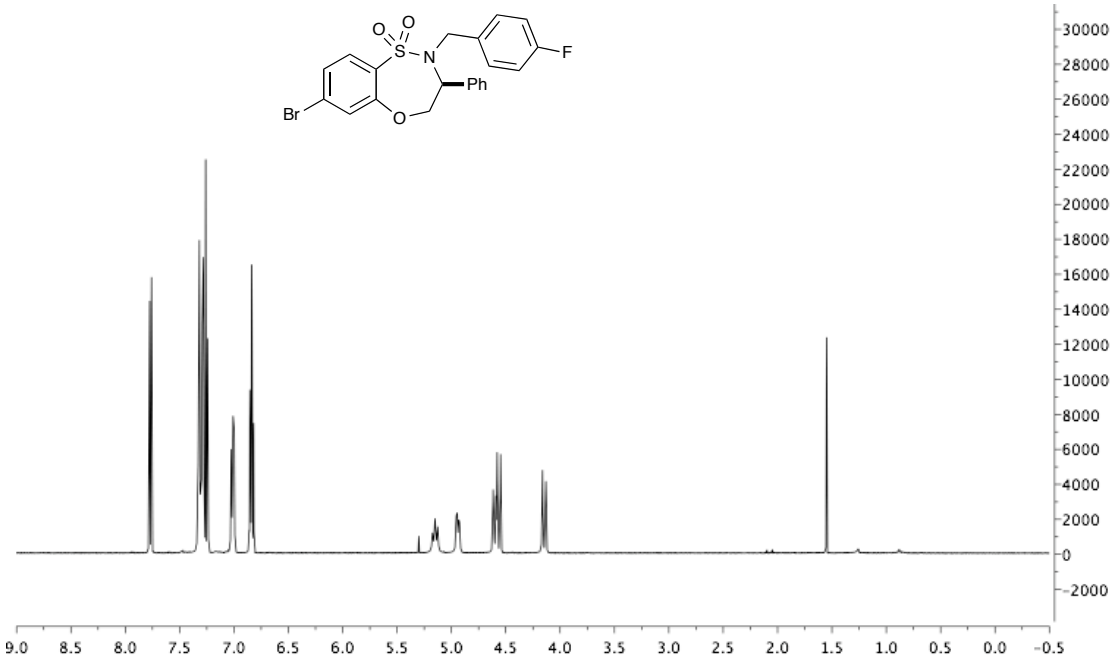

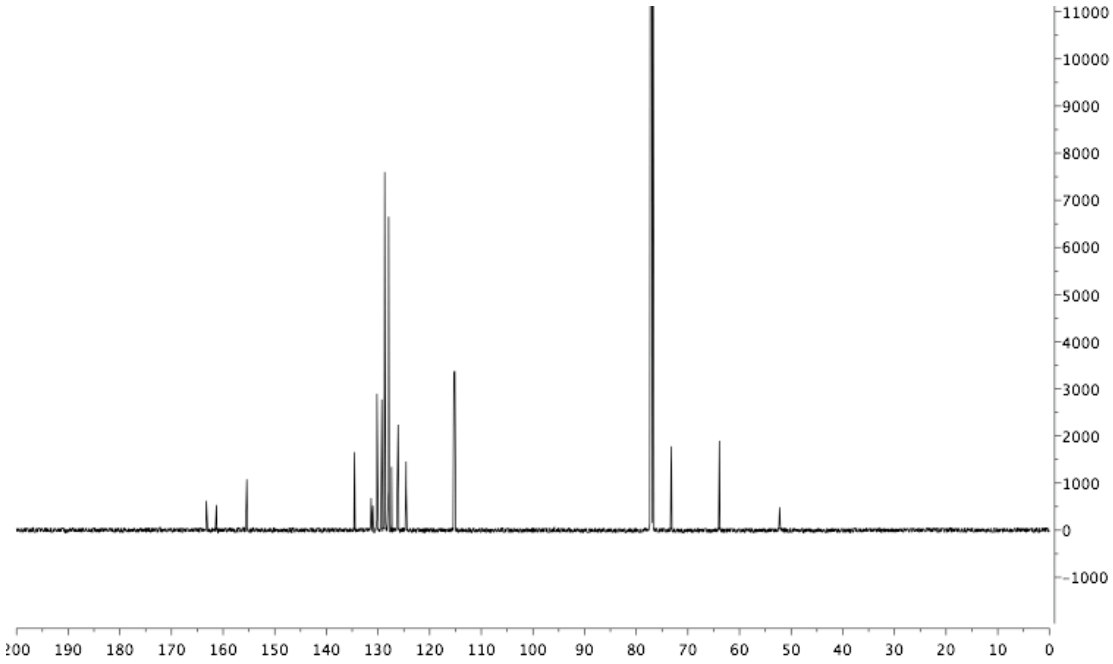

(*S*)-7-bromo-2-(4-fluorobenzyl)-3-isobutyl-3,4-dihydro-2H-benzo[b][1,4,5] oxathiazepine 1,1-dioxide (2.66d)

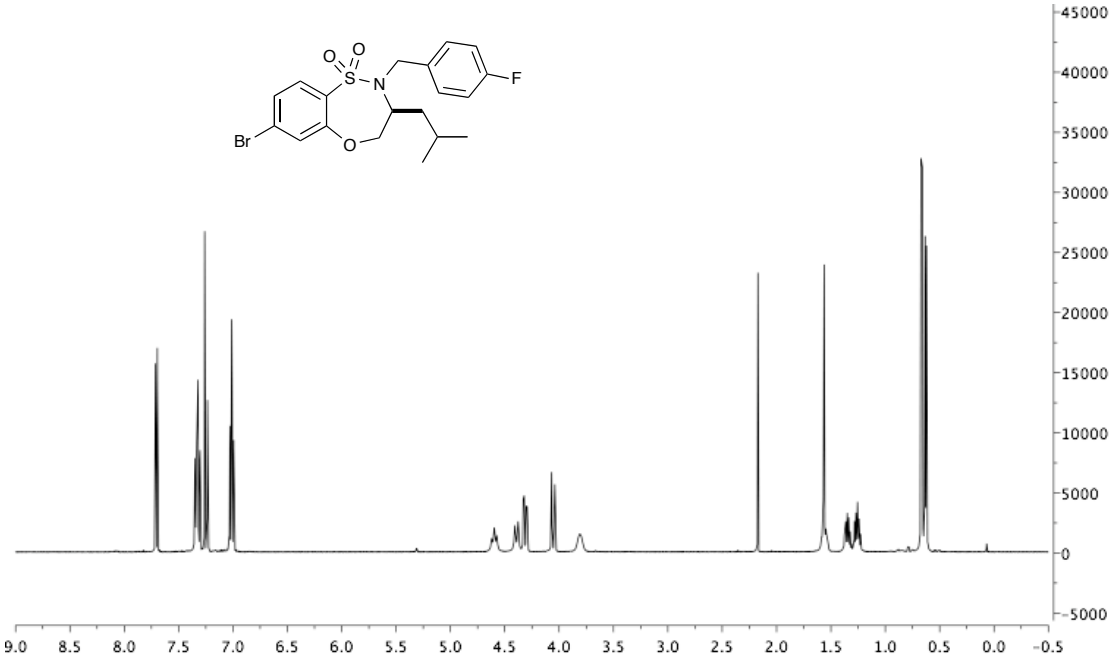

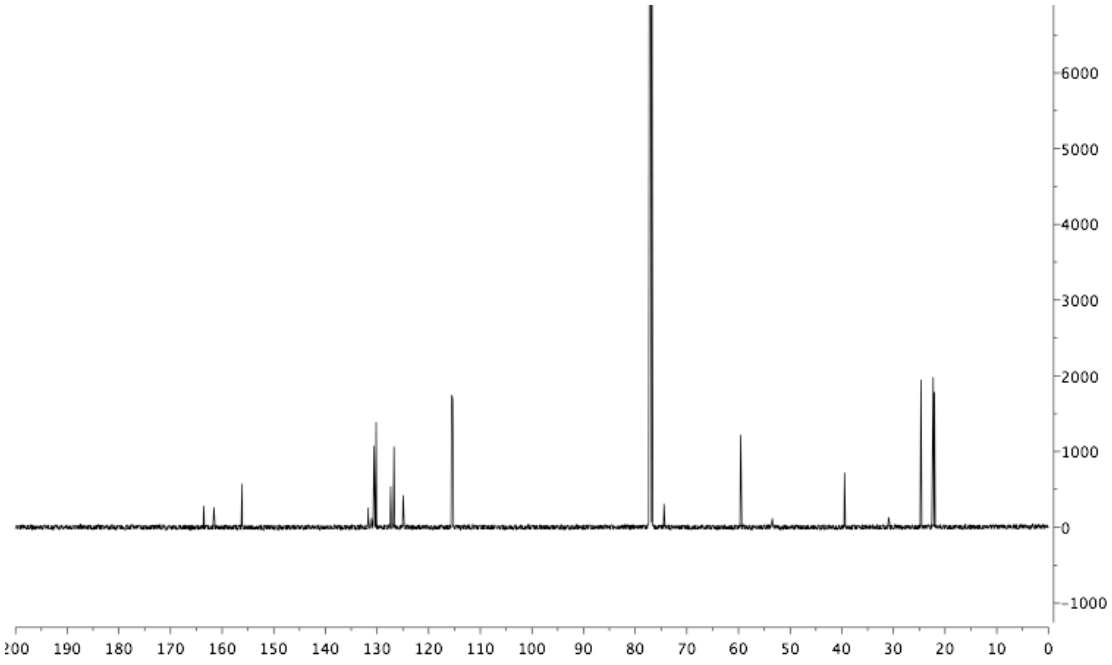

(±) tert-butyl-3,6,7,7a-tetrahydro-2H-3a,6-epoxybenzo[d] isothiazole-2-carboxylate 1,1-dioxide (3.15)

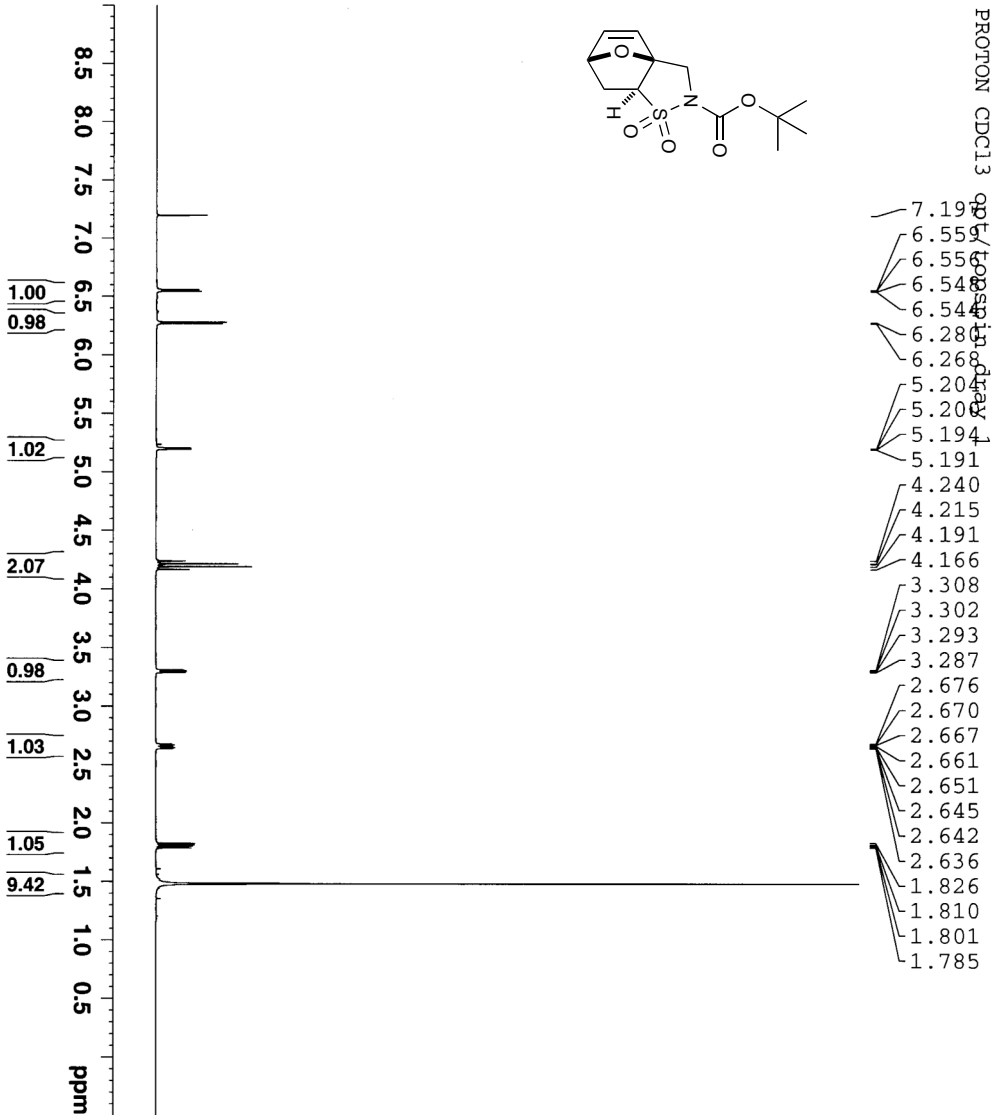

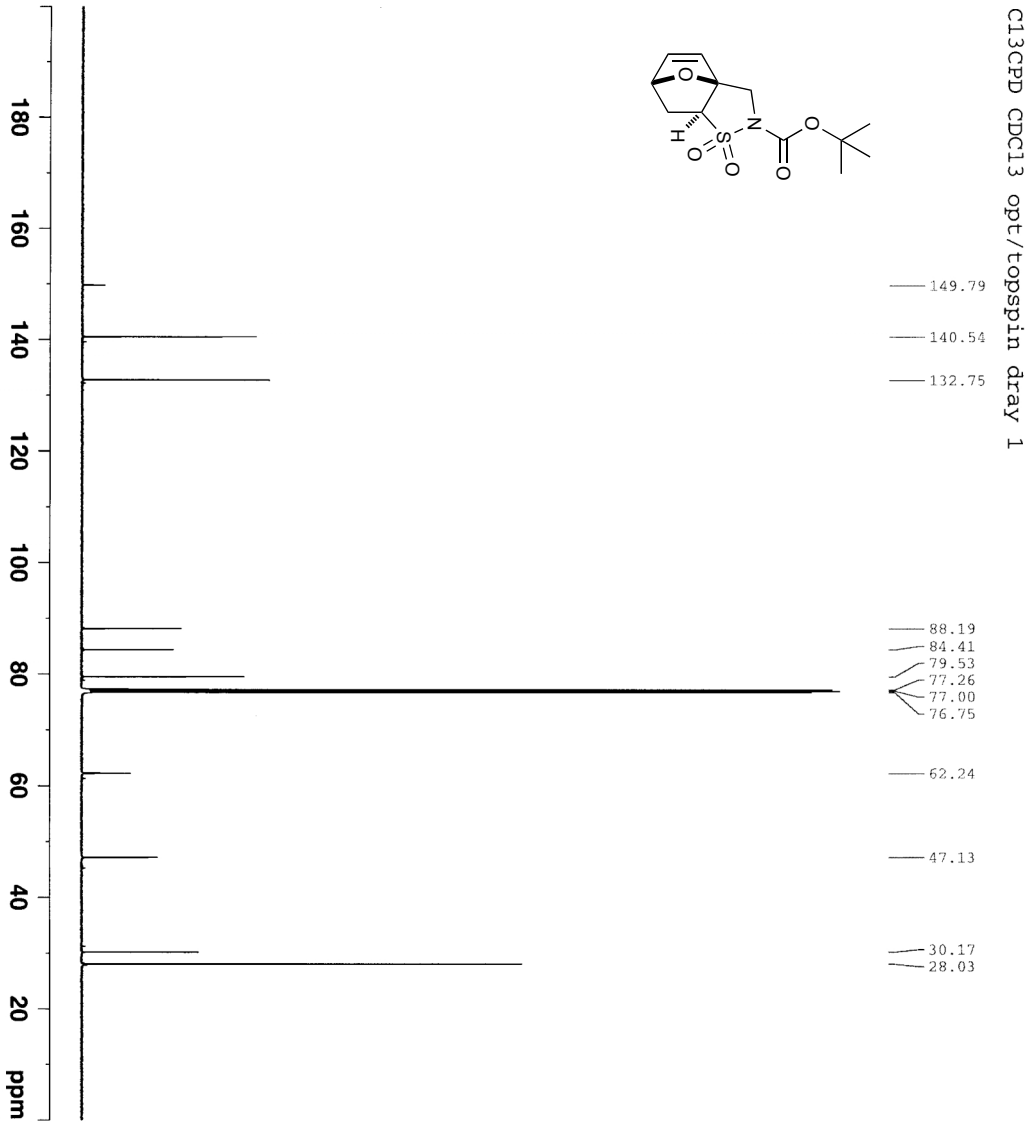
C13CPD CDCl3 opt/topspin dray 1
149.79
140.54
132.75
88.19
84.41
79.53
77.26
77.00
76.75
62.24
47.13
30.17
28.03
180
160
140
120
100
80
60
40
20
ppm

(±) tert-butyl-5-(4-acetylphenyl)hexahydro-2H-3a,6-epoxybenzo[d]isothiazole-2-carboxylate 1,1-dioxide (3.16a)

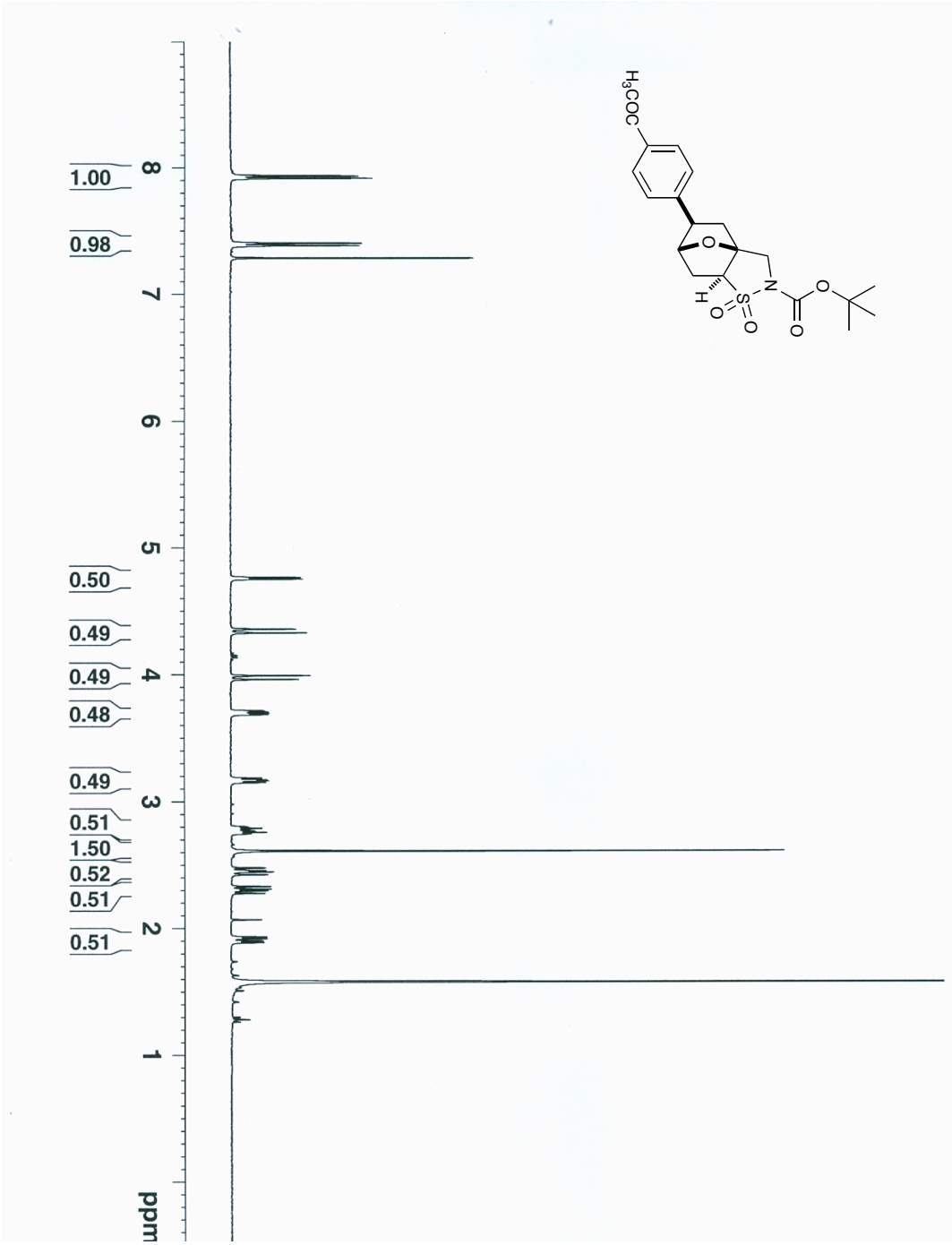

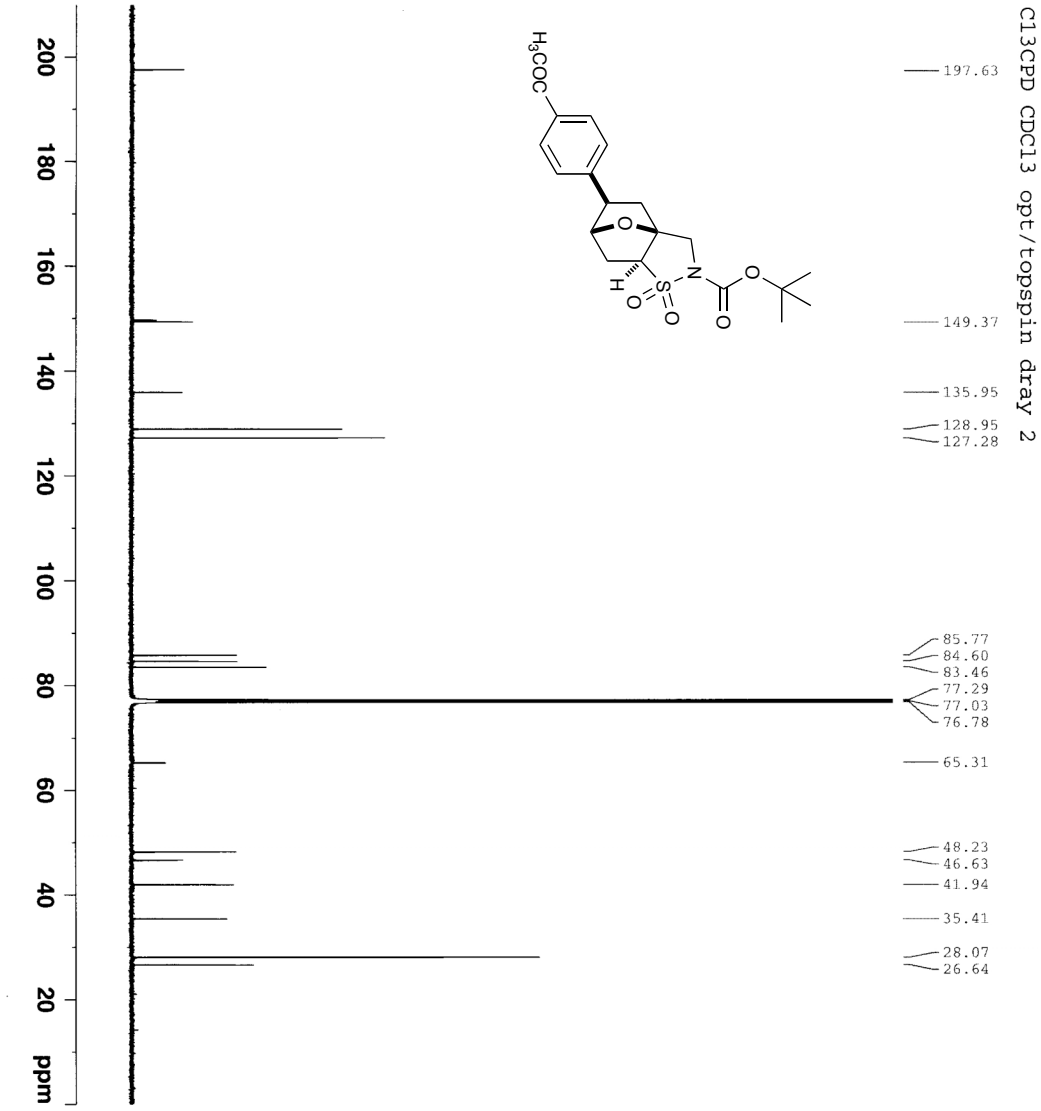
C13CPD CDCl3 opt/topspin dray 2
197.63
149.37
135.95
128.95
127.28
85.77
84.60
83.46
77.29
77.03
76.78
65.31
48.23
46.63
41.94
35.41
28.07
26.64
200
180
160
140
120
100
80
60
40
20
ppm

(±) tert-butyl-5-(4-acetylphenyl)hexahydro-2H-3a,6-epoxybenzo[d]isothiazole-2-carboxylate 1,1-dioxide (3.16b)

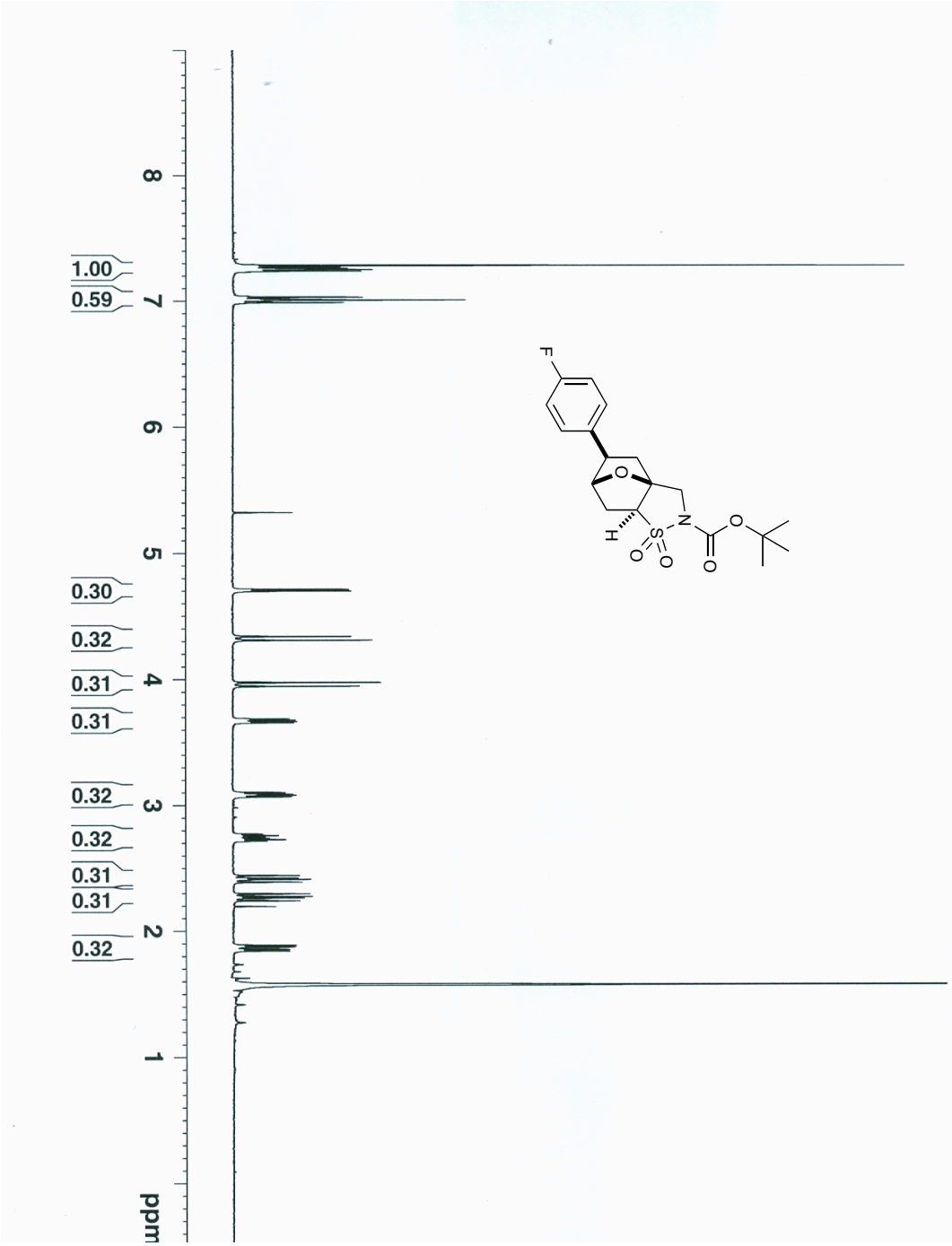

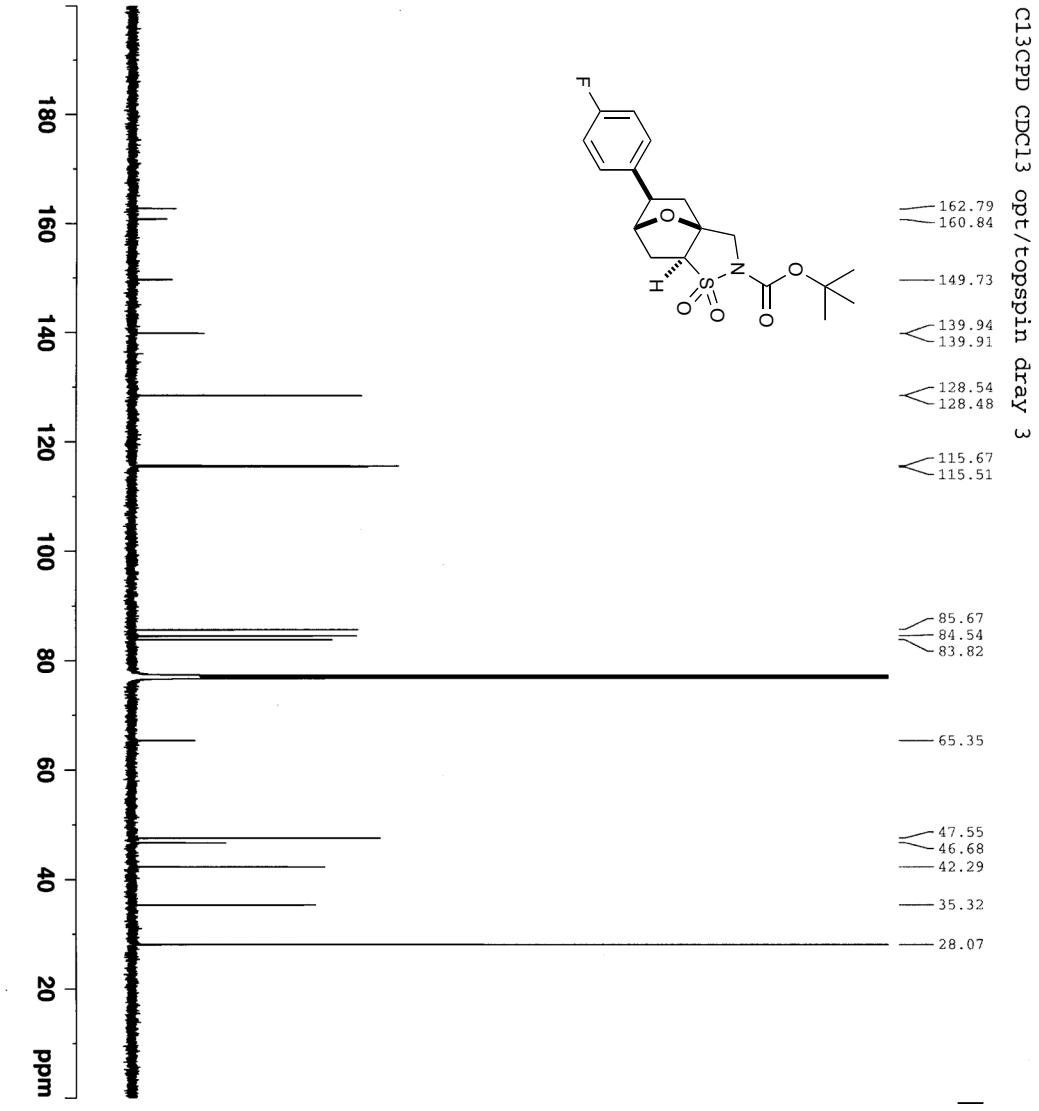
C13CPD CDCl3 opt/topspin dray 3
162.79
160.84
149.73
139.94
139.91
128.54
128.48
115.67
115.51
85.67
84.54
83.82
65.35
47.55
46.68
42.29
35.32
28.07
180
160
140
120
100
80
60
40
20
ppm

(±) tert-butyl 5-(4-(methoxycarbonyl)phenyl)hexahydro-2H-3a,6-epoxybenzo [d]isothiazole-2-carboxylate 1,1-dioxide (3.16c)

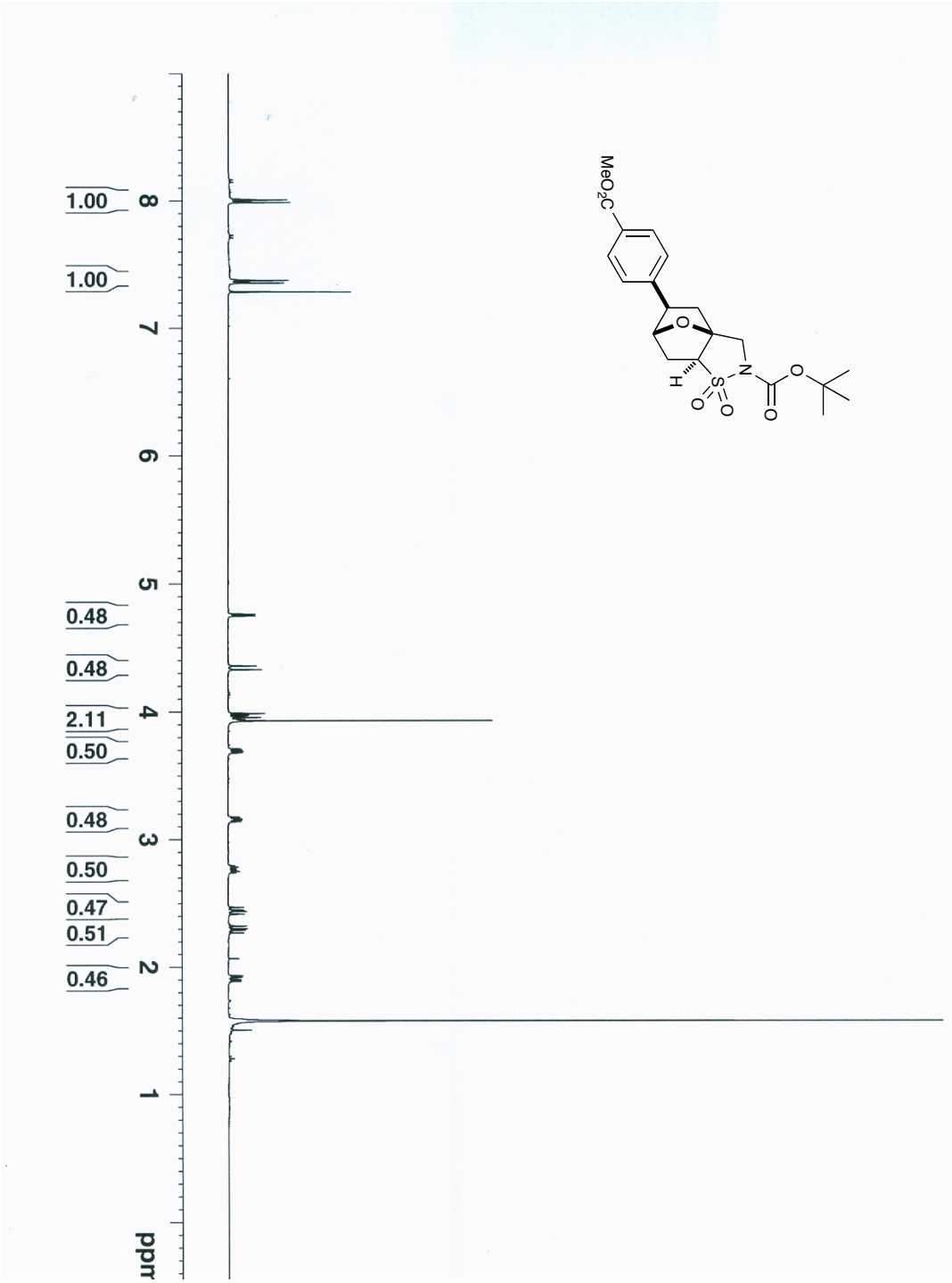

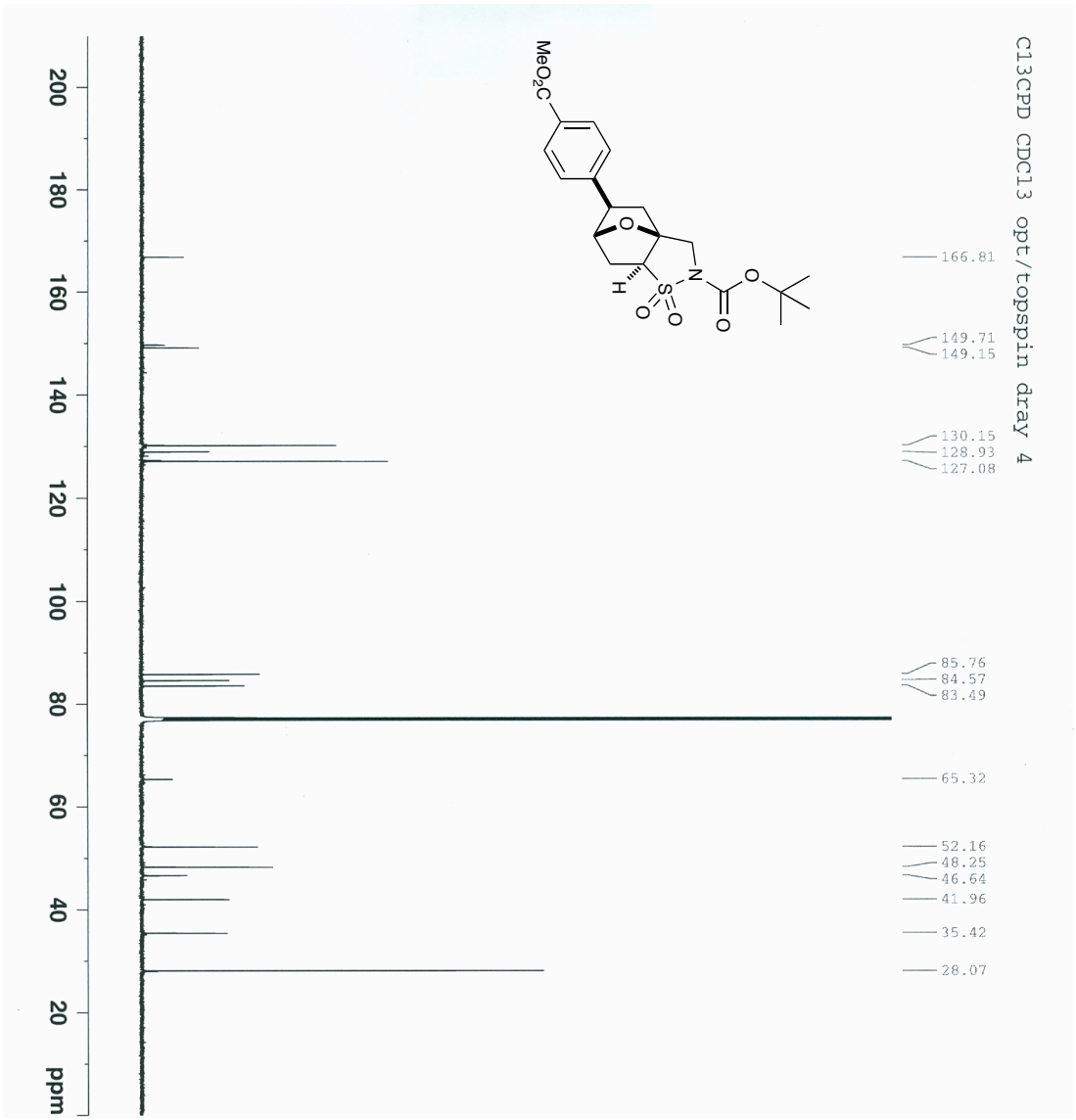
C13CPD CDCl3 opt/topspin dray 4
MeO2C
166.81
149.71
149.15
130.15
128.93
127.08
85.76
84.57
83.49
65.32
52.16
48.25
46.64
41.96
35.42
28.07
200
180
160
140
120
100
80
60
40
20
ppm

(±)-tert-butyl-5-(4-hydroxyphenyl)hexahydro-2H-3a,6-epoxybenzo[d]isothiazole-2-carboxylate 1,1-dioxide (3.16d)

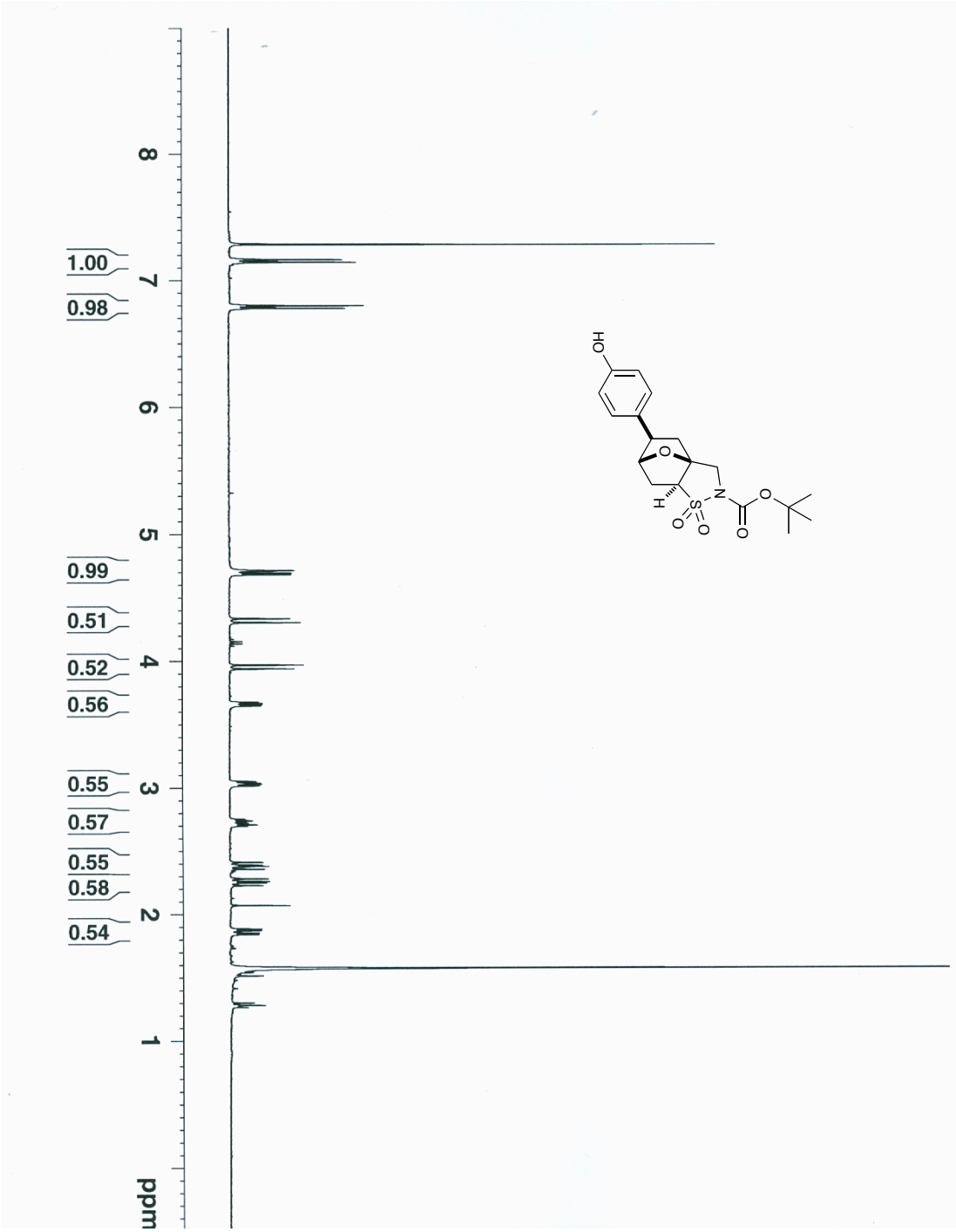

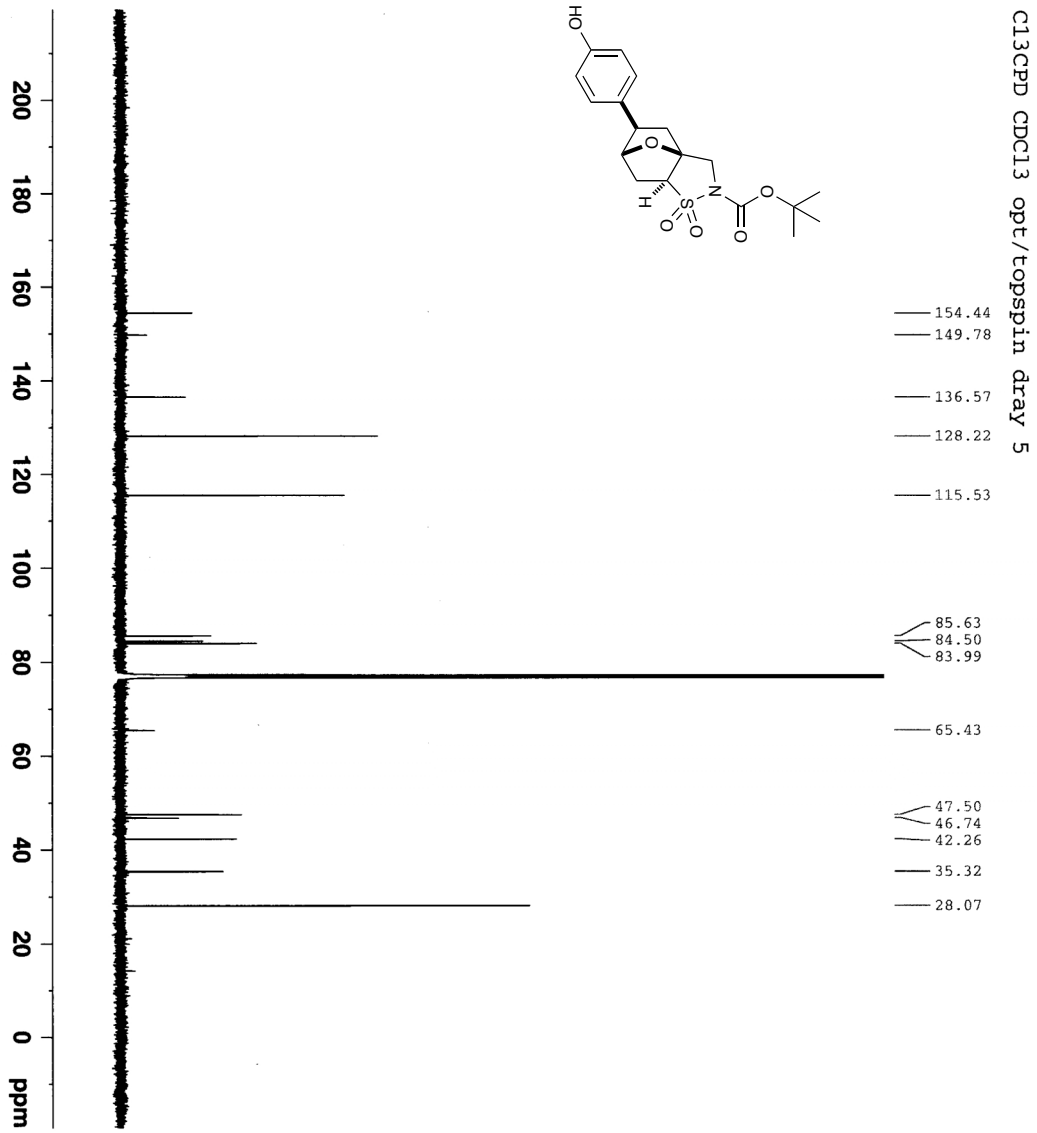
C13CPD CDC13 opt/topspin dray 5
154.44
149.78
136.57
128.22
115.53
85.63
84.50
83.99
65.43
47.50
46.74
42.26
35.32
28.07
200
180
160
140
120
100
80
60
40
20
0
ppm

(±) tert-butyl-5-(3-fluorophenyl) hexahydro-2H-3a,6-epoxybenzo[d]isothiazole-2-carboxylate 1,1-dioxide (3.16e)

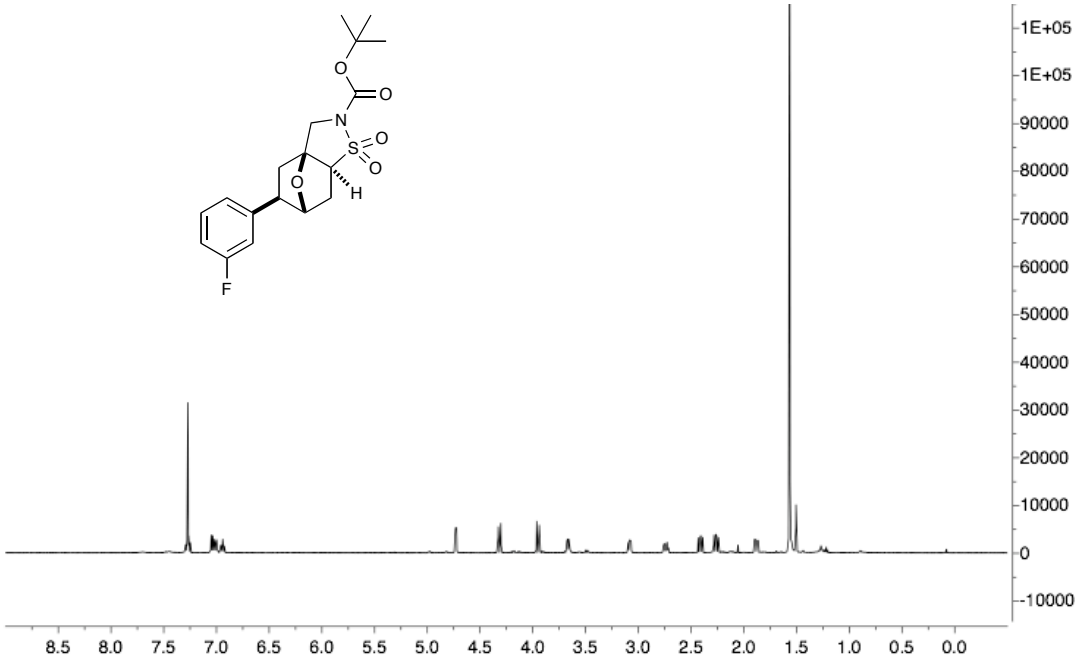

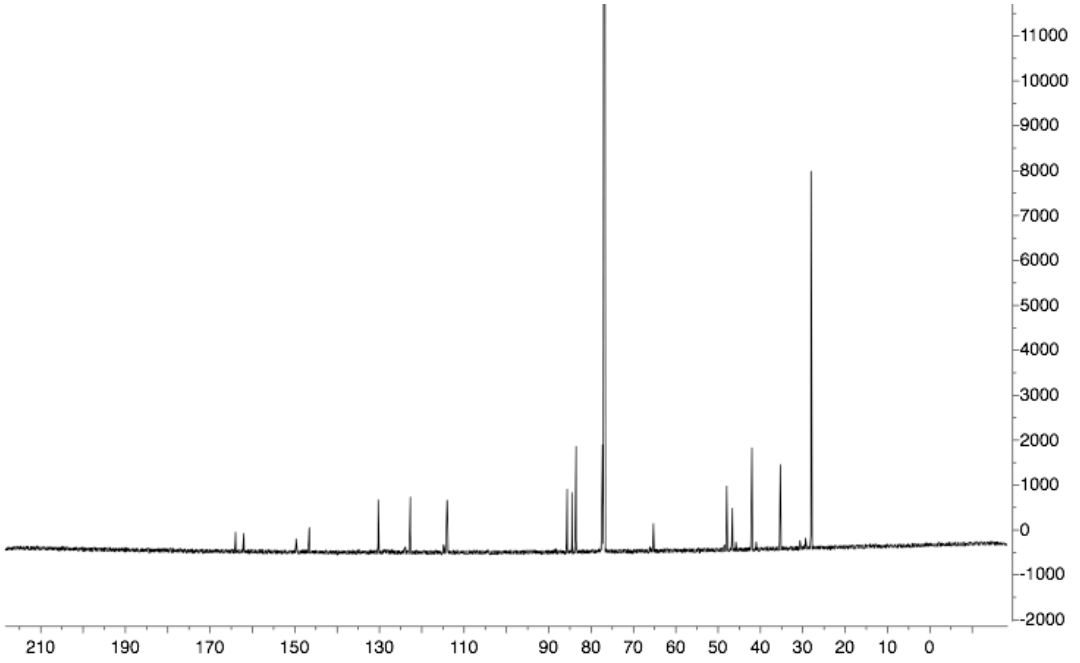

(±) tert-butyl 5-(3,5-dimethylphenyl) hexahydro-2H-3a,6 epoxybenzo [d]iso thiazole-2-carboxylate 1,1-dioxide (3.16f)

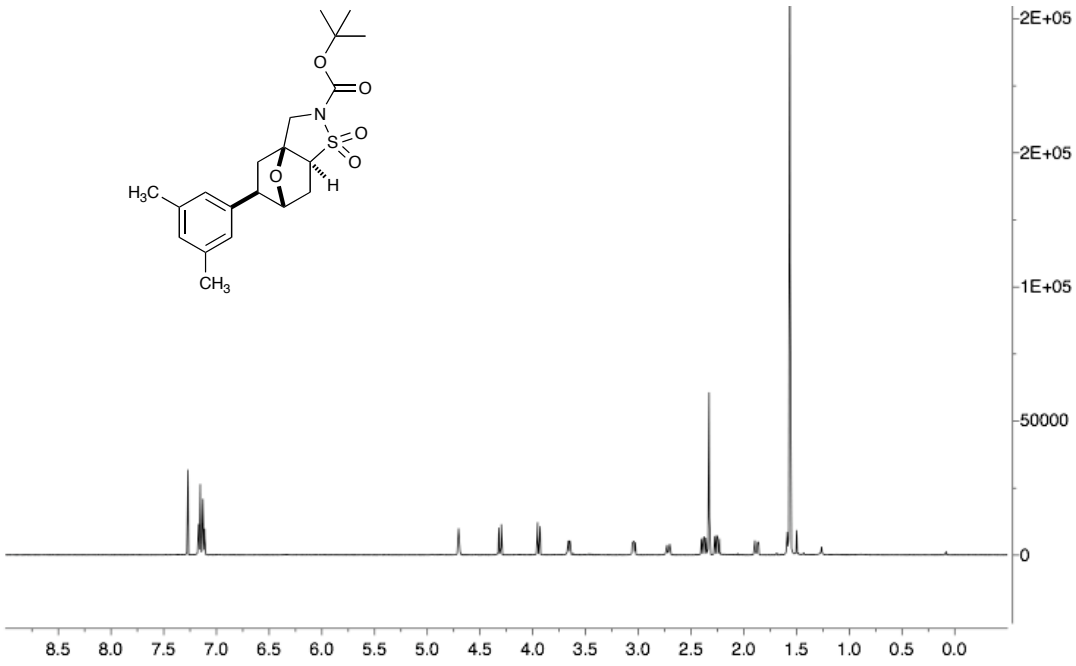

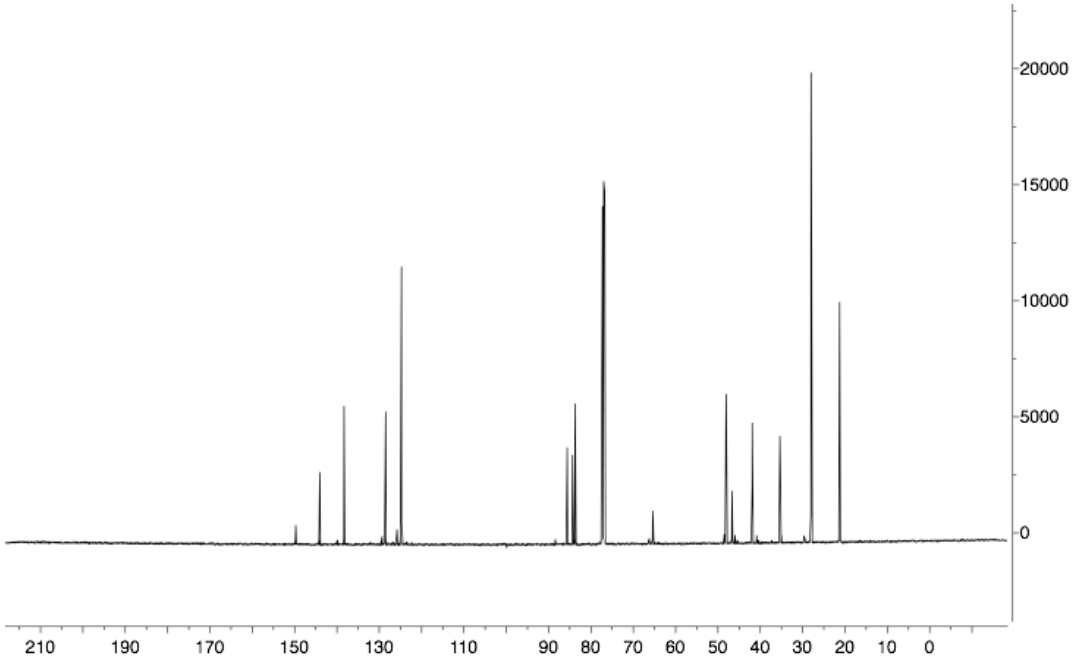

(±) *tert*-butyl-5-(*p*-tolyl) hexahydro-2*H*-3a,6-epoxybenzo[*d*]isothiazole-2-carboxylate 1,1-dioxide (3.16g)

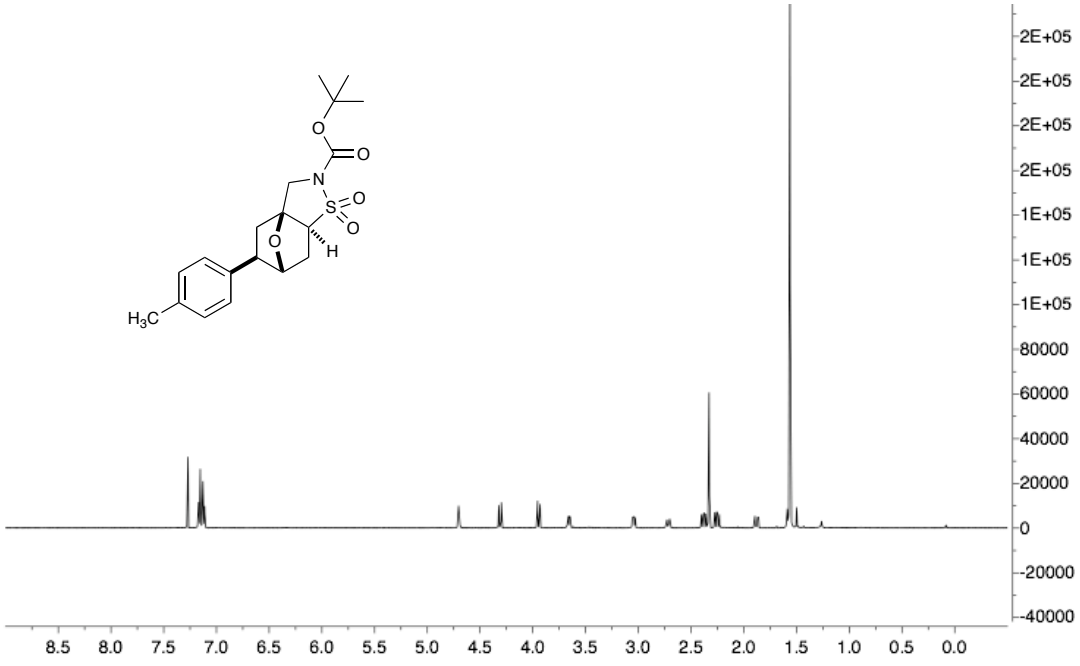

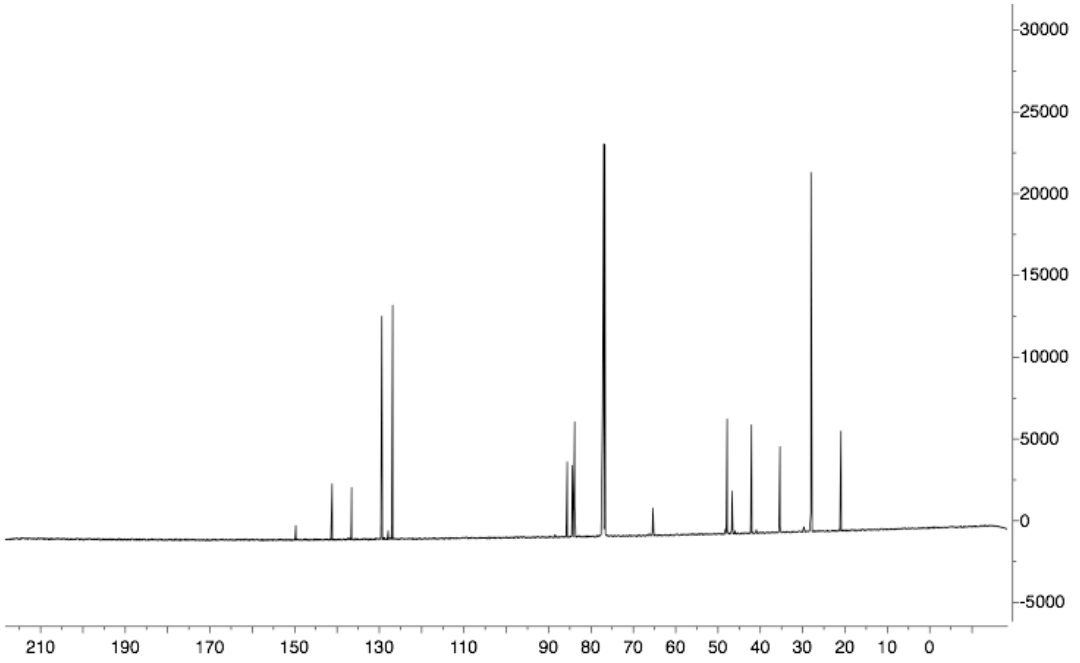

(±) tert-butyl-5-(4-(thiophen-3-yl)phenyl) hexahydro-2H-3a,6-epoxybenzo [d]iso-thiazole-2-carboxylate 1,1-dioxide (3.16h)

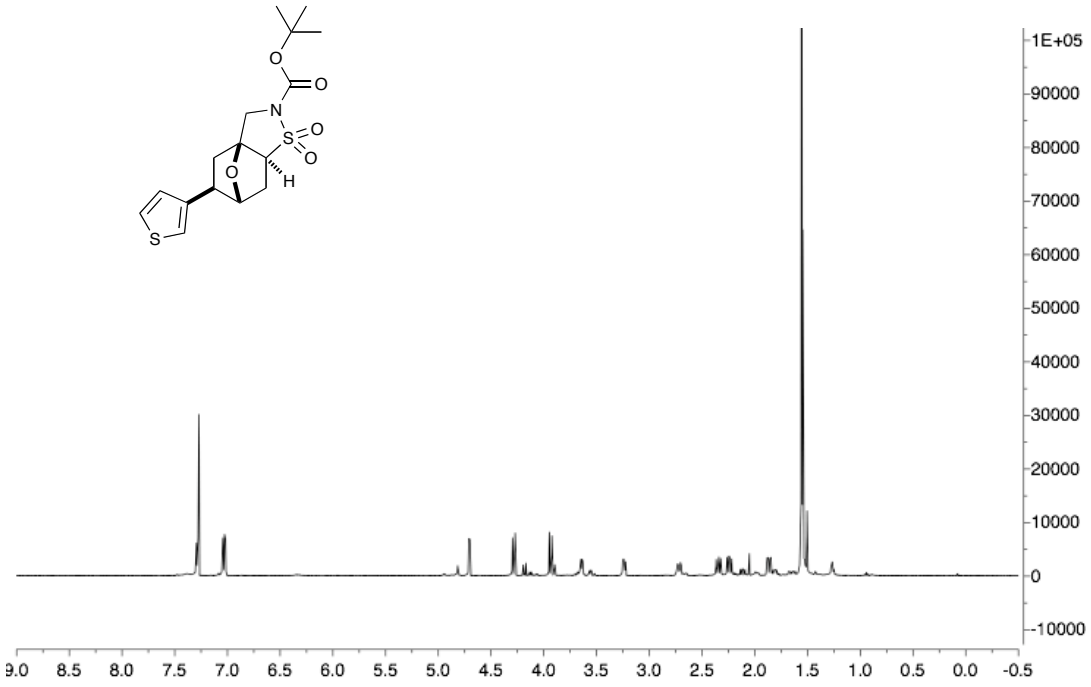

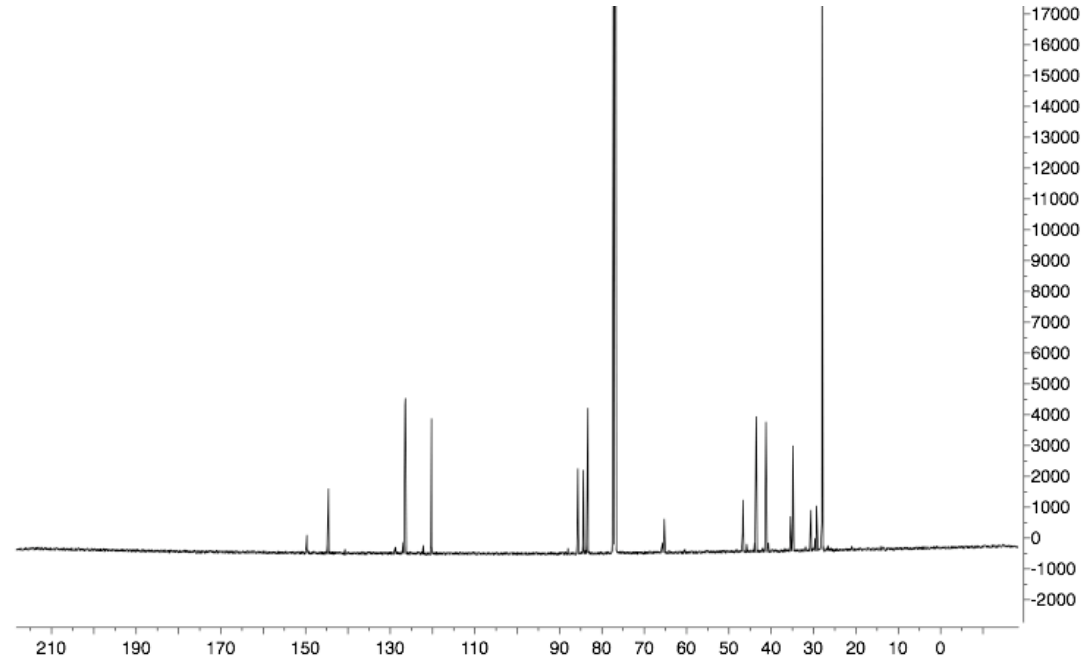

(±) tert-butyl-5-(4-(trifluoromethoxy)phenyl) hexahydro-2H-3a,6-epoxybenzo [d] isothiazole -2-carboxylate 1,1-dioxide (3.16i)

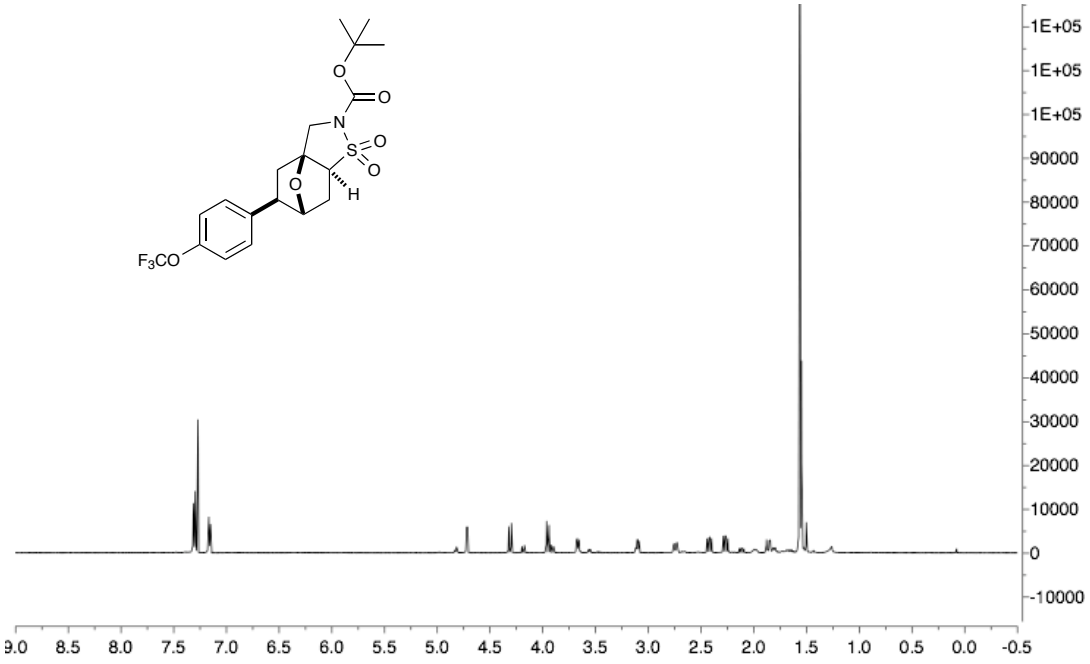

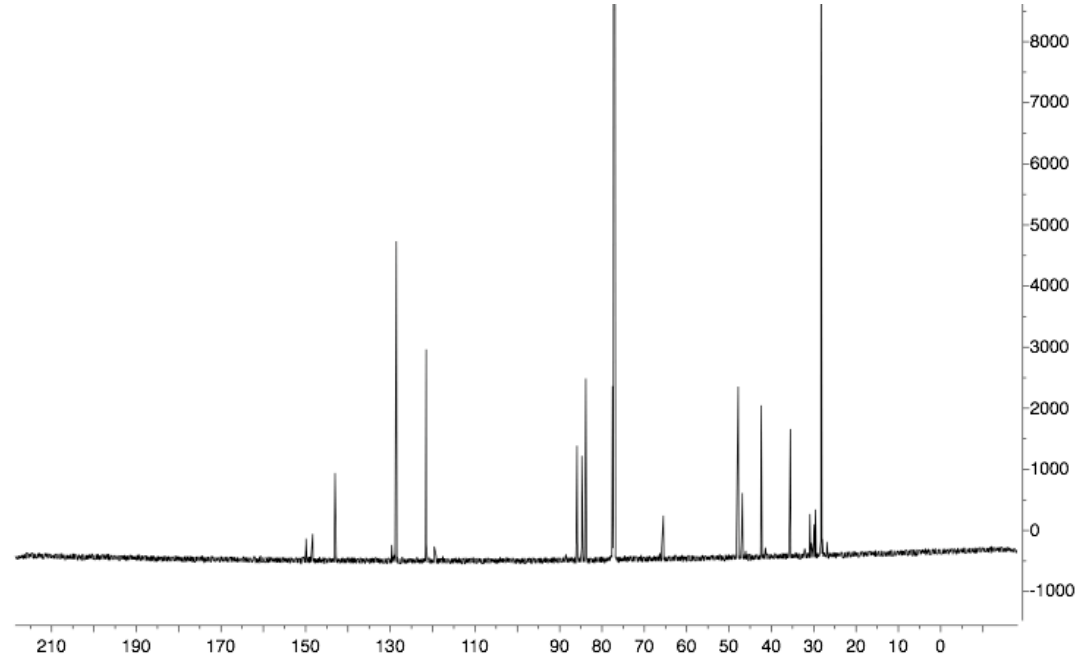

(±) tert-butyl-5-(4-cyanophenyl) hexahydro-2H-3a,6-epoxybenzo[d]isothiazole-2-carboxylate 1,1-dioxide (3.16j)

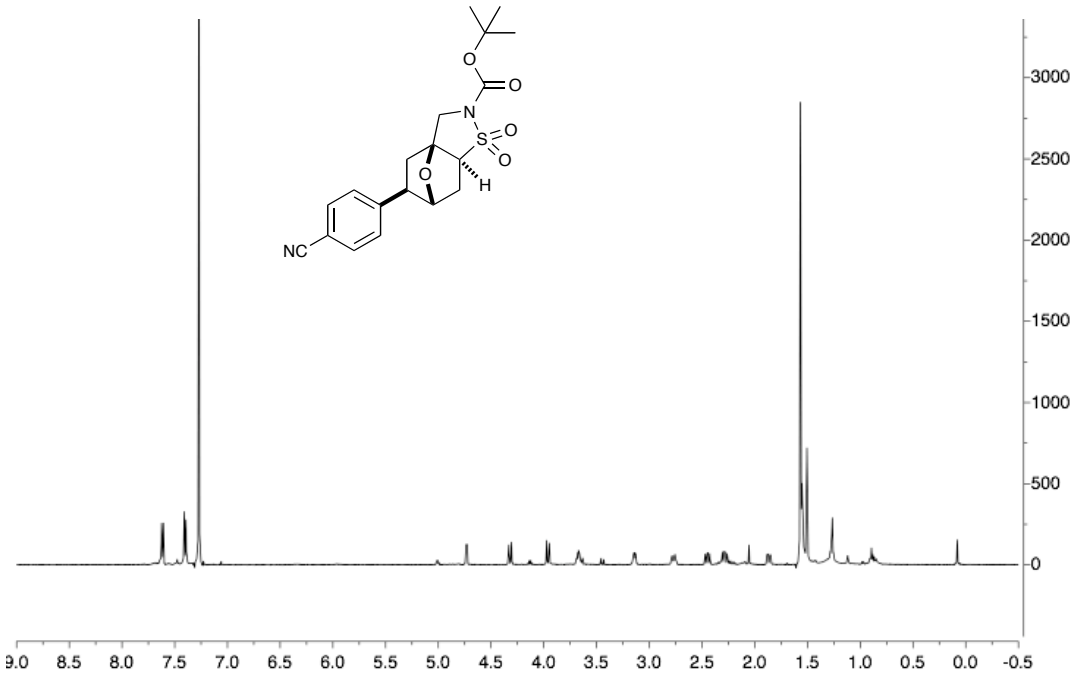

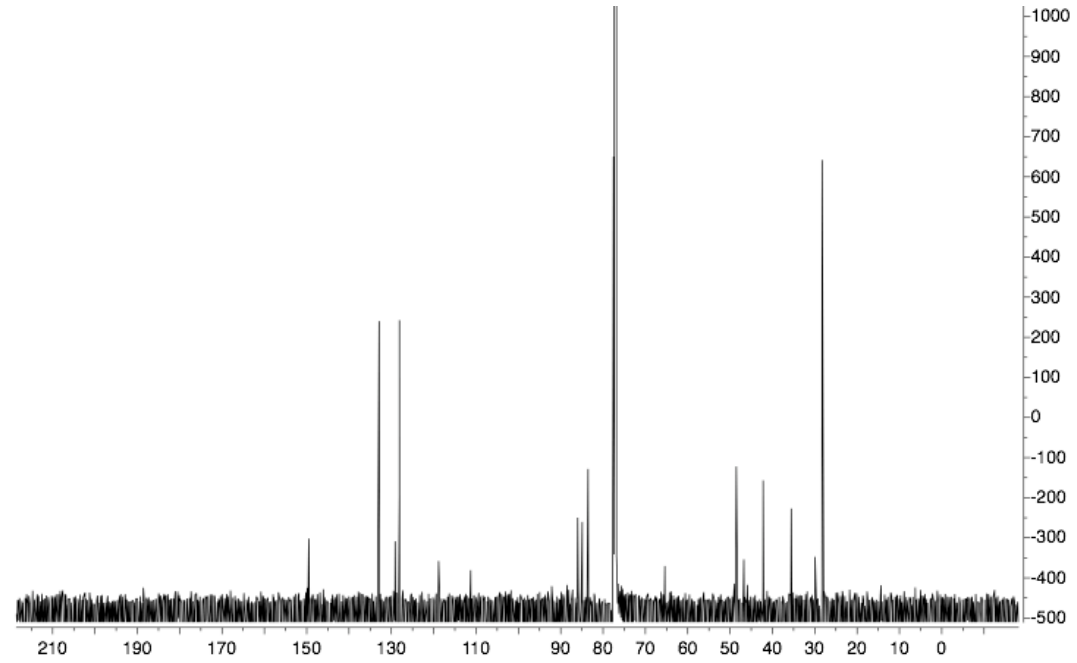

(±) hexahydro-2H-3a,7-epoxyoxepino[3,4-d]isothiazole 1,1-dioxide (3.19)

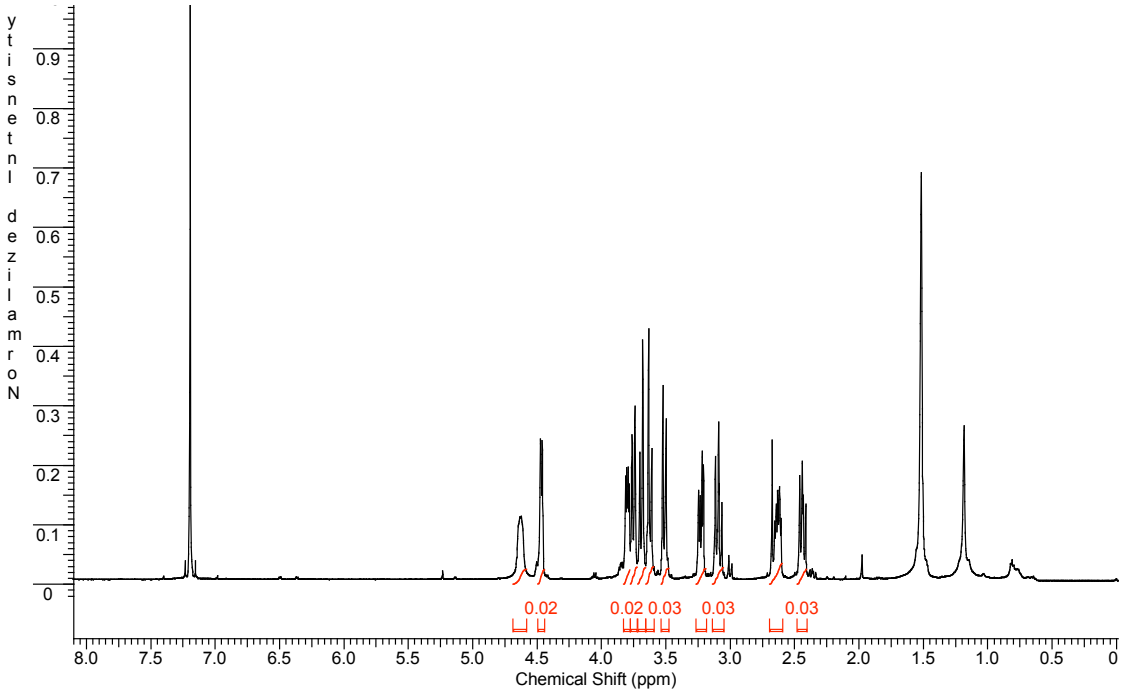

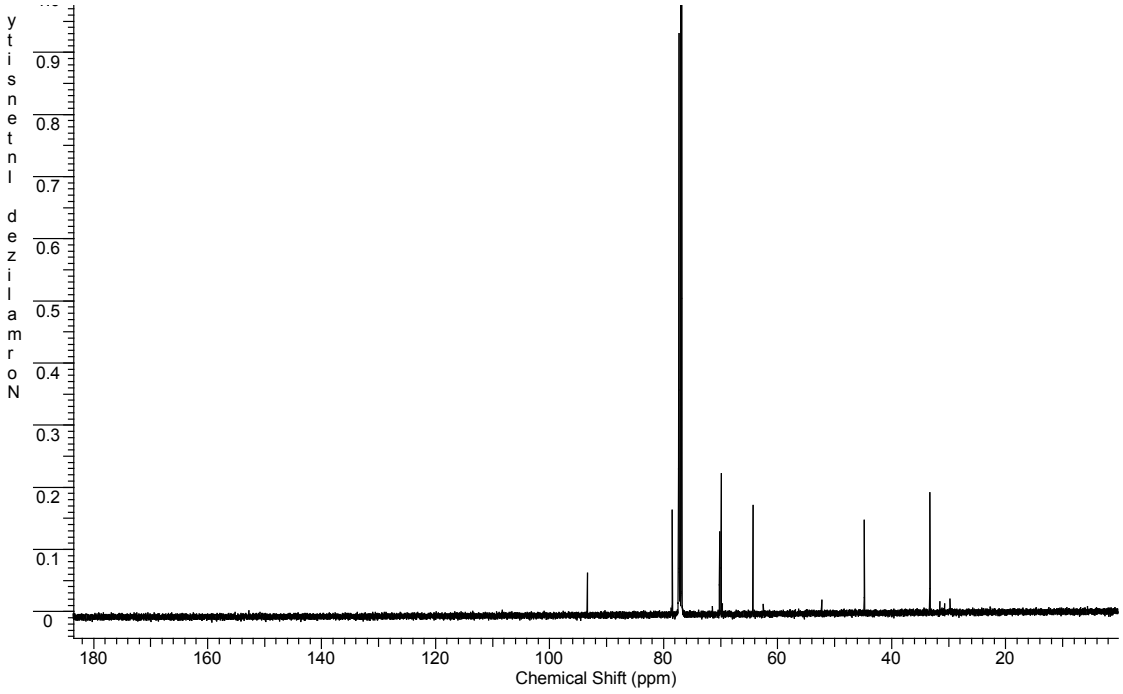

(±)-3a,5-bis(hydroxymethyl)-2-(4-methoxybenzyl)hexahydrofuro[2,3-d]isothiazole 1,1-dioxide (3.21)

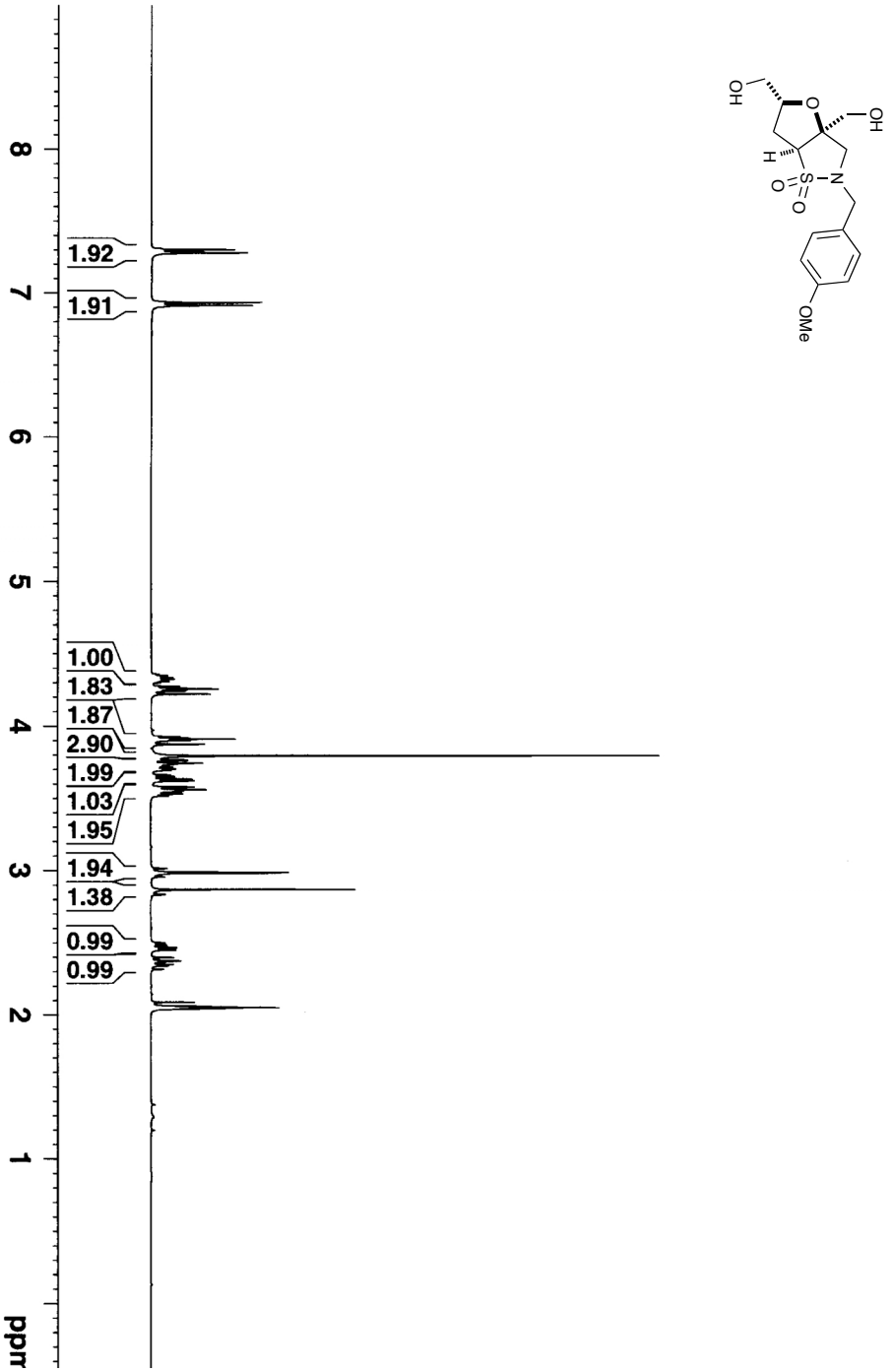

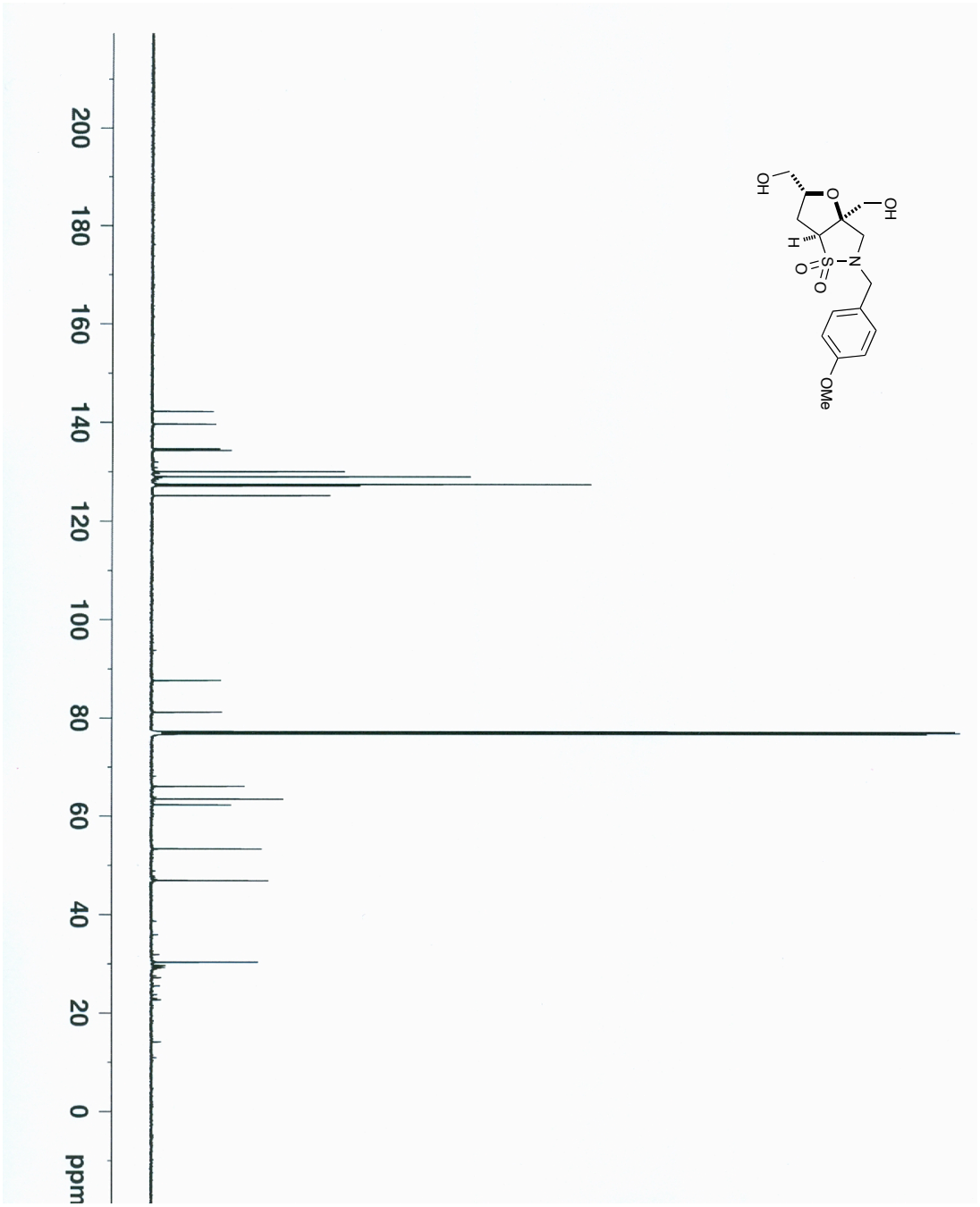
200
180
160
140
120
100
80
60
40
20
0
ppm
OH
O
OH
H
S
O
O
N
OMe

(±) 2-((4'-(tert-butyl)-[1,1'-biphenyl]-4-yl)methyl)-3a,5-bis(hydroxymethyl) hexahydrofuro[2,3-d]isothiazole 1,1-dioxide (3.23a)

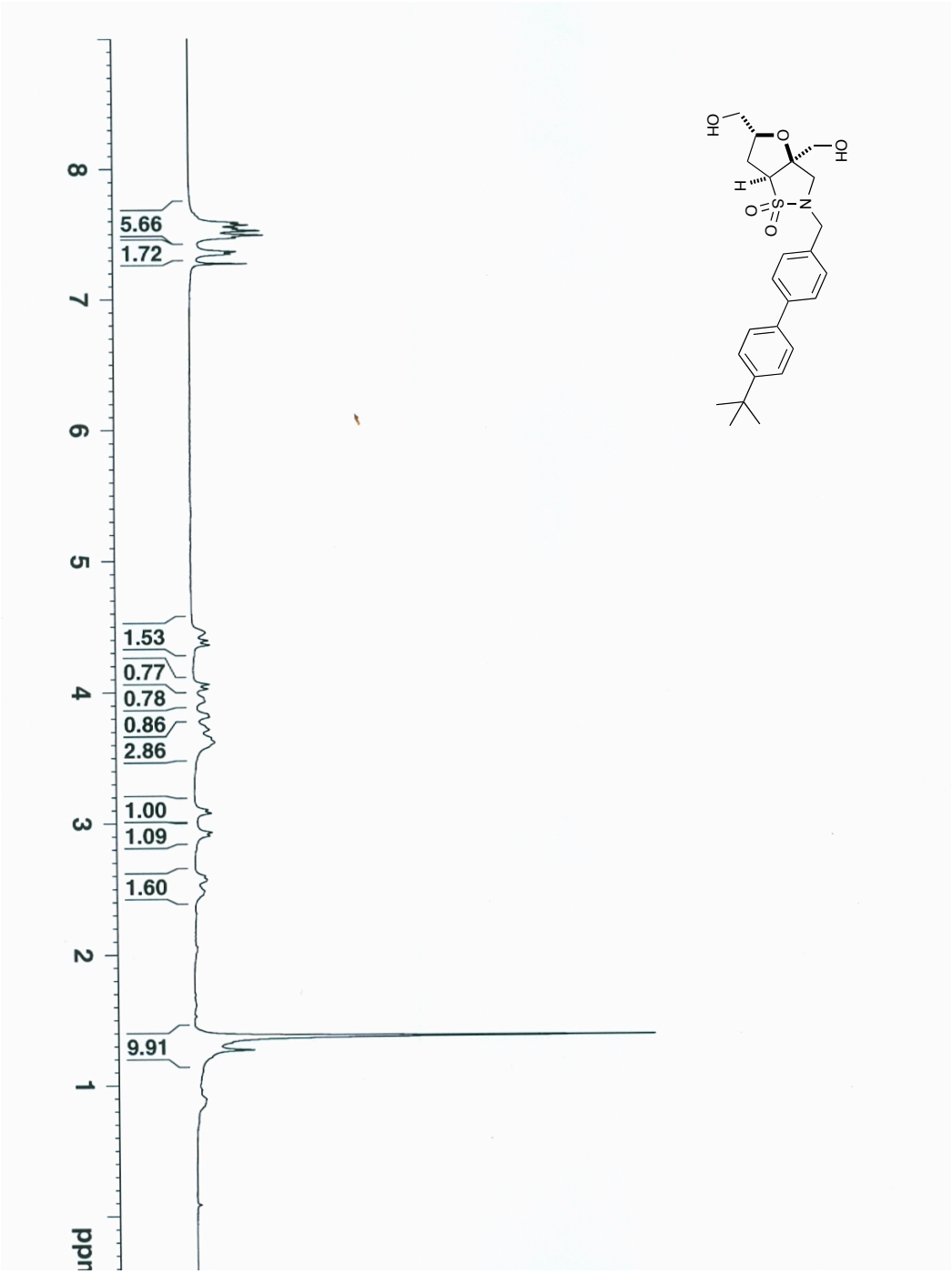

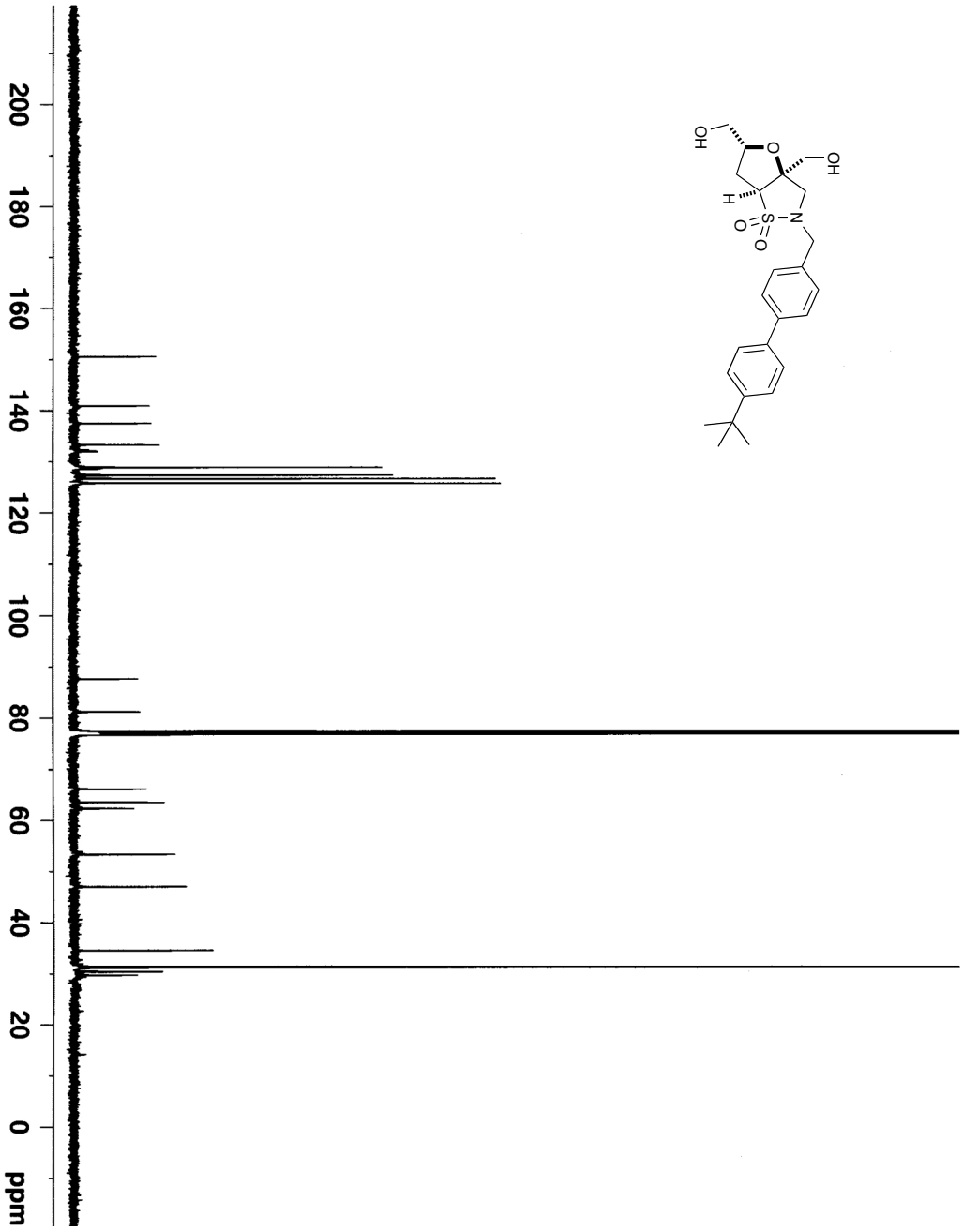
200
180
160
140
120
100
80
60
40
20
0
ppm
OH
O
OH
H
S
O
O
N

(±) 2-((3'-(1-hydroxyethyl)-[1,1'-biphenyl]-4-yl)methyl)-3a,5-bis(hydroxymethyl) hexa-hydrofuro[2,3-d]isothiazole 1,1-dioxide (3.23b) – mixture of diastereomers

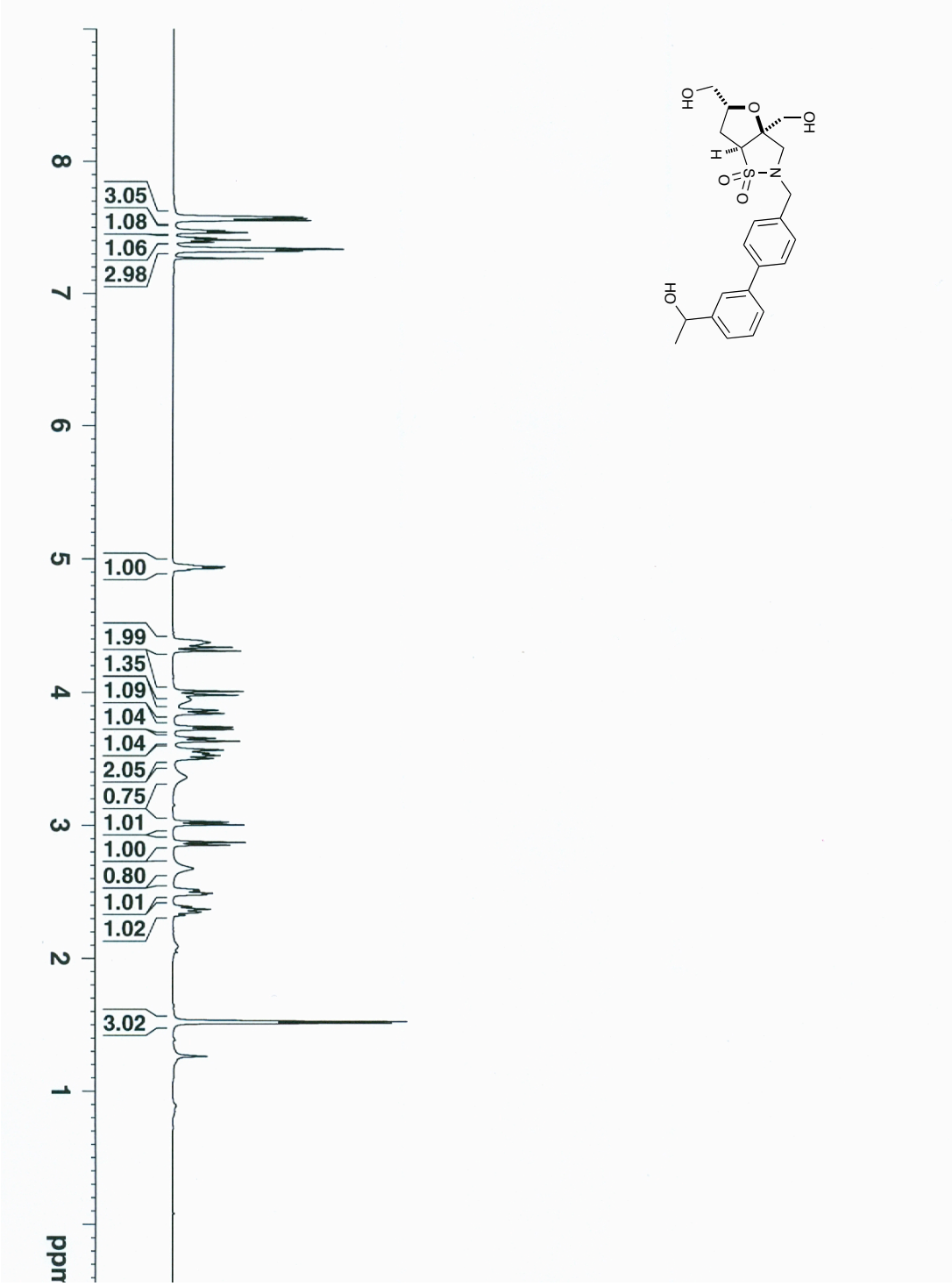

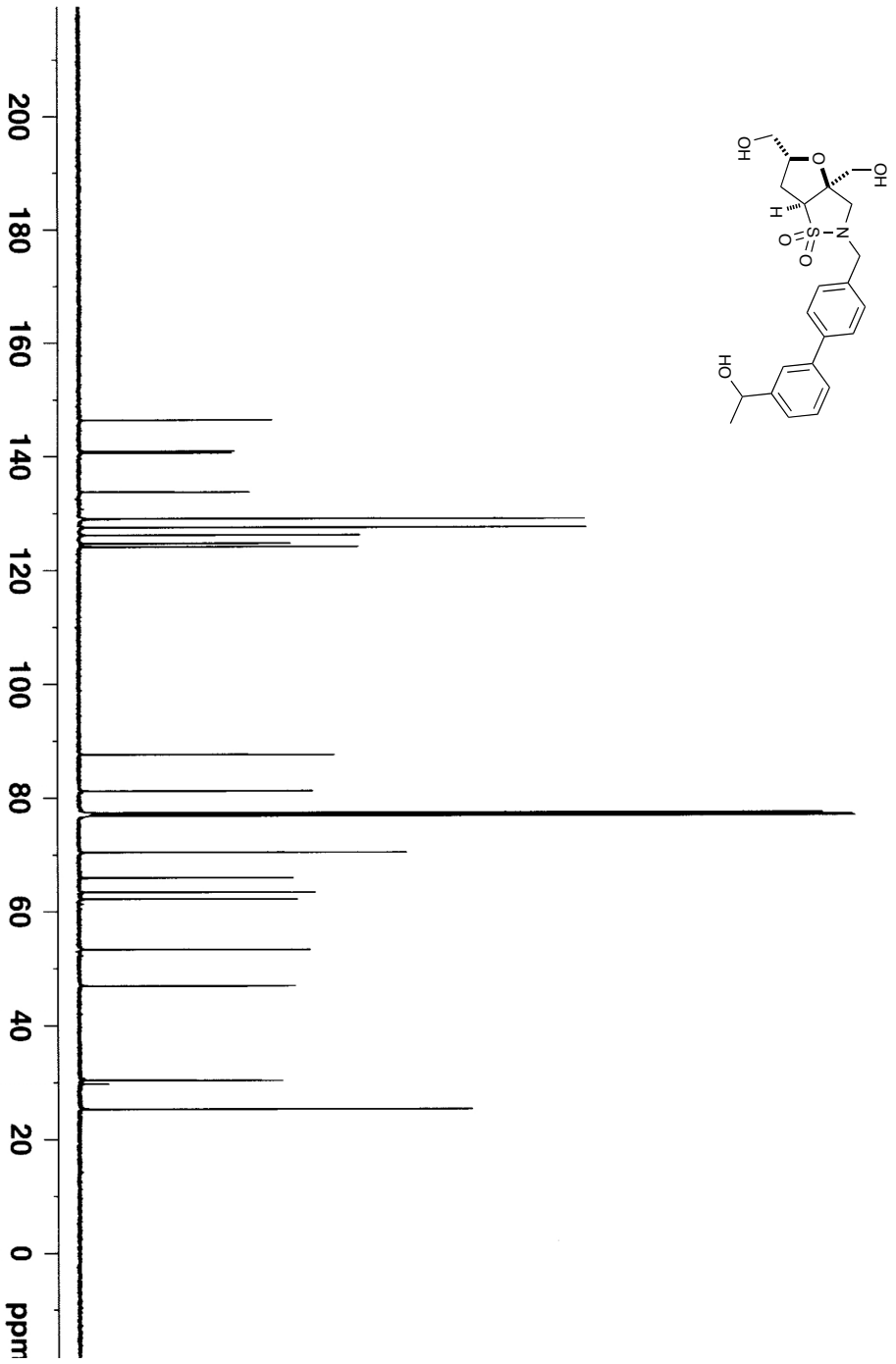
200
180
160
140
120
100
80
60
40
20
0
ppm
HO
O
HO
H
S
N
O
O
OH

(±) 4,5-dihydroxy-2-(4-iodobenzyl)hexahydro-2H-3a,6-epoxybenzo[d]isothiazole 1,1-dioxide (3.25)

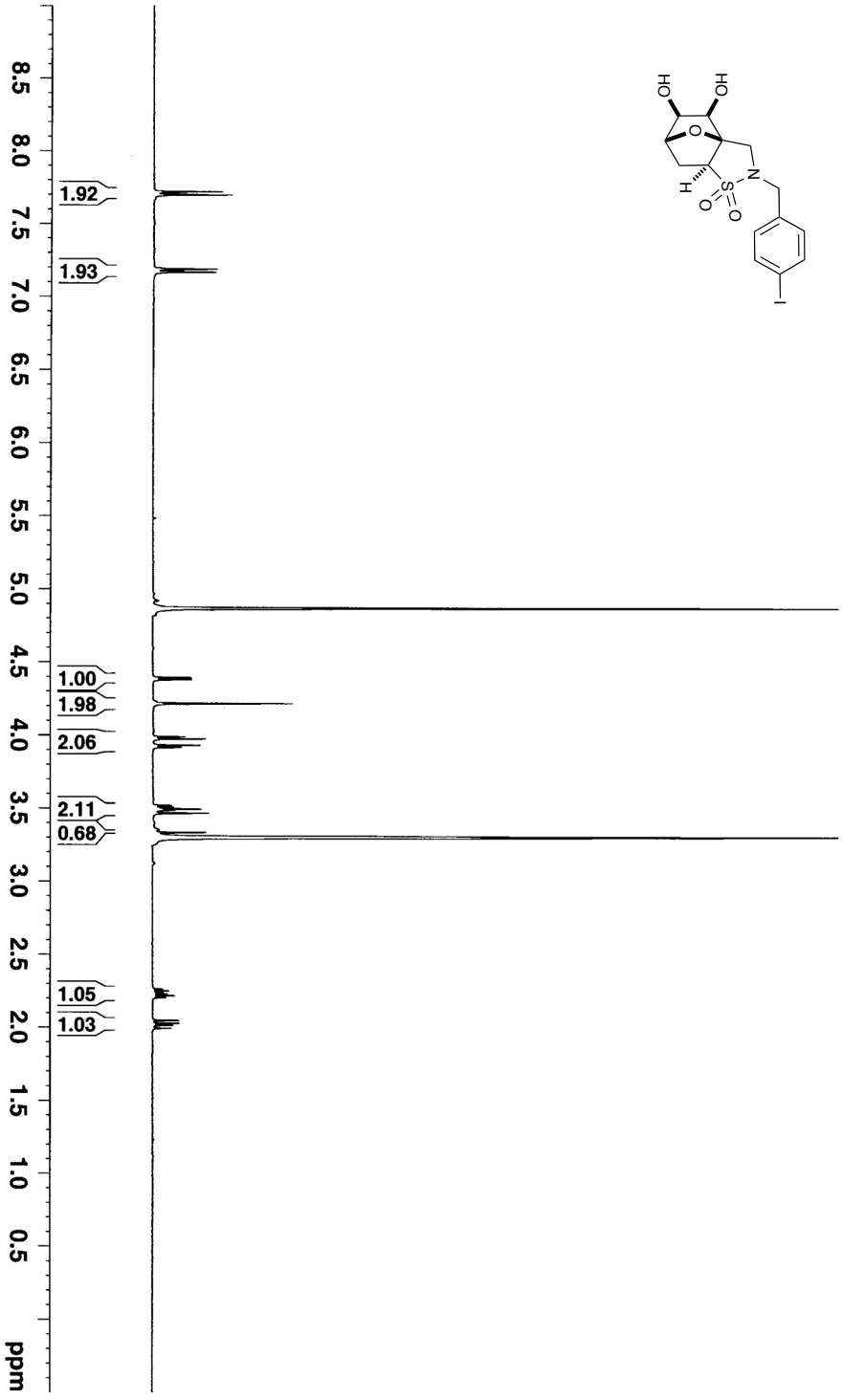

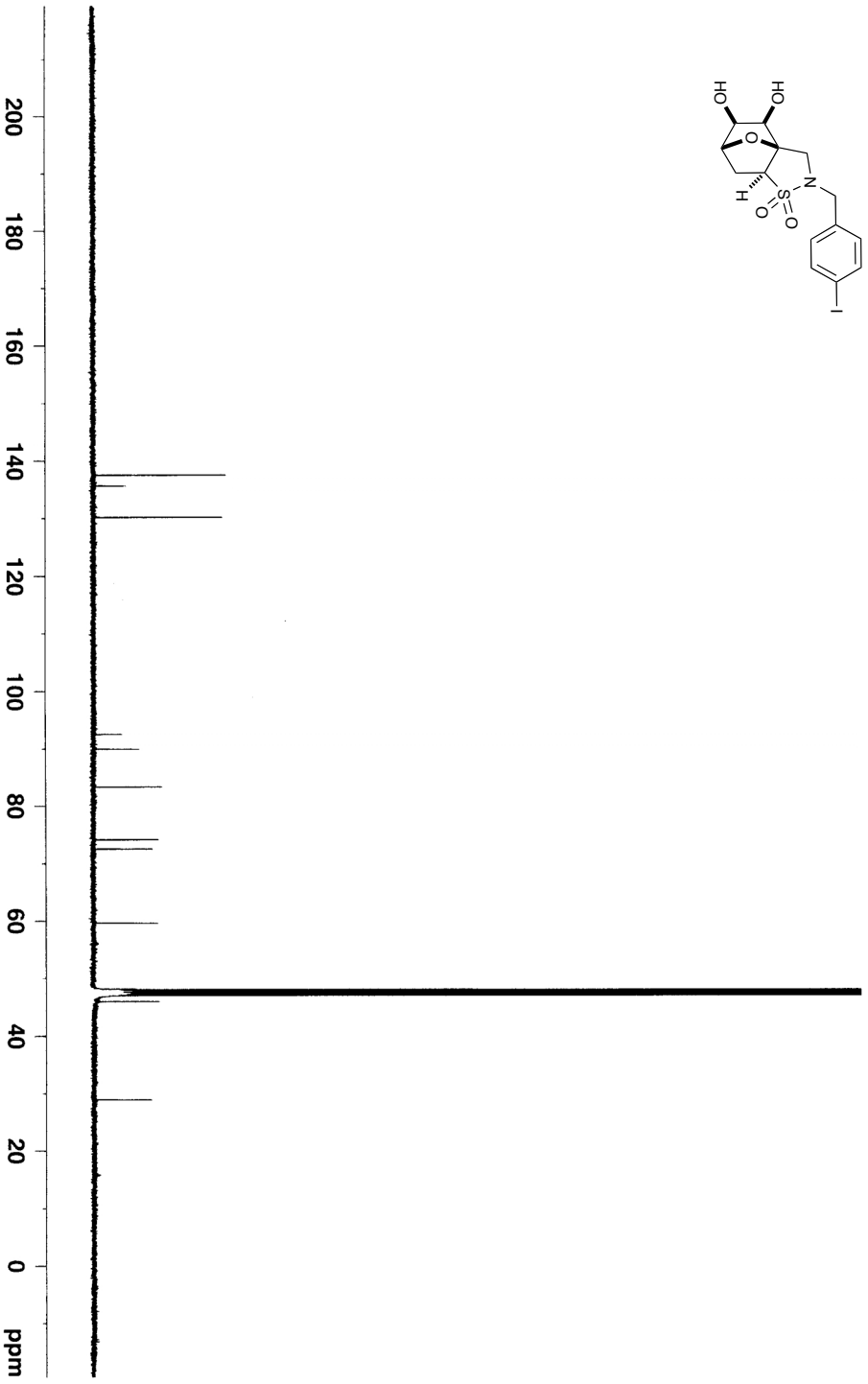
200
180
160
140
120
100
80
60
40
20
0
ppm
HO
HO
O
H
S
O
O
N
I

(±) 2-((4'-fluoro-[1,1'-biphenyl]-4-yl)methyl)-3a,5-bis(hydroxymethyl)hexahydro furo[2,3-d]isothiazole 1,1-dioxide (3.28a)

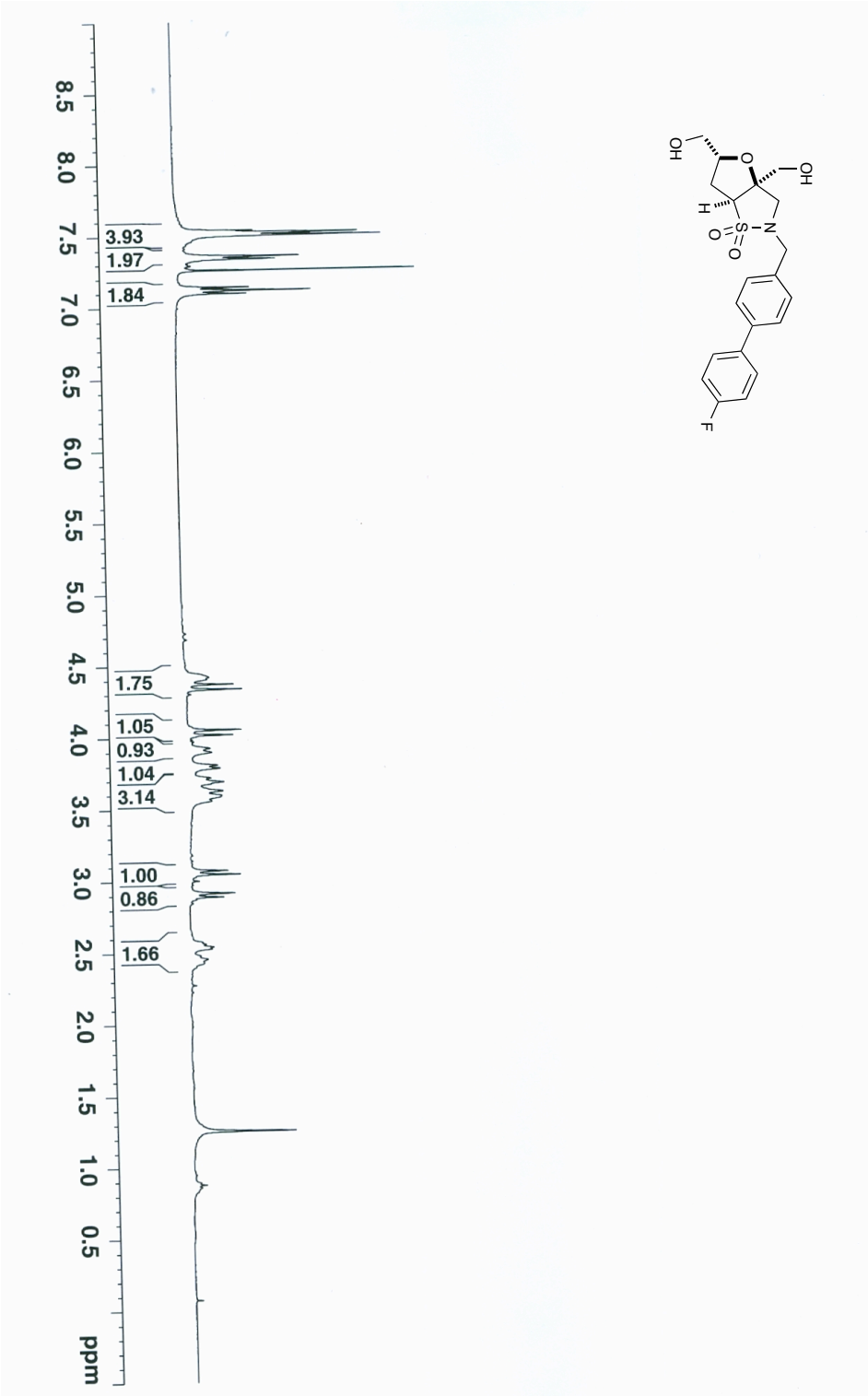

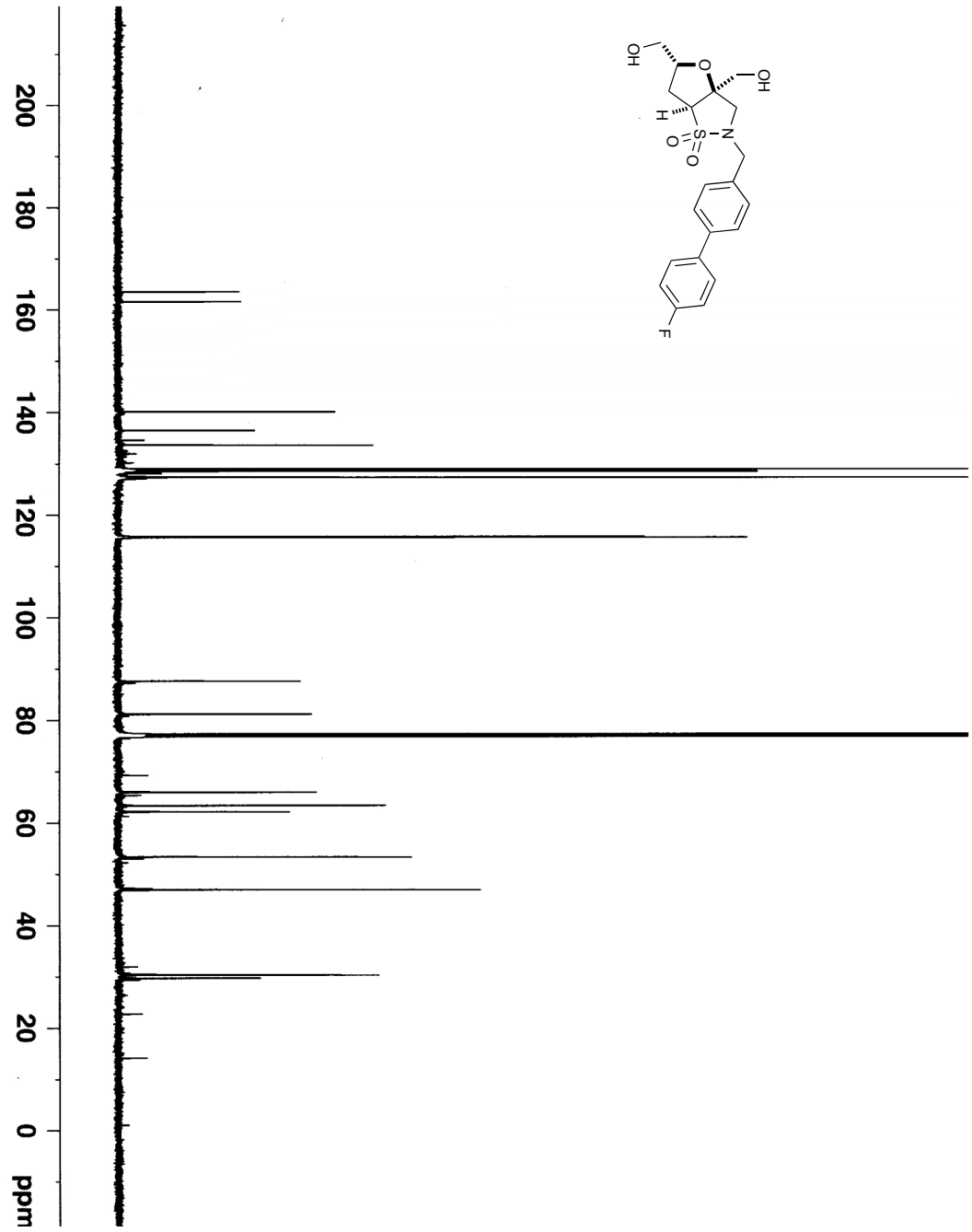
200
180
160
140
120
100
80
60
40
20
0
ppm
OH
O
OH
H
S
O
O
N
F

(±) 2-((3'-chloro-[1,1'-biphenyl]-4-yl)methyl)-3a,5-bis(hydroxymethyl) hexahydrofuro[2,3-d]isothiazole 1,1-dioxide (3.28b)

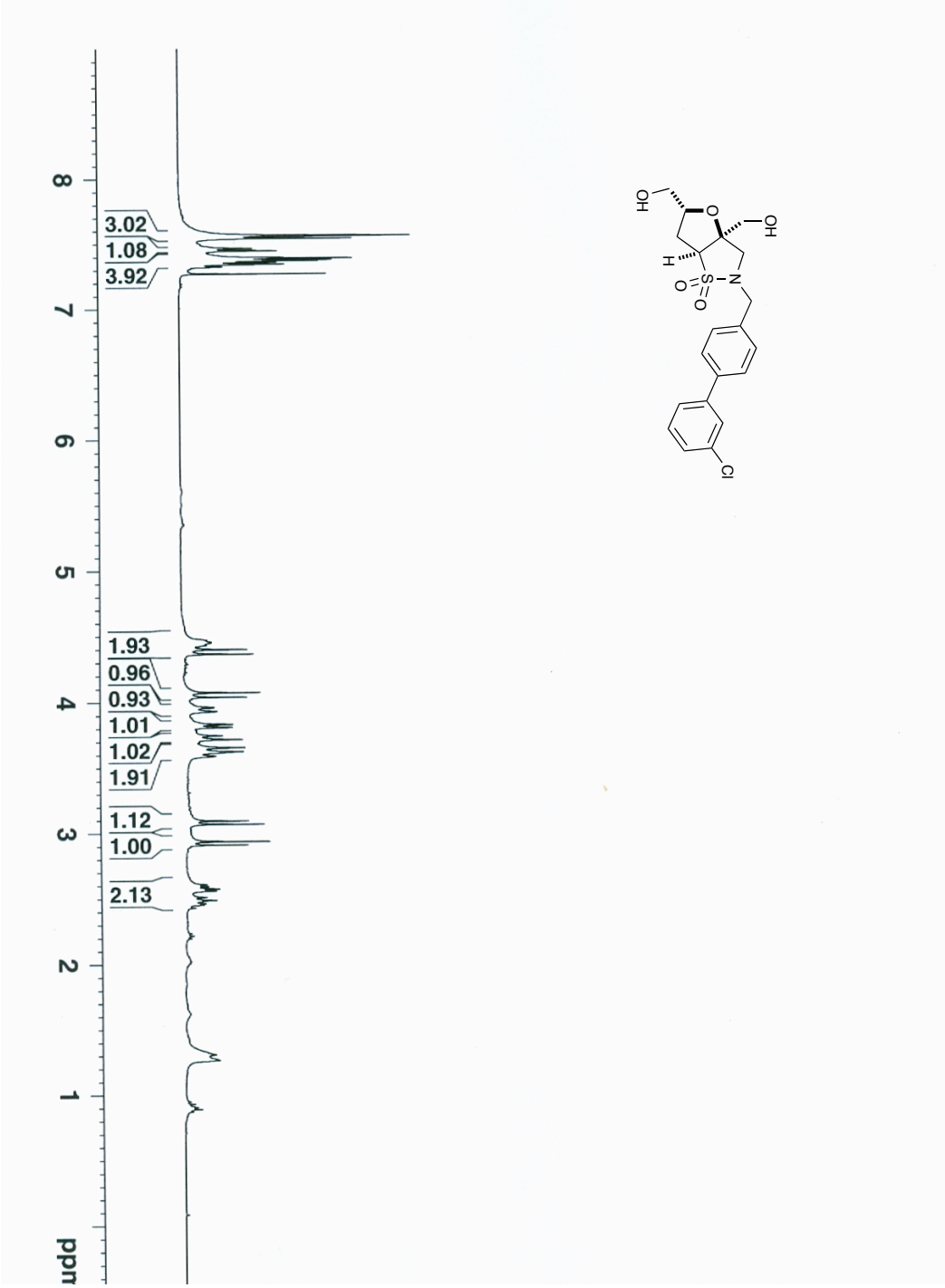

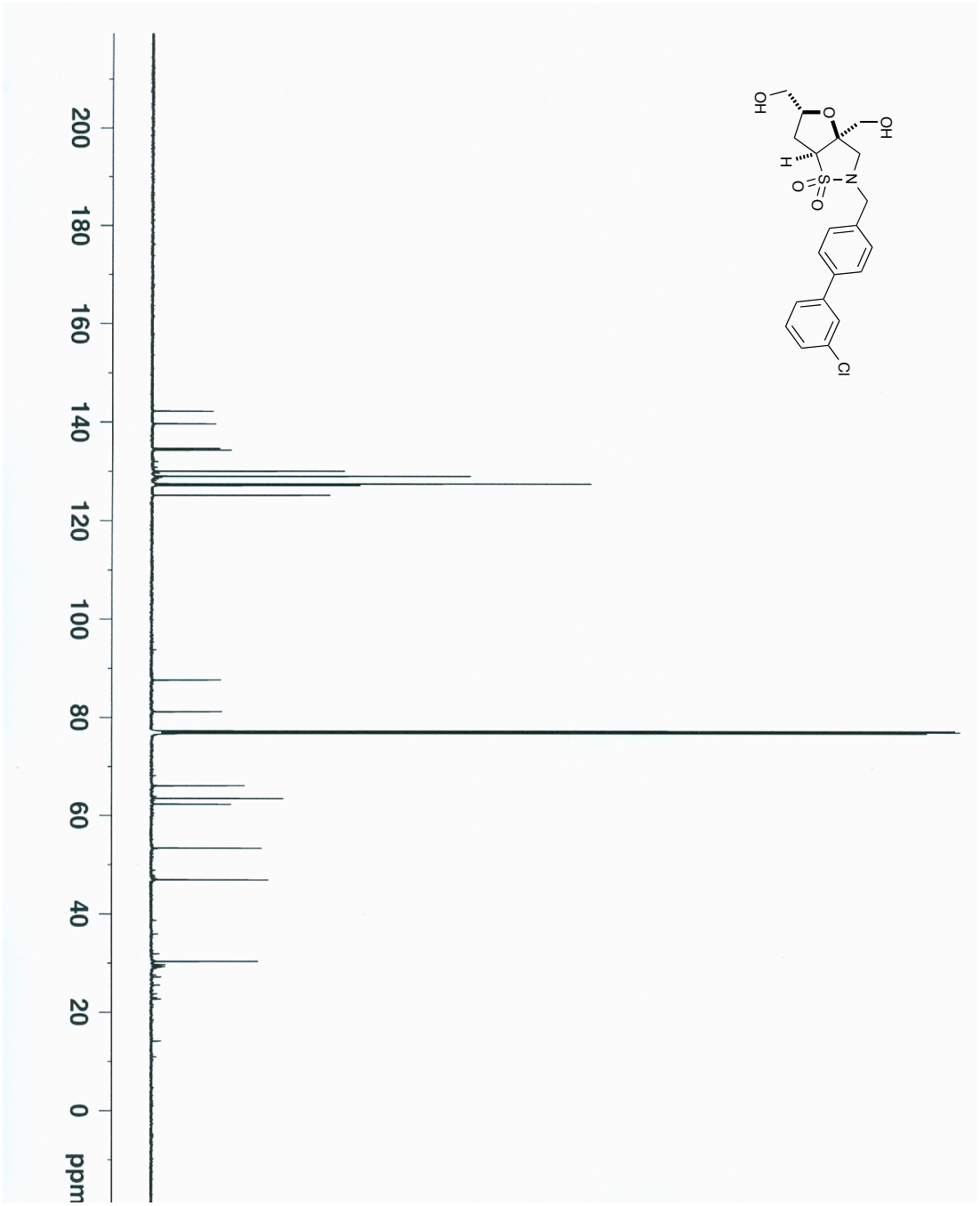
200
180
160
140
120
100
80
60
40
20
0
ppm
OH
O
OH
H
S
O
O
N
Cl

FTIR: Co/C-nanoparticles/ROMPgel (4.6, 4.10)

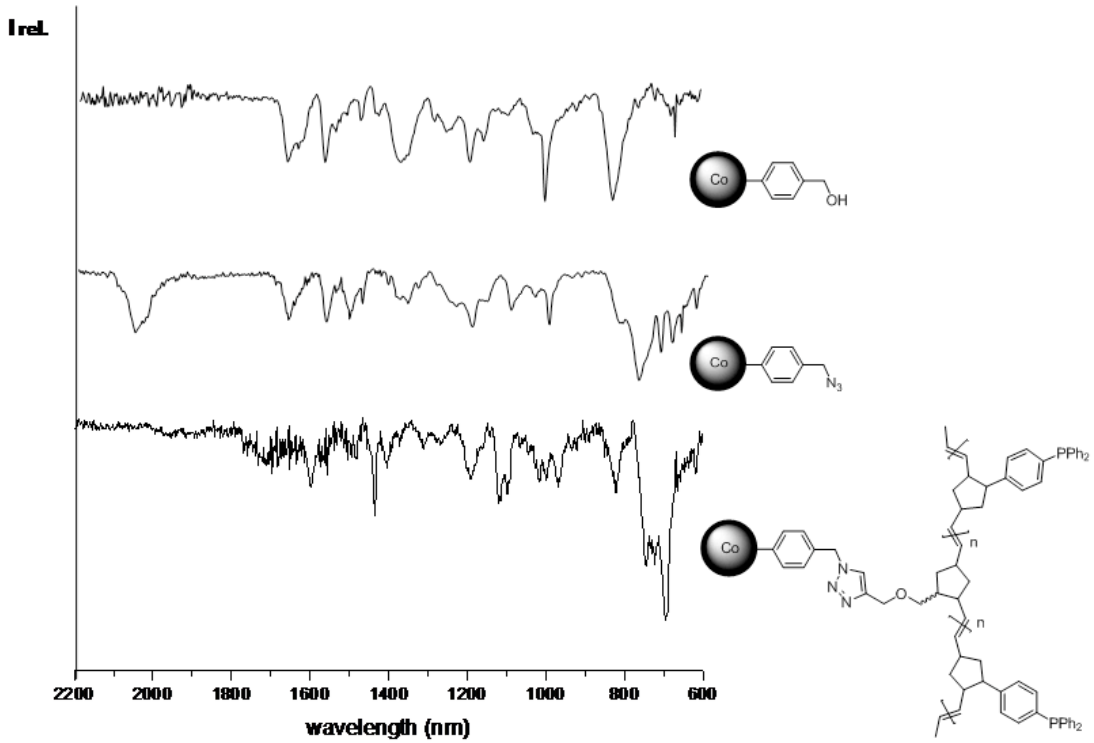

(*S*)-methyl 2-(*N*-(4-bromobenzyl)vinylsulfonamido)-3-methylbutanoate 5.6{*2*}

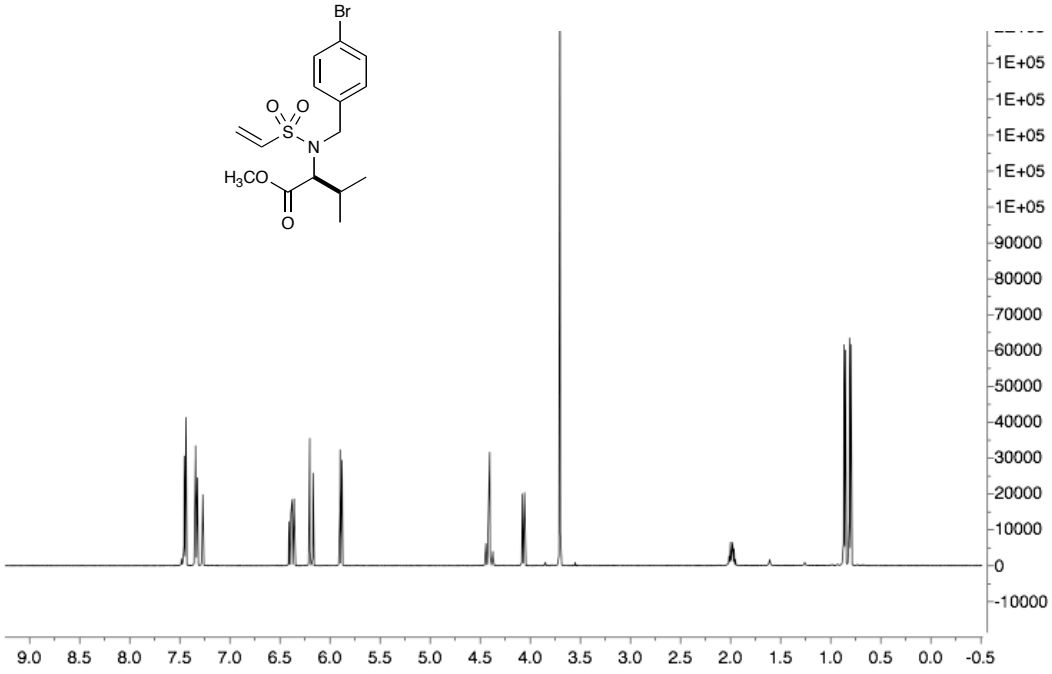

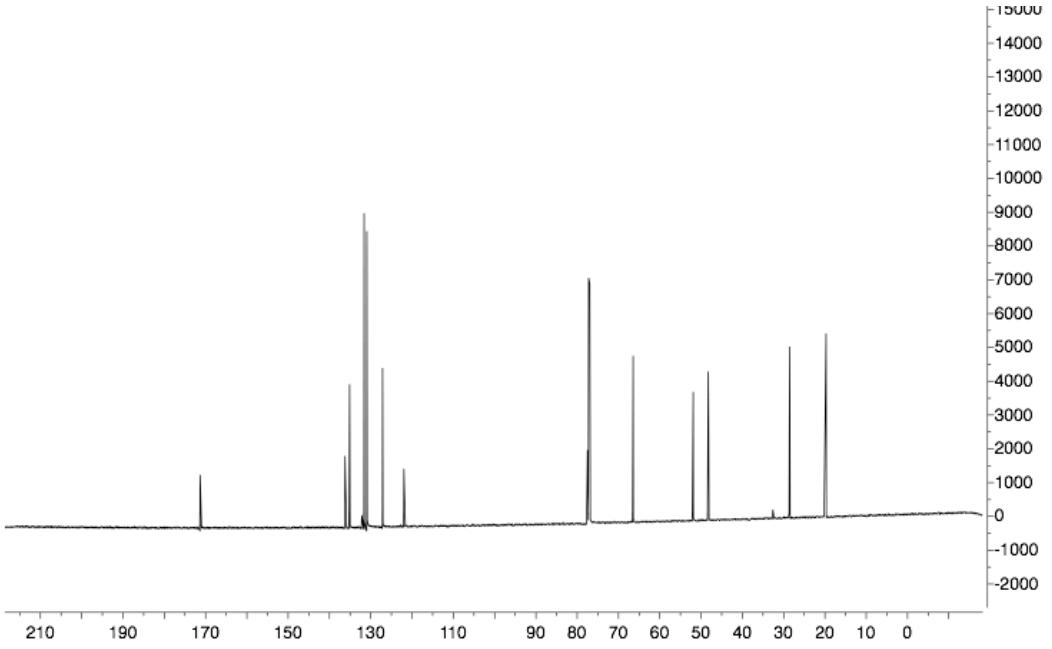

(*S*)-methyl 2-(*N*-(4-bromobenzyl)-2-(prop-2-yn-1-ylamino)ethylsulfonamido)-3-methylbutanoate 5.7{*2*}

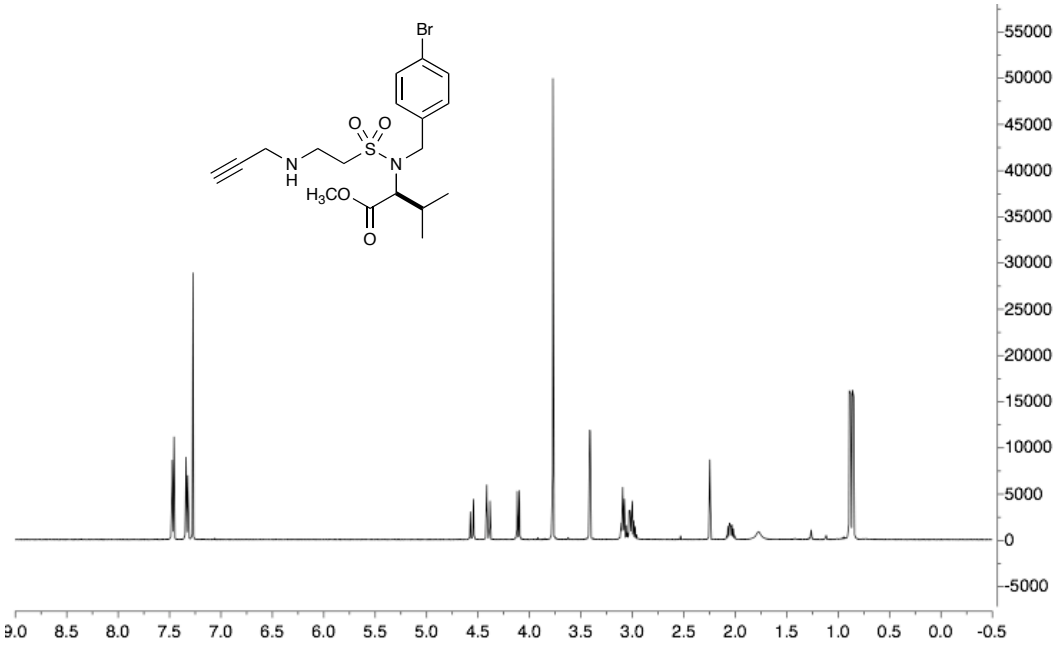

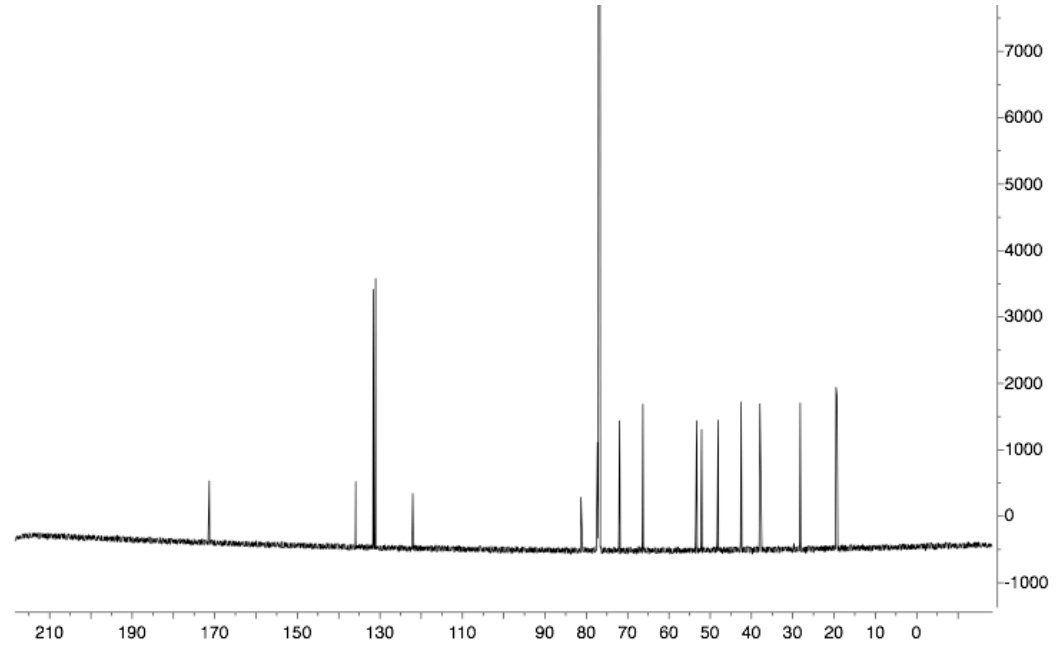

(*S*)-2-(4-bromobenzyl)-3-methyl-5-(prop-2-yn-1-yl)-1,2,5-thiadiazepin-1,1-dioxide-4-one 5.9{*1*}

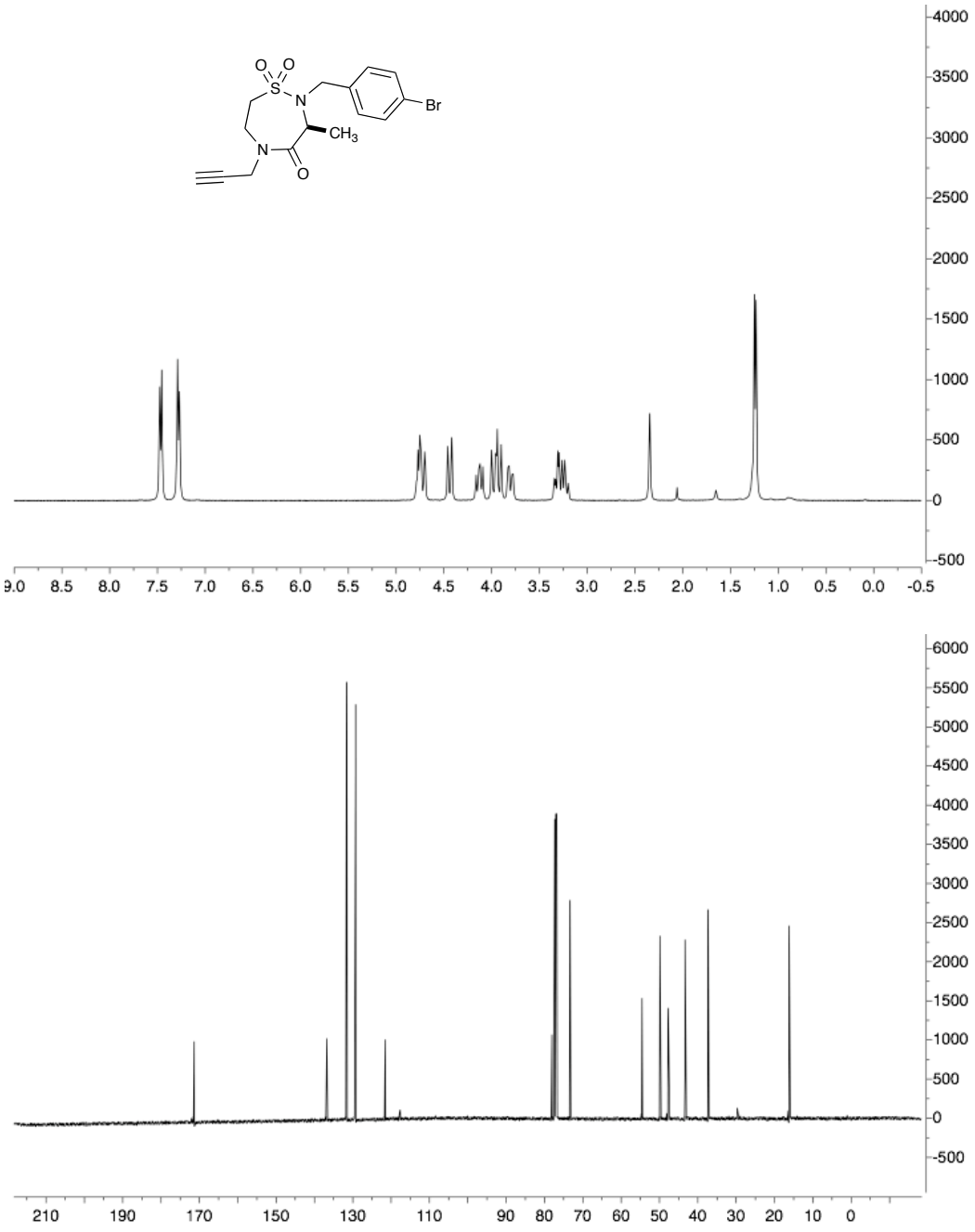

(*S*)-2-(4-bromobenzyl)-3-isopropyl-5-(prop-2-yn-1-yl)-1,2,5-thiadiazepin-1,1-dioxide-4-one 5.9{*2*}

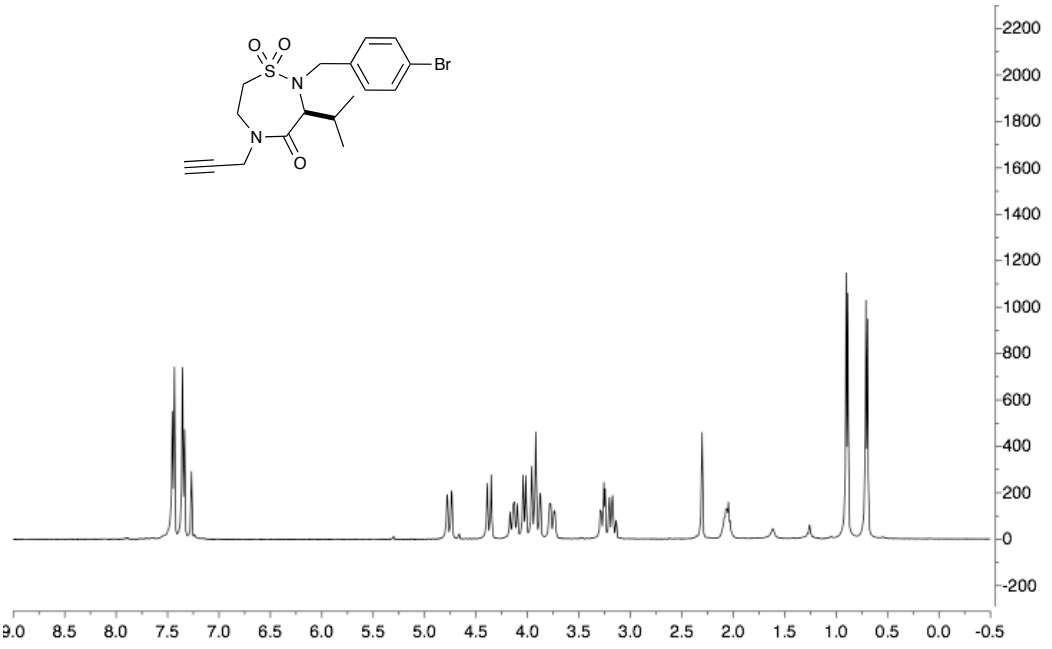

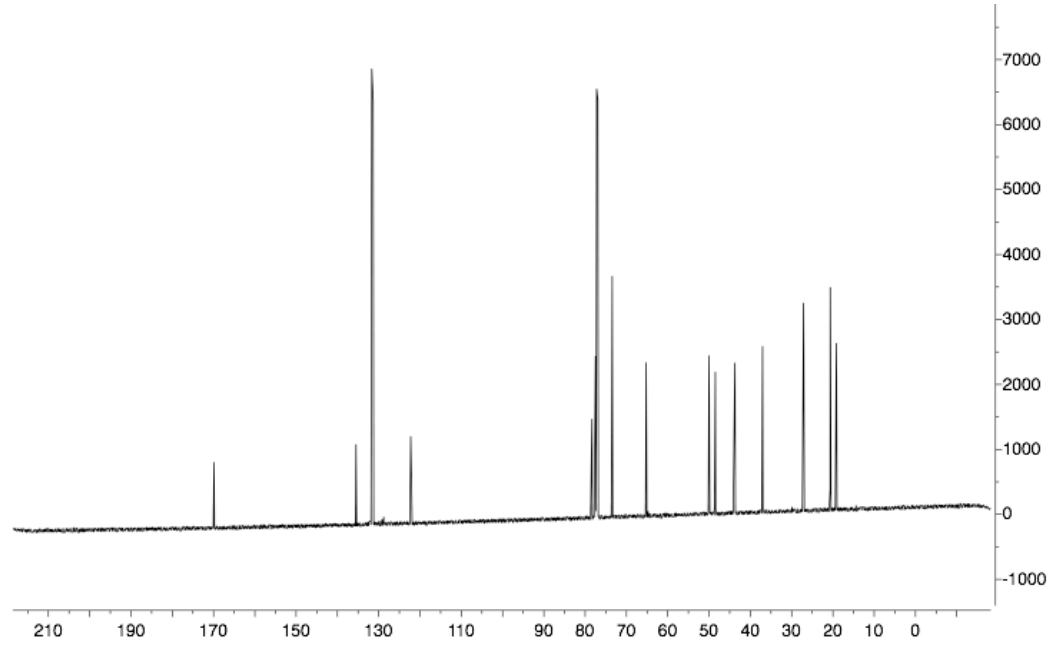

(*S*)-2-(4-bromobenzyl)-3-isobutyl-5-(prop-2-yn-1-yl)-1,2,5-thiadiazepin-1,1-dioxide-4-one 5.9{*3*}

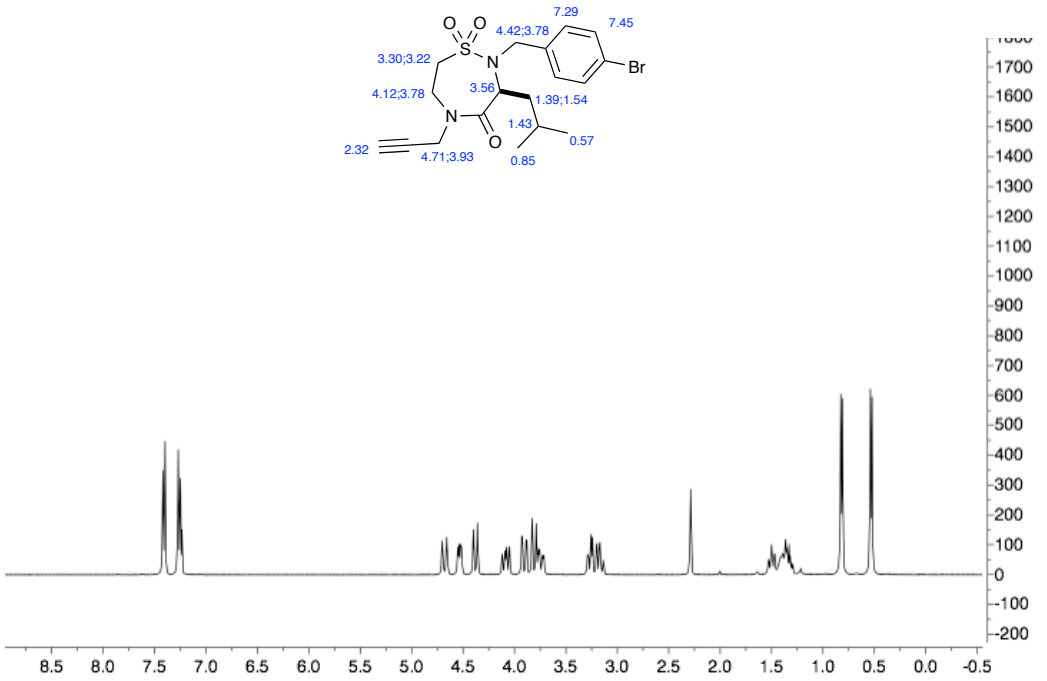

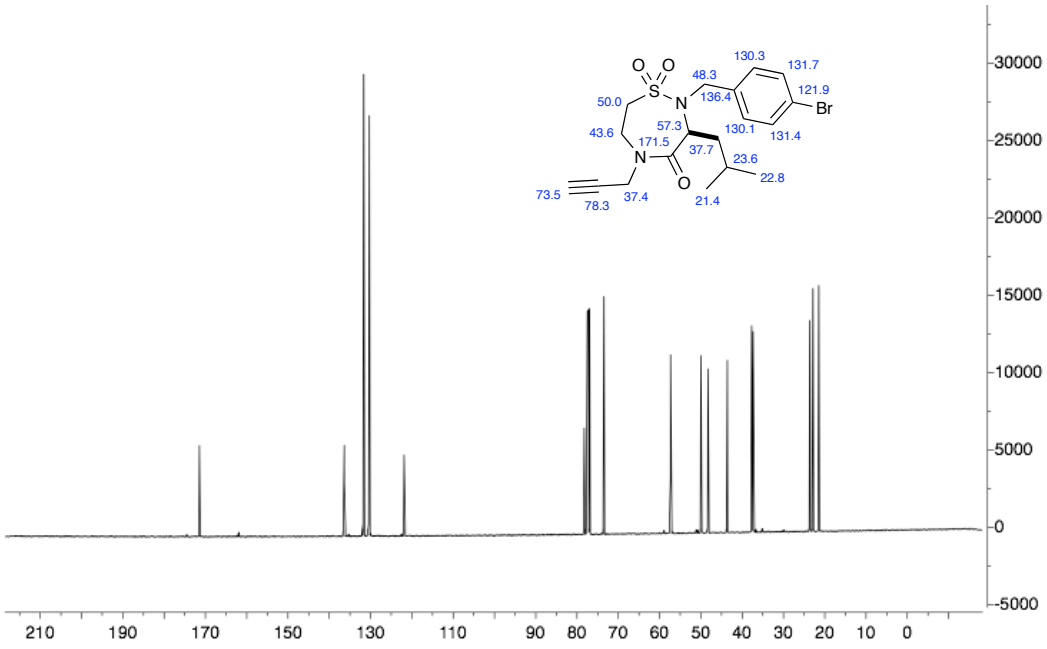

(±) 2-(4-bromobenzyl)-5-((1-(furan-2-ylmethyl)-1H-1,2,3-triazol-4-yl)methyl)-3-methyl-1,2,5-thiadiazepin-1,1-dioxide 4-one 5.10{*l*}

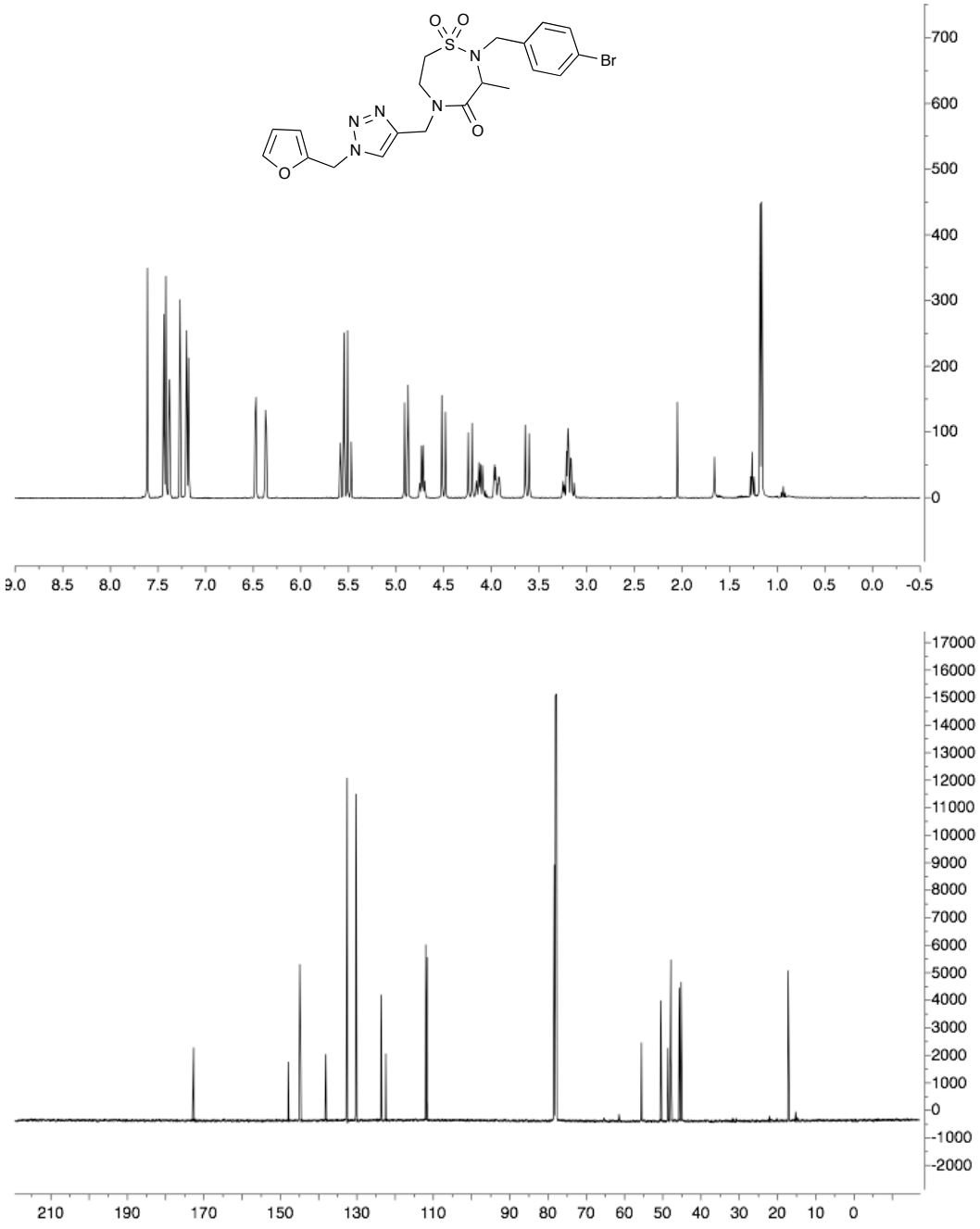

(*S*)-2-((4'-fluoro-[1,1'-biphenyl]-4-yl)methyl)-5-((1-(furan-2-ylmethyl)-1H-1,2,3-triazol-4-yl)methyl)-3-isopropyl-1,2,5-thiadiazepin-1,1-dioxide 4-one 5.13{*2,2,1*}

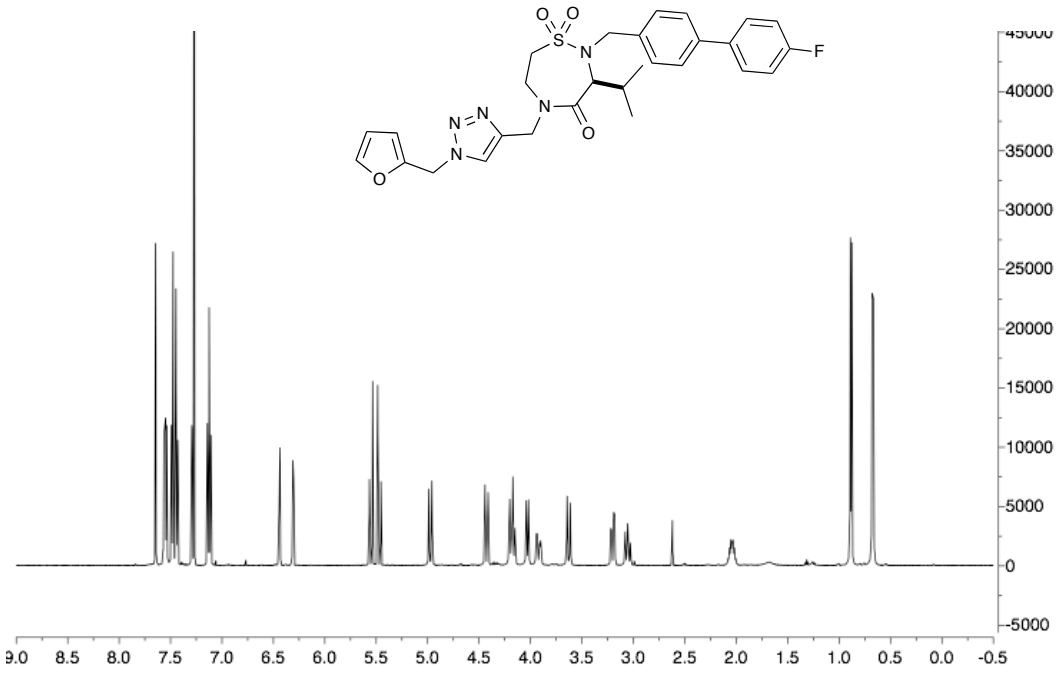

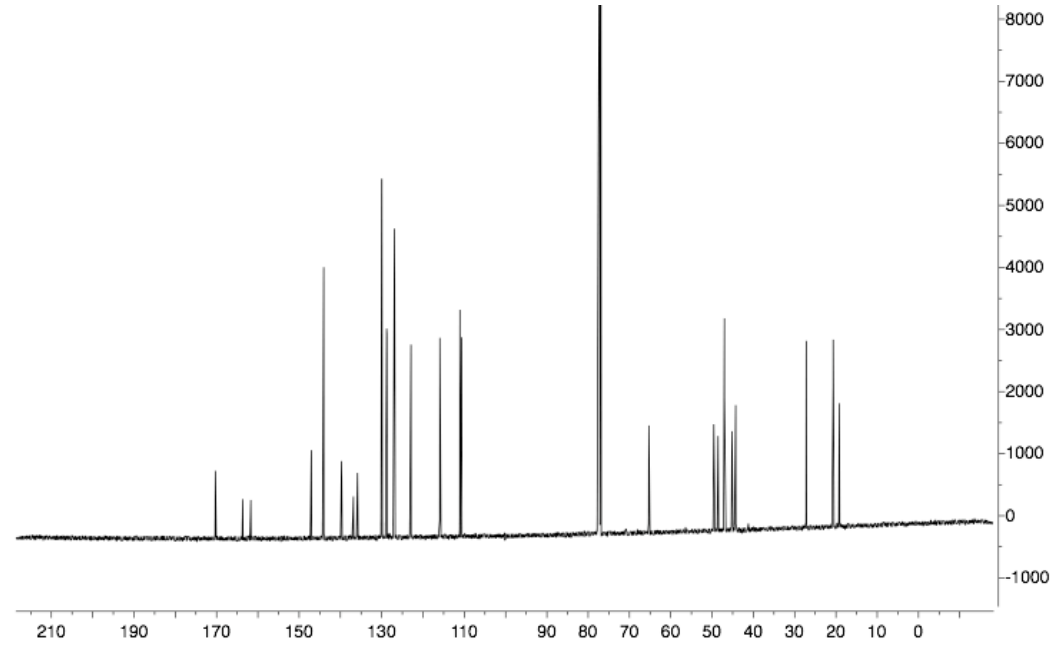

Appendix B

X-ray Data and Miscellaneous

CCD Experimental

A full hemisphere of diffracted intensities (1850 xx-second frames with a ω scan width of 0.30°) was measured at 100K using graphite-monochromated MoKα radiation (λ= 0.71073 Å) on a Bruker SMART APEX CCD Single Crystal Diffraction System equipped with an Oxford Cryosystems 700 Series Cryostream Low Temperature Device. X-rays were provided by a fine-focus sealed x-ray tube operated at 50kV and 30mA.

X-Ray Crystal Structure of Compound **3.21**

Comments

The asymmetric unit contains two crystallographically-independent $C_{15}H_{21}NO_6S$ molecules. The two hydroxyl groups in the first crystallographically-independent $C_{15}H_{21}NO_6S$ molecule are each disordered with two preferred orientations about their O-C bonds. The major occupancy orientation for oxygen atom O(4) is occupied 75% of the time and the minor orientation [O(4)] is occupied 25% of the time. The major occupancy orientation for oxygen atom O(5) is occupied 65% of the time and the minor orientation [O(5)] is occupied 35% of the time. The structure was refined as a 53/47 racemic twin. All displacement ellipsoids are drawn at the 50% probability level.

Experimental Description

Colorless lathe-shaped crystals of $C_{15}H_{21}NO_6S$ are, at 100(2) K, orthorhombic, space group $P2_12_12_1 - D_2^4$ (No. 19) (1) with **a** = 9.226(1) Å, **b** = 10.670(1) Å, **c** = 32.049(2) Å, V = 3154.8(3) $Å^3$ and Z = 8 molecules {d_{calcd} = 1.446 g/cm^3; $_a$(MoK) = 0.236 mm^{-1}}. A full hemisphere of diffracted intensities (1850 10-second frames with a scan width of 0.30) was measured using graphite-monochromated MoK radiation (= 0.71073 Å) on a Bruker SMART APEX CCD Single Crystal Diffraction System (2). X-rays were provided by a fine-focus sealed x-ray tube operated at 50kV and 30mA.

Lattice constants were determined with the Bruker SAINT software package using peak centers for 3105 reflections. A total of 29074 integrated reflection intensities having 2((MoK)< 52.00 were produced using the Bruker program SAINT(3); 6217 of these were unique and gave R_{int} = 0.068 with a coverage which was 100.0% complete. The data were corrected empirically for variable absorption effects using equivalent reflections; the relative transmission factors ranged from 0.827 to 1.000. The Bruker software package SHELXTL was used to solve the structure using "direct methods" techniques. All stages of weighted full-matrix least-squares refinement were conducted using F_o^2 data with the SHELXTL Version 6.10 software package (4).

The hydroxyl protons were included in the structural model at fixed idealized positions (assuming sp^3-hybridization of the oxygen atom and an O-H bond length of 0.84 Å). All methyl groups were incorporated into the structural model as rigid groups (using idealized sp^3-hybridized geometry and a C-H bond length of 0.98 Å) that were allowed to rotate about their O-C bonds during least-squares refinement cycles. The remaining hydrogen atoms were included into the structural model as idealized atoms (assuming sp^2- or sp^3-hybridization of the carbon atoms and C-H bond lengths of 0.95 – 1.00 Å). The isotropic thermal parameters of all hydrogen atoms were fixed at values 1.2 (nonmethyl) or 1.5 (methyl) times the equivalent isotropic thermal parameter of the oxygen or carbon atom to which they are covalently bonded.

The two hydroxyl groups in the first crystallographically-independent $C_{15}H_{21}NO_6S$ molecule are each disordered with two preferred orientations about their O-C bonds. The major orientation for oxygen atom O(4) is occupied 75% of the time and the minor orientation [O(4)] is occupied 25% of the time. The major orientation for oxygen atom O(5) is occupied 65% of the time and the minor orientation [O(5)] is occupied 35% of the time. The structure was refined as a 53/47 racemic twin.

The final structural model incorporated anisotropic thermal parameters for all nonhydrogen atoms and isotropic thermal parameters for all hydrogen atoms. A total of 438 parameters were refined using no restraints, 6217 data and weights of w = 1/

$[^2(F^2) + (0.0503\ P)^2 + 1.045\ P]$, where $P = [F_o^2 + 2F_c^2] / 3$. Final agreement factors at convergence are: R_1(unweighted, based on F) = 0.048 for 5309 independent absorption-corrected "observed" reflections having 2(MoK)< 52.00 and I>2(I); R_1(unweighted, based on F) = 0.060 and wR_2(weighted, based on F^2) = 0.107 for all 6217 independent absorption-corrected reflections having 2(MoK)< 52.00. The largest shift/s.u. was 0.000 in the final refinement cycle. The final difference Fourier had maxima and minima of 0.47 $e^-/Å^3$ and -0.38 $e^-/Å^3$, respectively.

Acknowledgments

Special thanks to the National Science Foundation (grant CHE-0079282) and the University of Kansas for funds to purchase the x-ray instrument and computers.

References

(1) International Tables for Crystallography, Vol A, 4th ed., Kluwer: Boston (1996).
(2) Data Collection: SMART Software Reference Manual (1998). Bruker-AXS, 5465 E. Cheryl Parkway, Madison, WI 53711-5373 USA.
(3) Data Reduction: SAINT Software Reference Manual (1998). Bruker-AXS, 6300 Enterprise Dr., Madison, WI 53719-1173, USA.
(4) G. M. Sheldrick (2000). SHELXTL Version 6.10 Reference Manual. Bruker-AXS, 5465 E. Cheryl Parkway, Madison, WI 53711-5373 USA.

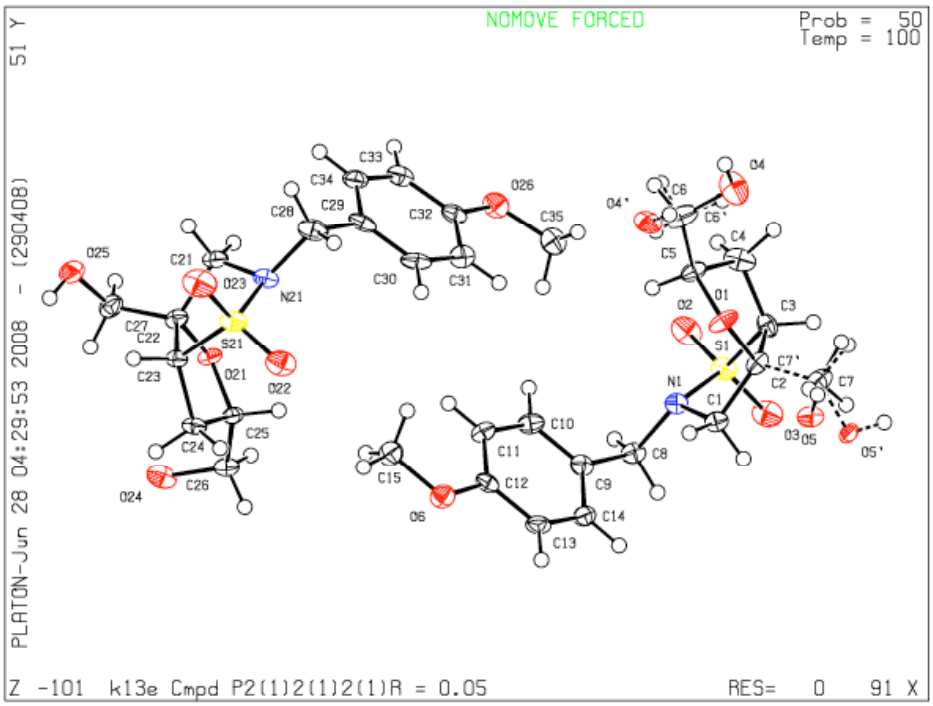
NOMOVE FORCED
Prob = 50
Temp = 100
51 Y
PLATON-Jun 28 04:29:53 2008 - (290408)
Z -101 k13e Cmpd P2(1)2(1)2(1)R = 0.05
RES= 0 91 X
O4
O4'
C6
C6'
C5
C4
O2
O1
C3
S1
C7'
C2
C7
N1
C1
O3
O5
O5'
C8
C9
C10
C11
C12
C13
C14
C15
O6
O26
C35
C33
C34
C29
C28
C32
C30
C31
O25
C21
O23
N21
C27
C22
S21
C23
O21
O22
C24
C25
O24
C26

Table 1. Crystal data and structure refinement for $C_{15}H_{21}NO_6S$.

Empirical formula	$C_{15}H_{21}NO_6S$	
Formula weight	343.39	
Temperature	100(2) K	
Wavelength	0.71073 Å	
Crystal system	Orthorhombic	
Space group	$P2_12_12_1 - D_2^4$ (No. 19)	
Unit cell dimensions	**a** = 9.226(1) Å	= 90.000°
	b = 10.670(1) Å	= 90.000°
	c = 32.049(2) Å	= 90.000°
Volume	3154.8(3) Å3	
Z	8	
Density (calculated)	1.446 Mg/m^3	
Absorption coefficient	0.236 mm^{-1}	
F(000)	1456	
Crystal size	0.46 x 0.14 x 0.06 mm^3	
Theta range for data collection	2.01° to 26.00°	
Index ranges	-11 h 11, -13 k 13, -39 l 39	
Reflections collected	29074	
Independent reflections	6217 [R_{int} = 0.068]	
Completeness to theta = 26.00°	100.0 %	
Absorption correction	Semi-empirical from equivalents	
Max. and min. transmission	1.000 and 0.827	
Refinement method	Full-matrix least-squares on F^2	
Data / restraints / parameters	6217 / 0 / 438	
Goodness-of-fit on F^2	1.039	
Final R indices [I>2sigma(I)]	R_1 = 0.048, wR_2 = 0.103	
R indices (all data)	R_1 = 0.060, wR_2 = 0.107	
Absolute structure parameter	0.0(14)	
Largest diff. peak and hole	0.47 and -0.38 $e^-/Å^3$	

$R_1 = \| |F_o| - |F_c| \| / |F_o|$

$wR_2 = \{ [w(F_o^2 - F_c^2)^2] / [w(F_o^2)^2] \}^{1/2}$

Table 2. Atomic coordinates (x 10^4) and equivalent isotropic displacement parameters ($Å^2$ x 10^3) for $C_{15}H_{21}NO_6S$. U(eq) is defined as one third of the trace of the orthogonalized U_{ij} tensor.

	x	y	z	U(eq)
S(1)	-543(1)	2889(1)	830(1)	21(1)
O(1)	2991(2)	1576(2)	766(1)	24(1)
O(2)	-640(3)	4093(2)	1028(1)	32(1)
O(3)	-1812(2)	2468(2)	603(1)	32(1)
O(6)	2146(2)	-931(2)	2782(1)	26(1)
N(1)	3(3)	1849(2)	1173(1)	18(1)
C(1)	597(3)	791(3)	935(1)	20(1)
C(2)	1573(3)	1366(3)	600(1)	19(1)
C(3)	991(3)	2704(3)	494(1)	20(1)
C(4)	2240(3)	3572(3)	593(1)	28(1)
C(5)	3150(3)	2844(3)	901(1)	20(1)
C(6)	4726(4)	3169(3)	916(1)	34(1)
O(4)	5347(3)	3193(3)	538(1)	40(1)
C(6')	4726(4)	3169(3)	916(1)	34(1)
O(4')	5547(9)	2590(8)	1131(3)	29(3)
C(7)	1733(4)	518(3)	225(1)	32(1)
O(5)	2153(4)	-632(3)	317(1)	22(1)
C(7')	1733(4)	518(3)	225(1)	32(1)
O(5')	502(6)	-45(5)	93(2)	20(2)
C(8)	-1019(3)	1535(3)	1512(1)	21(1)
C(9)	-207(3)	889(3)	1855(1)	20(1)
C(10)	624(3)	1582(3)	2133(1)	23(1)
C(11)	1420(3)	1022(3)	2447(1)	23(1)
C(12)	1417(3)	-279(3)	2481(1)	19(1)
C(13)	609(4)	-988(3)	2202(1)	24(1)
C(14)	-195(3)	-409(3)	1896(1)	21(1)
C(15)	3026(4)	-230(3)	3064(1)	27(1)
S(21)	5383(1)	2143(1)	3918(1)	23(1)

O(21)	2140(2)	3664(2)	4124(1)	19(1)
O(22)	5087(3)	1067(2)	3664(1)	32(1)
O(23)	6818(2)	2227(3)	4090(1)	38(1)
O(24)	-127(2)	2485(2)	4581(1)	29(1)
O(25)	4843(3)	4510(2)	4909(1)	38(1)
O(26)	2185(3)	6122(2)	2104(1)	28(1)
N(21)	4902(3)	3410(2)	3663(1)	20(1)
C(21)	4542(3)	4377(3)	3969(1)	23(1)
C(22)	3589(3)	3743(3)	4290(1)	19(1)
C(23)	4106(3)	2362(3)	4334(1)	17(1)
C(24)	2729(3)	1582(3)	4302(1)	20(1)
C(25)	1713(3)	2391(3)	4044(1)	18(1)
C(26)	122(3)	2254(3)	4150(1)	22(1)
C(27)	3483(4)	4443(3)	4700(1)	25(1)
C(28)	5794(3)	3771(3)	3301(1)	29(1)
C(29)	4861(3)	4392(3)	2977(1)	23(1)
C(30)	4152(3)	3674(3)	2677(1)	25(1)
C(31)	3266(3)	4210(3)	2378(1)	25(1)
C(32)	3032(3)	5498(3)	2381(1)	22(1)
C(33)	3699(3)	6223(3)	2683(1)	24(1)
C(34)	4622(4)	5685(3)	2973(1)	25(1)
C(35)	1507(4)	5421(3)	1778(1)	33(1)

Table 3. Bond lengths [Å] for $C_{15}H_{21}NO_6S$.

S(1)-O(2)	1.436(2)
S(1)-O(3)	1.449(2)
S(1)-N(1)	1.642(2)
S(1)-C(3)	1.789(3)
O(1)-C(5)	1.428(4)
O(1)-C(2)	1.430(3)
O(6)-C(12)	1.368(4)
O(6)-C(15)	1.427(4)
N(1)-C(1)	1.469(4)
N(1)-C(8)	1.476(4)
C(1)-C(2)	1.530(4)
C(2)-C(7)	1.511(4)
C(2)-C(3)	1.562(4)
C(3)-C(4)	1.513(4)
C(4)-C(5)	1.511(4)
C(5)-C(6)	1.496(4)
C(6)-O(4)	1.341(5)
C(7)-O(5)	1.321(5)
C(8)-C(9)	1.499(4)
C(9)-C(10)	1.389(4)
C(9)-C(14)	1.392(4)
C(10)-C(11)	1.382(4)
C(11)-C(12)	1.392(4)
C(12)-C(13)	1.388(4)
C(13)-C(14)	1.375(4)
S(21)-O(22)	1.434(2)
S(21)-O(23)	1.437(2)
S(21)-N(21)	1.641(2)
S(21)-C(23)	1.794(3)
O(21)-C(25)	1.437(3)
O(21)-C(22)	1.441(3)
O(24)-C(26)	1.422(4)

O(25)-C(27)	1.425(4)
O(26)-C(32)	1.357(4)
O(26)-C(35)	1.429(4)
N(21)-C(21)	1.463(4)
N(21)-C(28)	1.473(4)
C(21)-C(22)	1.512(4)
C(22)-C(27)	1.513(4)
C(22)-C(23)	1.555(4)
C(23)-C(24)	1.522(4)
C(24)-C(25)	1.518(4)
C(25)-C(26)	1.513(4)
C(28)-C(29)	1.503(4)
C(29)-C(30)	1.392(5)
C(29)-C(34)	1.396(4)
C(30)-C(31)	1.385(5)
C(31)-C(32)	1.391(5)
C(32)-C(33)	1.382(5)
C(33)-C(34)	1.386(5)

Table 4. Bond angles [°] for $C_{15}H_{21}NO_6S$.

O(2)-S(1)-O(3)	116.7(2)
O(2)-S(1)-N(1)	109.1(1)
O(3)-S(1)-N(1)	112.0(1)
O(2)-S(1)-C(3)	114.5(2)
O(3)-S(1)-C(3)	107.6(1)
N(1)-S(1)-C(3)	94.9(1)
C(5)-O(1)-C(2)	110.8(2)
C(12)-O(6)-C(15)	117.5(2)
C(1)-N(1)-C(8)	116.5(2)
C(1)-N(1)-S(1)	106.6(2)
C(8)-N(1)-S(1)	116.7(2)
N(1)-C(1)-C(2)	106.0(2)
O(1)-C(2)-C(7)	107.5(2)
O(1)-C(2)-C(1)	109.9(2)
C(7)-C(2)-C(1)	112.0(3)
O(1)-C(2)-C(3)	104.6(2)
C(7)-C(2)-C(3)	114.1(3)
C(1)-C(2)-C(3)	108.4(2)
C(4)-C(3)-C(2)	104.6(2)
C(4)-C(3)-S(1)	114.1(2)
C(2)-C(3)-S(1)	104.1(2)
C(5)-C(4)-C(3)	104.2(3)
O(1)-C(5)-C(6)	109.2(2)
O(1)-C(5)-C(4)	103.4(2)
C(6)-C(5)-C(4)	116.2(3)
O(4)-C(6)-C(5)	113.0(3)
O(5)-C(7)-C(2)	114.1(3)
N(1)-C(8)-C(9)	109.0(2)
C(10)-C(9)-C(14)	117.7(3)
C(10)-C(9)-C(8)	120.2(3)
C(14)-C(9)-C(8)	122.0(3)
C(11)-C(10)-C(9)	122.0(3)

C(10)-C(11)-C(12)	119.1(3)
O(6)-C(12)-C(13)	116.3(3)
O(6)-C(12)-C(11)	124.0(3)
C(13)-C(12)-C(11)	119.7(3)
C(14)-C(13)-C(12)	120.2(3)
C(13)-C(14)-C(9)	121.2(3)
O(22)-S(21)-O(23)	116.3(2)
O(22)-S(21)-N(21)	108.9(1)
O(23)-S(21)-N(21)	112.9(2)
O(22)-S(21)-C(23)	113.6(1)
O(23)-S(21)-C(23)	108.2(2)
N(21)-S(21)-C(23)	94.9(1)
C(25)-O(21)-C(22)	112.1(2)
C(32)-O(26)-C(35)	118.3(3)
C(21)-N(21)-C(28)	118.1(2)
C(21)-N(21)-S(21)	107.9(2)
C(28)-N(21)-S(21)	117.2(2)
N(21)-C(21)-C(22)	105.8(2)
O(21)-C(22)-C(21)	108.3(2)
O(21)-C(22)-C(27)	106.8(2)
C(21)-C(22)-C(27)	114.0(3)
O(21)-C(22)-C(23)	105.2(2)
C(21)-C(22)-C(23)	107.9(2)
C(27)-C(22)-C(23)	114.1(2)
C(24)-C(23)-C(22)	104.8(2)
C(24)-C(23)-S(21)	115.2(2)
C(22)-C(23)-S(21)	104.9(2)
C(25)-C(24)-C(23)	104.0(2)
O(21)-C(25)-C(26)	108.5(2)
O(21)-C(25)-C(24)	105.7(2)
C(26)-C(25)-C(24)	115.0(2)
O(24)-C(26)-C(25)	111.0(2)
O(25)-C(27)-C(22)	112.1(3)
N(21)-C(28)-C(29)	109.9(2)

C(30)-C(29)-C(34)	117.6(3)
C(30)-C(29)-C(28)	120.2(3)
C(34)-C(29)-C(28)	122.2(3)
C(31)-C(30)-C(29)	121.9(3)
C(30)-C(31)-C(32)	119.6(3)
O(26)-C(32)-C(33)	116.1(3)
O(26)-C(32)-C(31)	124.7(3)
C(33)-C(32)-C(31)	119.3(3)
C(32)-C(33)-C(34)	120.7(3)
C(33)-C(34)-C(29)	120.8(3)

Table 5. Anisotropic displacement parameters ($Å^2 x\ 10^3$) for $C_{15}H_{21}NO_6S$. The anisotropic displacement factor exponent takes the form: $-2^2[\ h^2\ a^{*2}U_{11} + ... + 2\ h\ k\ a^*\ b^*\ U_{12}\ ]$

	U_{11}	U_{22}	U_{33}	U_{23}	U_{13}	U_{12}
S(1)	14(1)	20(1)	28(1)	3(1)	1(1)	7(1)
O(1)	15(1)	14(1)	43(1)	-7(1)	-10(1)	2(1)
O(2)	39(2)	19(1)	38(1)	3(1)	11(1)	14(1)
O(3)	15(1)	38(2)	42(1)	10(1)	-5(1)	3(1)
O(6)	30(1)	19(1)	29(1)	1(1)	-4(1)	1(1)
N(1)	16(1)	15(1)	24(1)	1(1)	1(1)	3(1)
C(1)	17(2)	17(2)	26(2)	0(1)	-1(1)	1(1)
C(2)	14(2)	19(2)	24(2)	-4(1)	-4(1)	4(1)
C(3)	17(2)	26(2)	17(2)	4(1)	3(1)	5(1)
C(4)	17(2)	24(2)	44(2)	10(2)	4(2)	6(1)
C(5)	15(2)	16(2)	31(2)	-7(1)	1(1)	0(1)
C(6)	21(2)	22(2)	60(2)	-6(2)	-6(2)	-2(1)
O(4)	17(2)	69(3)	34(2)	11(2)	-1(2)	7(2)
C(6')	21(2)	22(2)	60(2)	-6(2)	-6(2)	-2(1)
O(4')	13(4)	42(6)	33(5)	11(4)	-1(4)	-6(4)
C(7)	24(2)	36(2)	37(2)	-17(2)	7(2)	-8(2)
O(5)	17(2)	18(2)	32(2)	-1(2)	4(1)	1(1)
C(7')	24(2)	36(2)	37(2)	-17(2)	7(2)	-8(2)
O(5')	18(3)	24(3)	18(3)	-7(2)	1(3)	-7(3)
C(8)	15(2)	21(2)	29(2)	-3(1)	4(1)	1(1)
C(9)	17(2)	21(2)	23(2)	-2(1)	6(1)	3(1)
C(10)	22(2)	15(2)	33(2)	1(1)	-1(2)	1(1)
C(11)	22(2)	17(2)	28(2)	-3(1)	-3(1)	-3(1)
C(12)	18(2)	19(2)	21(2)	3(1)	7(1)	2(1)
C(13)	30(2)	14(2)	29(2)	-2(1)	8(2)	-5(1)
C(14)	20(2)	19(2)	24(2)	-3(1)	2(1)	-3(1)
C(15)	28(2)	24(2)	28(2)	1(1)	-5(2)	1(2)
S(21)	14(1)	22(1)	34(1)	7(1)	1(1)	2(1)

O(21)	14(1)	15(1)	29(1)	1(1)	-4(1)	-3(1)
O(22)	37(1)	17(1)	41(1)	-1(1)	9(1)	4(1)
O(23)	14(1)	48(2)	51(2)	15(1)	-6(1)	2(1)
O(24)	26(1)	23(1)	37(1)	3(1)	12(1)	4(1)
O(25)	42(2)	41(1)	30(1)	8(1)	-14(1)	-21(1)
O(26)	31(1)	23(1)	30(1)	4(1)	1(1)	5(1)
N(21)	17(1)	16(1)	27(1)	4(1)	4(1)	1(1)
C(21)	19(2)	19(2)	31(2)	4(1)	-2(1)	-7(1)
C(22)	14(2)	18(2)	25(2)	2(1)	-5(1)	0(1)
C(23)	14(1)	16(2)	21(2)	4(1)	-1(1)	-1(1)
C(24)	17(2)	16(2)	27(2)	6(1)	0(1)	-3(1)
C(25)	16(2)	16(2)	21(2)	-1(1)	1(1)	-5(1)
C(26)	17(2)	20(2)	29(2)	1(1)	1(1)	-3(1)
C(27)	31(2)	18(2)	27(2)	1(1)	-9(2)	-2(1)
C(28)	19(2)	28(2)	39(2)	7(2)	5(1)	-1(1)
C(29)	16(2)	23(2)	30(2)	8(1)	12(1)	1(1)
C(30)	21(2)	12(2)	42(2)	4(1)	10(2)	-1(1)
C(31)	22(2)	22(2)	30(2)	-2(1)	3(1)	2(1)
C(32)	17(2)	23(2)	26(2)	3(1)	10(1)	-1(1)
C(33)	26(2)	17(2)	30(2)	0(1)	12(1)	1(1)
C(34)	25(2)	21(2)	28(2)	-1(1)	9(1)	-7(1)
C(35)	37(2)	34(2)	29(2)	4(2)	-1(2)	-1(2)

Table 6. Hydrogen coordinates (x 10^4) and isotropic displacement parameters ($Å^2$ x 10^3) for $C_{15}H_{21}NO_6S$.

	x	y	z	U(eq)
H(1A)	-194	300	805	24
H(1B)	1164	230	1119	24
H(3)	704	2768	194	24
H(4A)	2803	3769	338	34
H(4B)	1887	4364	718	34
H(5)	2724	2935	1187	25
H(6A)	4839	4002	1049	41
H(6B)	5236	2548	1093	41
H(4O)	6253	3186	565	48
H(6C)	5096	3123	627	41
H(6D)	4794	4058	1003	41
H(4O')	6175	2244	980	35
H(7A)	791	476	77	39
H(7B)	2446	894	31	39
H(5O)	3020	-731	243	27
H(7C)	2131	1018	-9	39
H(7D)	2451	-140	293	39
H(5O')	292	213	-147	24
H(8A)	-1792	979	1404	26
H(8B)	-1477	2309	1619	26
H(10)	646	2469	2107	28
H(11)	1962	1517	2638	27
H(13)	610	-1876	2222	29
H(14)	-752	-905	1709	25
H(15A)	3528	-806	3254	40
H(15B)	2413	341	3227	40
H(15C)	3741	256	2907	40
H(24O)	-740	3062	4607	35
H(25O)	4906	3919	5081	45

H(21A)	4018	5079	3835	27
H(21B)	5432	4709	4102	27
H(23)	4584	2228	4611	20
H(24A)	2922	774	4160	24
H(24B)	2317	1414	4581	24
H(25)	1859	2200	3742	21
H(26A)	-450	2853	3981	26
H(26B)	-204	1397	4079	26
H(27A)	3126	5303	4646	30
H(27B)	2771	4017	4882	30
H(28A)	6259	3017	3180	34
H(28B)	6567	4354	3391	34
H(30)	4279	2791	2679	30
H(31)	2821	3701	2171	29
H(33)	3523	7100	2691	29
H(34)	5098	6201	3172	30
H(35A)	935	5988	1602	50
H(35B)	870	4784	1900	50
H(35C)	2252	5012	1608	50

Table 7. Torsion angles [°] for $C_{15}H_{21}NO_6S$.

O(2)-S(1)-N(1)-C(1)	-159.30(19)
O(3)-S(1)-N(1)-C(1)	70.0(2)
C(3)-S(1)-N(1)-C(1)	-41.3(2)
O(2)-S(1)-N(1)-C(8)	68.5(2)
O(3)-S(1)-N(1)-C(8)	-62.2(2)
C(3)-S(1)-N(1)-C(8)	-173.5(2)
C(8)-N(1)-C(1)-C(2)	178.3(2)
S(1)-N(1)-C(1)-C(2)	46.0(3)
C(5)-O(1)-C(2)-C(7)	140.9(3)
C(5)-O(1)-C(2)-C(1)	-96.9(3)
C(5)-O(1)-C(2)-C(3)	19.3(3)
N(1)-C(1)-C(2)-O(1)	85.8(3)
N(1)-C(1)-C(2)-C(7)	-154.8(3)
N(1)-C(1)-C(2)-C(3)	-28.0(3)
O(1)-C(2)-C(3)-C(4)	3.4(3)
C(7)-C(2)-C(3)-C(4)	-113.8(3)
C(1)-C(2)-C(3)-C(4)	120.6(3)
O(1)-C(2)-C(3)-S(1)	-116.6(2)
C(7)-C(2)-C(3)-S(1)	126.2(2)
C(1)-C(2)-C(3)-S(1)	0.6(3)
O(2)-S(1)-C(3)-C(4)	23.3(3)
O(3)-S(1)-C(3)-C(4)	154.8(2)
N(1)-S(1)-C(3)-C(4)	-90.3(2)
O(2)-S(1)-C(3)-C(2)	136.69(19)
O(3)-S(1)-C(3)-C(2)	-91.8(2)
N(1)-S(1)-C(3)-C(2)	23.1(2)
C(2)-C(3)-C(4)-C(5)	-22.9(3)
S(1)-C(3)-C(4)-C(5)	90.2(3)
C(2)-O(1)-C(5)-C(6)	-158.4(3)
C(2)-O(1)-C(5)-C(4)	-34.1(3)
C(3)-C(4)-C(5)-O(1)	34.4(3)
C(3)-C(4)-C(5)-C(6)	154.0(3)

O(1)-C(5)-C(6)-O(4)	66.8(4)
C(4)-C(5)-C(6)-O(4)	-49.6(4)
O(1)-C(2)-C(7)-O(5)	67.8(4)
C(1)-C(2)-C(7)-O(5)	-53.0(4)
C(3)-C(2)-C(7)-O(5)	-176.7(3)
C(1)-N(1)-C(8)-C(9)	69.0(3)
S(1)-N(1)-C(8)-C(9)	-163.4(2)
N(1)-C(8)-C(9)-C(10)	78.4(3)
N(1)-C(8)-C(9)-C(14)	-98.4(3)
C(14)-C(9)-C(10)-C(11)	-1.3(5)
C(8)-C(9)-C(10)-C(11)	-178.2(3)
C(9)-C(10)-C(11)-C(12)	1.5(5)
C(15)-O(6)-C(12)-C(13)	177.9(3)
C(15)-O(6)-C(12)-C(11)	-3.8(4)
C(10)-C(11)-C(12)-O(6)	-178.9(3)
C(10)-C(11)-C(12)-C(13)	-0.6(5)
O(6)-C(12)-C(13)-C(14)	178.0(3)
C(11)-C(12)-C(13)-C(14)	-0.5(5)
C(12)-C(13)-C(14)-C(9)	0.7(5)
C(10)-C(9)-C(14)-C(13)	0.2(5)
C(8)-C(9)-C(14)-C(13)	177.0(3)
O(22)-S(21)-N(21)-C(21)	153.2(2)
O(23)-S(21)-N(21)-C(21)	-76.0(2)
C(23)-S(21)-N(21)-C(21)	36.1(2)
O(22)-S(21)-N(21)-C(28)	-70.6(3)
O(23)-S(21)-N(21)-C(28)	60.2(3)
C(23)-S(21)-N(21)-C(28)	172.3(2)
C(28)-N(21)-C(21)-C(22)	178.0(2)
S(21)-N(21)-C(21)-C(22)	-46.2(3)
C(25)-O(21)-C(22)-C(21)	113.0(3)
C(25)-O(21)-C(22)-C(27)	-123.8(3)
C(25)-O(21)-C(22)-C(23)	-2.2(3)
N(21)-C(21)-C(22)-O(21)	-79.6(3)
N(21)-C(21)-C(22)-C(27)	161.6(2)

N(21)-C(21)-C(22)-C(23)	33.8(3)
O(21)-C(22)-C(23)-C(24)	-15.6(3)
C(21)-C(22)-C(23)-C(24)	-131.1(3)
C(27)-C(22)-C(23)-C(24)	101.1(3)
O(21)-C(22)-C(23)-S(21)	106.2(2)
C(21)-C(22)-C(23)-S(21)	-9.3(3)
C(27)-C(22)-C(23)-S(21)	-137.1(2)
O(22)-S(21)-C(23)-C(24)	-13.3(3)
O(23)-S(21)-C(23)-C(24)	-144.1(2)
N(21)-S(21)-C(23)-C(24)	99.8(2)
O(22)-S(21)-C(23)-C(22)	-128.01(19)
O(23)-S(21)-C(23)-C(22)	101.2(2)
N(21)-S(21)-C(23)-C(22)	-14.9(2)
C(22)-C(23)-C(24)-C(25)	26.5(3)
S(21)-C(23)-C(24)-C(25)	-88.2(3)
C(22)-O(21)-C(25)-C(26)	143.2(2)
C(22)-O(21)-C(25)-C(24)	19.3(3)
C(23)-C(24)-C(25)-O(21)	-28.2(3)
C(23)-C(24)-C(25)-C(26)	-147.9(3)
O(21)-C(25)-C(26)-O(24)	-62.8(3)
C(24)-C(25)-C(26)-O(24)	55.4(3)
O(21)-C(22)-C(27)-O(25)	176.1(2)
C(21)-C(22)-C(27)-O(25)	-64.3(3)
C(23)-C(22)-C(27)-O(25)	60.3(3)
C(21)-N(21)-C(28)-C(29)	-80.5(3)
S(21)-N(21)-C(28)-C(29)	147.8(2)
N(21)-C(28)-C(29)-C(30)	-87.6(3)
N(21)-C(28)-C(29)-C(34)	89.7(4)
C(34)-C(29)-C(30)-C(31)	1.6(5)
C(28)-C(29)-C(30)-C(31)	179.0(3)
C(29)-C(30)-C(31)-C(32)	-2.1(5)
C(35)-O(26)-C(32)-C(33)	178.0(3)
C(35)-O(26)-C(32)-C(31)	-1.6(5)
C(30)-C(31)-C(32)-O(26)	-179.9(3)

C(30)-C(31)-C(32)-C(33)	0.5(5)
O(26)-C(32)-C(33)-C(34)	-178.0(3)
C(31)-C(32)-C(33)-C(34)	1.6(5)
C(32)-C(33)-C(34)-C(29)	-2.2(5)
C(30)-C(29)-C(34)-C(33)	0.6(4)
C(28)-C(29)-C(34)-C(33)	-176.8(3)

Table 8. Hydrogen bonds for $C_{15}H_{21}NO_6S$ [Å and °].

D-H...A	d(D-H)	d(H...A)	d(D...A)	<(DHA)
O(4)-H(4O)...O(3)#1	0.84	1.95	2.740(4)	157.3
O(4')-H(4O')...O(3)#1	0.84	2.23	2.968(9)	147.1
O(24)-H(24O)...O(5')#2	0.84	2.25	2.857(6)	129.5
O(25)-H(25O)...O(24)#3	0.84	1.85	2.684(3)	172.7

Symmetry transformations used to generate equivalent atoms: #1: x+1, y, z; #2: -x, y+1/2, -z+1/2; #3: x+1/2, -y+1/2, -z+1.

X-Ray Crystal Structure of Compound **3.25**

Comments

The asymmetric unit contains one $C_{14}H_{16}INO_5S$ molecule. All displacement ellipsoids are drawn at the 50% probability level.

Experimental Description

Colorless plate-shaped crystals of $C_{14}H_{16}INO_5S$ are, at 100(2) K, orthorhombic, space group $Pna2_1$ – C_{2v}^9 (No. 33) (1) with **a** = 7.9664(5) Å, **b** = 34.946(2) Å, **c** = 5.2792(4) Å, V = 1469.7(2) $Å^3$ and Z = 4 molecules {d_{calcd} = 1.976 g/cm^3; $_a$(MoK) = 2.345 mm^{-1}}. A full hemisphere of diffracted intensities (1850 10-second frames with a scan width of 0.30) was measured for a single-domain specimen using graphite-monochromated MoK radiation (= 0.71073 Å) on a Bruker SMART APEX CCD Single Crystal Diffraction System (2). X-rays were provided by a fine-focus sealed x-ray tube operated at 50kV and 30mA. Lattice constants were determined with the Bruker SAINT software package using peak centers for 6619 reflections. A total of 16743 integrated reflection intensities having 2((MoK)< 61.09 were produced using the Bruker program SAINT(3); 4416 of these were unique and gave R_{int} = 0.098 with a coverage which was 99.4% complete. The data were corrected empirically for variable absorption effects using equivalent reflections; the relative transmission factors ranged from 0.786 to 1.000. The Bruker software package SHELXTL was used to solve the structure using "direct methods" techniques. All stages of weighted full-matrix least-squares refinement were conducted using F_o^2 data with the SHELXTL Version 6.10 software package (4).

The hydroxyl protons were included in the structural model at fixed idealized positions (assuming sp^3-hybridization of the oxygen atom and an O-H bond length of 0.84 Å). The remaining hydrogen atoms were included into the structural model as idealized atoms (assuming sp^2- or sp^3-hybridization of the carbon atoms and C-H bond lengths of 0.95 – 1.00 Å). The isotropic thermal parameters of all hydrogen atoms were fixed at values 1.2 times the equivalent isotropic thermal parameter of the

oxygen or carbon atom to which they are covalently bonded.

The final structural model incorporated anisotropic thermal parameters for all nonhydrogen atoms and isotropic thermal parameters for all hydrogen atoms. A total of 199 parameters were refined using one restraint, 4416 data and weights of w = 1/ [^{2}(F^2) + (0.0221 P)^2 + 8.007 P], where P = [F_o^2 + 2F_c^2] / 3. Final agreement factors at convergence are: R_1(unweighted, based on F) = 0.057 for 4245 independent absorption-corrected "observed" reflections having 2(MoK)< 61.09 and I>2(I); R_1(unweighted, based on F) = 0.060 and wR_2(weighted, based on F^2) = 0.113 for all 4416 independent absorption-corrected reflections having 2(MoK)< 61.09. The largest shift/s.u. was 0.000 in the final refinement cycle. The top six peaks (1.45 – 1.05 $e^-/Å^3$) in the final difference map were within 0.88 Å of the iodine atom. The minima and next highest maxima in this final difference Fourier were –2.69 $e^-/Å^3$ and 1.05 $e^-/Å^3$, respectively.

Acknowledgment

Special thanks to the National Science Foundation (grant CHE-0079282) and the University of Kansas for funds to purchase the x-ray instrument and computers.

References

(1) International Tables for Crystallography, Vol A, 4th ed., Kluwer: Boston (1996).
(2) Data Collection: SMART Software Reference Manual (1998). Bruker-AXS, 5465 E. Cheryl Parkway, Madison, WI 53711-5373 USA.
(3) Data Reduction: SAINT Software Reference Manual (1998). Bruker-AXS, 6300 Enterprise Dr., Madison, WI 53719-1173, USA.
(4) G. M. Sheldrick (2000). SHELXTL Version 6.10 Reference Manual. Bruker-AXS, 5465 E. Cheryl Parkway, Madison, WI 53711-5373 USA.

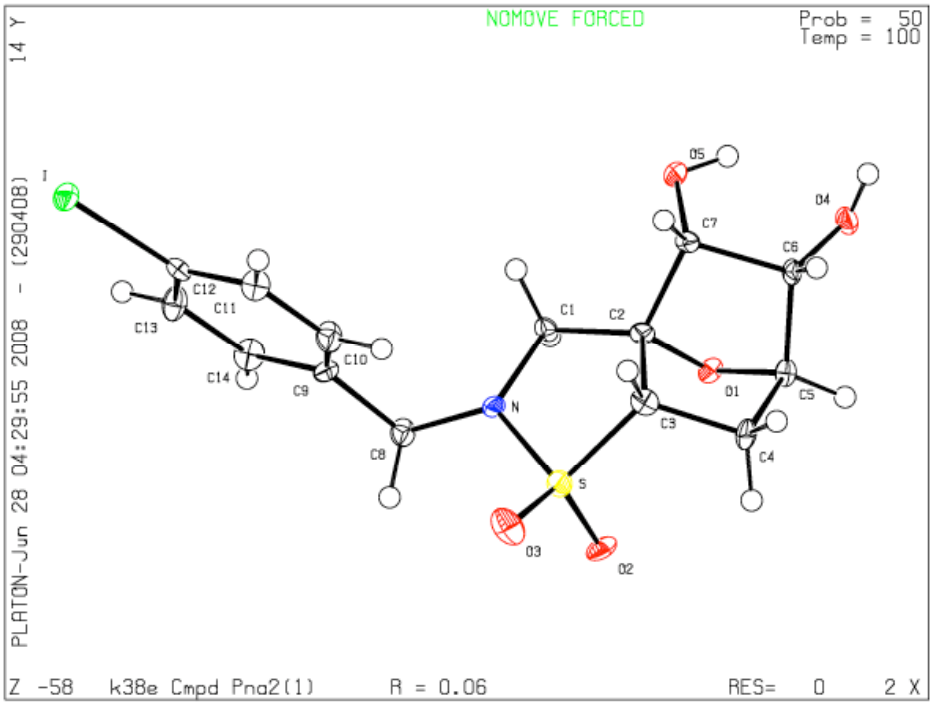
NOMOVE FORCED
Prob = 50
Temp = 100
14 Y
PLATON-Jun 28 04:29:55 2008 - (290408)
I
C12
C11
C13
C14
C10
C9
C8
N
C1
C2
C7
O5
O4
C6
O1
C5
C3
C4
S
O3
O2
Z -58 k38e Cmpd Pna2(1) R = 0.06 RES= 0 2 X

Table 1. Crystal data and structure refinement for $C_{14}H_{16}INO_5S$.

Empirical formula	$C_{14}H_{16}INO_5S$	
Formula weight	437.24	
Temperature	100(2) K	
Wavelength	0.71073 Å	
Crystal system	Orthorhombic	
Space group	$Pna2_1 - C_{2v}^9$ (No. 33)	
Unit cell dimensions	a = 7.9664(5) Å	= 90.000°
	b = 34.946(2) Å	= 90.000°
	c = 5.2792(4) Å	= 90.000°
Volume	1469.7(2) $Å^3$	
Z	4	
Density (calculated)	1.976 Mg/m^3	
Absorption coefficient	2.345 mm^{-1}	
F(000)	864	
Crystal size	0.39 x 0.05 x 0.03 mm^3	
Theta range for data collection	2.33° to 30.54°	
Index ranges	-11 h 11, -49 k 49, -7 l 7	
Reflections collected	16743	
Independent reflections	4416 [R_{int} = 0.098]	
Completeness to theta = 30.54°	99.4 %	
Absorption correction	Semi-empirical from equivalents	
Max. and min. transmission	1.000 and 0.786	
Refinement method	Full-matrix least-squares on F^2	
Data / restraints / parameters	4416 / 1 / 199	
Goodness-of-fit on F^2	1.143	
Final R indices [I>2sigma(I)]	R_1 = 0.057, wR_2 = 0.112	
R indices (all data)	R_1 = 0.060, wR_2 = 0.113	
Absolute structure parameter	0.00(3)	
Largest diff. peak and hole	1.45 and -2.69 $e^-/Å^3$	

$-R_1 = \; ||F_o| - |F_c|| \; / \; |F_o|$

$wR_2 = \{ \; [w(F_o^2 - F_c^2)^2] \; / \; [w(F_o^2)^2] \; \}^{1/2}$

Table 2. Atomic coordinates (x 10^4) and equivalent isotropic displacement parameters ($Å^2$ x 10^3) for $C_{14}H_{16}INO_5S$. U(eq) is defined as one third of the trace of the orthogonalized U_{ij} tensor.

	x	y	z	U(eq)
I	-1085(1)	3152(1)	8551(1)	19(1)
S	-1041(2)	803(1)	5986(3)	14(1)
N	-719(6)	1210(1)	4553(9)	13(1)
O(1)	1598(5)	544(1)	1871(7)	12(1)
O(2)	-1879(5)	521(1)	4431(8)	16(1)
O(3)	-1844(5)	879(1)	8376(11)	23(1)
O(4)	5269(5)	402(1)	1503(8)	15(1)
O(5)	4291(5)	1104(1)	1598(9)	17(1)
C(1)	755(7)	1205(2)	2870(10)	12(1)
C(2)	1785(6)	859(1)	3629(14)	11(1)
C(3)	1130(7)	688(2)	6114(11)	15(1)
C(4)	1609(8)	263(2)	5879(11)	15(1)
C(5)	2555(6)	271(2)	3328(13)	12(1)
C(6)	4252(6)	471(1)	3640(16)	12(1)
C(7)	3698(6)	902(2)	3795(12)	11(1)
C(8)	-2115(7)	1473(2)	4073(10)	15(1)
C(9)	-1777(8)	1871(2)	5049(11)	15(1)
C(10)	-847(7)	1928(2)	7255(13)	19(1)
C(11)	-625(8)	2295(2)	8187(10)	14(1)
C(12)	-1351(7)	2604(2)	6969(11)	15(1)
C(13)	-2272(8)	2552(2)	4787(11)	17(1)
C(14)	-2481(7)	2182(2)	3844(11)	16(1)

Table 3. Bond lengths [Å] for $C_{14}H_{16}INO_5S$.

I-C(12)	2.100(6)
S-O(3)	1.439(5)
S-O(2)	1.447(4)
S-N	1.631(5)
S-C(3)	1.777(6)
N-C(8)	1.463(7)
N-C(1)	1.472(7)
O(1)-C(5)	1.444(7)
O(1)-C(2)	1.447(7)
O(4)-C(6)	1.410(8)
O(5)-C(7)	1.438(7)
C(1)-C(2)	1.516(7)
C(2)-C(3)	1.533(9)
C(2)-C(7)	1.534(7)
C(3)-C(4)	1.536(8)
C(4)-C(5)	1.543(9)
C(5)-C(6)	1.531(7)
C(6)-C(7)	1.569(7)
C(8)-C(9)	1.509(8)
C(9)-C(14)	1.377(8)
C(9)-C(10)	1.395(8)
C(10)-C(11)	1.386(8)
C(11)-C(12)	1.382(8)
C(12)-C(13)	1.378(8)
C(13)-C(14)	1.395(8)

Table 4. Bond angles [°] for $C_{14}H_{16}INO_5S$.

O(3)-S-O(2)	114.7(3)
O(3)-S-N	108.4(3)
O(2)-S-N	113.9(3)
O(3)-S-C(3)	116.2(3)
O(2)-S-C(3)	108.4(3)
N-S-C(3)	93.6(3)
C(8)-N-C(1)	120.6(4)
C(8)-N-S	120.5(4)
C(1)-N-S	113.2(4)
C(5)-O(1)-C(2)	96.1(4)
N-C(1)-C(2)	106.4(4)
O(1)-C(2)-C(1)	112.4(5)
O(1)-C(2)-C(3)	102.6(4)
C(1)-C(2)-C(3)	110.7(5)
O(1)-C(2)-C(7)	102.3(4)
C(1)-C(2)-C(7)	118.4(4)
C(3)-C(2)-C(7)	109.1(5)
C(2)-C(3)-C(4)	102.9(5)
C(2)-C(3)-S	102.1(4)
C(4)-C(3)-S	117.3(4)
C(3)-C(4)-C(5)	100.1(4)
O(1)-C(5)-C(6)	102.8(4)
O(1)-C(5)-C(4)	102.6(4)
C(6)-C(5)-C(4)	110.2(6)
O(4)-C(6)-C(5)	110.1(5)
O(4)-C(6)-C(7)	111.5(5)
C(5)-C(6)-C(7)	101.3(4)
O(5)-C(7)-C(2)	109.1(5)
O(5)-C(7)-C(6)	109.7(5)
C(2)-C(7)-C(6)	100.5(4)
N-C(8)-C(9)	112.5(5)
C(14)-C(9)-C(10)	119.3(6)

C(14)-C(9)-C(8)	119.8(5)
C(10)-C(9)-C(8)	120.7(5)
C(11)-C(10)-C(9)	119.7(6)
C(12)-C(11)-C(10)	120.3(5)
C(13)-C(12)-C(11)	120.6(6)
C(13)-C(12)-I	120.4(4)
C(11)-C(12)-I	119.0(4)
C(12)-C(13)-C(14)	119.0(6)
C(9)-C(14)-C(13)	121.1(6)

Table 5. Anisotropic displacement parameters ($Å^2 x\ 10^3$) for $C_{14}H_{16}INO_5S$. The anisotropic displacement factor exponent takes the form: $-2^2[\ h^2\ a^{*2}U_{11}\ ...\ +\ 2\ h\ k\ a^*\ b^*\ U_{12}\ ]$

	U_{11}	U_{22}	U_{33}	U_{23}	U_{13}	U_{12}
I	20(1)	13(1)	23(1)	-3(1)	5(1)	0(1)
S	16(1)	14(1)	13(1)	-1(1)	4(1)	1(1)
N	10(2)	9(2)	20(2)	5(2)	-1(2)	0(2)
O(1)	15(2)	10(2)	10(2)	1(1)	-3(2)	-1(2)
O(2)	18(2)	12(2)	20(2)	-1(2)	-6(2)	-6(2)
O(3)	24(2)	34(2)	12(2)	0(2)	8(2)	6(2)
O(4)	14(2)	15(2)	17(2)	-3(2)	3(2)	3(2)
O(5)	16(2)	10(2)	26(2)	5(2)	6(2)	1(2)
C(1)	12(2)	14(3)	10(2)	3(2)	4(2)	2(2)
C(2)	12(2)	13(2)	9(2)	6(3)	3(3)	0(2)
C(3)	15(3)	18(3)	10(2)	1(2)	0(2)	0(2)
C(4)	19(3)	10(2)	15(2)	3(2)	-1(2)	5(2)
C(5)	15(2)	11(2)	9(2)	0(2)	-1(2)	3(2)
C(6)	13(2)	10(2)	14(2)	-5(3)	1(3)	2(2)
C(7)	12(2)	13(2)	7(3)	-2(2)	4(2)	-2(2)
C(8)	14(2)	14(2)	16(3)	0(2)	-4(2)	2(2)
C(9)	15(3)	10(2)	21(3)	0(2)	5(2)	-3(2)
C(10)	15(3)	17(3)	25(3)	-4(2)	-8(2)	3(2)
C(11)	20(2)	18(2)	6(3)	0(2)	-2(2)	1(2)
C(12)	8(3)	16(3)	20(3)	0(2)	3(2)	1(2)
C(13)	26(3)	14(3)	12(2)	1(2)	0(2)	5(2)
C(14)	21(2)	20(2)	6(3)	-3(2)	-5(2)	0(2)

Table 6. Hydrogen coordinates (x 10^4) and isotropic displacement parameters ($Å^2$ x 10^3) for $C_{14}H_{16}INO_5S$.

	x	y	z	U(eq)
H(4O)	6283	431	1898	18
H(5O)	4966	965	795	20
H(1A)	1420	1442	3078	15
H(1B)	399	1185	1078	15
H(3)	1683	809	7614	17
H(4A)	606	97	5806	18
H(4B)	2345	180	7285	18
H(5)	2640	14	2503	14
H(6)	4825	388	5234	15
H(7)	4062	1026	5411	13
H(8A)	-3140	1371	4896	18
H(8B)	-2327	1485	2227	18
H(10)	-368	1715	8116	23
H(11)	28	2335	9669	17
H(13)	-2756	2764	3937	21
H(14)	-3120	2143	2346	19

Table 7. Torsion angles [°] for $C_{14}H_{16}INO_5S$.

O(3)-S-N-C(8)	-55.6(5)
O(2)-S-N-C(8)	73.3(5)
C(3)-S-N-C(8)	-174.8(5)
O(3)-S-N-C(1)	150.8(4)
O(2)-S-N-C(1)	-80.2(4)
C(3)-S-N-C(1)	31.7(4)
C(8)-N-C(1)-C(2)	-170.2(5)
S-N-C(1)-C(2)	-16.7(6)
C(5)-O(1)-C(2)-C(1)	-173.9(4)
C(5)-O(1)-C(2)-C(3)	-55.0(5)
C(5)-O(1)-C(2)-C(7)	58.1(5)
N-C(1)-C(2)-O(1)	103.5(5)
N-C(1)-C(2)-C(3)	-10.5(6)
N-C(1)-C(2)-C(7)	-137.5(6)
O(1)-C(2)-C(3)-C(4)	31.8(5)
C(1)-C(2)-C(3)-C(4)	152.0(5)
C(7)-C(2)-C(3)-C(4)	-76.1(5)
O(1)-C(2)-C(3)-S	-90.2(4)
C(1)-C(2)-C(3)-S	29.9(6)
C(7)-C(2)-C(3)-S	161.9(4)
O(3)-S-C(3)-C(2)	-147.1(4)
O(2)-S-C(3)-C(2)	82.1(4)
N-S-C(3)-C(2)	-34.6(4)
O(3)-S-C(3)-C(4)	101.3(5)
O(2)-S-C(3)-C(4)	-29.5(5)
N-S-C(3)-C(4)	-146.1(4)
C(2)-C(3)-C(4)-C(5)	3.0(5)
S-C(3)-C(4)-C(5)	114.1(5)
C(2)-O(1)-C(5)-C(6)	-56.8(5)
C(2)-O(1)-C(5)-C(4)	57.6(5)
C(3)-C(4)-C(5)-O(1)	-37.3(5)
C(3)-C(4)-C(5)-C(6)	71.7(5)

O(1)-C(5)-C(6)-O(4)	-84.6(5)
C(4)-C(5)-C(6)-O(4)	166.6(4)
O(1)-C(5)-C(6)-C(7)	33.5(6)
C(4)-C(5)-C(6)-C(7)	-75.3(6)
O(1)-C(2)-C(7)-O(5)	78.8(5)
C(1)-C(2)-C(7)-O(5)	-45.4(8)
C(3)-C(2)-C(7)-O(5)	-173.1(4)
O(1)-C(2)-C(7)-C(6)	-36.5(6)
C(1)-C(2)-C(7)-C(6)	-160.7(6)
C(3)-C(2)-C(7)-C(6)	71.6(6)
O(4)-C(6)-C(7)-O(5)	4.0(6)
C(5)-C(6)-C(7)-O(5)	-113.1(5)
O(4)-C(6)-C(7)-C(2)	118.9(5)
C(5)-C(6)-C(7)-C(2)	1.8(7)
C(1)-N-C(8)-C(9)	-81.3(6)
S-N-C(8)-C(9)	127.1(5)
N-C(8)-C(9)-C(14)	149.8(5)
N-C(8)-C(9)-C(10)	-34.4(8)
C(14)-C(9)-C(10)-C(11)	-0.8(9)
C(8)-C(9)-C(10)-C(11)	-176.7(6)
C(9)-C(10)-C(11)-C(12)	1.4(9)
C(10)-C(11)-C(12)-C(13)	-1.4(9)
C(10)-C(11)-C(12)-I	176.9(5)
C(11)-C(12)-C(13)-C(14)	0.9(9)
I-C(12)-C(13)-C(14)	-177.4(5)
C(10)-C(9)-C(14)-C(13)	0.3(9)
C(8)-C(9)-C(14)-C(13)	176.3(6)
C(12)-C(13)-C(14)-C(9)	-0.4(9)

Table 8. Hydrogen bonds for $C_{14}H_{16}INO_5S$ [Å and °].

D-H...A	d(D-H)	d(H...A)	d(D...A)	<(DHA)
O(4)-H(4O)...O(2)#1	0.84	2.01	2.780(6)	152.3
O(5)-H(5O)...O(4)	0.84	2.01	2.572(6)	123.2

Symmetry transformations used to generate equivalent atoms: #1: x+1, y, z.

Hanson Lab
Dry Solvent System
Manual

4-2-09

Toby R. Long

Table of Contents

I. Introduction

The dry solvent system is a replacement for conventional distillations of large volumes of solvents to be used for virtually all chemistries that take place in an organic chemistry research laboratory. The system is based upon a drying technique using activated alumina (Al_2O_3) whereby solvents are forced through packed columns containing the drying agent under inert gas atmosphere and are collected in small storage flasks. The purpose of the following manual is to familiarize the user with the system as a whole in order to demonstrate proper usage and maintenance providing greater awareness and overall safety for the entire lab.

II. Daily Use and Care

a. Inert gas replacement and monitoring

The most important issue for maintaining the solvent system on a daily/weekly basis is to closely monitor the total argon pressure. As the argon tank is being used, small periodic changes in pressure may require adjustment of the upper manifold metering valves (Figure 1) that control the argon halo over the collection flasks to minimize solvent exposure to outside air and moisture. Careful adjustment of the argon pressure aids in minimizing the amount of argon being used throughout the week and helps keep the system dry. Each attached argon bubbler should have a slow flow rate (~ 1 bubble/5 seconds). The lower argon manifold distributes argon to the solvent storage tanks. Each needle valve on this manifold should remain open at all times unless isolation from the system is required during regeneration or repair.

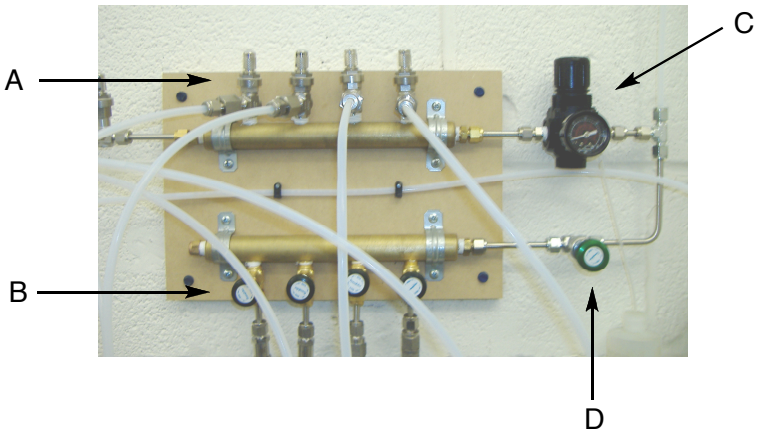

A. Upper manifold/ metering valves
B. Lower manifold/ needle valves
C. Halo system regulator
D. Fill valve

Figure 1: Argon manifold assembly

When the system argon pressure is low (< 50 psi – right-hand gauge) it is best to replace the tank before it completely runs out. The first step is to place the (NO ARGON – DO NOT USE!!) sign on the system to alert users that the solvent system is down. Next, sequentially shut off the argon related valves starting with the green fill valve located near the halo system regulator followed next by the closure of the black valve that is directly attached to the tank regulator. Lastly, close the argon tank valve and disconnect the regulator from the tank. Place the safety cap back on the argon tank and exchange for a full tank. Once the new tank is secured on the wall with the chain, remove the safety cap and reconnect the tank regulator. While tightening the regulator, SLOWLY open the main valve to purge any air from the regulator housing and continue to tighten the regulator until the gauges are reading at full pressure. Finish tightening the regulator to an acceptable torque rating and open the argon related valves in reverse order starting from the tank. Allow the system 5-10 minutes to re-pressurize and readjust the upper manifold metering valves that control the argon halo.

b. Solvent replacement and delivery

Replacement of the solvent in the system should only be performed by someone who is trained on the system. This process begins by closing the green fill valve (Figure 1) that controls the argon flow to the solvent storage tanks (Figure 2). After

shutting the valve, locate the tank valve (B) on the storage tank that corresponds to the solvent being replaced and close this valve. Next, remove the argon pressure line (C) leading to the tank by pressing down on the larger part of the quick-connect assembly until it releases. Locate the quick-connect bleeder hose and place this on the tank to bleed the tank pressure to atmospheric level. Open the top of the storage tank by lifting the lever. ****IMPORTANT** If the solvent is flammable, double check that the tank is securely grounded by tracing the ground wire to the source of the ground. Also, if the solvent container being used to fill is metal, attach a ground lead to this container as well prior to opening or filling.** Continue to fill the tank to the fill line located on the upper outer rim of the tank. Once the tank is full, replace the cap loosely and connect the argon pressure line to the degassing quick connect valve (A) on the tank by pressing downward on the upper, thinner part of the quick connect until it clicks. Slowly open the green fill valve until out-gassing occurs in the tank. Continue degassing the solvent for 5 minutes. After such time pull the cap on the tank closed while the degassing is continues. Switch the argon pressure line from the degassing quick connect valve (A) to the pressure inlet quick connect valve (C). Continue pressurizing the storage tank for 5 minutes. Lastly, reopen the tank valve (B) leading to the column and continue pressurizing for another 5 minutes. The system is now ready to be used.

A. Degassing quick connect valve
B. Tank shut-off valve
C. Pressure inlet quick connect valve
D. Ground cable connection

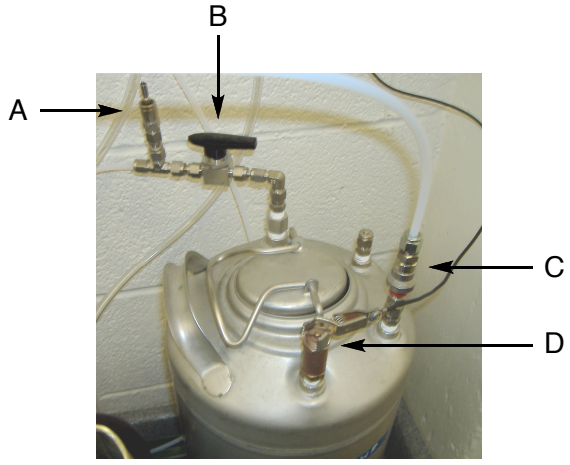

Figure 2: Solvent storage container

c. Proper solvent extraction technique

Proper extraction technique is just as vital as maintaining the argon supply as poor technique will lead to exposing the system to excess air and moisture. ****IMPORTANT – Make sure your syringe and needle is clean and dry before using to extract solvent from the system. Only 12 in. long needles should be used for this process.** Proceed to enter into the flask by piercing the upper inlet septum (A) on the flask (Figure 3) and turn the 2-way valve (C) until the needle can be pushed though to the solvent level. Withdraw the solvent into the syringe barrel being careful not to put pressure on the glass joint with the septum (B) as this can lead to breakage and possible injury. Expel excess argon from the top of the syringe without returning excess amounts of solution to the flask This helps prevent contamination of the solvent flask. Once the desired amount is withdrawn, bring the needle out of the solvent and pull argon into your syringe. Withdraw the needle back through the two-way valve (C), close the valve and remove from the septum (B). ****Do not remove the needle through the valve and out the septum in one motion.** If you are filling the flask to withdraw large quantities of solvent, insure that the system is well pressurized before proceeding. Check the argon level on the tank first and proceed to open the green fill valve (five full turns counter clockwise) and wait for several minutes. Remove the lower round bottom flask and place it on the cork ring located at the solvent station. Open the lower two-way valve on the flask and collect the desired amount of solvent. ****Do not leave behind large amounts of solvent in the flask unless you know you or someone else will be using it.**

A. Argon halo inlet
B. Syringe inlet septum
C. 2-way valve
D. Dry solvent inlet

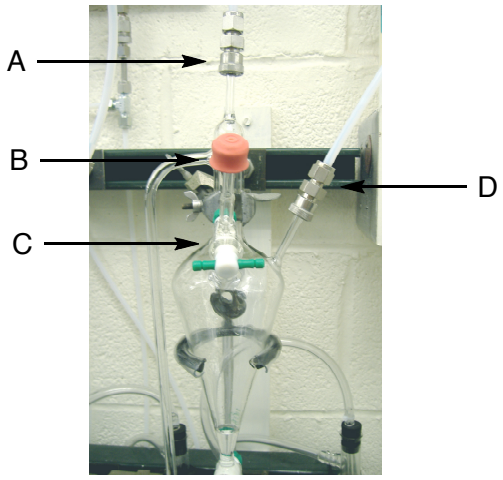

Figure 3: Solvent collection flask

d. Cleaning solvent collection flasks

During the regeneration period it is good practice to go ahead and critically clean the solvent collection flask to the corresponding solvent. Proceed to carefully remove the connectors attached to the flask (Figure 3) by un-tightening the connector by hand and removing it from the glass joint. **It is easier to keep the connector together in one piece while removing or replacing it in order to keep the seal and ferule properly aligned inside of the housing. Afterwards, carefully remove the flask and begin cleaning it using a diluted solution of Micro 90 cleaning soap. Rinse thoroughly with deionized water and acetone and place in a drying oven at 90 ºC overnight. Replace the flask and only connect the upper argon connection. Proceed to flame dry the flask while flowing argon into the flask. ****IMPORTANT** Make sure the solvent feed line is empty/dry and there are no flammables nearby. If the nearby flask on the system contains a flammable solvent, empty and dry the flask before proceeding.**

III. Safety Issues

a. Static electricity/discharge

Storage containers containing flammable solvents (diethyl ether, THF, and toluene) require an external ground wire to be securely attached to a nearby ground source. This can be located in Figure 2(D). ****Make sure the connection is secure before refilling the storage container. **When refilling flammable solvents, ground the solvent can to the storage container being filled.** Also, use caution that other people nearby are not using an open flame. Do not use your cell phone or other electronics at or nearby the dry solvent system.

b. Over-pressurization

Over-pressurization of the system can be easily prevented by carefully monitoring the inert gas total pressure on the left-hand (secondary) gauge on the gas regulator. By securing the large regulator valve with tape, this will prevent accidental changes in pressure due to the occasional brush of an arm by a person walking nearby. The total pressure on the solvent storage containers should not exceed 20 psi. A good working pressure is 15-20 psi.

c. Solvent overflow

Overflowing the solvent system can be kept at a minimum by carefully thinking your way through the process of using the system. **If an overflow occurs, quickly absorb the solvent/oil off the floor and report it to the person in charge. The inert gas bubbler corresponding to this solvent will need to be emptied and refilled with light mineral oil located near the system. If significant damage has occurred to the vinyl tubing, then it should be replaced as well.

IV. Column Regeneration

a. Materials and Apparatus

- Activated alumina beads (2-5 mm dia)
- Inert gas tank and regulator
- ¼ in. Swagelok drying tube w/ dessicant
- Heating blanket (Figure 7)
- 110 V Voltage regulator
- Digital thermometer and probe
- Glass wool
- Nickel Anti-Seize Tape
- Particulate breathing mask
- Small plastic funnel
- Two large crescent wrenches
- Rubber mallet

b. Regeneration Procedure

1. Turn off the solvent storage tank valve located on top of the tank corresponding to the column needing regeneration. **Leave the storage tank under inert gas during this process.
2. Disconnect the upper feed line at the glass collection flask and plug the glass feed stem with a 14/20 septum.
3. Disconnect the lower and upper feed lines leading at the valves on the column using caution to slowly bleed the solvent remaining in each line.
4. Loosen the large U clamps that secure the column to the wall with the aid of another person and lower the column out of the clamps.

5. Carry and place the end of the column in the top of an open solvent waste container and slowly open the valve to allow the excess solvent to spray and drain from the column.
6. Once the majority of the solvent is removed, place the column in a hood and attach an air line to one end. Apply pressure to the column and open both valves to purge out any remaining solvent liquid or vapor.
7. Once the column is dry, use two large crescent wrenches to loosen each threaded valve adapter – removing one adapter and valve on any given end.
8. Empty the dry spent alumina beads into the solid waste container and attach an air line to the other valve to help force out any remaining beads.
9. When the column is empty, unthread and remove the remaining valve assembly. Each valve assembly contains glass wool plugs that should be replaced. **Do not over pack.
10. Replace the nickel anti-seize tape on threads and replace. Wrap one loop over the threads in a clockwise direction with the glass wool plug facing your direction. Remove any remaining tape on the inner threads of the column before replacing each adapter and valve assembly.
11. Thread one adapter and valve assembly onto one end of the column as tight as possible with a wrench leaving the other end of the column open.
12. Using a dust/particulate mask over your mouth and safety glasses, place the small funnel in the end of the column upright. With the help of another person, slowly pour the beads into the column. Use the rubber mallet to occasionally rap the side of the column to ensure proper packing/settling of the beads.
13. Once the column is full and packed well, replace the other valve adapter assembly and concentrically tighten each assembly using both persons and both crescent wrenches until firmly tight (55-60 ft.lbs – torque).
14. Place the column in the heating blanket with the un-insulated end of the temperature probe and tie up the column with the probe securing them well in the

blanket. **Check to make sure there is no plastic insulation touching the blanket as it will melt and catch fire.

15. Connect one end of the column to the drying tube and the inert gas tank regulator. Set the regulator to 6 psi while flowing inert gas through the column. Continue gas flow until regeneration is finished. Test the flow is sufficient with a small drop of water on your wrist.
16. ****Important** – Before beginning the heating process, remove the valve on the opposite end of the column as excess steam being ejected will damage the valve. This valve should be replaced once the column is finished and cool to the touch.
17. Connect the heating blanket to the voltage regulator and slowly increase the voltage until the desired temperature has been reached. (**375 ºC**)
18. Continue heating at 375 ºC for 6-8 hours. Place a caution sign nearby to alert people of the high temperature and closely monitor the column during this time period.
19. After such time, carefully untie the blanket and allow the column to return to room temperature while maintaining inert gas flow. Use a fan to speed up the process.
20. Once the column has reached room temperature, reconnect the end valve to the threaded valve adapter and align each set of valve handles with each other.
21. Close the valves on the column starting from the end furthest from the inert gas inlet to seal off the column from the outer atmosphere.
22. Disconnect the column from the inert gas and reattach it to the U clamps on the wall.
23. Reattach the feed lines in no specific order. Do not over-tighten.
24. Make sure there is pressure on the corresponding solvent storage tank.
25. ****Important** - Open the storage tank valve and loosen the lower feed line at the valve on the column to bleed the solvent up to the valve.
26. Once the solvent is up to the valve, open the lower valve to the column. Wait a few minutes and open the upper valve on the column slowly. ****Important** –

Excess heat generated from the adsorption in the column can cause the solvent to boil creating a large amount of volatile fumes. If this occurs, remove the feed line at the glass collection flask and place it directly in an open 4 L bottle until the column cools and the vapor begins to condense back to a liquid. **Also, make sure no one in the vicinity is using an open flame if the solvent is flammable.

27. Check the system for leaks and tighten any needed fittings.
28. Monitor the argon flow and pressure and make any necessary adjustments.